Organometallic tetrazoles

Bhandari, Sonali

Award date:
1998

Awarding institution:
University of Bath

ORGANOMETALLIC TETRAZOLES

Submitted by Sonali Bhandari

For the degree of PhD

of the University of Bath

1998

Department of Chemistry

University of Bath

Supervisor: Dr.K.C.Molloy

COPYRIGHT

S. Bhandari

ProQuest LLC
789 East Eisenhower Parkway
P.O. Box 1346
Ann Arbor, MI 48106-1346

Contents

ABSTRACT

The syntheses and characterisation by standard spectroscopic techniques of organotin-, organolead- and organothallium-substituted tetrazoles and thio-tetrazoles have been undertaken.

Chapter two of this thesis describes the preparation of organotin-substituted tetra-tetrazoles by the established ring-building 1,3-dipolar cycloaddition. The crystal structures of 1,4-phenylene-bis-(tributylstannyl tetrazole) and 1,2,4,5-tetra-benzene-(triethylstannyl tetrazole) have been included.

In chapter 3, the employment of the cycloaddition route to synthesise organotin-substituted functionalised tetrazoles has been described. The crystal structure of anhydrous 4-pyridyl-(triethyltin tetrazole), the crystal structure of monohydrate 3-pyridyl-(triethyltin tetrazole) and the structure of dihydrate 4-pyridyl-(tributyltin tetrazole) have also been included.

Chapter 4 extends the study to the syntheses and characterisation of triphenyllead-substituted tetrazoles. This class of compounds was synthesised by the reaction of triphenyllead hydroxide with the appropriate hydro-tetrazole. Little success has been achieved with these compounds on the crystallography front.

In chapter 5, the preparation and characterisation of thallium(I) tetrazolates and diphenylthallium-substituted tetrazoles have been described. The latter class of compounds were prepared by the reaction of diphenylthallium hydroxide with the appropriate hydro-tetrazole. The structures of 1-diphenyl thallium-5-(phenyl tetrazole).MeOH, 1,4-butylene-bis-(diphenyl thallium tetrazole). 2MeOH and 1,2-phenylene-bis-(diphenyl thallium tetrazole). 2MeOH. $2H_2O$. Ph_2TlCl have been crystallographically determined.

Finally, chapter 6 contains the preparation and characterisation of triorganotin-substituted thio-tetrazoles. Two different routes have been invoked to prepare these compounds- the 1,3 dipolar cycloaddition route and the salt elimination of NH_4Cl route. The structures of 1,4-phenylene-bis-(5′-thiolato-tributylstannyl-1′-tetrazole) and 1,4-phenylene-bis-(5′-thiolato-trimethylstannyl-1′-tetrazole) have been determined by X-ray crystallography. 1,4-phenylene-bis-(5′-thiolato-tributylstannyl-1′-tetrazole) has also been used as a precursor to synthesise Ni(II)-, Ag(I)-, Hg(II)-, organomercury-, organolead- and organothallium-substituted tetrazoles.

List of Abbreviations Used in this Work

Bu	Butyl
^{n}Bu	n-butyl
Calc.	calculated
CO	Carbonyl
cod	1,5 Cyclooctadiene
CHN	Carbon-hydrogen-nitrogen (microanalysis)
CN	coordination number
dec.	decomposed
DMSO	Dimethyl sulphoxide
Et	Ethyl
esds(σ)	estimated standard deviations
Glx	Glutamine or glutamic acid
g	grams
HMPT	Hexamethyl phosphoramide
HOMO	Highest occupied molecular orbital
Hz	Hertz
i.s.	Isomer shift
IR	Infra-red
I	Intensity
K	Kelvin
keV	Kilo electron volt
LUMO	Lowest occupied molecular orbital

Met	Methionine
Me	Methyl
MHz	Megahertz
MeOH	Methanol
Me_2pz	Dimethyl pyrazolyl
m.p.	melting point
mms^{-1}	millimeter per second
mmol	millimoles
mL	millilitre
NMR	Nuclear magnetic resonance
Phe	Phenylalanine
^{i}Pr	iso-propyl
^{n}Pr	normal propyl
Ph	Phenyl
pmtta	Pentamethylene tetrazole
PVC	Polyvinyl chloride
ppm	Parts per million
q.s.	Quadrupole splitting
Trp	Tryptophan
TMS	Tetramethyl silane
vs.	versus
XS	Excess

DEDICATION

I dedicate this thesis to my grandparents and parents.

A Road Not Taken

Two roads diverged in a yellow wood,
And sorry I could not travel both
And be one traveller, long I stood
To where it bent in the undergrowth;

Then took the other, as just as fair,
And having perhaps the better claim,
Because it was grassy and wanted wear;
Though as for that the passing there
Had worn them really about the same,

And both that morning equally lay
In leaves no step had trodden black.
Oh, I kept the first for another day!
Yet knowing how way leads on to way,
I doubted if I should ever come back.

I shall be telling this with a sigh
Somewhere ages and ages hence:
Two roads diverged in a wood, and I-
I took the one less travelled by,
And that has made all the difference.

Robert Frost

ACKOWLEDGEMENTS

First and foremost, I would like to thank Dr.Kieran Molloy for giving me the opportunity to work towards a Ph.D under his supervision. I would also like to thank him for all his advice and friendship during the course of the past three and a half years. My special gratitude is extended to Dr.Mary Mahon for her skills involved in the crystallographic data contained in this thesis. She has also been a great friend and I applaud her fortitude and courage in being a woman professional.

I would like to express my sincere gratitude to all the technical staff of the University of Bath, Mr.Dave Wood for the majority of the NMR data, Mr.Alan Carver for all the CHN analyses and the wonderful moral support and encouragement provided by Mr.Robert Stevens, Mr.Ahmed Sheibani and Mrs.Sheila Osborne.

My ambition to get a Ph.D has been a very personal quest for answers about the role of women in society. I would like to thank my sisters, Anjali and Bornali, and all my friends, especially Alia Lodi, in this long journey who have believed in me and made it possible. I would also like to thank my critics for pointing out my defects and thus have given me the determination to overcome them. My list of acknowledgements will not be complete without thanking the two most important people in my life - my parents. I bow down to their fortitude, determination, hard work and for being pillars of support and encouragement to me.

Chapter 1

The Synthesis and Structural Variations of Organometallic Tetrazoles

This thesis describes the syntheses and structural characteristion of various classes of organometallic tetrazoles containing tin, lead, and thallium via cycloaddition between an organometallic azide and an organic nitrile or elimination of water using a preformed heterocycle. In addition, the syntheses of a series of triorganotin thio-tetrazoles and the use of these compounds as precursors to other organometallic thio-tetrazoles is described. In order to introduce this work, the synthetic and structural aspects of organometallic tetrazoles will be reviewed.

1.1 INTRODUCTION

Biological activity is encountered in tetrazoles due to the tetrazole ring being isosteric with a carboxylic acid group and of comparable acidity.[1] The increased metabolic activity of the tetrazole ring has generated biochemical and pharmacological uses. For instance, the tetrazole analogue of tetrapeptide (I) has been prepared and was found to show comparable acidity to the normal peptide for stimulating gastric acid secretion.[1]

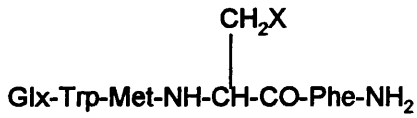

X = CN_4H, CO_2H

I

Tetrazole analogues of amino acids and natural carboxylic acids have been prepared and have found uses in antitumour, antiflammatory, antimicrobial, antiallergic,

and antihypotensive activities.[2,3] For instance, pentamethylene tetrazole (**II**) is used as a stimulant for the central nervous system and counteracts the effects of barbiturate overdose.[1] The medicinal uses of tetrazole have been covered by extensive reviews.[4]

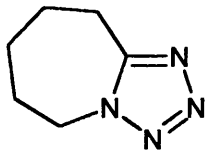

II

Tetrazoles have also found potential uses in agriculture, photography, polymer chemistry, explosives, and as rocket propellants.[1] In addition, a number of substituted tetrazoline-5-thiones are used for gravimetric determinations of transition metals because of their complexing ability. Ions such as Cu^{2+}, Cu^{+}, Ag^{+}, Au^{+}, Hg^{+}, and Cd^{2+} can be detected in the 0.5-5.0 mg range by precipitation.[5] Tetrazole polymers have also been prepared and are used as thermally stable propellant binders and as plastics.[6]

1.2 STRUCTURE

The tetrazole subunit is a five-membered heterocyclic ring with four nitrogens. It is a 6π azopyrrole ring system with two tautomeric forms - the 1,5-disubstituted (**IIIa**) and the 2,5-disubstituted (**IIIb**) - as shown in the following diagram.[1]

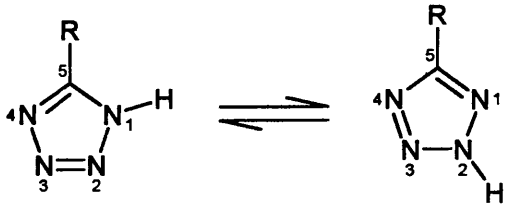

IIIa **IIIb**

The tetrazole ring is planar with bond lengths characteristic of aromatic systems. The tetrazolate anion (**IVa**, **IVb**, and **IVc**) is isoelectronic with the cyclopentadienyl anion and the acidity of these two species is also comparable.[7]

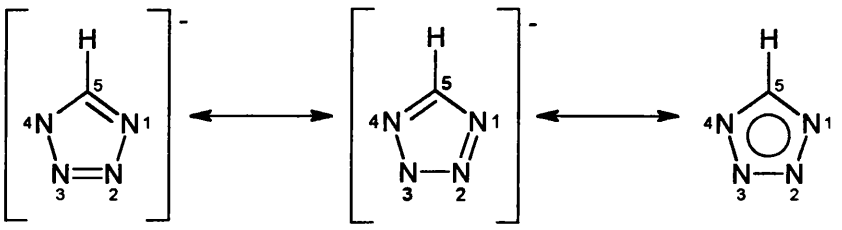

IVa **IVb** **IVc**

1.3 SYNTHESIS

In this section, some general methods of syntheses of organic tetrazoles will be described. This will be followed by a discussion of more specific routes reported in the literature for the preparation of main group and transition metal derivatives of tetrazoles.

1.3.1 General Methods For Synthesis Of Organic Tetrazoles

The following sections describe four major routes used to synthesise organic tetrazoles.

1.3.1.1 Production and cyclization of imidoyl azides

One of the main routes for the synthesis of 1-substituted and 1,5-disubstituted tetrazoles is the production and cyclization of imidoyl azides as shown in the following equilibrium.[8]

Equilibrium 1.1

X = O, S, NR^1

When X is an oxygen atom, the acyclic form predominates and when X is a sulphur atom the cyclic form predominates. When X is an NR^1 moiety, there can be an equilibrium of both acyclic and cyclic forms or either form can predominate.

1.3.1.2 Cyclization of formazan and tetrazene derivatives

Formazan ($RN{=}N\text{-}R^1{=}N\text{-}NHR^2$)[9] and tetrazene (R-NH-N=N-NHR)[10] systems are acyclic systems other than the imidoyl azides which can cyclize into a tetrazole. For instance, formazans can be oxidised to give tetrazolium salts. If one of the N-substituents of formazans is a good leaving group, it cyclizes to form a 2,5-disubstituted tetrazole (Scheme 1.1).[9]

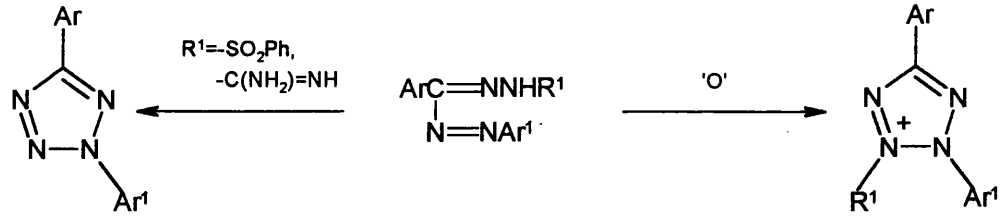

Scheme 1.1

1.3.1.3 Addition of azide ion to nitriles, nitrilium ions and isonitriles

The most prevalent route for the synthesis of tetrazoles is the 1,3-dipolar cycloaddition of hydrazoic acid or azide ion with compounds containing carbon-nitrogen multiple bonds. Reaction of azide ion with nitriles, nitrilium salts, and isocyanides leads to the synthesis of 5-substituted tetrazoles[11], 1,5-disubstituted tetrazoles[12], and 1-substituted tetrazoles[13], respectively (Scheme 1.2).

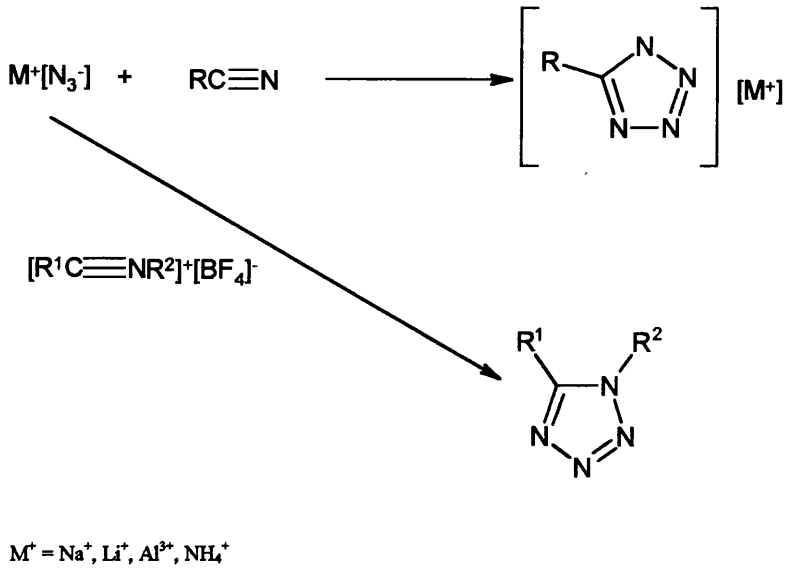

Scheme 1.2

1.3.1.4 Cycloaddition of azides to -C=N- and -C≡N- systems

Cycloaddition of organic azides with compounds containing carbon-nitrogen multiple bonds leads to the formation of 1,5- and 2,5- disubstituted tetrazoles as depicted in the following equation.[14]

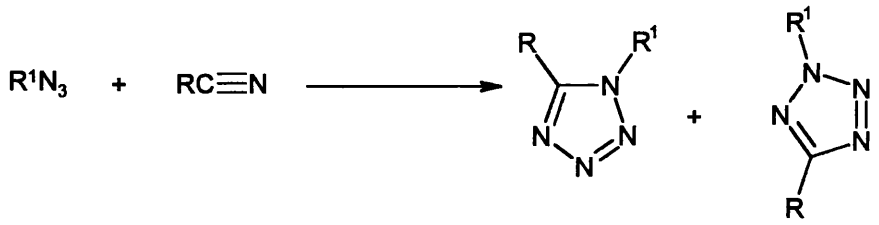

Eq. 1.1

Scheme 1.3 summarises the reactions between organic azides and isocyanate and related systems. Addition of the azide group across the carbon-nitrogen multiple bond can be exploited to form a variety of tetrazole containing organic compounds.

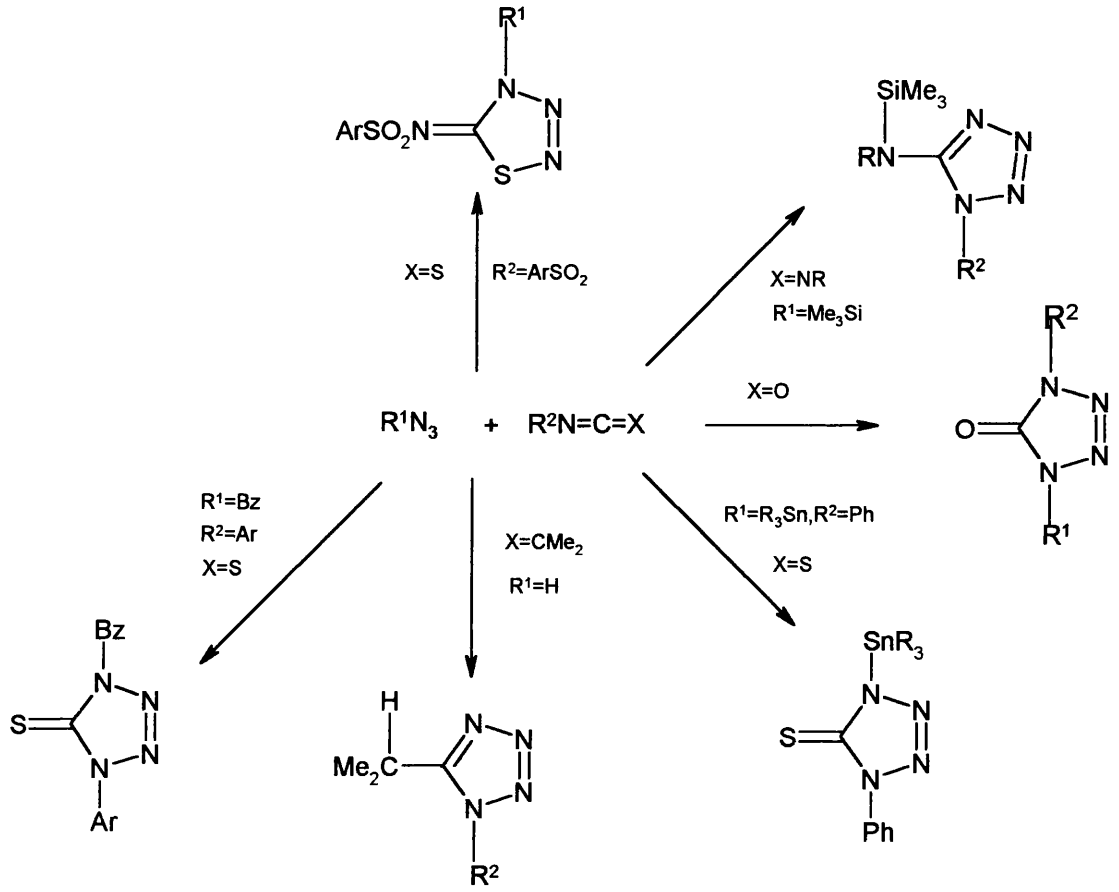

Scheme 1.3

1.3.2 Synthetic Routes To Main Group Derivatives Of Tetrazoles

Three routes have been widely used to synthesise main group derivatives of tetrazoles and will be discussed in the following sections.

1.3.2.1 Cycloaddition of organometallic azides to organonitriles involving formation of the tetrazole ring

The most prevalent route for the synthesis of main group derivatives of tetrazoles involves the 1,3 dipolar cycloaddition of metal-substituted azides to compounds containing carbon-nitrogen multiple bonds (equation 1.2).[15,16,17,18,19] Steric factors and identity of the coordinated metal determine the position and degree of substitution.

Eq.1.2

Cycloaddition reactions for ($4\pi + 2\pi$) systems are concerted processes involving two components - HOMO (highest occupied molecular orbital) of one species and LUMO (lowest occupied molecular orbital) of another.[20] The feasibility of cycloaddition reactions is determined by whether overlap can take place between the HOMO of one component and LUMO of another. The extent of overlap in turn is determined by the symmetry, phases, and energies of the two orbitals in question. The closer the two orbitals are in energy, the better is the overlap. The 4π component in a ($4\pi + 2\pi$) cycloaddition need not involve carbon atoms only nor be a four-atom system. The commonest of these non-dienic 4π systems involve three atoms and have one or more dipolar canonical structures, e.g. N_3^- and O_3, hence the term - 1,3 dipolar cycloaddition. The frontier orbitals for 1,3 dipolar cycloadditions are given in Fig. 1.1.[20,21]

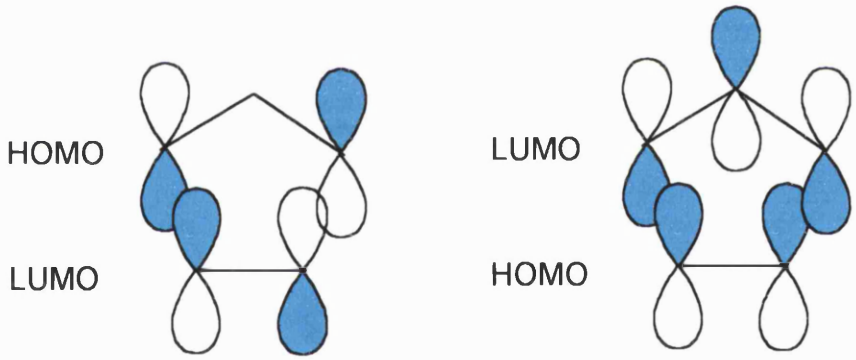

Fig. 1.1

The mechanism of the metal azide - nitrile cycloaddition is given below (Figs.1.2a and 1.2b).[22] The reaction is favoured if the azide is strongly "nucleophilic" and the nitrile is strongly "electrophilic" and nucleophilicity of the azide in turn is affected by the nature of the metal. For instance, low conversions were obtained for the reaction between trimethylsilyl azide with aryl and alkyl nitriles.[23] However, in the presence of a catalytic

amount of dibutyltin oxide the yields of the cycloaddition product increased dramatically. Two mechanisms have been invoked to explain this observation, both of which involve the formation and breakdown of the intermediate diakyl(o-trimethylsilyl)azidostannyl hydrin (VI) which reacts with the organonitrile (Schemes 1.4 and 1.5).

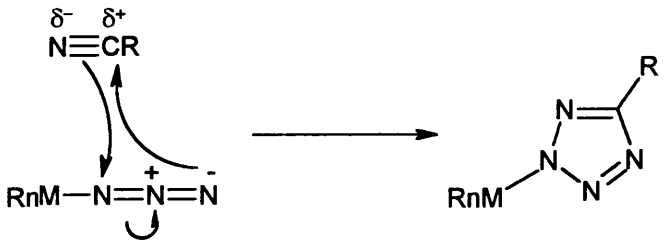

Fig. 1.2a

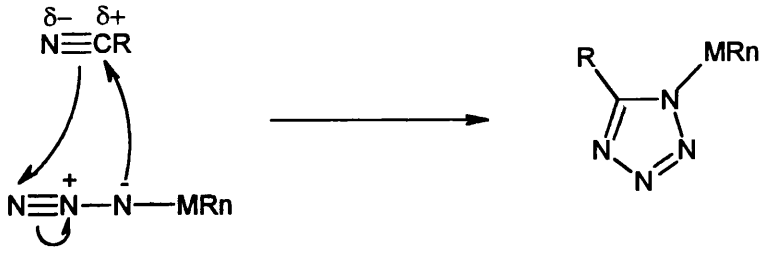

Fig.1.2b

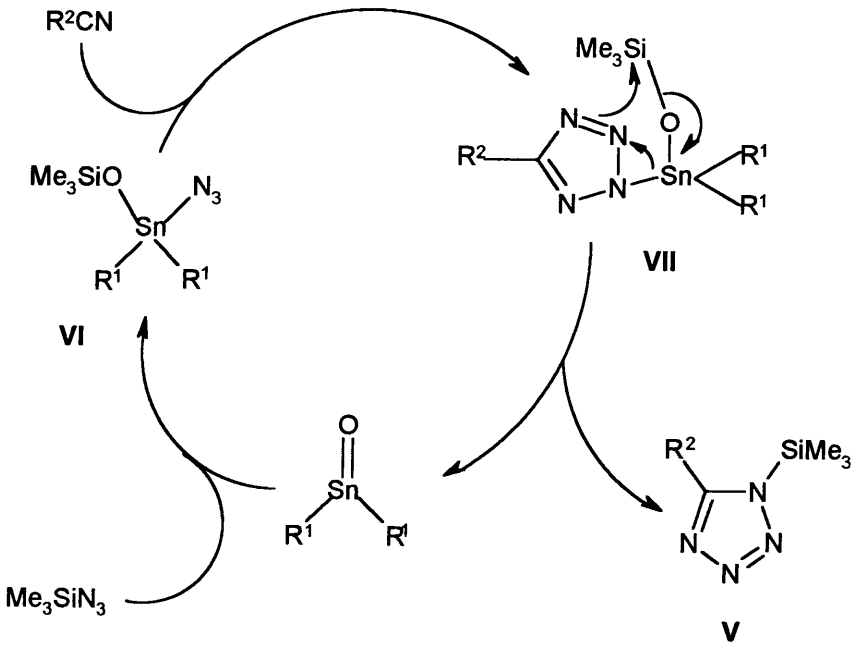

Scheme 1.4

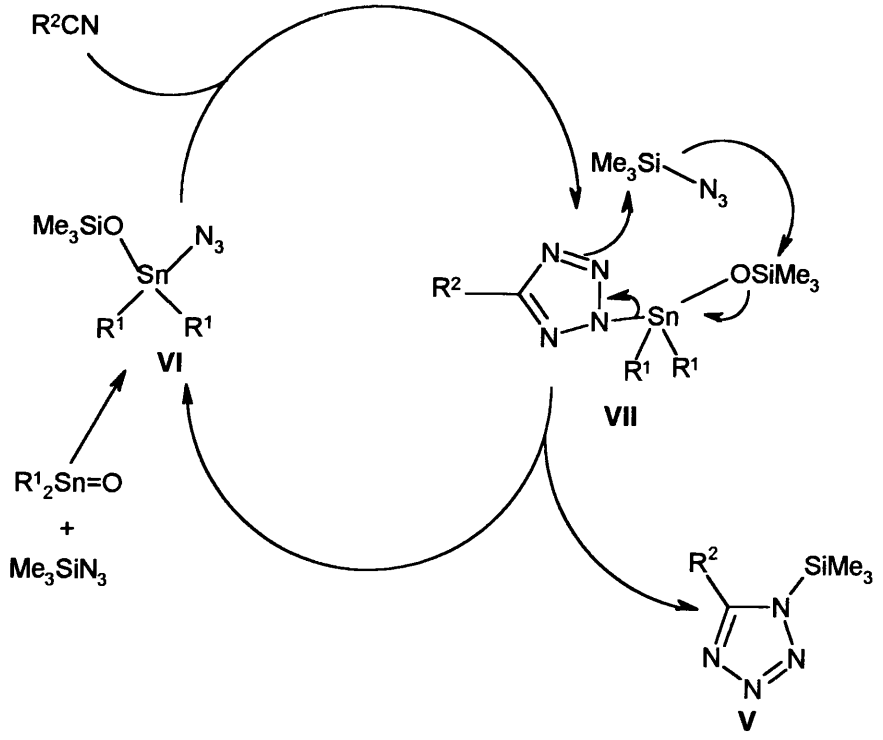

Scheme 1.5

Triorganotin azide, however, readily undergoes cycloaddition reactions with mono-, bis-, and tris-, aliphatic and aromatic nitriles and gives nearly 100% yields of triorganotin tetrazoles.[24]

1.3.2.2 Condensation of preformed tetrazoles with organometallic oxides and hydroxides

Other preparative routes for organometallic tetrazoles involve the reaction of the parent hydro-tetrazole with an organometallic oxide or hydroxide. For instance, synthetic routes reported by Sisido *et al* involve the treatment of a free 5-substituted tetrazole with bis(tri-n-butyltin)oxide or trimethyltin hydroxide to give **VIII** and **IX,** respectively (equations 1.3 and 1.4).[25]

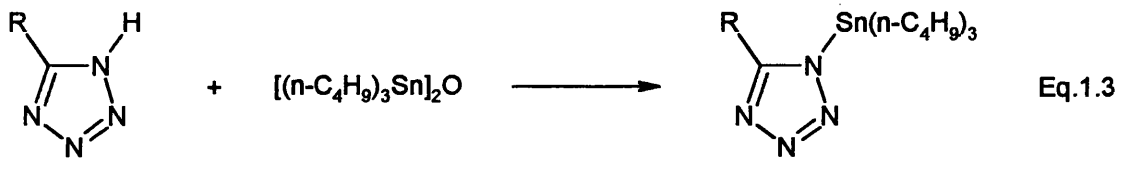

Eq.1.3

VIII

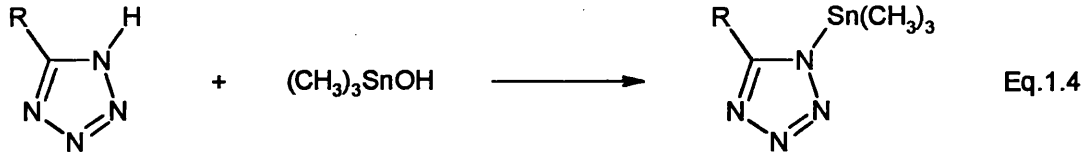

Eq.1.4

IX

1.3.2.3 Reaction of preformed tetrazole salts of the tetrazole ring with organometallic chlorides

A less prevalent synthetic procedure for organometallic tetrazoles involves the reaction of tetrazole salts with organometallic chlorides with the elimination of metal chloride. An example of this procedure was reported by Molloy *et al* and involves the simple metathesis between an organotin chloride and the sodium salt of the preformed

tetrazole (equation 1.5).[26] Triorganotin tetrazole is formed by the elimination of sodium chloride.

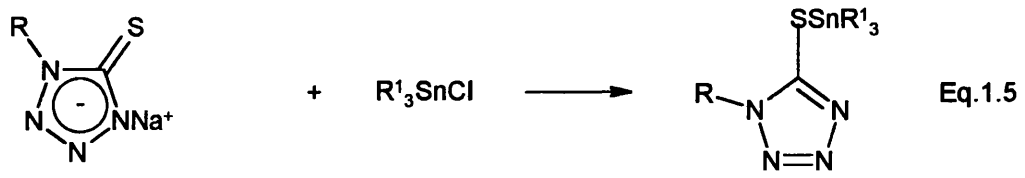

Eq.1.5

	X	XI	XII	XIII
R	Me	Ph	Ph	Ph
R^1	Bu	Me	Bu	Ph

Organotin(IV) derivatives of thio-tetrazoles have also been prepared by Raymundo-Cea-Olivares *et al* using this metathesis route.[27] Stoichiometric amounts of methyl and benzyl tin(IV) chlorides were reacted with the ammonium salt of 1-phenyl-*1H*-tetrazole-5-thiol to give the respective organotin(IV) thio-tetrazoles (equation 1.6).

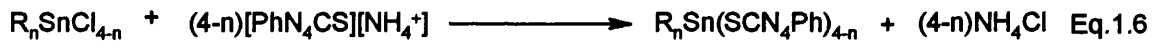

Eq.1.6

1.3.3 Synthetic Routes To Transition Metal Derivatives Of Tetrazoles

A wide variety of transition metal complexes containing the parent tetrazole (**III**) and the tetrazolate anion (**IV**) have been synthesised to date.[28] The only groups for which such complexes are not known are the scandium, titanium, and the vanadium groups.

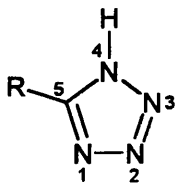

III

Tetrazole

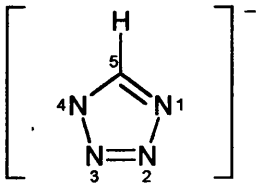

IV

Tetrazolate

1.3.3.1 Synthesis of complexes of transition metals containing the parent tetrazole from transition metal perchlorates or tetrafluoroborates

Hydrated metal (II) perchlorates or tetrafluoroborates react with 1,5-pentamethylenetetrazole and 1- or 2- substituted tetrazoles in the presence of a dehydrating agent to form complex salts $[M(1,5\text{-pmtta})_6][Y]_2$, $[M(1\text{-R}, 5\text{-R}^1\text{-}CN_4)_6][Y]_2$, and $[M(2\text{-R}, 5\text{-R}^1\text{-}CN_4)_6][Y]_2$, where M = Mn^{2+}, Fe^{2+}, Co^{2+}, Ni^{2+}, Cu^{2+}, or Zn^{2+}; Y = ClO_4^- or BF_4^-, as shown in equation 1.7.[29]

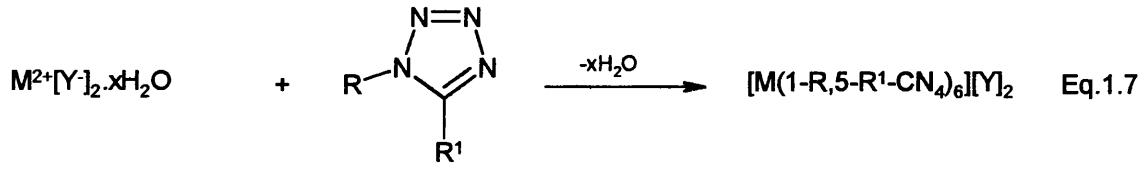

1.3.3.2 Synthesis of complexes of transition metals containing the parent tetrazole from transition metal carbonyls

Thermal or photolytic displacement of CO from carbonyl complexes of chromium, molybdenum, and tungsten lead to the formation of tetrazole complexes of the chromium group (equation 1.8).[30]

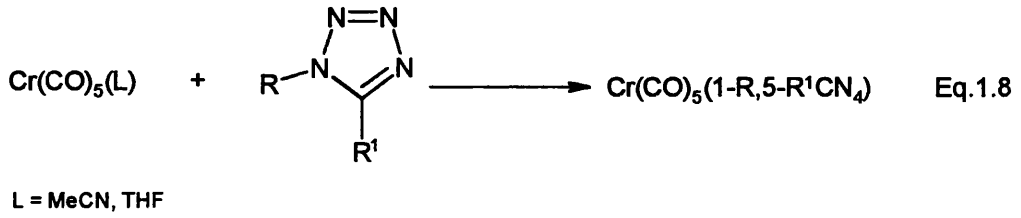

1.3.3.3 Synthesis of complexes of transition metals containing the tetrazolate anion

There are three possible routes for the syntheses of tetrazolate complexes (Scheme 1.6). In the presence of base such as triethylamine[31], hydrazine[32], or potassium hydroxide[33], metal salts react with the free tetrazoles to form tetrazolate complexes. They can also be formed by reacting transition metal halides with alkali metal salts of tetrazoles and 5-substituted tetrazoles.[34] Cycloaddition of organic nitriles (RCN)[35] or isonitriles

(RNC)[36] with coordinated azides results in the synthesis of 1- or 5-substituted tetrazolate anions.

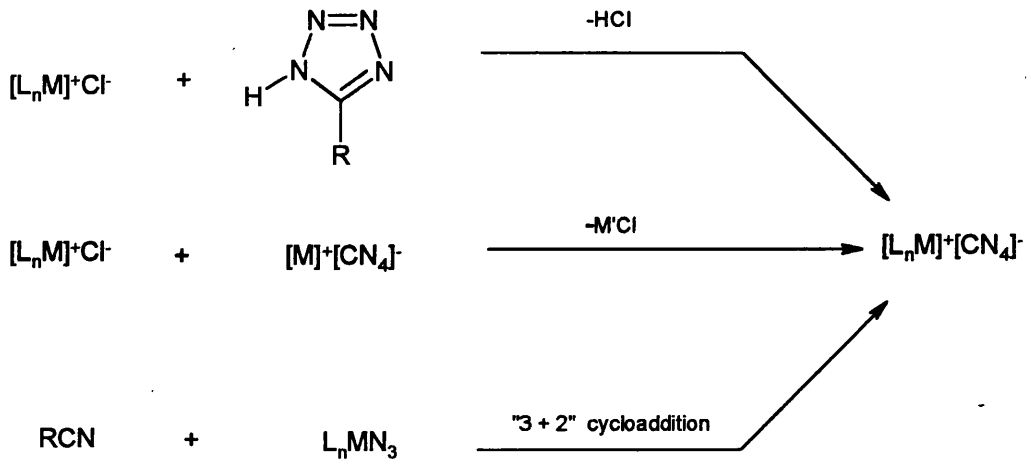

Scheme 1.6

1.4 STRUCTURAL VARIATIONS OF METAL DERIVATIVES OF TETRAZOLES

Due to the isoelectronic nature of the tetrazole and cyclopentadienyl anions, η^5 coordination of the tetrazolate ligands had been proposed.[37] However, all established structures exhibit localised M-N σ-bonds between the metal centres and tetrazolate anions or tetrazoles.[28] In principle, all four nitrogen atoms in the tetrazole ring can act as coordination sites. The nature and position of the substituent on the ring determines its electronic and steric properties, which in turn determines the coordination site.

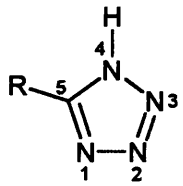

III

Molecular orbital calculations indicate N^1 and N^2 positions of the tetrazole ring (III) to be essentially equivalent electronically and energetically, with only a slight preference for N^1.[38] However, if the ring substituent is large and the coordination site crowded, steric factors favour N^2.[39,40] Several syntheses afford mixtures of N^1 and N^2 coordinated isomers.[41] It must be noted that N^1 and N^4 are energetically equivalent, as are N^2 and N^3.

For the purposes of a review of published crystallographically determined structures, metal derivatives of tetrazoles and tetrazolates have been broadly classified as tetrazole derivatives which exhibit 1) coordination through $N^1(N^4)$ 2) coordination through $N^2(N^3)$ 3) coordination through C^5 and 4) coordination through more than one nitrogen in the tetrazole ring. To date, complexes with a maximum of three coordinated nitrogens have been reported.[42] Individual examples for each of these categories are discussed in the subsequent sections.

1.4.1 Structural Variations Of Transition Metal Derivatives Of Tetrazoles And Tetrazolates

A wide variety of coordination modes of the tetrazole ring have been observed for transition metal derivatives of tetrazoles and tetrazolates and these are discussed in the following sections. To date no tetrazole complexes have been reported for scandium, titanium, and vanadium groups.

1.4.1.1 Coordination through $N^1(N^4)$

Monodentate coordination of 1-substituted tetrazoles is believed to take place through the $N^1(N^4)$ position. In this bonding model, this most basic of the tetrazole nitrogen acts as a donor through a charge-transfer σ-type bond. N^1 coordination has indeed been reported by Guilard *et al* in the crystal structure of (5-methyltetrazolato)-(2,3,7,8,12,13,17,18-octaethylporphyrinato)-iron(III) (Fig.1.3).[43] Analysis of the crystal structure reveals that the metal atom lies 0.412(2)Å above the plane of the four porphyrin nitrogens. The small methyl group at the 5-position of the tetrazolato ring enables

coordination to the metal centre to occur through N^1. This is consistent with the discussion in Section 1.4.

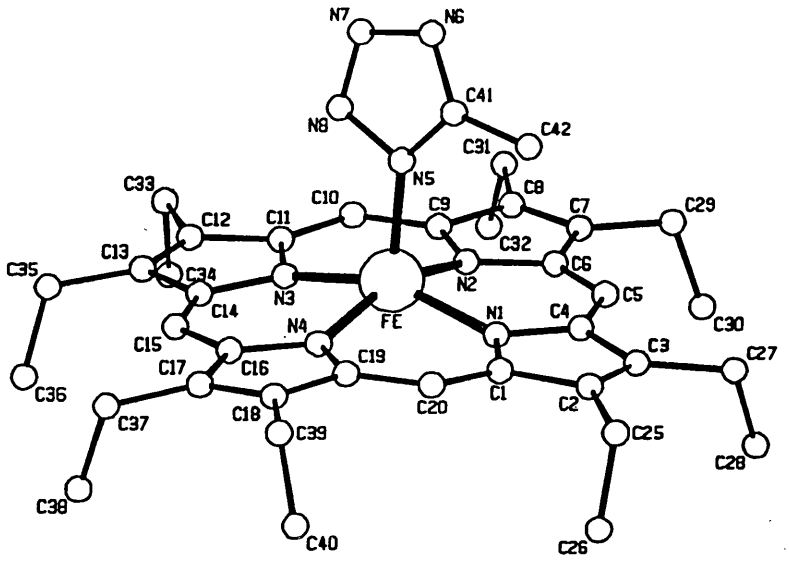

Fig.1.3

1.4.1.2 Coordination through $N^2(N^3)$

An example of a sterically driven tetrazolate complex is that of [Pd(L)($N_4CC_6H_4OMe$-3] (HL = methyl 2-(((2-diethylamino)ethyl)amino)cyclopent-1-enedithiocarboxylate) (Fig. 1.4).[44] The Pd atom sits in a distorted square-planar environment provided by the N_2S donor set of the complimentary ligand and by the N^2 nitrogen of the tetrazole. The bulky C_6H_4OMe-3 substituent on the tetrazole ring carbon makes the N^1 coordination site crowded. Steric factors, thus, result in coordination of the tetrazole ring to the metal centre through N^2.

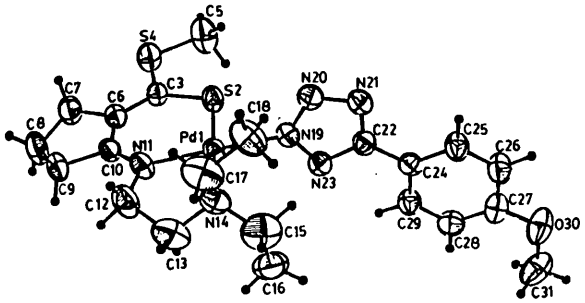

Fig. 1.4

1.4.1.3 Coordination through carbon

The existence of a unique tetrazolato metal complex with a metal-carbon σ-bonded covalent linkage has been provided by the X-ray crystal structure of $[As(C_6H_5)_4]^+[Au(CN_4R)_4]^-$, where R = *i*-$C_3H_7$ (Fig. 1.5).[44] The sterically most favourable geometry is provided by the four Au-C σ-bonded tetrazole rings being in an almost perpendicular alignment with respect to the central AuC_4 plane. Coordination occurs through carbon instead of nitrogen, probably due to the soft nature of the Au(III) ion.

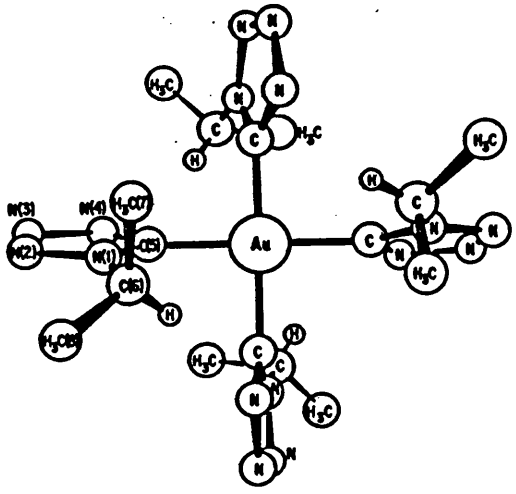

Fig. 1.5

1.4.1.4 Mixed coordination

The ability of each of the nitrogen atoms in the tetrazole ring to act as coordination sites allows the formation of complexes containing bidentate and even tridentate tetrazoles. A considerable number of complexes have been characterised involving various permutations and combinations of the four coordination sites (see Table 1.1). For bidentate complexes, the most common combination is the N^1 + N^3 coordination mode, presumably as the least sterically demanding combination of ligating atoms. Other coordination modes observed in bidentate tetrazoles are N^1 + N^4 and N^2 + N^3 (see Table 1.1). An example of a complex exhibiting the N^1 + N^3 coordination mode is that of $[Ni(Me(H)CN_4)_6](BF_4)_2$[46] (Fig.1.6). Analysis of the crystal structure revealed a perfect NiN_6 core with the six $Me(H)CN_4$ ligands arranged in an octahedral arrangement around the metal centre. Coordination of the tetrazole to the metal takes place via N^1 while the methyl substituent is on N^3.

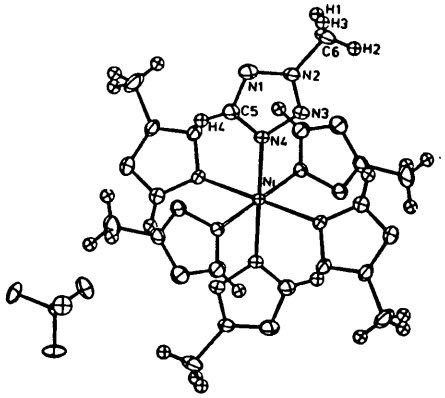

Fig. 1.6

In all of the tridentate complexes characterised to date, the N^1 + N^2 + N^4 coordination mode has been observed. This is typified by the structure of a tridentate tetrazolate complex, $[Rh_3(\mu_3\text{-}CN_4)(\mu\text{-}Cl)Cl(CO)_6]$, reported by Oro *et al* (Fig.1.7).[42] Each of the three rhodium atoms is in a distorted square-planar environment and is linked to a

nitrogen of the bridging tetrazole. The tetrazole is coordinated to the metal centres via the N^1, N^2 and N^4 coordination sites.

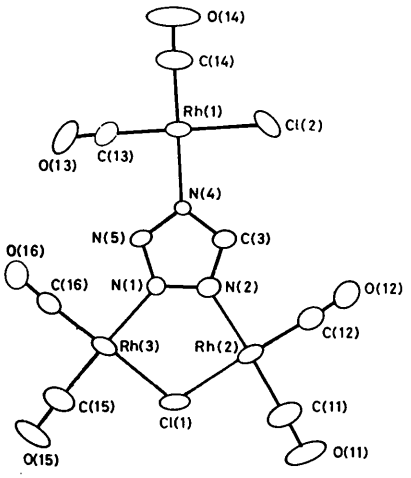

Fig.1.7

1.4.2 Structural Variations Of Main Group Derivatives Of Tetrazoles

A characteristic feature of the known main group derivatives of tetrazoles is the formation of supramolecular arrays. This is made possible by the multidentate nature of the tetrazole moiety combined with the availability of various combination modes, e.g. N^1 + N^3, N^2 + N^3, N^1 + N^4. Formation of supramolecular arrays is especially a feature of organotin-substituted tetrazoles due to the tendency of tin to attain a trigonal bipyramidal geometry (as discussed later in Section *1.4.2.3*).

1.4.2.1 Groups 1 and 2

The crystal structure of sodium tetrazolate monohydrate is the only structure reported in the literature for elements of these two Groups.[47] Analysis of the structure reveals an infinite chain of water molecules and tetrazolate ions (Fig. 1.8). Layers of water molecules are hydrogen-bonded to tetrazolate ions and are separated by the positive

sodium ion. The water molecule forms hydrogen bonds to two tetrazolate ions in the same layer. The chains are linked by Van der Waals contact between the hydrogen on the carbon of one ring and the two N^2 atoms of the tetrazolate ion.

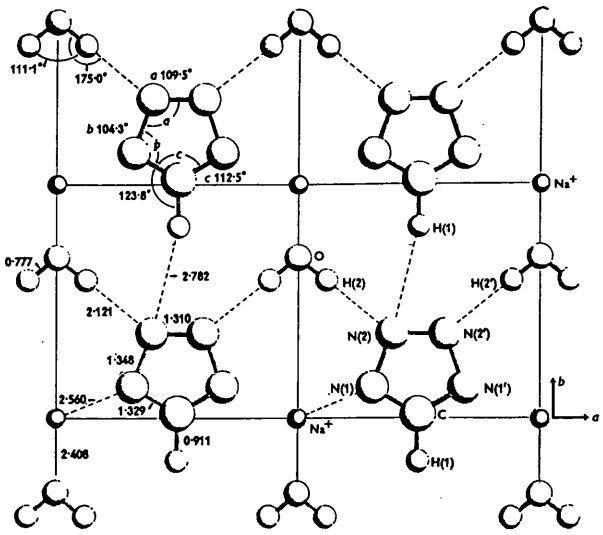

Fig. 1.8

1.4.2.2 Group 13

In this group, boron and indium are the only two elements whose tetrazole derivatives have been crystallographically characterised.

An interesting modification of the scorpionate, or poly(pyrazolyl)borate ligand, is obtained by substituting the pyrazolyl moiety with tetrazolyl.[48] This gives rise to ambidentate tetrazolyl-borate anions $[H_2B(CHN_4)_2]^-$ **(XIV)** with multiple bonding centres. The introduction of additional donor sites in the scorpionate ligand results in a supramolecular architecture in the solid-state with the formation of two-dimensional rhombic grid sheets (Fig.1.9).

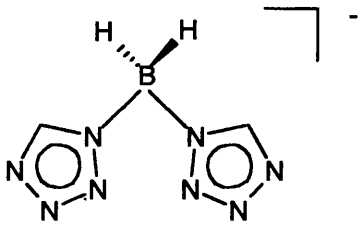

XIV

The potassium salt of the dihydrobis(tetrazolyl)borate anion reacts with MCl_2 [M = Mn(II), Co(II), Cd(II)], $Fe(II)SO_4$, and $Zn(II)(CH_3COO)_2$ in water to form diaquabis[μ-dihydrobis-(tetrazolyl)borate]metal(II) complexes (equation 1.9).

$$MX_2 + 2K[H_2B(CHN_4)_2] \longrightarrow \{[M(H_2O)_2\{H_2B(CHN_4)_2\}_2].2H_2O\} + 2KX \quad \text{Eq.1.9}$$

The crystal structures of these complexes exhibit two-dimensional coordination polymerisation (Fig. 1.9). The metal centres are octahedrally coordinated with the octahedral polyhedron being formed using four nitrogen atoms from the two bis(tetrazolyl)borate ligands and two *trans*-coordinated water molecules. The dihydrobis(tetrazolyl)borate ligand forms bridges between the metal atom and the boron atom. Typically N^1 of the tetrazole ring is bonded to the boron and N^4 is bonded to the metal centre. The rhombohedral openings in the coordination polymer are filled with two water molecules of crystallization, which hydrogen bond to the N^3 atoms of the tetrazolyl rings and to the metal-coordinated water ligands. Thus, this is an example of a complex where three of the four available nitrogens on the tetrazole ring are coordinated. The aqua ligand hydrogen bonds with the two adjacent water molecules of crystallization giving rise to one-dimensional chains of water molecules which run parallel to the two-dimensional metal-ligand grid sheets (Fig. 1.10).

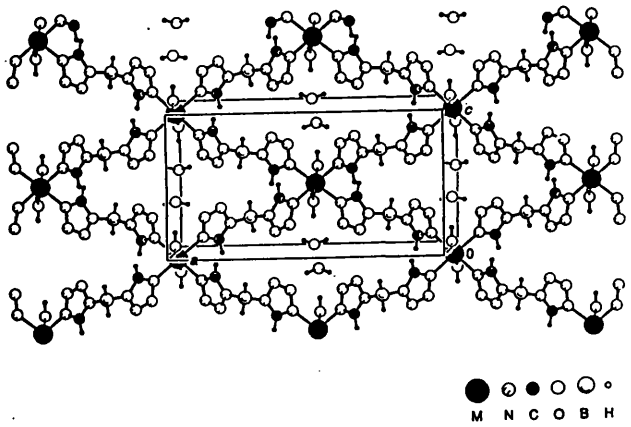

Fig.1.9

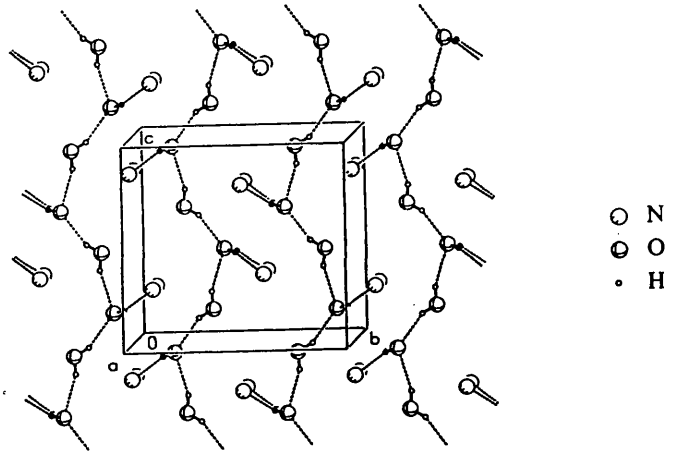

Fig. 1.10

The biological interest of the metal-nitrogen bond led Guilard *et al* to investigate the reactivity of a series of metalloporphyrins with an axial azide ligand.[49] The first investigation performed was the 1,3 dipolar cycloaddition of an azido-(octaethylporphinato)indium(III) with organic nitriles (e.g. PhCN or MeCN). These

reactions lead to two isomers (**XV** and **XVI**) in which indium is coordinated to either N^1 or N^2.

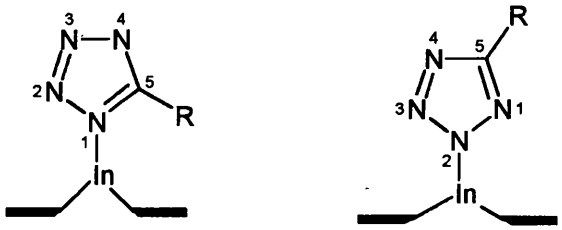

XV **XVI**

Crystal structures of (octaethylporphyrin)In[$N_4C(C_6H_5)$] and (octaethylporphyrin)In[$N_4C(CH_3)$] were obtained (Figs. 1.11 and 1.12 respectively). The phenyl group of the former is located on the N^2 of the tetrazole ring, while the methyl group of the latter is on the N^1. These results are consistent with the discussion in Section 1.4 and confirm that in a one-substituted tetrazole ring, N^1 position is the most nucleophilic of the nitrogen positions. However, presence of bulky groups favours N^2 coordination due to the steric congestion associated with the N^1 coordination site.

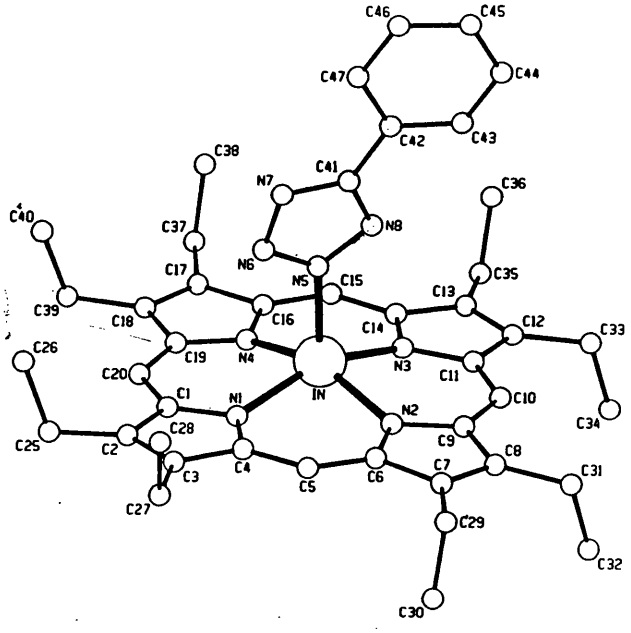

Fig. 1.11

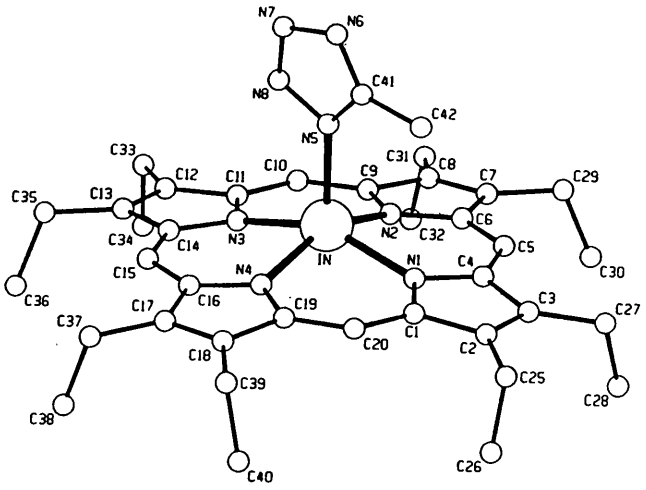

Fig. 1.12

1.4.2.3 Group 14

Crystallographic characterisation of organosilicon and organotin tetrazoles have been reported in the literature.

Eaborn *et al* have reported an organosilicon tetrazole, where the silicon centre of a bulky silyl group is bonded to the N^2 position of the tetrazole.[50] This compound was prepared by reacting the iodide $(Me_2PhSi)_3CSiMe_2I$ with MeCN in the presence of NaN_3 and its structure was determined by X-ray diffraction (Fig.1.13). Two isomers involving coordination through N^1 and N^2 nitrogens of the tetrazole respectively (analogous to **IIIa** and **IIIb**) of the product $(PhMeSi)_3CSiMe_2N$-N=C(Me)-N=N (**XVII**) are possible although the latter is likely to be preferred due to reduced steric hindrance. The crystal structure unambiguously confirmed this expectation. However, no reliable parameters could be obtained for the heterocyclic ring system, due to the similarity between the space-filling properties of the 5-methyltetrazolyl and phenyl groups, which gives rise to 50-50 disorder involving the heterocyclic and the phenyl groups.

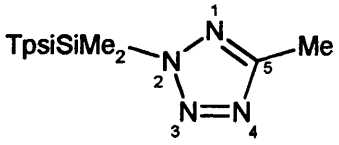

Tpsi = $(PhMe_2Si)_3C$

XVII

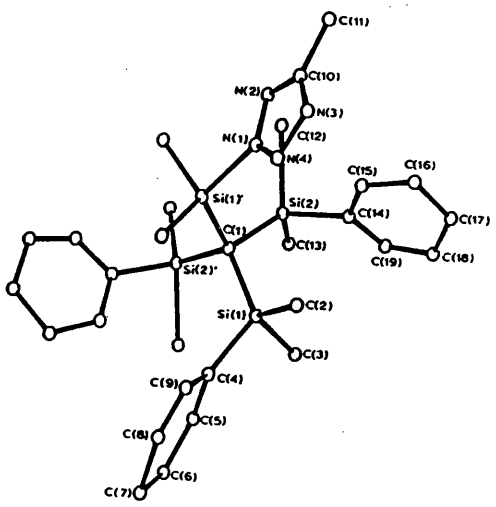

Fig. 1.13

Cycloadditions reactions of organotin azides with organonitriles and organoisothiocyanates as dipolarophiles have been used to synthesise a series of organotin-substituted heterocycles. These reactions were first reported by Dunn and Oldfield.[51] The structural chemistry of organotin tetrazoles produced by the cycloaddition of organotin azide with organonitriles has been extensively investigated by Molloy *et al.*[18,19,52,53] The central *trans*-N_2SnC_3 unit with a near-linear N-Sn-N component is a consistent feature of crystal structures of organotin tetrazoles. This tendency of tin to attain a trigonal bipyramidal geometry coupled with the multidentate nature of the tetrazoles and the need to arrange the organo-(alkyl and phenyl) groups on the tin within the lattice leads to the formation of two- or three- dimensional supramolecular arrays.

The crystal structure of 1,2-phenylene-bis-5,5'-(tributylstannyltetrazole) is described below as an example.[18] The asymmetric unit (Fig. 1.14) consists of two unique 1,2-phenylene substituted bis(tetrazole) ligands and four tri-n-butyltin centres. Each tin centre adopts the *trans*-trigonal bipyramidal N_2SnC_3 geometry. This is a structure which comprises of bidentate tetrazole rings involving the N^1 and N^2 coordination modes. Each tin is axially bound to two nitrogen atoms, one from the N^1 of a tetrazole ring and the other from the N^2 position of a second tetrazole from an alternative bis(tetrazole) ligand within the asymmetric unit.

The supramolecular structure consists of a three-dimensional array (Fig.1.15). Propagation along the *b* axis is achieved via N(2)-Sn(1)-N(12) and N(4)-Sn(3)-N(10) linkages resulting in a zigzag polymer consisting of a single tetrazole ring of each bis(tetrazole) ligand linked through its N^1 and N^3 centres by tributyltin units. A similar polymer propagation takes place along the *c* axis via N(5)-Sn(2)-N(13) and N(7)-Sn(4)-N(15) linkages involving the tetrazole rings not involved in propagation along the *b* axis. The net result of these two interactions is the formation of a two-dimensional sheets bearing pseudo-four-fold symmetry parallel to the *bc*-plane. These sheets are intermoleculary linked along the *a* axis by bridges comprising of the two complete phenyl-bridged bis(tetrazole) ligands. Typically bridges comprise of N(12)-Sn(1)-N(2) and N(13)-Sn(2)-N(5) linkages. The overall effect of all these interactions is a three-dimensional framework as shown in Fig.1.15, where coordination along *a* arranges the sheets lying in the *bc* plane above each other to form channels which run throughout the lattice. The large cavities in this open framework are, however, filled with butyl groups attached to the tin.

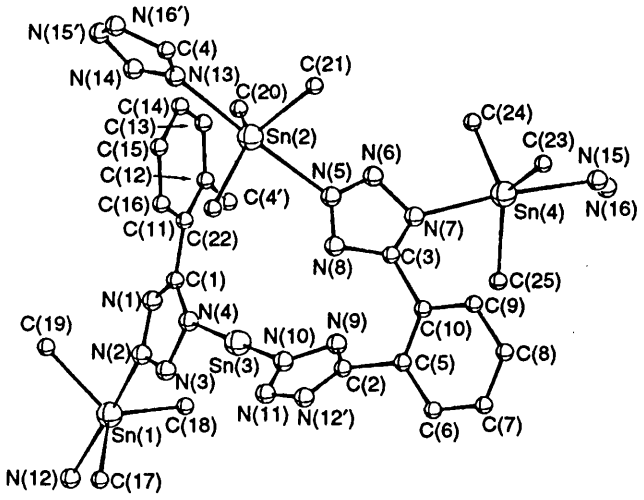

Fig.1.14

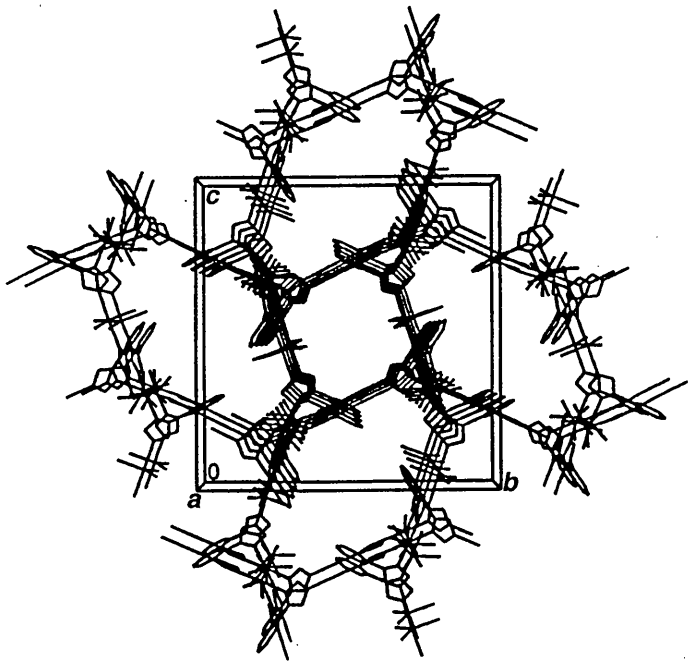

Fig.1.15

Table 1.1 summarises the various coordination modes exhibited by a selected number of crystallographically characterised tetrazole and tetrazolate complexes.

Table 1.1: Summary of coordination modes of crystallographically characterised tetrazole and tetrazolate complexes

Coordination through $N^1(N^4)$	**Ref**
[octaethylporphyrin]Fe[$N_4C(Me)$]	43
Bis-[dimethyl-(phenyl)-phosphine]-bis-(5-methyl-tetrazolato)-palladium(II)	54
[octaethylporphyrin]In[$N_4C(CH_3)$]	49
[octaethylporphyrin]In[$N_4C(C_2H_5)$]	49
Coordination through $N^2(N^3)$	
$[Co(5\text{-}CN\text{-}CN_4)(NH_3)_5](ClO_4)_2$	55
[Pd(L)($N_4CC_6H_4OMe$] [a]	44
[octaethylporphyrin]In[$N_4C(CMe_3)$]	49
[octaethylporphyrin]In[$N_4C(C_6H_5)$]	49
$(PhMe_2Si)_3CSiMe_3N\text{-}N{=}C(Me)\text{-}N{=}N$	50
Coordination through C^5	
$[As(C_6H_5)_4][Au(CN_4Pr^i)_4]$	45
Mixed Coordination ($N^1 + N^4$)	
$ZnCl_2(1\text{-}Me\text{-}CN_4H)_2$	56
$[Ag(NO_3)(1,5\text{-pmtta})_2]_2$	57
$[Fe(CHN_4C_3H_7)_6][BF_4]_2$	58
$[Fe(CHN_4CH_3)_6][BF_4]_2$	58
$1,6\text{-}[2\text{-}(Bu_3Sn)N_4C]_2[CH_2]_6$	19

Table 1.1: Summary of coordination modes of crystallographically characterised tetrazole and tetrazolate complexes (contd.)

Mixed Coordination ($N^2 + N^3$)	
$[Mn_2(CO)_6(N_4CCF_3)_3]^-$	59
Mixed Coordination ($N^1 + N^3$) / ($N^2 + N^4$)	
$[Ni(2\text{-}Me\text{-}CN_4H)_6](BF_4)_2$	46
$1,6\text{-}[2\text{-}(Bu_3Sn)N_4C]_2(CH_2)_6$	19
$1,3\text{-}C_6H_4\text{-}bis\text{-}[CN_4(SnBu_3)]_2.2MeOH$	18
$1,2\text{-}C_6H_4\text{-}bis\text{-}[CN_4(SnEt_3)]_2$	18
$1,2\text{-}C_6H_4\text{-}bis\text{-}[CN_4(SnBu_3)]_2$	18
$1,3,5\text{-}C_6H_3\text{-}[5\text{-}CN_4(SnBu_3)]_3$	52
Mixed Coordination ($N^1 + N^2$) / ($N^3 + N^4$)	
No examples	
Mixed Coordination ($N^1 + N^2 + N^4$)	
$[Rh_3(\mu_3\text{–}CN_4)(\mu\text{–}Cl)Cl(cod)_2(CO)_2]$	42
$[Rh_3(\mu_3\text{–}CN_4)(\mu\text{–}Cl)Cl(CO)_6]$	42
$[Ag(NO_3)(1,5\text{-}pmtta)_2]_2$	57
$\{M[H_2B(CHN_4)_2]_2(H_2O)_2\}.(H_2O)_2$	48
Mixed Coordination ($N^1 + N^2 + N^3 + N^4$)	
No examples	

[a] HL = 2-{[(2-di-ethyl-amino)-ethyl]-amino}cyclopent-1-ene dithiocarboxylate

1.5 SPECTROSCOPY

An overview of the main spectroscopic techniques used in this thesis are described in this section.

1.5.1 Mössbauer Spectroscopy

Mössbauer spectroscopy is, perhaps, more aptly described as nuclear gamma resonance spectroscopy as the effect being observed is the emission and absorption of γ-rays by the nuclei of certain elements.

Extensive reviews[60,61,62,63] and books[64,65,66,67,68] have been written about the basic principles and theory behind ^{119m}Sn Mössbauer spectroscopy. Only a brief summary involving the practical processes is given here. The Mössbauer effect for tin is observed when the source, the metastable ^{119m}Sn isotope, emits a 23.875 keV γ-ray and excites another ^{119}Sn nucleus to its first excited state. The exciting radiation is strictly monochromatic as γ-rays have quantized energies. The energy, E, perceived by the sample is modulated by the Doppler effect by mounting the source on a vibrator and applying to it a controlled velocity. The energy scale, therefore, is expressed in units of mms^{-1}.

The sample must be in the solid state to prevent nuclei from recoiling when they absorb γ-radiation. In practice, even in a solid, only a fraction of nuclei do not suffer recoil and it is this fraction which gives rise to the observed spectrum. The recoil-free fraction is usually denoted as the f-factor and it is this property which determines the amount of sample required for a Mössbauer experiment. For a low γ energy nucleus like ^{119}Sn (23.8 keV), recoil effects are small and only small amounts of material are required. The recoil free fraction also increases with decreasing temperature. For this reason, ^{119}Sn Mössbauer samples are routinely cooled to liquid N_2 temperatures.

The two most important Mössbauer parameters are isomer shift, δ (mms^{-1}), and quadrupole splitting, ΔEq (mms^{-1}), with δ usually denoted relative to SnO_2 or $BaSnO_3$ as 0.00 mms^{-1}.

Isomer shift represents the displacement of the resonance from zero velocity. There are two compounds involved in a Mössbauer experiment- the emitter (source) and the absorber. When the two are identical, the isomer shift is 0. When the compounds are different, the isomer shift represents the mismatch between the two sets of nuclear levels arising from the interaction of the two nuclei with their electronic environments (Fig. 1.16). Thus, it follows that differing isomer shifts correspond to differing chemical environments. This is due to changes in the electron density of the valence *5s* electrons, which have a finite probability of existing at the nucleus. This results in the isomer shifts of Sn(II) and Sn(IV) compounds falling into characteristic ranges. Sn(IV) compounds appear between -0.5 and 2.7 mms^{-1} while Sn(II) compounds have higher isomer shifts (above 2.10 mms^{-1}). This is because of increased electron density in the case of the latter compounds due to the availability of the *5s* lone pair of electrons on the Sn.

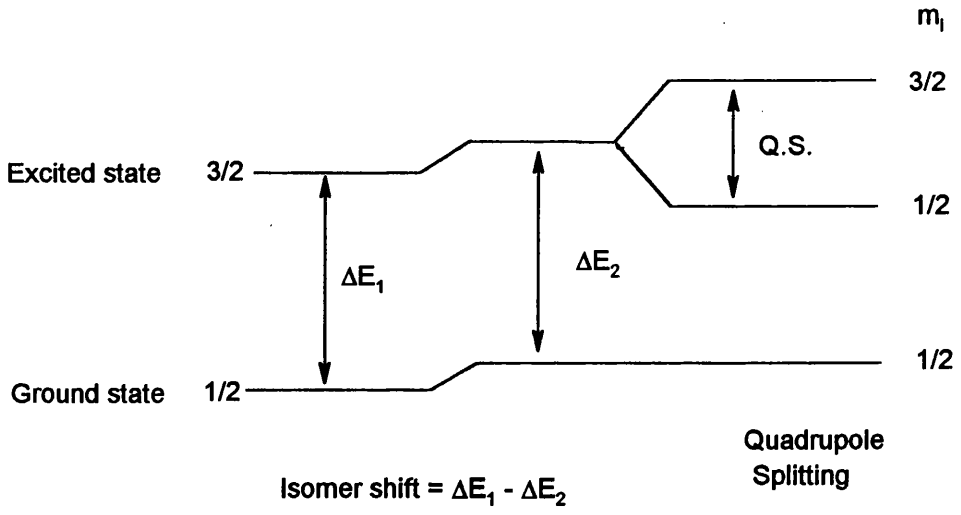

Fig. 1.16: The origin of isomer shift and quadrupole splitting[60]

For tetrahedral sp^3 hybridised organotin(IV) compounds, the isomer shift will be affected by the nature of the ligands as this affects the environment of tin. The following

Table illustrates how δ varies with the inductive effect of R.[60,61] As the organic ligand becomes more electron donating, the value of δ increases.

Table 1.2: Variation of δ with organic ligands coordinated to tin

R	R_4Sn, δ (mm sec^{-1})	R_3SnCl, δ (mms^{-1})
Me	1.29	1.43
Et	1.31	1.62
Pr	1.30	1.62
Bu	1.35	1.65

Electron withdrawing groups attached to tin result in decreasing the value of δ. For a series of iso-organyl R_3SnL compounds, δ decreases as the electronegativity of L increases due to the reduction of electron density on tin. This is illustrated in Table 1.3.[60,61]

Table 1.3: Variation of δ with L for a series of iso-organyl compounds

L	Et_3SnL, δ (mm sec^{-1})	Bu_3SnL, δ (mms^{-1})
F	1.46	1.31
Cl	1.55	1.38
Br	1.62	1.48
I	1.70	1.52

Quadrupole splitting is the second most important Mössbauer parameter and it arises from the asymmetry of the electron cloud around the nucleus. A zero field gradient is obtained for cubic symmetry (tetrahedral or octahedral arrangement of attached atoms), e.g. Bu_4Sn gives rise to a single line. However, an electric field gradient is generated at the nucleus by an asymmetric arrangement of ligands or by a coordination sphere of lower symmetry e.g. trigonal bipyramidal. In the case of ^{119}Sn, this results in the lifting of degeneracy of the quadrupolar first excited spin 3/2 state and produces a characteristic two line spectrum. Quadrupole splitting (ΔEq) is the energy difference between the two transitions and δ is measured as the centroid of the two peaks relative to the source. ΔEq gives valuable information about the stereochemistry of organotin compounds as it falls in characteristic ranges for specific ligand configurations of di-and tri-organotin compounds (Table 1.4).[67,69]

Table 1.4: Quadrupole splitting ranges (mms^{-1}) for organotin (IV) compounds

Geometry	$RSnX_3$	R_2SnX_2	R_3SnX
Tetrahedral	1.3-2.1	2.1-2.4	1.5-2.8
cis-Trigonal bipyramidal	1.6-2.4	2.9-3.7	1.7-2.2
trans-Trigonal bipyramidal			3.0-4.0
cis-Octahedral	1.6-2.4	1.7-2.2	
trans-Octahedral		3.5-4.2	

1.5.2 ^{119}Sn AND ^{207}Pb NMR SPECTROSCOPY

Elemental tin has ten isotopes of which only three - ^{115}Sn (abundance = 0.34%, relative sensitivity[a] = 0.069), ^{117}Sn (abundance = 7.61%, relative sensitivity = 2.0×10^1),

[a] Sensitivity is quoted relative to carbon

^{119}Sn (abundance = 8.56%, relative sensitivity = 2.5×10^1) - have spin of 1/2 and are therefore NMR active. The selected nucleus for NMR is usually ^{119}Sn due to its superior receptivity. Several reviews[67,68,74,75] and books[70,71,72,73] have been written covering the theoretical and practical aspects of ^{119}Sn NMR spectroscopy. Chemical shifts for ^{119}Sn cover a range of greater than ± 600 ppm and are quoted with reference to Me_4Sn as 0 ppm. The values for chemical shifts are dependent on a number of structure and solvent dependent factors and therefore give valuable information about the composition of the compound in question.

Elemental lead contains sixteen isotopes of which only ^{207}Pb is NMR active. Lead-207 has a nuclear spin of 1/2, a natural abundance of 23%, and relative sensitivity of 1.18×10^1 that of a proton.[74,75] However, despite the favourable NMR properties of this nuclide, only a small amount of work has been done on it.[74,75] Tetramethyl lead is the accepted standard for ^{207}Pb NMR chemical shifts, values of which are spread over a range of ±5000 ppm. Changes in non-coordinating solvent and temperature have little effect over Group IV chemical shifts in comparison with the overall chemical shift ranges. These effects are greatest for lead and least for silicon.[75]

The lead nucleus is more sensitive to changes in its substituents than tin and this can be attributed to its greater polarisability. Otherwise, the factors that control shielding of tin seem to control shielding of lead as well. A plot of $\delta(^{207}Pb)$ against $\delta(^{119}Sn)$ in analogous compounds show a marked correlation as shown in Fig.1.17.

Electron withdrawing groups decrease the ^{119}Sn shielding and give higher frequency resonances. However, whilst replacement of one R group in R_4Sn by an electron withdrawing X group will decrease ^{119}Sn shielding, the trend will be reversed by further replacement. This behaviour is most extreme when X is bulky and polarisable, e.g. I. However, the causes for this effect have not yet been determined. The following figure illustrates the effect on ^{119}Sn chemical shifts by progressive substitution of R by X in various $R_{4-n}SnX_n$ compounds.[68]

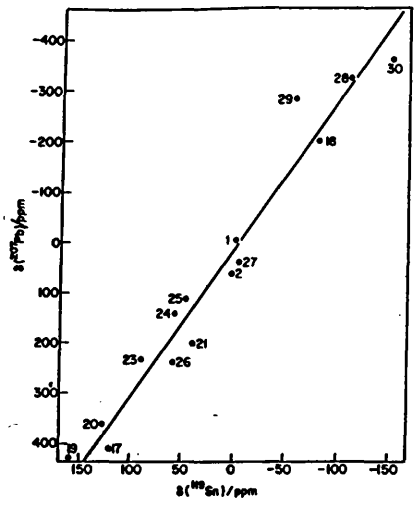

Fig.1.17

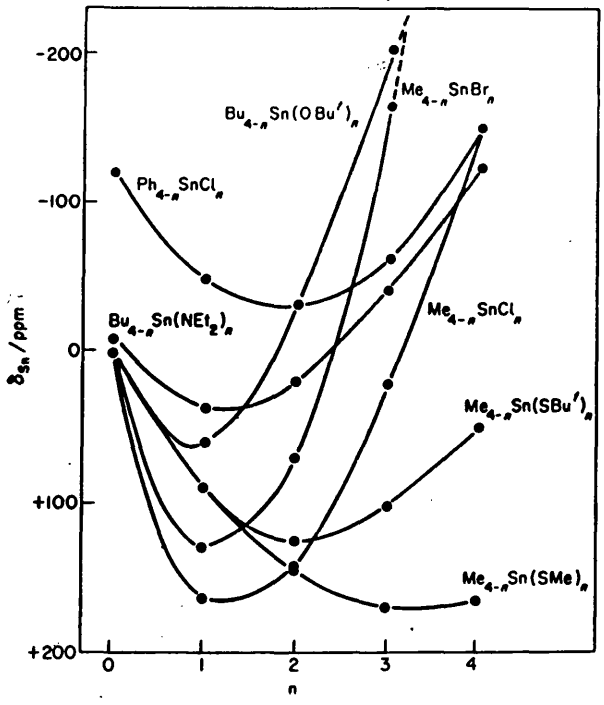

Fig. 1.18

Electron releasing groups increase ^{119}Sn shielding and give lower frequency resonances as shown in Table 1.5.[73] In the case of the phenyl group, however, its electron withdrawing nature would be expected to result in more downfield chemical shifts. In reality, this does not happen and this is due to the increased polarisability of the phenyl ring.

Table 1.5: ^{119}Sn chemical shifts (ppm) of alkyl and phenyl-tin chlorides

R	$RSnCl_3$	R_2SnCl_2	R_3SnCl
Me	+20	+141	+164
Et	+6.5	+126	+155
^{n}Bu	+6.0	+122	+141
Ph	-63	-32	-48

Electron withdrawing substituents decrease lead shielding (Table 1.6)[74] while bulky substituents in most cases increase it (Table 1.7)[74]. An exception to the latter rule is observed by substitution of Sn by Pb in passing from $Me_3PbSnMe_3$ to $Me_3PbPbMe_3$. This has been attributed to the non-availability of electrons in orbitals of suitable symmetry to form π-bonds with Sn.[74] As in the case of ^{119}Sn, progressive substitution of R by an electron withdrawing group X in $R_{4-n}SnX_n$ compounds produces U-shaped plots of δ (^{207}Pb) against n.[75]

Table 1.6: Effect of electron withdrawing substituents on lead shielding

Compound	δ (^{207}Pb) (Hz)
Me_3PbCl	432
Me_3PbBr	367
Me_3PbI	203

Table 1.7: Effect of bulky substituents on lead shielding

Compound	δ (^{207}Pb) (Hz)
Me_3PbCl	432
Me_3PbSMe	239
Me_3PbSBu^t	161
$Me_3PbSeMe$	98
$Me_3PbSnMe_3$	-324
$Me_3PbPbMe_3$	-281

A second substituent effect is the interbond angle at the tin. In compounds where tin is part of a ring system, reduction of the cyclic interbond angles at the metal in the five-membered rings gives reduced shielding. For instance, introduction of S in the five-membered ring in **XIX** reduces the shielding of Sn dramatically compared to **XVIII**.[74]

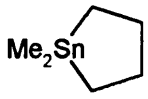

XVIII

$\delta(^{119}Sn) = +54$ ppm

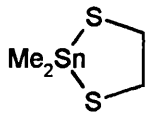

XIX

$\delta(^{119}Sn) = +190$ ppm

Enlargement of interbond angles in six-membered rings increases the shielding. For example, in **XX** where Sn is part of a six-membered ring, it is more shielded than **XVIII**.[74s]

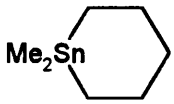

XX

$\delta(^{119}Sn) = -43$ ppm

As in the case of tin, reduction of cyclic interbond angles at the lead centre reduces shielding while enlargement in six-membered rings increase shielding.[75]

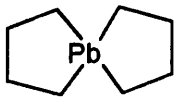

$\delta\ (^{207}Pb) = +416$ ppm

XXI

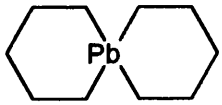

$\delta(^{207}Pb) = -200$ ppm

XXII

Changes in coordination number also have a dramatic influence on the ^{119}Sn chemical shifts. In general, increase in the coordination number from 4 to 5 leads to increase in tin shielding of 150 ppm. This effect can be explained by increased electron density on the tin due to occupancy of the *5d* orbitals and increased π-bonding.

Normally, solvent and concentration only affect the chemical shift by a few ppm. Thus, results obtained in benzene, carbon tetrachloride, chloroform, or dichloromethane are comparable with those obtained on neat liquids. However, donor solvents, e.g. dimethyl sulfoxide, pyridine, and acetone can form *in situ* adducts with the tin compounds and affect the chemical shifts. For instance, chemical shift of a saturated solution of Me_2SnCl_2 in DMSO (-246 ppm) is almost 400 ppm to low frequency of that in CH_2Cl_2 or CCl_4 and probably corresponds to the six coordinate octahedral complex $Me_2SnCl_2.2DMSO$ (**XXIII**).[73]

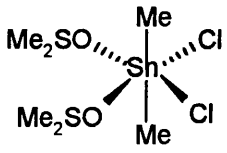

XXIII

Tin compounds which form associated polymeric species in the solid-state auto-associate in the solution state. Auto-association causes changes in coordination number and therefore, changes in chemical shifts. A chemical shift-concentration study of trimethyltin formate in $CDCl_3$ solution revealed a dramatic shift from +2.5 ppm for a 3M solution to +152 ppm on dilution to 0.05M in the same solvent (equilibrium 1.2).[73] This phenomenon has been explained by the self-association of monomeric tetrahedral trimethyltin formate molecules in more concentrated solutions to yield the five-coordinate oligomeric species known in the solid-state.

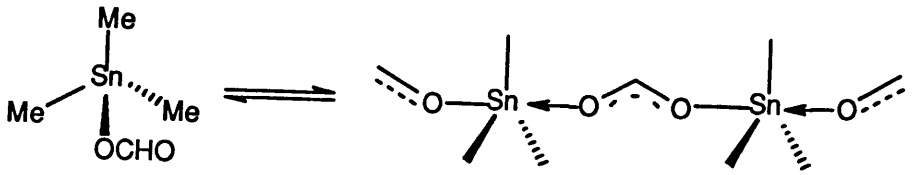

Equilibrium 1.2

Coordination number also has an important effect on shielding of the ^{207}Pb nucleus and is confirmed by solvent studies. Addition of ligands DMSO or HMPT to solutions of Me_3PbBr or Me_3PbCl in CH_2Cl_2 produces increases in shielding of upto 270 ppm, which can be attributed to the formation of species containing five-coordinate lead.[74]

A wealth of information is available for coupling constants between ^{119}Sn and other nuclei [$^{n}J(Sn,X)$, n = 1-4], particularly when X = C or H.[73,74,75]

Coupling constants are related by the Fermi contact term and therefore reflect the amount of *s* electron density in a Sn-C bond. This can lead to important inferences about the valence electron distribution and structure and bonding of the compound in question. This is illustrated in the following series of compounds (Table 1.8).[74] With progressive replacement of Me by Cl, the $^{2}J(^{119}Sn\text{-}^{1}H)$ increases due to the increased *s* electron density in the remaining Sn-C bonds with concomitant increase in *p* character in the bonds to chlorine. The $^{1}J(^{119}Sn\text{-}^{13}C)$ and $^{2}J(^{119}Sn\text{-}^{1}H)$ are, therefore, proportional to the amount of *s* electron density in the Sn-C bond.

Table 1.8: $^{2}J(^{119}Sn\text{-}^{1}H)$ for a series of Me_nSnCl_{4-n} compounds

Compound	$^{2}J(^{119}Sn\text{-}^{1}H)$
Me_4Sn	54.7 Hz
Me_3SnCl	58.2 Hz
Me_2SnCl_2	68.9 Hz
$MeSnCl_3$	96.9 Hz

The $^{1}J(^{119}Sn\text{-}^{13}C)$ and $^{2}J(^{119}Sn\text{-}^{1}H)$ are related quantitatively to CSnC bond angles in Me- and Bu-Sn(IV) compounds. For butyltin(IV) compounds[76,77], the linear relationship is:-

$$|^{1}J(^{119}Sn\text{-}^{13}C)| = (9.99 \pm 0.73)\theta - (746 \pm 100)$$

For Me(IV)Sn compounds $^{2}J(^{119}Sn\text{-}^{1}H)$ and θ are related by[78] :-

$$\theta = 0.0161|^{2}J(^{119}Sn\text{-}^{1}H)|^{2} - 1.32|^{2}J(^{119}Sn\text{-}^{1}H)| + 133.4$$

The importance of the values of coupling constants between tin and carbon is highlighted by the fact that they fall into characteristic ranges for specified coordination numbers and geometries. Examples for triphenyltin[79] and tributyltin[76] compounds are given in the following Table.

Table 1.9: $^{1}J(^{119}Sn\text{-}^{13}C)$ values (Hz) for R_3SnX compounds

Structure	R = Bu; $^{1}J(^{119}Sn\text{-}^{13}C)$ (Hz)	R = Ph; $^{1}J(^{119}Sn\text{-}^{13}C)$ (Hz)
monomeric R_3SnX	320-390	550-660
cis-trigonal bipyramidal	350-395	600-660
trans-trigonal bipyramidal	440-510	750-850

There is very little information available about coupling constants between lead and nuclei other than proton. Results to date available for $^{1}J(^{207}Pb, X)$ strongly suggest against drawing close parallels between tin and lead as illustrated in Table 1.10.[74] There are more similarities between tin and lead when $^{2}J(^{207}Pb, H)$ and $^{3}J(^{207}Pb, H)$ couplings in alkyl lead compounds are concerned (Table 1.10). The lead couplings are 20-50% larger than the analogous tin ones but opposite in sign as $\gamma(^{207}Pb)$ is positive. Couplings to lead over more than three bonds have been studied very little but the relevant ^{207}Pb satellites can be easily detected. For instance, $^{4}J(^{207}Pb, H) = 5.3 \pm 0.1$ Hz in $(Me_3CCH_2)_4Pb$ and $^{4}J(^{207}Pb, ^{13}C) = 20$ Hz in Ph_4Pb.[74]

Table 1.10: $^{n}J(^{207}Pb,X)$ and $^{n}J(^{119}Sn,X)$ for analogous organotin and organolead compounds (values in Hz).

Compound	$^{1}J_{PbC}$	$^{1}J_{SnC}$	$^{2}J_{PbH}$	$^{2}J_{SnH}$	$^{3}J_{PbH}$	$^{3}J_{SnH}$
Me_4M	250	-340	-60.5	54.3		
Et_4M		-307	-41	32.2	128.6	-71.2
Me_3MBr	246	-380	-68			
Me_2MCl_2		-566	-154.5	68.9		

1.5.3 Infrared Spectroscopy

IR spectroscopy is a useful tool in organotetrazole chemistry and has the dual purposes of providing a means of comparison between the product and starting material and also being able to identify the presence of functional groups in the product.

The main IR absorption bands assigned to tetrazoles are in the region of 1000-1100 cm^{-1} and between 1095-1120 cm^{-1}.[1] Other absorptions assigned to the ring have been observed in the ranges :- 1045-1085 cm^{-1}, and 1265-1298 cm^{-1}.

1.6 PREVIOUS WORK AND AIMS OF THIS THESIS

Compounds of the type $R_3Sn(CH_2)_nR^1$ (R^1 = tetrazolyl), were synthesized in this laboratory to enhance the aerobic and hydrolytic stability of potentially biocidal C-bonded triorganotin heterocycles.[80] In the synthesis of such compounds the established 1,3-dipolar cycloaddition of an organonitrile and a triorganotin azide was employed. Variable temperature and concentration ^{119}Sn and ^{13}C NMR experiments on related tin-substituted tetrazoles have revealed migratory behaviour of the tin around the tetrazole ring. This

cycloaddition chemistry was subsequently extended further to the syntheses of mono-, bis-, and tris-organotin tetrazoles.[24] A plethora of crystal structures of these compounds were obtained which revealed extensive multi-dimensional arrays.

The research described in this thesis seeks to expand the above work to the

- formation of organotin tetra-tetrazoles
- formation of functionalised organotin tetrazoles
- formation of organotin thio-tetrazoles and their use as precursors to other organometallic thio-tetrazoles
- formation of other organometallic tetrazoles e.g., lead, thallium

Each of these topics will be addressed in the following chapters.

Chapter 2

The Synthesis and Characterisation of Organotin-Substituted Tetra-tetrazoles

2.1 INTRODUCTION

Tin occurs in nature as oxides and sulphides. Tin has ten stable isotopes and many unstable isotopes with half-lives from 2.2 mins to ~10^5years.[68] Tin has an electronic configuration of [Kr]$5s^2 5p^2$ and therefore has two oxidation states (II and IV). The IV oxidation state is more stable than the II although the energy difference between the two states is quite small.[68] 'Organotin' compounds are derivatives of Sn(IV) and Sn(II) which contain the Sn-C bond. The applications, preparative methods and structural aspects of organotin chemistry have been covered in several reviews[81-84] and books[85-94].

Some important biocidal uses of organotin compounds are as fungicides for potato blight, leaf spot on sugar beet and celery, rice blast, coffee leaf rust[95-97] and as disinfectant in hospitals[98]. The major non-biocidal applications include the use of di- and mono-alkyltin compounds for the stabilisation of PVC[99-101] and in the chemical vapour deposition of thin surface films of SnO_2 on glass.[102,103]

2.1.1 Structural Chemistry Of Organotin-Substituted Tetrazoles

Table 2.1 summarises all the structures known to date of organotin-substituted tetrazoles, their coordination modes and the various lattice types associated with them. Organotin-substituted thio-tetrazoles will be dealt with in Chapter 6.

The trigonal bipyramidal *trans*-N_2SnC_3 geometry at the tin centre is universal in all triorganotin-substituted tetrazoles. The only exception is provided by 1,3-[C_6H_4-$(Bu_3SnCN_4)_2$].2MeOH where the methanol molecules are coordinated to the tin centres forming a *trans*-$NOSnC_3$ centre.

Table 2.1: Coordination Modes And Lattice Types Of Known Organotin-Substituted Tetrazoles With Respect To The Tin Centre

	Compound	Metal-Tetrazole Coordination with respect to Tin	Lattice Type
XXIV	2,3,4,5-tetraza-6-diphenylstannyl-[3,4]-bicyclonona-1,3-diene	Two N_2SnC_3: $N^1 + N^1$	Polymeric Chains[80]
XXV	1,3-phenylene-bis-5,5′-(tributylstannyltetrazole)Bis-methanolate	Two $NOSnC_3$	Two-dimensional planar sheet[24]
XXVI	1,2-phenylene-bis-5,5′-(triethylstannyltetrazole)	Two N_2SnC_3: $N^2 + N^2$, $N^1 + N^1$	Zigzagged two-dimensional sheets[24]
XXVII	1,2-phenylene-bis-5,5′-(tributylstannyltetrazole)	Four N_2SnC_3: $N^1 + N^2$	Three-dimensional array[24]
XXVIII	Tris-[2-(5-tributylstannyl-tetrazolyl)-ethyl]-nitromethane	Three N_2SnC_3: $N^1 + N^2$	Two-dimensional puckered sheet[24]
XXIX	1,3,5-phenylene-tris-5-(tributylstannyl)tetrazole	Three N_2SnC_3: $N^1 + N^2$	Two-dimensional planar sheet[24]

With respect to tin, the metal can coordinate to hindered (N^1/N^4) or more open nitrogens (N^2/N^3) on the tetrazole ring. In the compounds listed in Table 2.1, $N^1 + N^1$, $N^1 + N^2$ and $N^2 + N^2$ coordination modes of the tetrazole have been observed.

A variety of lattice types have been observed for **XXIV-XXIX**. The lattice types can be broadly classified into three categories.

a) **Polymeric Chains:** This is exhibited by **XXIV** and involves one-dimensional polymers running side by side (Fig.2.1).[80]

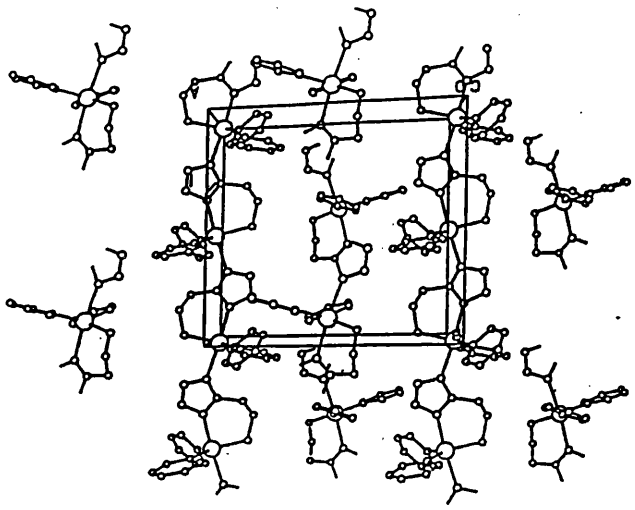

Fig.2.1: The molecular structure of **XXIV**

b) **Two-dimensional sheets:** This lattice type is exhibited by **XXV, XXVI, XXVIII** and **XXIX**. The sheets can be planar as in **XXV** and **XXIX** or puckered as in **XXVI** and **XXVIII**. In **XXV**, linear polymers along the *b*-axis are further held together by hydrogen bonds along the *a*-axis. In **XXIX**, the molecule is linked with its lattice neighbours to form a two-dimensional infinitely polymeric network of tetrazole hexamers. In **XXVI**, heavily zigzagged sheet polymers are obtained. In **XXVIII**, the highly polymeric lattice is propagated in two-dimensions via *trans*-N_2SnC_3 bridging interactions. The resultant sheet-like array is dominated by a 24 atom hexagonal motif constructed from six pairs of molecules of symmetry-related asymmetric units. The ethyl chains of the substituted nitromethane units interlink the hexagonal constructions which lead to the overall

honeycomb-like appearance. The interlammelar region consists of tin-bonded butyl groups and the tripodal nitromethane units which alternately project above and below the individual sheets rendering them puckered (Fig.2.2).[24]

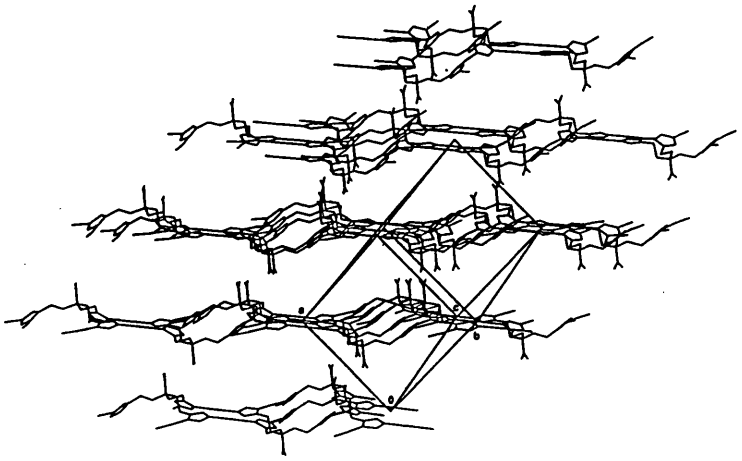

Fig.2.2: Side view of the sheet structure of **XXVIII**. Tributyltin groups omitted for clarity.

c) **Three-dimensional arrays:** A three-dimensional array is exhibited by **XXVII**. A linear polymer evolves along the *b*-axis constructed from a single tetrazole ring of each bis-tetrazole ligand. A similar polymer propagates along the *c*-axis involving the tetrazole rings not involved in propagation along the *b*-axis. Both these interactions result in a two-dimensional array parallel to the *bc*-plane and are intermolecularly cemented along the *a*-axis by alternate bridging by the two unique phenyl-bridged bis-tetrazole ligands (Fig.2.3).[24]

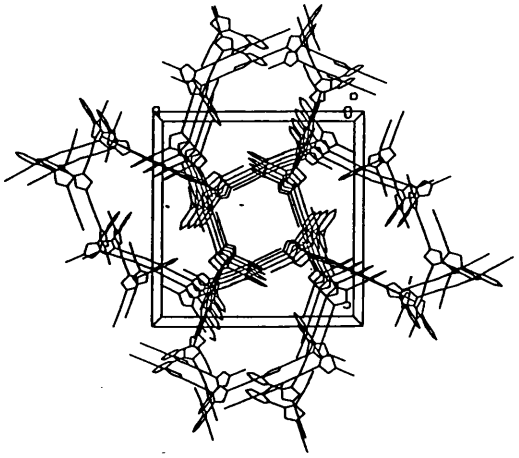

Fig.2.3: Perspective view of **XXVII** along the *a*-axis illustrating the microchannels extending through the lattice.

This chapter describes an extension of these studies to species containing four tetrazole units.

2.2 SYNTHESIS OF ORGANOTIN-SUBSTITUTED TETRA-TETRAZOLES

Six triorganotin-substituted tetra-tetrazoles (**1-6**) have been synthesised using the well-established cycloaddition route of Sisido *et al*[104] and Molloy *et al*[53] (see discussion in Section 1.3.2.1) (equations 2.1-2.3). Typically, a tetra-nitrile was heated with a slight excess of the appropriate azide under nitrogen in the absence of any solvent. Reactions usually reached completion at elevated temperatures (100-170°C) over one hour. The course of the reaction was followed by the disappearance of the IR bands due to the $\nu(N_3)$ at ~2060 cm^{-1} and ν(CN) at ~2250 cm^{-1}. 1,4-phenylene-bis(tributylstannyl)tetrazole.H_2O (**7**), which had been synthesised in this laboratory was re-prepared for purposes of crystallographic studies (equation 2.4), as X-ray analyses of the isomeric 1,2-phenylene-bis(tributylstannyl)tetrazole and 1,3- phenylene-bis(tributylstannyl)tetrazole species had previously been carried out. Slow crystallisation from ethanol yielded the monohydrate, rather than the anhydrous material previously obtained. Compounds **1**, **2,** and **7** showed characteristic aromatic bands in their IR spectrum at 1618 cm^{-1} confirming the presence of the phenylene ring.[105] The expected strong CH stretches and deformations of tetra-tetrazolyl compounds appeared at 2900 cm^{-1} and 1460 cm^{-1} respectively.[1] A band at 1290 cm^{-1} assigned to the -(N-N=N)- moiety in azole systems was present in all spectra.[1] Medium strength bands characteristic of tetrazole rings appeared at 1000-1100 cm^{-1}.[1]

The crude solid products in all cases were recrystallized from methanol. Cooling the methanolic solution gave gummy materials for **1**, **3-6**. While **1**, **3**, **5** and **6** were anhydrous, **4** was obtained as a tetrahydrate. These had to be stirred in hexanes to give the respective products in a powder form. **2** crystallised from methanol with two water molecules incorporated in its lattice structure (see Section 2.4.2). Although **2** has been referred to as being a dihydrate, the complicated nature of the crystal structure suggests a fractional number of water molecules per unit molecule of **2**.

Detailed synthetic procedures and work-up for compounds **1-7** are included in Section 2.5.

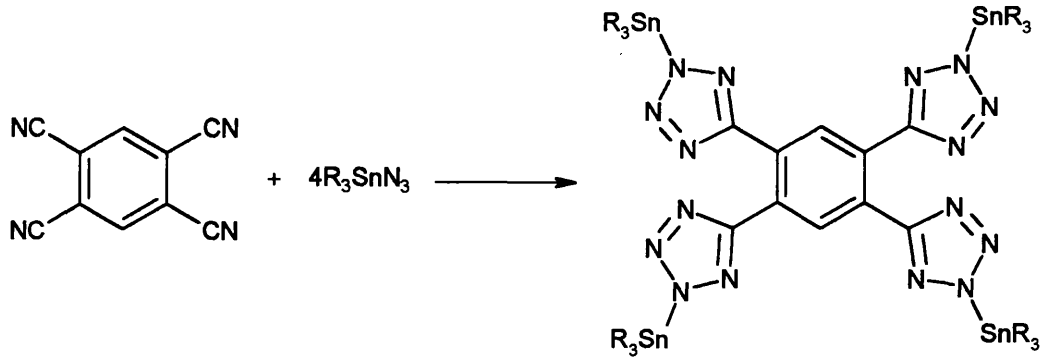

Eq.2.1

R = Bu (**1**), R = Et (**2**)

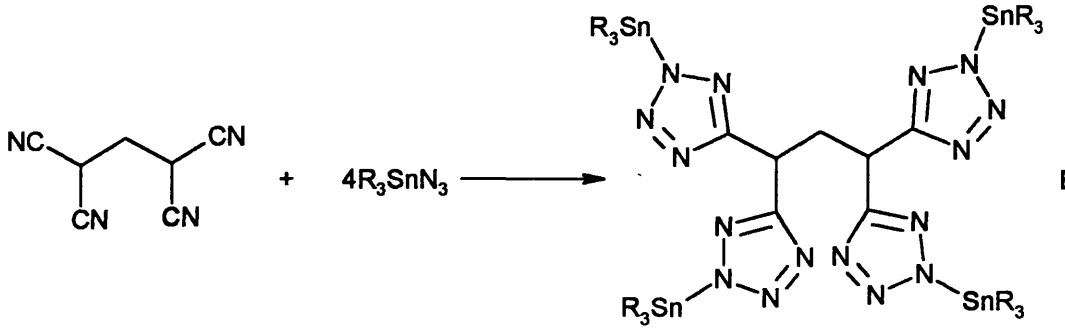

Eq.2.2

R = Bu (**3**), R = Et (**4**)

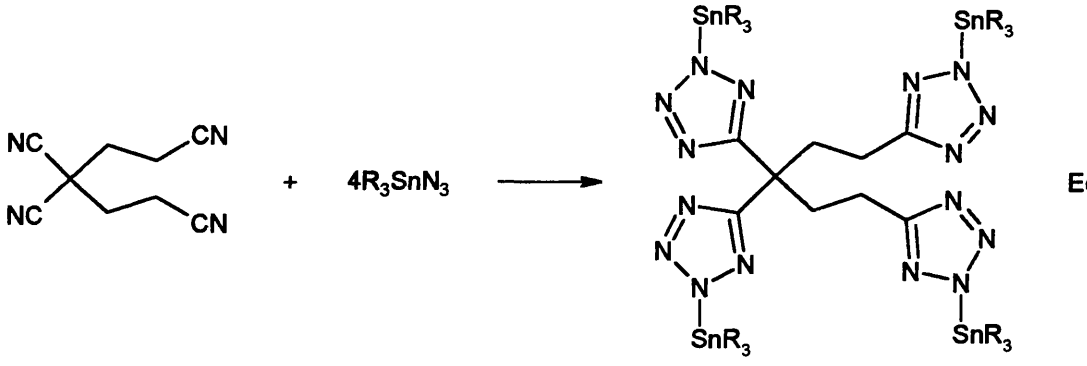

Eq.2.3

R = Bu (**5**), R = Et (**6**)

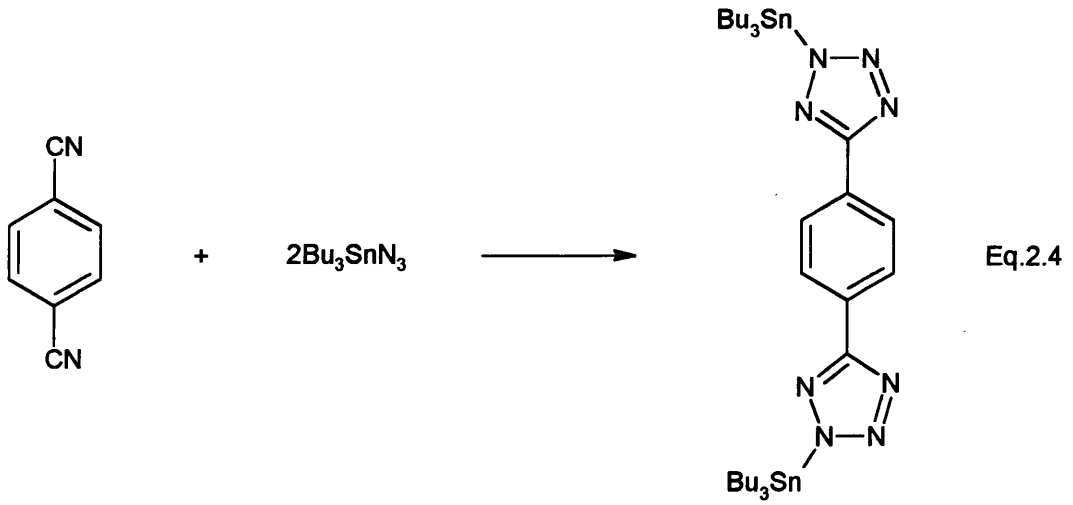

Eq.2.4

(7)

2.3 SPECTROSCOPY

2.3.1 Mössbauer Spectroscopy

The Mössbauer data for triorganotin-substituted tetra-tetrazoles are given in Table 2.2. The isomer shifts fall within the range 1.40-1.55 mms^{-1} and quadrupole splitting (q.s.) falls within the range 3.5-3.9 mms^{-1}. The former confirms the +4 oxidation state of tin while the latter points towards a *trans*-trigonal bipyramidal geometry around tin (see Section 1.5.1). Five-coordination is a characteristic feature of many triorganotin compounds and the preparation of now well-established examples date back to 1923.[106] Based on point-charge models, Fitzsimmons and co-workers[107] calculated quadrupole splittings for *cis* and *trans* trigonal bipyramidal geometries of the type R_3SnX_2. The q.s. calculated for *cis*- trigonal bipyramidal was 1.57 mms^{-1} and for *trans*- trigonal bipyramidal was 3.12 mms^{-1}.

Trans-trigonal bipyramidal geometry about tin is consistent with all published organotin tetrazole structures. For instance, q.s. values of 1,2-[C_6H_4-(SnR_3CN_4)$_2$] (R = Et, ^{n}Bu, ^{i}Pr), 1,3-[C_6H_4-(SnR_3CN_4)$_2$] (R = Et, ^{n}Bu), 1,4-[C_6H_4-(SnR_3CN_4)$_2$] (R = ^{n}Bu, ^{i}Pr) fall within the narrow range of 3.60-3.86 mms^{-1}.[18] The *trans*-trigonal bipyramidal geometry

Table 2.2: ^{119}Sn NMR[a] And Mössbauer[b] Data For Organotin-Substituted Tetra-(tetrazoles) And Related Species

Compound	$\delta(^{119}Sn)$[c]	$^{1}J(Sn-C)$ (Hz)	(δ)	ΔEq	Γ_1, Γ_2[d]
(1)	-48.6	-	1.50	3.67	0.92, 0.96
(2)	-43.2	478	1.50	3.76	0.87, 0.94
(3)	-50.2	-	1.47	3.65	0.88, 0.98
(4)	-45.1	478	1.53	3.87	0.86, 0.94
(5)	-53.5	476	1.47	3.59	0.98, 1.07
(6)	-51.8	482	1.43	3.63	0.83, 1.05
(7)	-48.6	470	1.48	3.84	0.99, 1.02

[a] All spectra recorded as DMSO-d^6 solutions at 25°C

[b] Mössbauer data recorded at 78K and data given in mms^{-1}

[c] Values given in ppm

[d] Refers to full width at half height of the high and low velocity resonances

about tin is achieved via *trans*-N_2SnC_3 type coordination which is also consistent with all published organotin tetrazole structures. Possible exceptions may arise in the case of hydrated **2**, **4** and **7**. In these three cases, both *trans*-N_2SnC_3 and *trans*-$NOSnC_3$ coordinations are possible and both are consistent with the Mössbauer data, the latter arising if the intermolecular N→Sn interaction is replaced by H_2O→Sn interaction. The quadrupole splittings for both possibilities (N_2SnC_3 *vs.* $NOSnC_3$) fall within the same range. For instance, q.s. for crystallographically characterised 1,3-phenylene-bis-5,5′-(tributylstannyltetrazole).bis-methanolate is 3.65 mms^{-1}.[24] A precedent for simultaneous observation of both tin environments exists in the structure of bis(trimethylstannyl)-5,5′-azotetrazole hydrate for which similar Mössbauer data have been recorded (q.s. = 3.90 mms^{-1}).[108] Broad linewidths obtained for **7** (Γ = 0.99, 1.02) strongly support the presence of two environments. Mössbauer spectroscopy by itself is not sufficient to distinguish between the two environments.

The most likely way of attaining this *trans*-N_2SnC_3 trigonal bipyramidal geometry about tin is by the formation of structures of the type **XXX** in which the tin is covalently bonded to nitrogen of one tetrazole and intermolecularly to nitrogen of a neighbouring tetrazole. This is supported by viscosity measurements and low temperature NMR experiments on 2-(tri-n-butylstannyl)-5-substituted tetrazoles.[109] The degree of association in these compounds was found to be dependent on the 5-substituent of the tetrazoles. Steric hindrance of the 5-substituent decreases the degree of association.

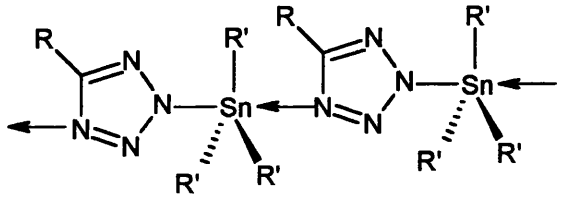

XXX

Broad linewidths for **5** (Γ = 0.98, 1.07) and **6** (Γ = 0.83, 1.05) are possibly caused by the asymmetry inherent in the tetra-tetrazole ligands. Organotin-substituted tetrazoles

synthesised to date contain -(SnR_3)CN_4 moieties connected by symmetrical aliphatic or aromatic units. This, however, is not the case for **5** and **6**. The asymmetrical organotin tetrazole -(SnR_3)CN_4 moieties, probably, give rise to slightly different tin environments which lead to broad linewidths. A combination of various coordination modes of the tin to the tetrazole nitrogen, e.g. $N^1 + N^2$, $N^1 + N^3$, $N^1 + N^4$ etc., (see numbering scheme in Section 1.4) can also give rise to broad linewidths.

2.3.2 NMR Spectroscopy

^1H, ^{13}C, and ^{119}Sn NMR data were collected in d^6-DMSO for all the organotin-substituted tetrazoles. ^{119}Sn NMR data for all the compounds included in this chapter are summarised in Table 2.2. ^1H and ^{13}C NMR data are consistent with the proposed structures and can be found in Section 2.6.

The ^1H NMR spectra for all the tributyltin-substituted compounds show butyl resonances as multiplets at 0.77 ppm corresponding to the δ-CH_3 protons and between 1.2-1.3 corresponding to the α, β, and γ-CH_2 protons. The triethyltin-substituted compounds show ethyl resonances as a multiplet at 0.8-1.4 ppm. In **1**, **2**, and **7** aromatic protons of the benzene ring are also visible. In **3** and **4**, the propyl protons of the ligand are completely masked by the resonances from the butyl and ethyl tin protons, respectively. However, in **5** and **6**, the ligand pentyl protons were observed as a multiplet at 2.5-2.8 ppm in addition to the signals due to groups bonded to tin. The ^{13}C NMR spectra of all the triorganotin-substituted tetrazoles listed in this chapter clearly show the quaternary carbon of the tetrazole at 160 ppm. For **1**, **3**, **5**, and **7**, the butyl resonances appear between 13 and 27 ppm. Resonances for C_β and C_γ are reversed due to the tetrahedral geometry of the methylene groups and the dihedral Sn-C-C-C angle. The net result is that C_γ is brought closer to the tin nucleus than C_β in a time-averaged picture. Literature precedents for this phenomenon are available.[24,71,72] The reversal of C_β and C_γ in relation to the tin nucleus is also reflected in the Sn-C coupling constants. The $^2J(Sn\text{-}C_\beta)$ coupling constant is ~28 Hz while the $^3J(Sn\text{-}C_\gamma)$ coupling constant is ~74 Hz. In **2**, **4** and **6**, the ethyl resonances appear between 10.0-10.1 ppm. The $^1J(Sn\text{-}C_\alpha)$ for the

organotin tetrazole compounds **1-7** is ~480 Hz. This value falls within the range for *trans*-trigonal bipyramidal geometry about tin (see Section 1.5.2). In addition, use of the semi-empirical relationship derived by Holecek and Lycka[77] for correlating ^1J and C-Sn-C angles suggests a value of 124° for compounds **1, 3, 5** and **7**, also consistent with *trans*-trigonal bipyramidal geometry about tin. Correlations between coupling constants and C-Sn-C bond angles have been established for Bu(IV)-Sn and Me(IV)-Sn compounds (see Section 1.5.2). No such relationship has been reported for Et(IV)-Sn compounds. However, the lower members of the homologous series of alkyl(IV)-Sn compounds are likely to exhibit similar NMR properties to that of Bu(IV)-Sn compounds, with the exception of Me(IV)-Sn compounds which have been reported to have a quadratic relationship (see Section 1.5.2). Therefore NMR information obtained about Bu(IV)-Sn compounds throws light on Et(IV)-Sn compounds.

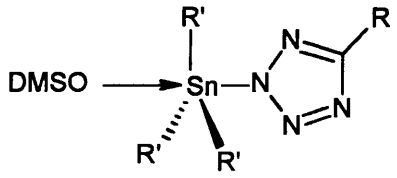

XXXI

^{119}Sn NMR exhibit resonances between -40 and -80 ppm. In comparison with previous work on organotin-substituted tetrazoles, this indicates a five-coordinate tin. The ^{119}Sn chemical shifts of 1,2-[C_6H_4-(SnR_3CN_4)$_2$] (R = Et, ^{n}Bu, ^{i}Pr), 1,3-[C_6H_4-(SnR_3CN_4)$_2$] (R = Et, ^{n}Bu), 1,4-[C_6H_4-(SnR_3CN_4)$_2$] (R = ^{n}Bu, ^{i}Pr)[18] fall within the range of -40 to -83 ppm and are to low frequency of four-coordinated $SnBu_3(NMe_2)$ (δ 36 ppm)[72]. The five-coordination at tin could be achieved in two ways as depicted in **XXX** and **XXXI**. In a coordinating solvent such as DMSO either structure could be formed and all that could be conclusively ascertained is that the tin is five-coordinate.

Another common feature between the work being described and the simple N-trialkylstannyl tetrazoles (R_3SnN_4CR') studied in reference 80 is the broad linewidths obtained for the ^{119}Sn NMR signals. Typically, half width at half height of the tin

resonance at 25°C for the former compounds is 470 Hz and for the latter compounds is 688 Hz. Although this could be ascribed to the tin being adjacent to the quadrupolar nucleus ^{14}N, this seems unlikely due to the temperature dependence of ^{119}Sn chemical shifts and linewidths. Variable temperature study on the trialkylstannyl tetrazoles has explained these linewidths as arising from a dynamic process in which tin oscillates around the CN_4 ring.

2.4 X-RAY CRYSTALLOGRAPHY

Crystallography is very important for the structural analysis of chemical compounds and is the ultimate tool available for the conclusive characterisation of organometallic tetrazole species. Mössbauer data merely point out the local geometry about tin and even then, they are not unambiguous, e.g. distinction between R_3SnN_2 and R_3SnNO cannot be made. As discussed in Sections 2.3.1 and 2.3.2, Mössbauer and multinuclear NMR spectroscopies provide a variety of possible structures but do not conclusively point towards any one structure.

2.4.1 Crystal Structure Of 1,4-Phenylene-Bis(tributylstannyltetrazole).H_2O, (7)

Crystals of 1,4-phenylene-bis(tributylstannyltetrazole).H_2O (**7**), previously synthesised in the laboratory, were grown from an ethanolic solution at room temperature. Full details of the crystallographic analysis, atomic coordinates and isotropic thermal parameters are included in Appendix II. The asymmetric unit of **7** is illustrated Fig.2.4 and selected bond lengths and bond angles are given in Tables 2.3 and 2.4, respectively. Examination of Fig.2.4 reveals that **7** crystallises from ethanol as a monohydrate. This is only the second hydrated organotin-substituted tetrazole known to date and provides a means of comparison with the dihydrate (**2**) discussed in Section 2.4.2. The asymmetric unit contains two trigonal bipyramidal tin centres- a *trans*-N_2SnC_3 and a $NOSnC_3$. As confirmed by spectroscopic evidence, all previously examined tin centres of organotin tetrazoles are trigonal bipyramidal (see Sections 2.3.1 and 2.3.2).

The axial positions of Sn(1) are occupied by N^2 atoms of two tetrazole moieties (see numbering scheme discussed in Section 1.4). The N-Sn-N bond angle is close to 180° [N(2)-Sn(1)-N(6′) 176.4(3)°] and the two individual bond lengths are equivalent within experimental error. Thus Sn(1) has N^2 + N^2 type coordination which has previously been seen in 1,2-[C_6H_4-($Et_3SnN_4C)_2$].[18] The axial positions of Sn(2) are occupied by tetrazole N(8) and oxygen of the water molecule [O(1)]. The N-Sn-O bond angle is also close to 180° [N(8)-Sn(2)-O(1) 178.7(2)°].

The structure also shows coordination polymerisation and hydrogen bonding. A one-dimensional polymer is formed along the *a*-axis involving Sn(1) bridged by bis-tetrazole ligands (Fig.2.5). The hydrated tin centre Sn(2) is pendant to this chain. Along the *b*-axis, a zigzag uni-dimensional polymer is formed as a result of a hydrogen bond between H(1) of the water molecule coordinated to Sn(2) and N(5) of the lattice neighbour generated by the operator *1.5-x, 0.5+y, 1.5-z* [H(1)....N(5), 2.048Å] (Fig.2.6). The net result of these two interactions is the formation of two-dimensional zigzag molecular sheets which compile along the *c*-axis. A second weaker hydrogen bond between H(2) of the same water molecule and N(4) of the lattice neighbour generated by the transformation *0.5+x, 0.5-y, 0.5+z* 'cements' these sheets together along *c* as shown in Fig.2.6 [H(2)....N(4), 2.125Å]. The net result of all these interactions is an array of lattice channels along various unit cell vectors. Fig.2.7 shows the view of the lattice structure along the *a*-axis. The large cavities seen in the lattice are, in reality, filled with butyl groups. In the categories of crystal structures of organotin-substituted tetrazoles known to date listed in Table 2.1, **XXVII** also forms a three-dimensional array. However, it must be noted that **XXVII** is an anhydrous compound while **7** is a hydrate.

As a final note to the description of the structure, the coordination modes with respect to the tetrazole ring must be mentioned. The tetrazole based on C(1) is bidentate and exhibits N^1 + N^3 mode of coordination. The tetrazole based on C(6) is tridentate and exhibits N^1 + N^2 + N^4 mode. While the N^1 + N^3 mode of coordination is the commonest among organotin tetrazoles (see Table 1.1), the less common N^1 + N^2 + N^4 mode has been observed in some organotransition metal[42,57] and organoboron tetrazoles[48].

A similar hydrogen bonding interaction has been observed in the crystal structure of $(Me_3SnN_4C)_2N_2.H_2O$.[108] As in **7**, a zigzag polymer is obtained along the *b*-axis consisting of Sn(2) moieties bridged by bis-tetrazole ligands with pendant hydrated Sn(1) groups alternating on either side of the backbone. These meandering polymers are 'cemented' together by two hydrogen bonding interactions which result in the formation of two-dimensional polymer sheets within the *bc*-plane. These sheets build up along the *a*-axis of the unit cell although unlike in **7**, there is no interaction between the sheets (Fig.2.8).

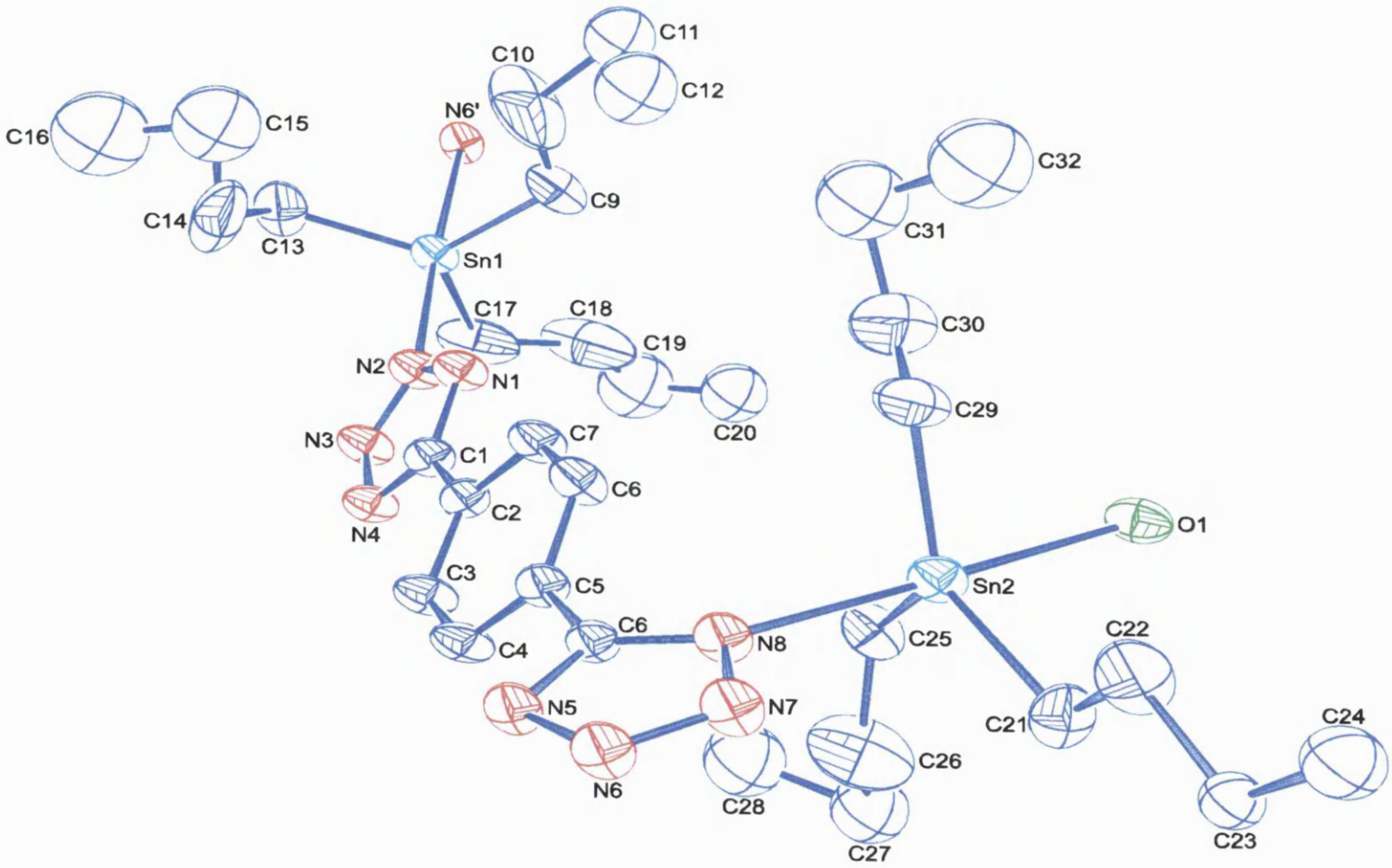

Fig.2.4: The asymmetric unit of **7** showing the atomic labelling scheme used in the text and tables. Hydrogen atoms omitted for clarity.

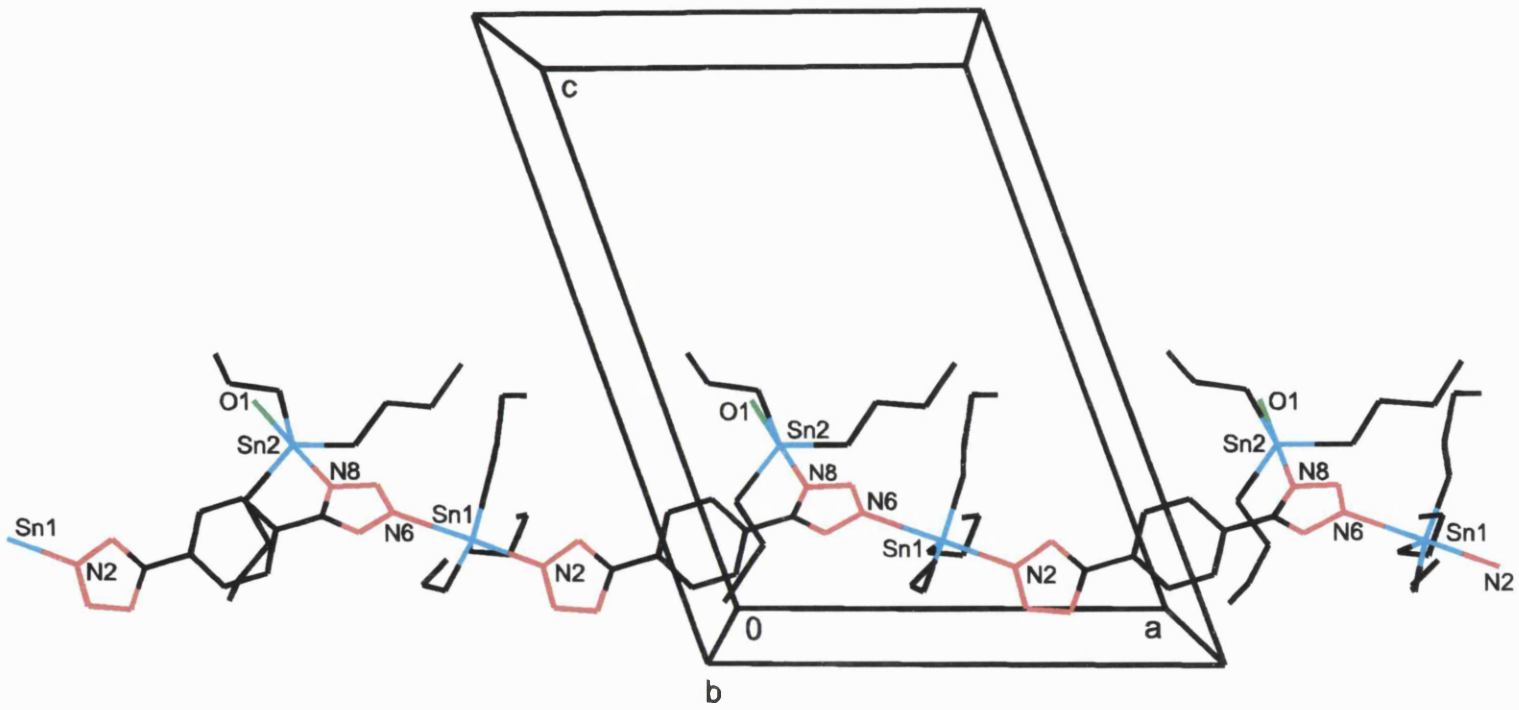

Fig.2.5: One-dimensional polymer of **7** along the *a*-axis.

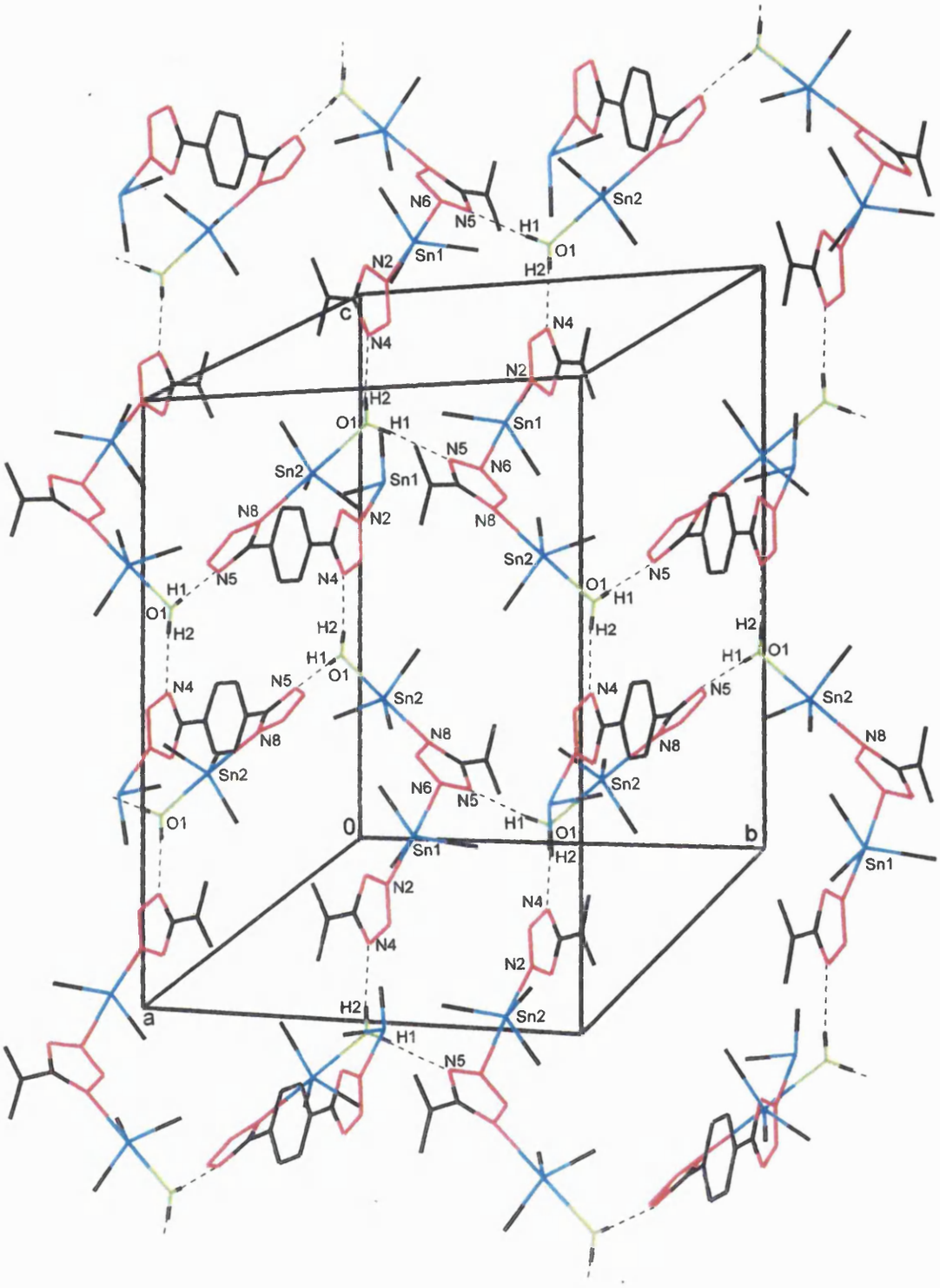

Fig.2.6: View of the three-dimensional array of 7 formed as a result of the two hydrogen-bonds along the *b* and *c* axes.

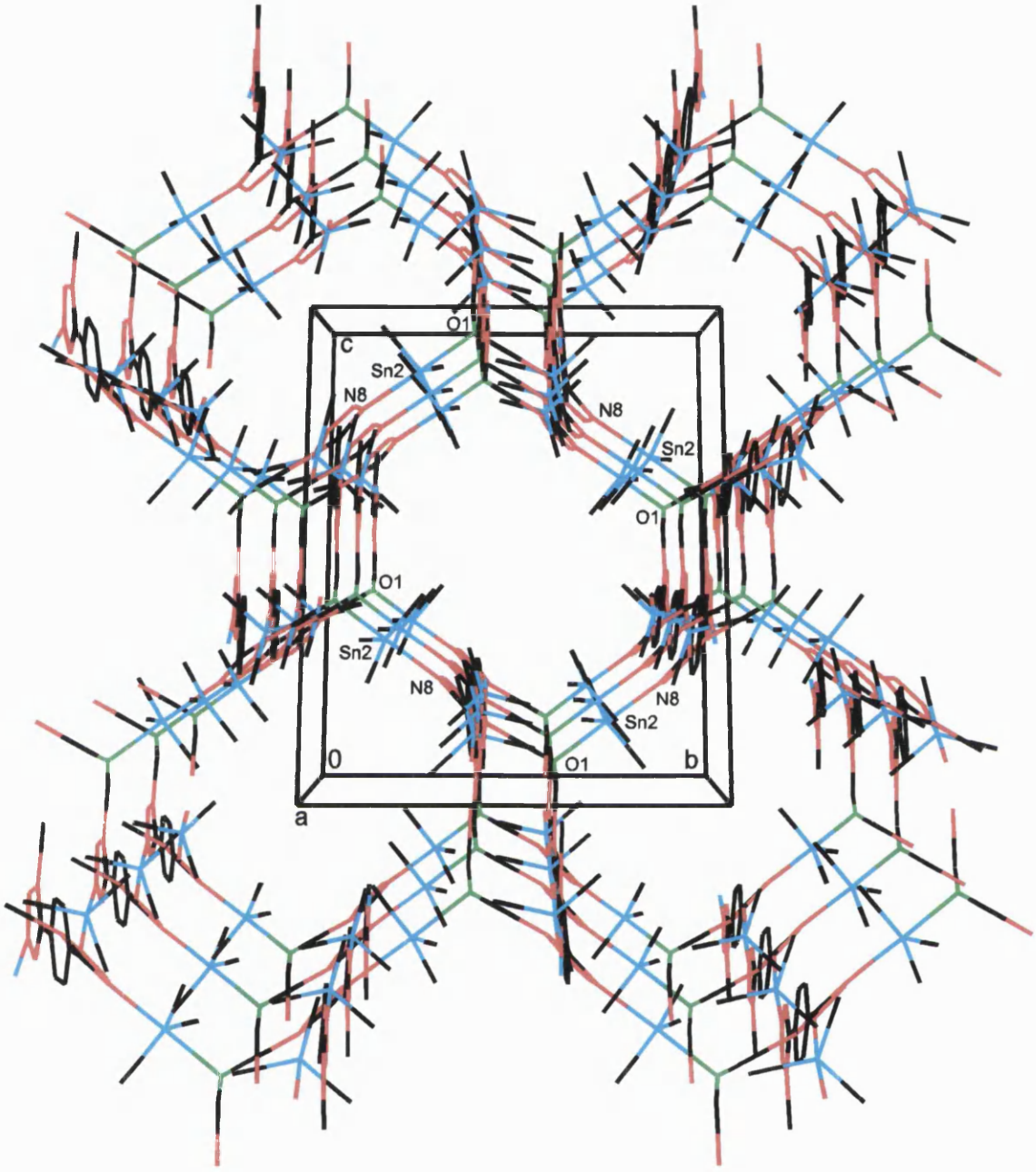

Fig.2.7: View of the lattice structure of **7** along the *a*-axis.

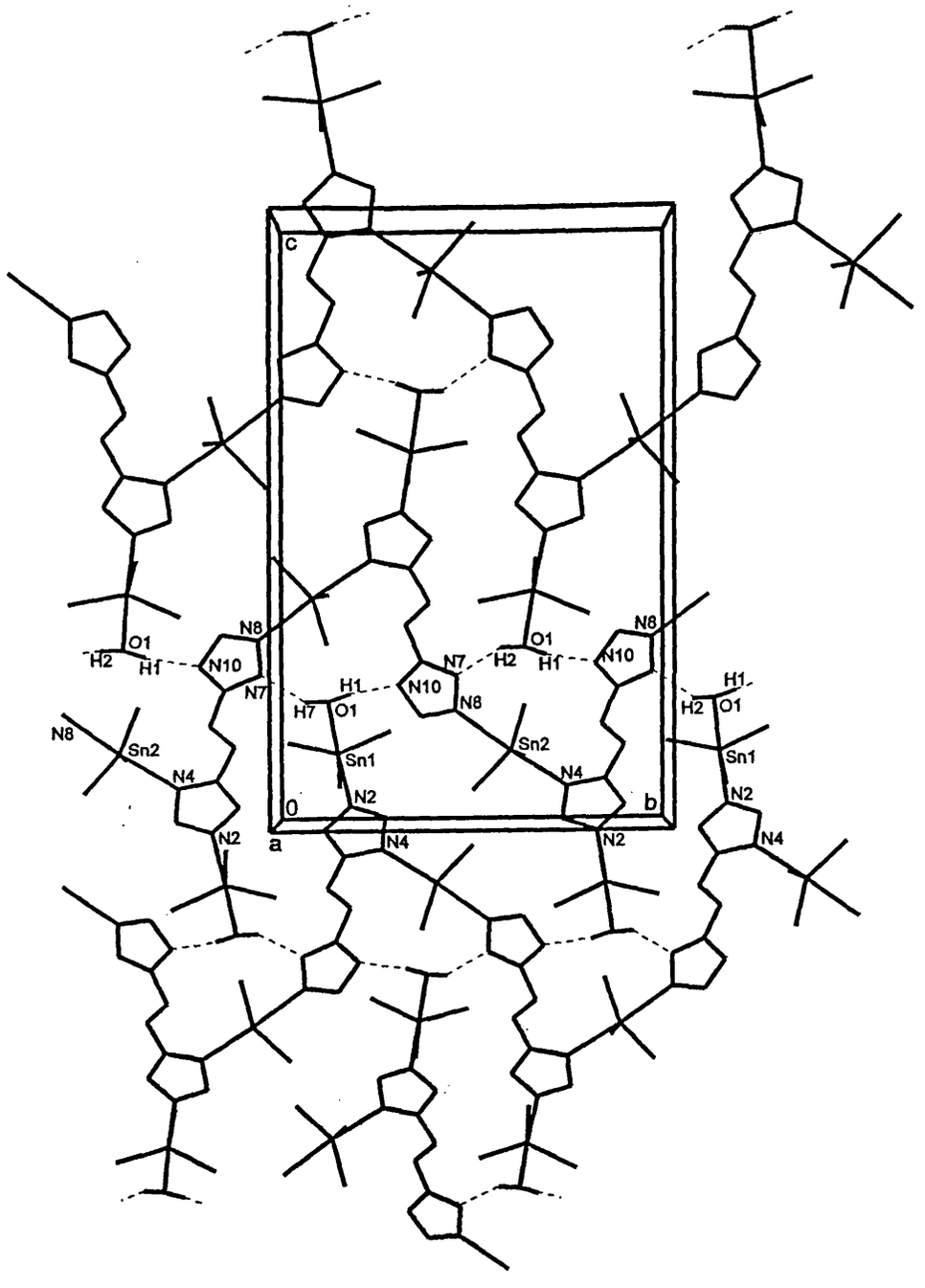

Fig.2.8: Two-dimensional polymeric sheets of $(Me_3SnN_4C)_2N_2.H_2O$ formed in the *bc*-plane.[108]

Table 2.3: Selected Bond Lengths (Å) For **7** With Their Estimated Standard Deviations In Parentheses.

Sn(1)-C(13)	2.135(11)	Sn(2)-C(21)	2.132(8)
Sn(1)-C(9)	2.127(9)	Sn(2)-C(25)	2.131(8)
Sn(1)-C(17)	2.147(12)	Sn(2)-C(29)	2.121(10)
Sn(1)-N(2)	2.293(6)	Sn(2)-O(1)	2.368(6)
Sn(1)-N(6)#1	2.573(6)	Sn(2)-N(8)	2.403(6)
O(1)-H(1)	0.820(1)	O(1)-H(2)	0.820(1)
N(1)-C(1)	1.323(9)	N(5)-C(8)	1.333(9)
N(1)-N(2)	1.349(9)	N(5)-N(6)	1.358(8)
N(2)-N(3)	1.303(9)	N(6)-N(7)	1.303(9)
N(3)-N(4)	1.323(8)	N(7)-N(8)	1.352(7)
N(4)-C(1)	1.343(10)	N(8)-C(8)	1.346(9)

Symmetry transformations used to generate equivalent atoms:

#1 x-1,y,z; #2 x+1,y,z.

Table 2.4: Selected Bond Angles (°) For **7** With Their Estimated Standard Deviations In Parentheses.

C(13)-Sn(1)-C(9)	120.5(5)	C(29)-Sn(2)-N(8)	91.3(4)
C(13)-Sn(1)-C(17)	120.4(6)	C(21)-Sn(2)-N(8)	91.9(3)
C(9)-Sn(1)-C(17)	117.7(5)	C(25)-Sn(2)-N(8)	91.7(3)
C(13)-Sn(1)-N(2)	95.7(3)	O(1)-Sn(2)-N(8)	178.7(2)
C(9)-Sn(1)-N(2)	93.4(3)	Sn(2)-O(1)-H(1)	113(6)
C(17)-Sn(1)-N(2)	92.5(4)	Sn(2)-O(1)-H(2)	101(8)
C(13)-Sn(1)-N(6)#1	87.4(3)	H(1)-O(1)-H(2)	135(9)
C(9)-Sn(1)-N(6)#1	86.6(3)	C(1)-N(1)-N(2)	102.5(6)
C(17)-Sn(1)-N(6)#1	84.3(4)	N(3)-N(2)-N(1)	111.6(5)
N(2)-Sn(1)-N(6)#1	176.4(3)	N(3)-N(2)-Sn(1)	124.9(5)
C(29)-Sn(2)-C(21)	120.6(4)	N(1)-N(2)-Sn(1)	123.5(5)
C(29)-Sn(2)-C(25)	124.4(4)	N(2)-N(3)-N(4)	108.3(6)
C(21)-Sn(2)-C(25)	114.8(4)	N(3)-N(4)-C(1)	105.1(6)
C(29)-Sn(2)-O(1)	87.4(3)	C(8)-N(5)-N(6)	103.7(6)
C(21)-Sn(2)-O(1)	88.6(3)	N(7)-N(6)-N(5)	111.1(5)
C(25)-Sn(2)-O(1)	89.3(3)	N(7)-N(6)-Sn(1)#2	118.4(4)
C(22)-C(21)-Sn(2)	115.0(7)	N(5)-N(6)-Sn(1)#2	126.3(5)

Table 2.4: Selected Bond Angles (°) For Compound (7) With Their Estimated Standard Deviations In Parentheses. (Contd.)

C(26)-C(25)-Sn(2)	114.5(8)	N(6)-N(7)-N(8)	108.4(6)
C(30)-C(29)-Sn(2)	113(1)	C(8)-N(8)-N(7)	105.2(6)
C(18)-C(17)-Sn(1)	112.2(9)	C(8)-N(8)-Sn(2)	139.9(4)
C(10)-C(9)-Sn(1)	115(1)	N(7)-N(8)-Sn(2)	114.0(5)
C(14)-C(13)-Sn(1)	116.2(8)	N(1)-C(1)-N(4)	112.5(6)
N(5)-C(8)-C(5)	122.8(7)	N(1)-C(1)-C(2)	122.3(7)
N(8)-C(8)-C(5)	125.5(6)	N(4)-C(1)-C(2)	125.2(6)
N(5)-C(8)-N(8)	111.6(6)		

Symmetry transformations used to generate equivalent atoms:

#1 x-1,y,z; #2 x+1,y,z.

2.4.2 Crystal Structure Of 1,2,4,5-Phenylene-Tetra(triethylstannyltetrazole).$2H_2O$, (2)

The structure of **2** is the most complicated obtained to date, is without literature precedent and does not fit into any of the categories described in Section 2.1.2. It is also unique in not only being a dihydrate but also exhibiting host-guest chemistry by having a water molecule embedded in the lattice structure.

Crystals of 1,2,4,5-phenylene-tetra(triethylstannyltetrazole).$2H_2O$ were grown from a methanolic solution at room temperature. Full details of the crystallographic analysis, atomic coordinates and isotropic thermal parameters are included in Appendix III. The asymmetric unit consists of three tins of unit occupancy [Sn(2), Sn(4), Sn(5)] and two tins of half occupancy [Sn(1), Sn(3)] which coincide with inversion centres, along with two separate ligand halves (Fig.2.9). Selected bond lengths and bond angles are given in Tables 2.5 and 2.6. As pointed out in Section 2.2, although the number of water molecules incorporated in the lattice structure of **2** is two, the number of waters per unit molecule of **2** is probably a fractional number.

All tin environments are trigonal bipyramidal with equatorial ethyl groups. The asymmetric unit contains four *trans*-N_2SnC_3 centres and a $NOSnC_3$ centre. The trigonal bipyramidal tin centre is found in all previously examined tin tetrazoles[18,19,52,53] and confirms the spectroscopic interpretation (see Sections 2.3.1 and 2.3.2). The axially ligating atoms for the five tins, the N-Sn-N/N-Sn-O bond angles and the modes of coordination of the tetrazole ring with respect to the tins are tabulated in Table 2.7. The nine Sn-N bond lengths are equivalent within experimental error. The $N^1 + N^2$ coordination mode has been seen in 1,2-[C_6H_4-($Bu_3SnN_4C)_2$] while the $N^2 + N^2$ mode has been seen in 1,2-[C_6H_4-($Et_3SnN_4C)_2$].[18]

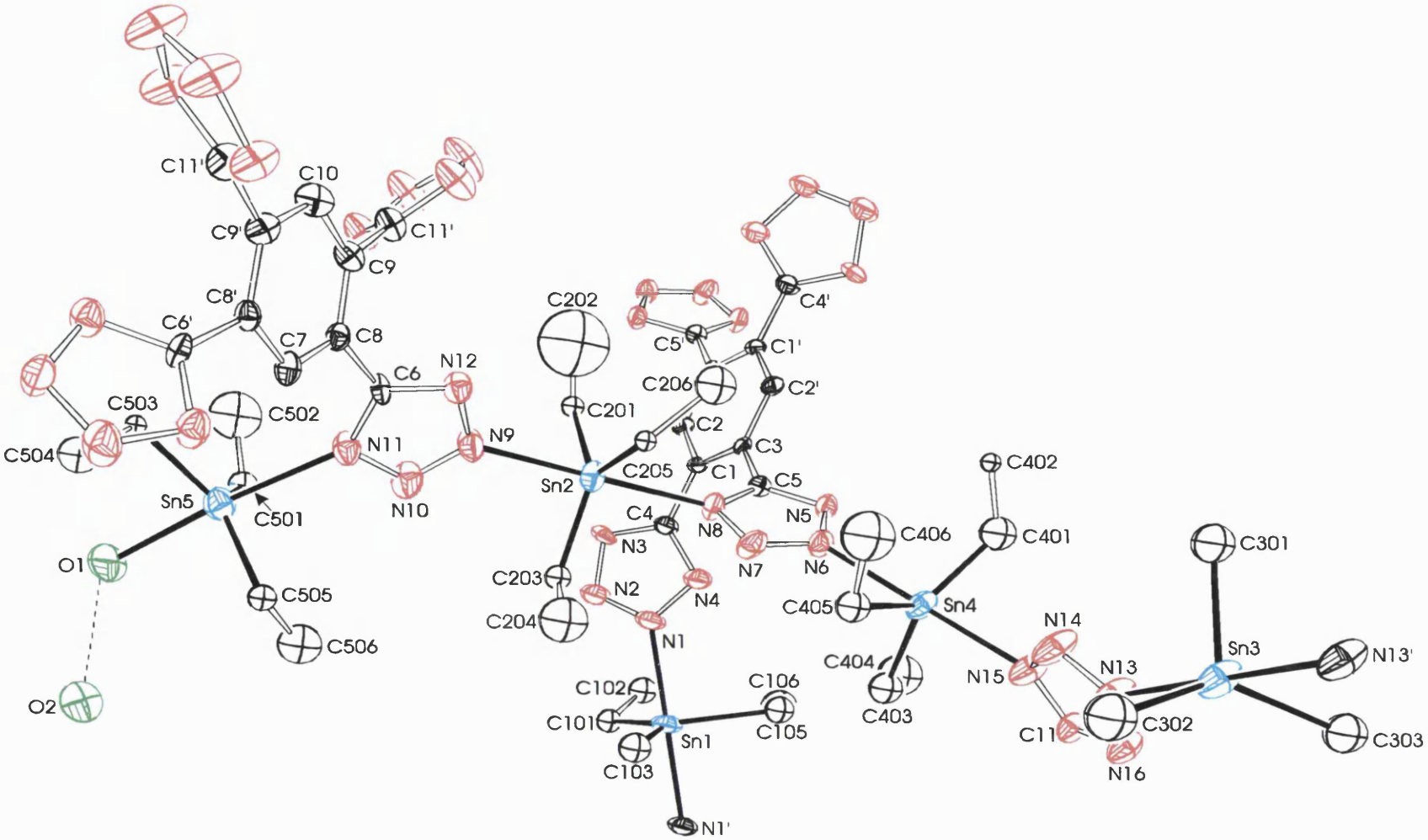

Fig.2.9: The asymmetric unit of **2** showing the atomic labeling scheme used in text and tables. Hydrogen atoms omitted for clarity.

Table 2.7: Axial Positions Of The Five Tins In The Asymmetric Unit Of **2** And Their N-Sn-N/N-Sn-O Bond Angles

Sn	Tetrazole coordination with respect to tin	N-Sn-N bond angle (°)
1	$N^2 + N^2$	N(1)-Sn(1)-N(1′) 180.0(2)
2	$N^1 + N^2$	N(9)-Sn(2)-N(8) 176.3(4)
3	$N^2 + N^2$	N(13)-Sn(3)-N(13′) 180.0(2)
4	$N^1 + N^2$	N(15)-Sn(4)-N(6) 179.2(4)
5	N^1	N(11)-Sn(5)-O(1) 175.6(5)

The three-dimensional structure of (**2**) shown in Fig.2.10 can be loosely described in terms of layers. Propagation along *b* takes place primarily through the *trans*-$N_2Sn(3)$ [Sn(3) sits on an inversion centre at 0, 0.5, 0 etc.], while propagation along *a* takes place via *trans*-$N_2Sn(2)$ and *trans*-$N_2Sn(4)$. In order to highlight the salient features of the structure, it is essential to point out that the ligands are of two distinct types. The ligand based on C(1) (Type A) has at the centre of the C_6 ring an inversion centre (0.25, 0.25, 0.5). This ligand is oriented asymmetrically with respect to *b* and is responsible for spanning the wider part of the elliptical cavities (Fig.2.11a and b). The ligand based on C(7) (Type B) has a two-fold axis through C(7)-C(10) (0, y, 0.25) and is thus symmetrically disposed with respect to *b*. It provides the link at the narrowest part of the elliptical cavity. A simplified pictorial depiction of the structure is given in Fig.2.14, where levels 1 and 2 have been used to focus on the narrower and wider part of an elliptical cavity.

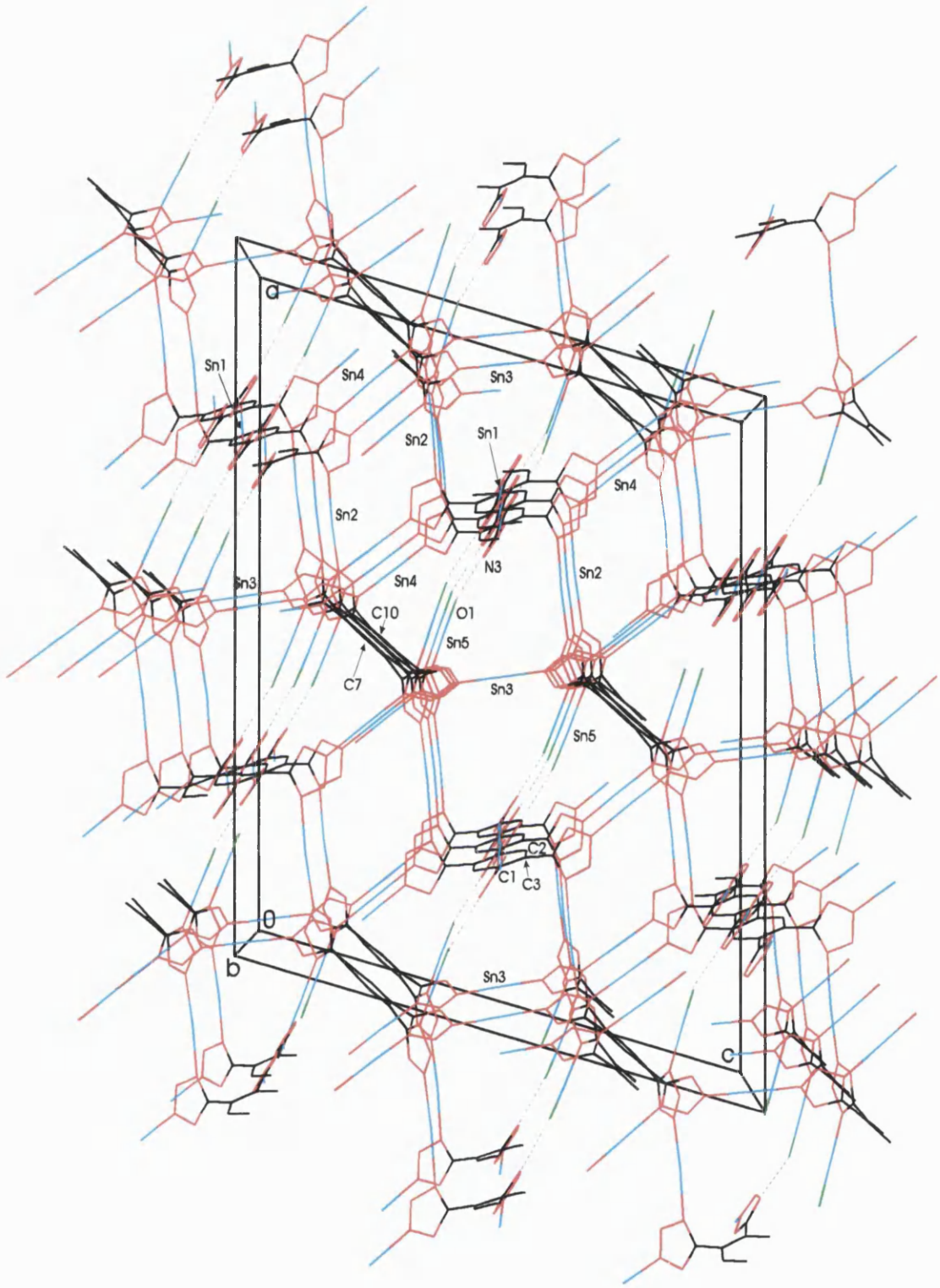

Fig.2.10: View of the three-dimensional lattice structure of **2**.

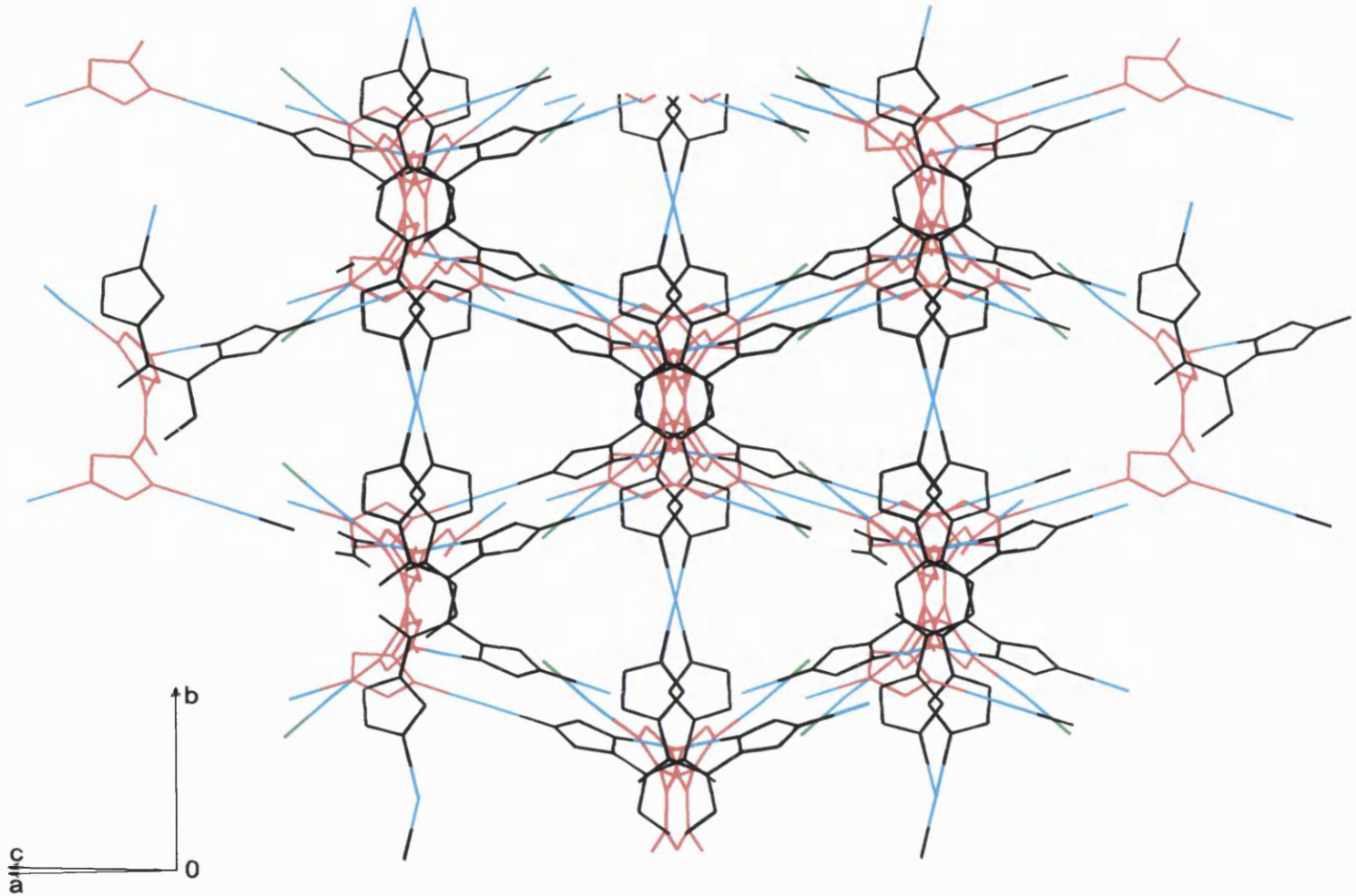

Fig.2.11a: View of the three-dimensional lattice structure of **2** along the (1, 0, -1) direction.

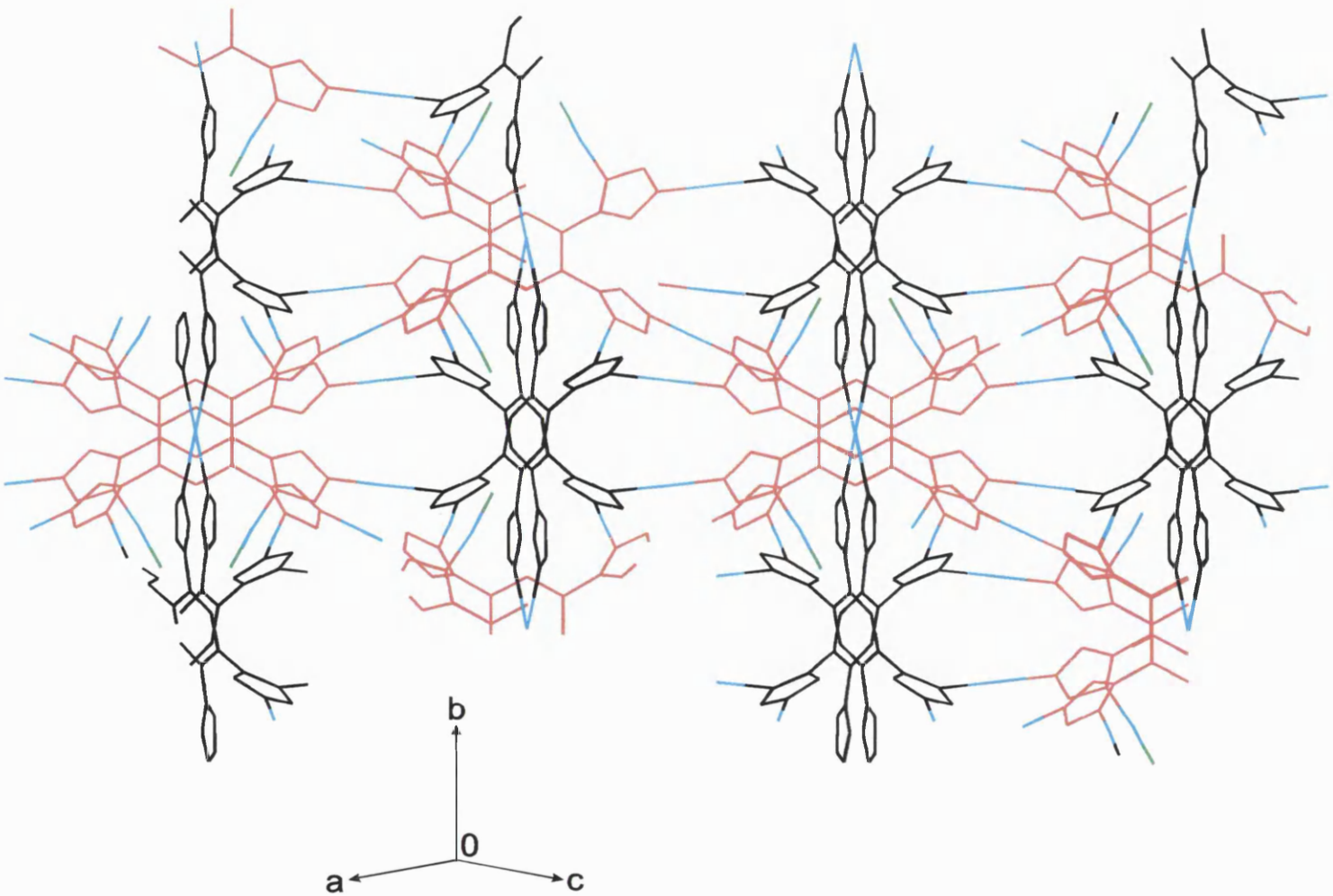

Fig.2.11b: View of the three-dimensional lattice structure of **2** in the (1, 0, 1) direction.

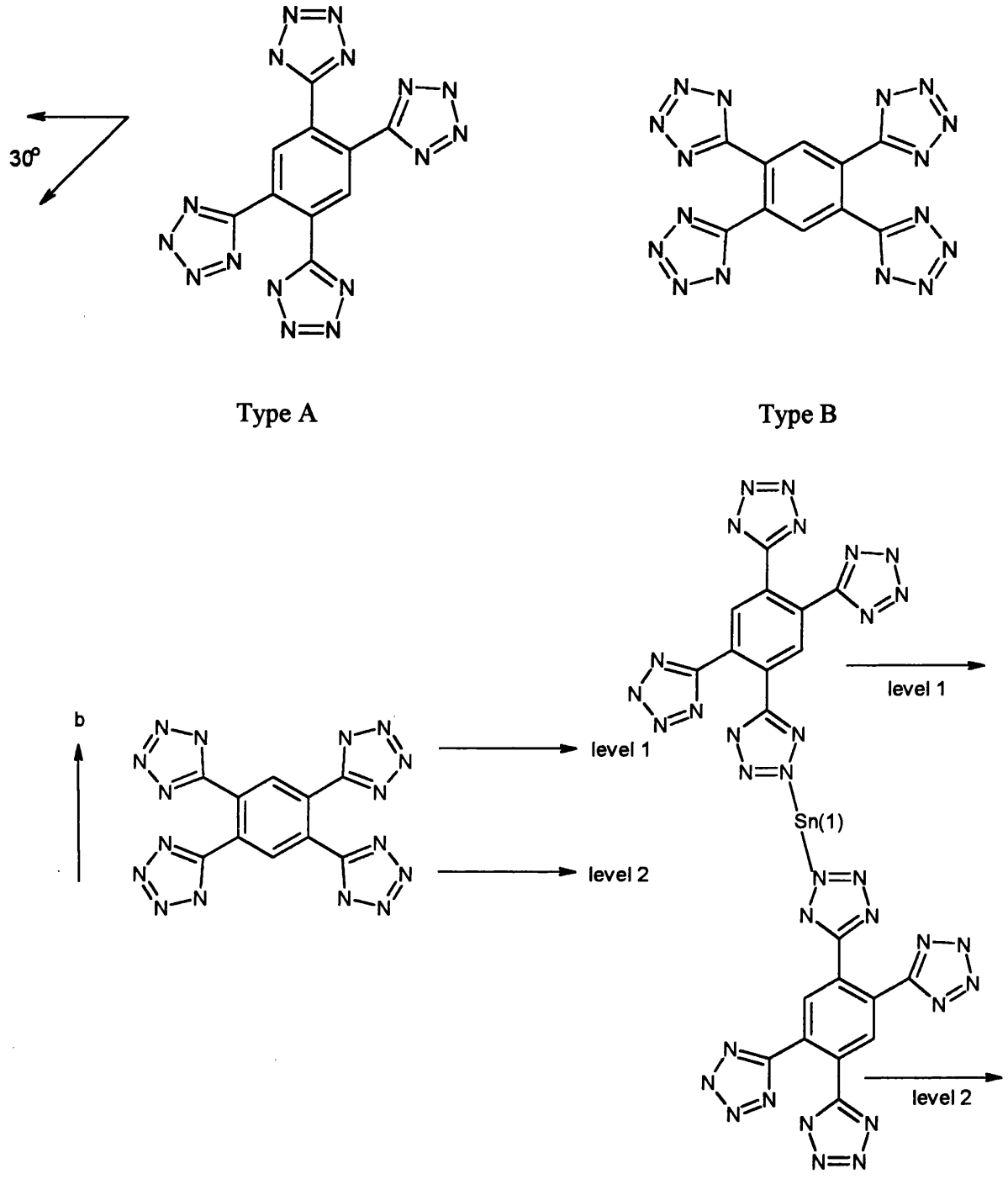

Type A

Type B

Narrow part of cavity

Wide part of cavity

Fig.2.14

The pseudo-five-sided rings visible in Fig.2.10 are made up of three tins (Sn2, Sn3 and Sn4). These rings are not planar and are tilted with respect to the *b* axis. These rings

start and finish at tetrazoles based on C(5) sharing a common phenylene bridge (type A) and the "top to bottom" cycle is accommodated by the 2_1 axis (0.25, y, 0.25) which spirals Sn2 and Sn4 along *b*. In addition, the angle between opposite tetrazoles on either side of the type A tetra-tetrazole is approximately 30° with respect to the *ac*-plane, which is the origin of the zigzag appearance of Fig.2.11. The five-sided rings contain 28 atoms and are shown in red on the stereo plot (Fig.2.12).

The formation of the three-dimensional lattice is complex as several features contribute to the propagation along *b*. Firstly, there are two distinct types of ligands as described above. The inversion centre at Sn(1) (0.25, 0.25, 0) generates the *trans*-$N_2Sn(1)$ unit which spans the widest part of the elliptical cavities. Secondly, the spirals associated with Sn(2) and Sn(4)- the pseudo four-sided rings (Fig.2.10) are not planar but are related by the screw axis at 0.25, y, 0.25 which propagate the lattice along *b*. Thirdly, H-bonding involving water [O(1)] which is coordinated to Sn(5) and N(3). This effectively anchors the position of the two tetrazoles based on C(4) [the ones not coordinating Sn(1)] and generate a new 24-membered centrosymmetric macrocycle (26 atom including the hydrogens of the H-bonds). These are shown in green on the stereo plot but share some common atoms with the red five-sided ring (Fig.2.12). Fig.2.13 is also a stereo plot of **2** with some labeled atoms. Finally, the lattice can also be viewed as an interpenetrating network. The pseudo-eight-sided rings comprising of 38 atoms and 6 *trans*-N_2Sn units and two type B ligands (shown in blue in Fig.2.12) have the *trans*-$N_2Sn(1)$ bridge centred on ligand type A threaded through them.

Hydrogen bonding interactions result from an interaction between the water molecule [O(1)] coordinated to Sn(5) and N(3) of the lattice neighbour generated by the operation *1-x, 1-y, 2-z* [O(1)-N(3), 2.650(2)Å]. Sn(5)-O(1) [2.273Å(11)] of **2** is slightly shorter than Sn(2)-O(1) [2.368(6)Å] of **7**. There is also an interstitial water molecule in the lattice, the [O(2)] of which is hydrogen bonded to both O(1) and N(5) of the lattice neighbour generated by *0.5-x, -0.5+y, z* [O(2)-O(1), 2.721 Å; O(2)-N(5), 2.481 Å]. It is the interstitial water molecule i.e. one not directly involved in coordination to tin as in previous hydrated tetrazole structures, that adds to the uniqueness of the structure.

Taking into account the hydrogen-bonding, the four tetrazoles in the asymmetric unit (Fig.2.9) exhibit different coordination modes with respect to themselves. The tetrazole based on C(4) and C(6) exhibit a bidentate $N^1 + N^3$ coordination mode; the tetrazole ring based on C(5) shows tridentate $N^1 + N^2 + N^4$ mode of coordination and the one based on C(11) shows a monodentate N^1 coordination mode.

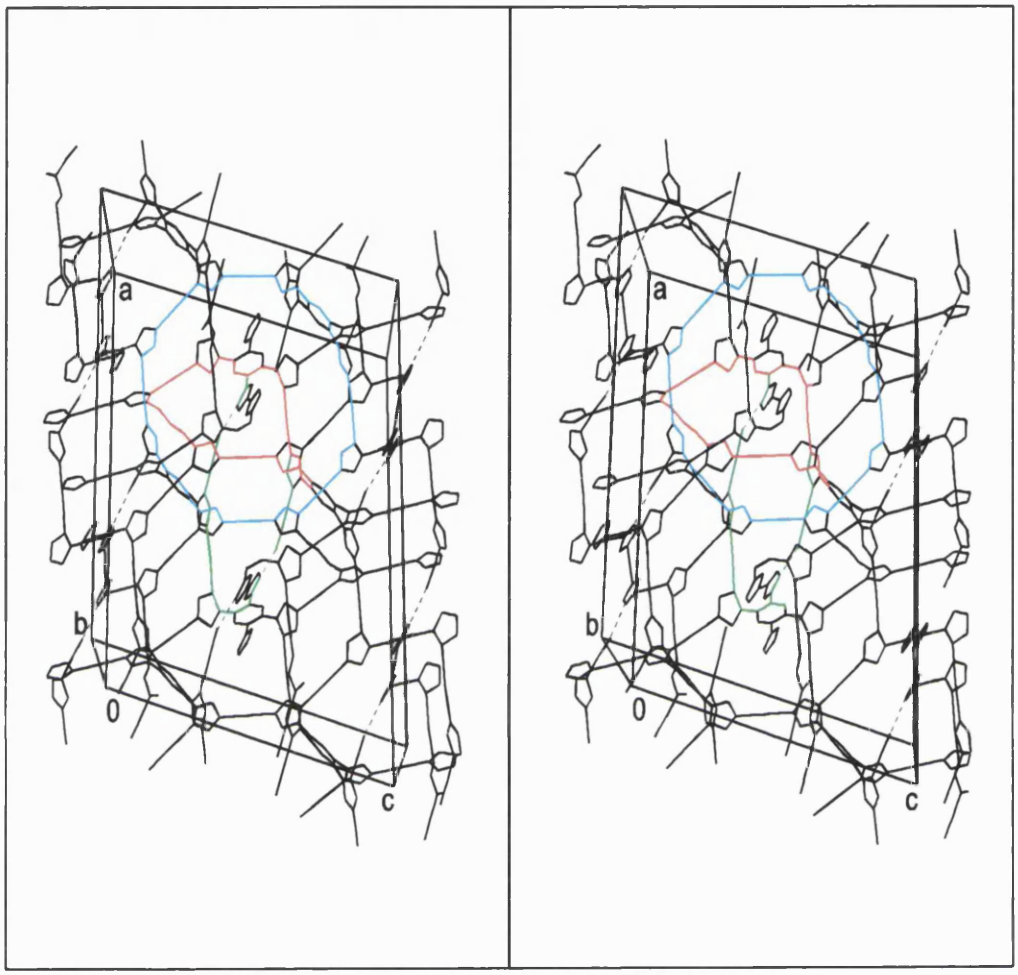

Fig.2.12: Stereo plot of **2.**

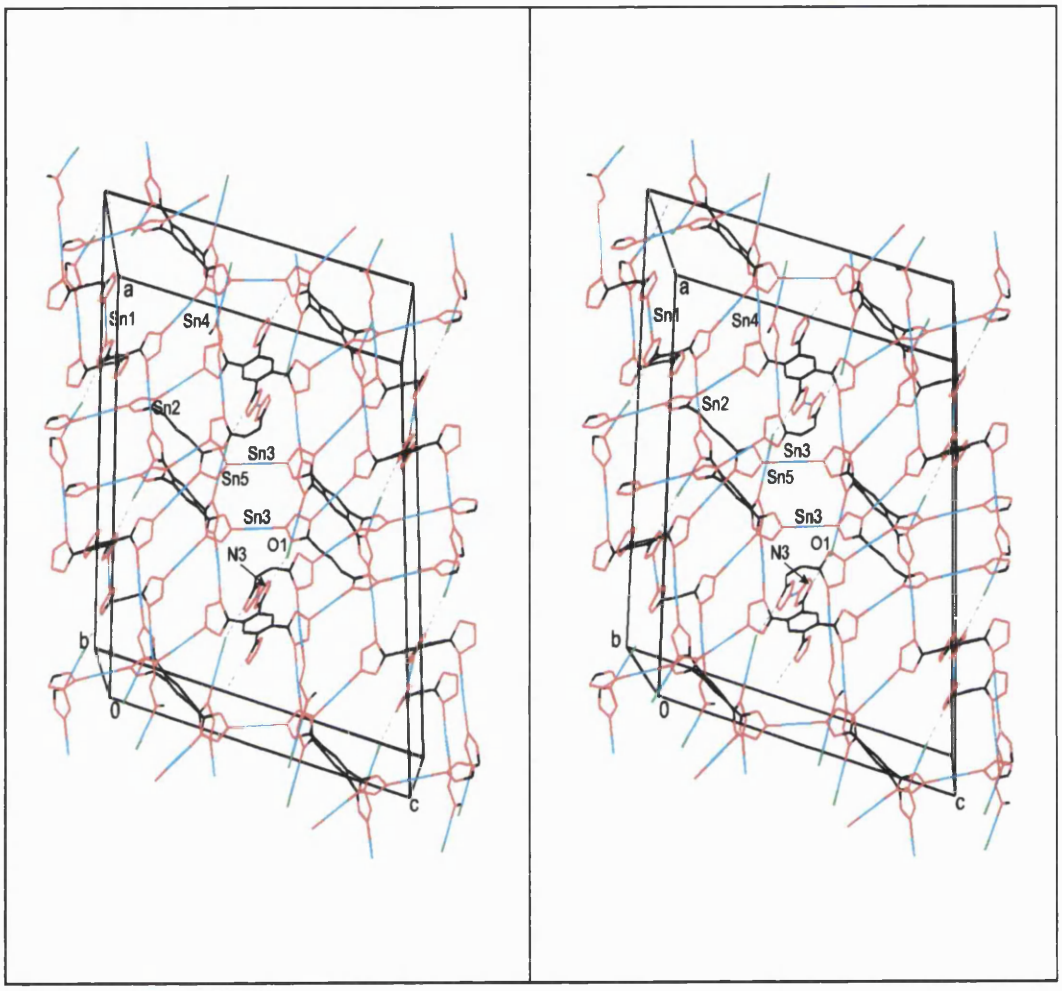

Fig.2.13: Stereo plot of **2**.

Table 2.5: Selected Bond Lengths (Å) For **2** With Their Estimated Standard Deviations In Parentheses.

Sn(1)-C(101)	2.11(5)	Sn(3)-C(305)	2.38(8)
Sn(1)-C(103)	2.13(6)	Sn(3)-C(303)	2.44(7)
Sn(1)-C(105)	2.28(6)	Sn(4)-C(401)	2.08(3)
Sn(1)-N(1)	2.36(1)	Sn(4)-C(403)	2.13(3)
Sn(2)-C(205)	2.14(2)	Sn(4)-C(405)	2.25(3)
Sn(2)-C(203)	2.15(2)	Sn(4)-N(15)	2.39(1)
Sn(2)-C(201)	2.15(2)	Sn(4)-N(6)	2.42(1)
Sn(2)-N(9)	2.37(1)	Sn(5)-C(501)	2.10(3)
Sn(2)-N(8)	2.43(1)	Sn(5)-C(503)	2.14(2)
Sn(3)-C(301)	2.26(6)	Sn(5)-C(505)	2.14(3)
Sn(5)-N(11)	2.42(1)	Sn(5)-O(1)	2.27(1)

Symmetry transformations used to generate equivalent atoms:

#1 -x+1/2,-y+1/2,-z+2; #2 -x,-y+1,-z+1; #3 x,y,z; #4 -x+1/2,-y+3/2,-z+2;

#5 -x+1,y,-z+3/2; #6 -x+1/2,y+1/2,-z+3/2; #7 -x+1/2,y-1/2,-z+3/2.

Table 2.6: Selected Bond Angles (°) For **2** With Their Standard Deviations In Parentheses

C(101)-Sn(1)-C(103)	125(2)	C(205)-Sn(2)-C(203)	122.7(9)
C(101)-Sn(1)-C(105)	122(2)	C(205)-Sn(2)-C(201)	121.5(9)
C(103)-Sn(1)-C(105)	112(2)	C(203)-Sn(2)-C(201)	115.6(9)
C(101)#1-Sn(1)-C(105)#1	122(2)	C(205)-Sn(2)-N(9)	87.0(7)
C(103)#1-Sn(1)-C(105)#1	112(2)	C(203)-Sn(2)-N(9)	91.5(7)
C(101)-Sn(1)-N(1)	93(1)	C(201)-Sn(2)-N(9)	87.3(7)
C(103)#1-Sn(1)-N(1)	88(2)	C(205)-Sn(2)-N(8)	89.5(7)
C(103)-Sn(1)-N(1)	92(2)	C(203)-Sn(2)-N(8)	89.7(7)
C(105)-Sn(1)-N(1)	91(2)	C(201)-Sn(2)-N(8)	95.3(6)
C(105)#1-Sn(1)-N(1)	89(2)	N(9)-Sn(2)-N(8)	176.3(4)
C(103)-Sn(1)-N(1)#1	88(2)	C(301)-Sn(3)-C(305)	100(2)
		C(301)#2-Sn(3)-C(305)#2	100(2)
		C(301)-Sn(3)-C(305)#2	80(2)

Symmetry transformations used to generate equivalent atoms:

#1 -x+1/2,-y+1/2,-z+2; #2 -x,-y+1,-z+1; #3 x,y,z; #4 -x+1/2,-y+3/2,-z+2;

#5 -x+1,y,-z+3/2; #6 -x+1/2,y+1/2,-z+3/2; #7 -x+1/2,y-1/2,-z+3/2.

2.5 SUMMARY

In conclusion, the cycloaddition route used to synthesise mono-, bis- and tris-triorganotin-substituted tetrazoles has been successfully extended to the synthesis and characterisation of tetra-triorganotin-substituted tetrazoles. Structural analysis of the second hydrated organotin-substituted tetrazole and the first organotin-substituted tetrazole exhibiting a host-guest type interaction has been obtained.

2.6 EXPERIMENTAL

The tributyltin and triethyltin azides were prepared by the literature methods.[110] The method of Belsky *et al* [111] was used to prepare 1,3,3,5-pentane tetracarbonitrile. All other reagents were of commercial origin (e.g. Aldrich) and used without further purification.

Preparation of 1,2,4,5-tetra-(tributylstannyl tetrazole) benzene (**1**).

A mixture of tributyltin azide (2.89g, 8.7 mmol) and 1,2,4,5-tetracyanobenzene (0.39g, 2.12 mmol) was heated under N_2 at 120°C for 45 mins. The reaction mixture formed a white solid at this temperature, which was then dissolved in hot methanol. Hot filtration afforded a green solution, which on cooling, afforded a green gum. The green gum, when washed with hexanes, gave **1** as a green powder (0.99g, 30%) (m.p. 210°C dec.).

Analysis: Found (Calc. for $C_{58}H_{110}N_{16}Sn_4$): C 46.2 (47.2); H 7.30 (7.20); N 14.9 (15.1)%.

^{1}H NMR [δ(ppm), DMSO-d^6 solution]: 8.49 [s,1H, *3*-C_6H_2]; 8.10 [s, 1H, *6*-C_6H_2]; 1.45 [m, 24H, $SnCH_2CH_2CH_2CH_3$]; 1.20-1.30 [m, 48H, $SnCH_2CH_2CH_2CH_3$]; 0.77 [m, 36H, $(CH_2)_3CH_3$].

^{13}C NMR [δ(ppm), DMSO-d^6 solution]: 159.9 [*C*N$_4$]; 134.2 [*3,6-C*$_6$H$_2$]; 117.7 [*1,2,4,5-C*$_6$H$_2$]; 27.7 [SnCH$_2$*CH$_2$*CH$_2$CH$_3$]; 26.5 [Sn(CH$_2$)$_2$*CH$_2$*CH$_3$]; 18.4 [Sn*CH$_2$*(CH$_2$)$_2$CH$_3$]; 13.5 [(CH$_2$)$_3$*CH$_3$*]; ^{2}J[^{13}*CH$_2$*-^{117,119}*Sn*] 77.2 Hz (unresolved); ^{3}J[^{13}*CH$_2$*-^{117,119}*Sn*] 28.6 Hz (unresolved).

^{119}Sn NMR [δ(ppm), DMSO-d^6 solution]: -48.6.

IR [(cm^{-1}), KBr disk]: 3406, 2957, 2924, 2872, 2856, 1658, 1618, 1464, 1417, 1377, 1358, 1292, 1217, 1157, 1080, 1047, 1026, 879, 769, 700, 679, 524, 432.

^{119m}Sn Mössbauer (mms^{-1}): I.S. = 1.50; Q.S. = 3.67.

Preparation of 1,2,4,5-tetra-(triethylstannyltetrazole) benzene.3½H$_2$O (**2**)

A mixture of triethyltin azide (0.92g, 3.71mmol) and 1,2,4,5-tetracyanobenzene (0.15g, 0.84mmol) was heated under N_2 at 105°C for 30 mins. The reaction mixture formed a white solid at this temperature, which was washed with hexanes and dried *in vacuo*. The resultant white powder was partially soluble in methanol. Hence, it was dissolved in hot methanol in a Soxhlet apparatus. Hot filtration afforded a clear solution, which on cooling at room temperature afforded colourless crystals (0.59g, 56%) (m.p. 200°C).

Analysis: Found (Calc. for C$_{34}$H$_{62}$N$_{16}$Sn$_4$.3½H$_2$O): C 33.5 (33.1); H 5.32 (5.60); N 17.8 (18.2)%.

^{1}H NMR [δ(ppm), DMSO-d^6 solution]: 8.0 [s, 2H, *3,6*-C$_6$*H$_2$*]; 0.8-1.4 [m, 60H, *CH$_2$CH$_3$*].

^{13}C NMR [δ(ppm), DMSO-d^6 solution]: 160.2 [*C*N$_4$]; 131.1 [*3,6-C*$_6$H$_2$]; 129.3 [*1,2,4,5-C*$_6$H$_2$]; 9.7 [*CH$_2$*CH$_3$]; 9.1 [CH$_2$*CH$_3$*]; ^{1}J[^{13}*C*-^{117,119}*Sn*] 478 Hz (unresolved); ^{2}J[^{13}*C*-^{117,119}*Sn*] 34.9 Hz (unresolved).

^{119}Sn NMR [δ(ppm), DMSO-d^6 solution]: -43.2.

IR [(cm^{-1}), KBr disk]: 3661, 3061, 2924, 2870, 1637, 1479, 1460, 1427, 1377, 1190, 1074, 1057, 1022, 997, 729, 698, 661, 524, 447.

^{119m}Sn Mössbauer (mms^{-1}): I.S. = 1.50; Q.S. = 3.76.

Preparation of 1,1,3,3-tetra-(tributylstannyltetrazole) propane (**3**)

A mixture of tributyltin azide (2.07g, 6.23mmol) and 1,1,3,3, tetrapropanenitrile (0.18g, 1.30mmol) was heated while stirring under N_2 at 130°C for half an hour. An orange brown glass was formed at this temperature, which was dissolved in hot methanol. Hot filtration resulted in a yellow solution, which, on cooling, gave a yellow gummy substance. The yellow gum, when washed with hexanes, gave **3** as a yellow powder (0.43g, 24%) (m.p. 195°C).

Analysis: Found (Calc. for $C_{55}H_{112}N_{16}Sn_4$): C 44.8 (44.0); H 7.61 (7.58); N 15.2 (14.9)%.

^{1}H NMR [δ(ppm), DMSO-d^6 solution]: 1.48 [m. 24H, Sn$CH_2$$CH_2CH_2CH_3$]; 1.2-1.3 [m, 48H, $SnCH_2CH_2CH_2CH_3$]; 0.78 [m, 36H, $(CH_2)_3CH_3$].

^{13}C NMR [δ(ppm), DMSO-d^6 solution]: 163.0 [CN_4]; 27.7 [$SnCH_2CH_2CH_2CH_3$]; 26.4 [$Sn(CH_2)_2CH_2CH_3$]; 18.1 [Sn$CH_2$$(CH_2)_2CH_3$]; 13.5 [$(CH_2)_3CH_3$]; ^{2}J[^{13}C-^{117,119}Sn] 76 Hz (unresolved).

^{119}Sn NMR [δ(ppm), DMSO-d^6 solution]: -50.2.

IR [(cm^{-1}), KBr disk]: 3420, 2957, 2924, 2872, 2855, 2073, 1653, 1635, 1464, 1377, 1342, 1292, 1155, 1126, 1026, 960, 879, 679, 611.

^{119m}Sn Mössbauer (mms^{-1}): I.S. = 1.47; Q.S. = 3.65.

Preparation of 1,1,3,3-tetra-(triethylstannyltetrazole) propane.4H_2O (**4**)

A mixture of triethyltin azide (1.83g, 7.38mmol) and 1,1,3,3-tetrapropanenitrile (0.26g, 1.81mmol) was heated while stirring under N_2 at 95°C for 30 mins. The resultant yellow glass was dissolved in hot methanol. Hot filtration afforded a yellow solution which, on cooling, gave a yellow gummy substance. The yellow gum, when washed with hexanes, gave **4** as a yellow powder (1.75g, 80%) (m.p. 205°C dec.).

Analysis: Found (Calc. for $C_{31}H_{64}N_{16}Sn_4.4H_2O$): C 31.8 (30.8); H 5.68 (5.96); N 19.0 (18.5)%.

^{1}H NMR [δ(ppm), DMSO-d^6 solution]: 1.0-1.3 [m, 60H, CH_2CH_3].

^{13}C NMR [δ(ppm), DMSO-d^6 solution]: 163.5 [CN_4]; 10.1 [CH_2CH_3]; 10.0 [CH_2CH_3]; ^{1}J[$^{13}C^{117,119}Sn$] 478 Hz (unresolved).

^{119}Sn NMR [δ(ppm), DMSO-d^6 solution]: -45.1.

IR [(cm^{-1}), KBr disk]: 3406, 3182, 2949, 2870, 2735, 1458, 1421, 1379, 1199, 1126, 1016, 956, 684.

^{119m}Sn Mössbauer (mms^{-1}): I.S. = 1.53; Q.S. = 3.87.

Preparation of 1,3,3,5-tetra-(tributylstannyltetrazole) pentane (**5**)

A mixture of tributyltin azide (2.13g, 6.42 mmol) and 1,3,3,5-tetracyanopentane (0.26g, 1.5 mmol) was heated under N_2 at 170°C for 15 mins. The reaction mixture formed an orange glass at this temperature, which was dissolved in hot methanol. Hot filtration afforded a yellow solution, which on cooling, gave a yellow gummy substance. The gummy solid, when washed with hexanes, gave **5** as a yellow powder (1.56g, 70%) (m.p. 209°C).

Analysis: Found (Calc. for $C_{57}H_{116}N_{16}Sn_4$): C 45.6 (44.1); H 7.73 (7.46); N 14.9 (14.7)%.

^{1}H NMR [δ(ppm), DMSO-d^6 solution]: 2.50-2.80 [m, 4H, C*(CH$_2$CH$_2$)$_2$*]; 1.48 [m, 24H, Sn*CH$_2$*CH$_2$CH$_2$CH$_3$]; 1.20-1.25 [m, 48H, SnCH$_2$*CH$_2$CH$_2$*CH$_3$]; 0.76 [m, 36H, (CH$_2$)$_3$*CH$_3$*].

^{13}C NMR [δ(ppm), DMSO-d^6 solution]: 160.0 [*C*N$_4$]; 27.7 [SnCH$_2$*CH$_2$*CH$_2$CH$_3$]; 26.4 [Sn(CH$_2$)$_2$*CH$_2$*CH$_3$]; 18.1 [Sn*CH$_2$*(CH$_2$)$_2$CH$_3$]; 13.5 [(CH$_2$)$_3$*CH$_3$*]; ^{1}J[^{13}*C*-^{117,119}*Sn*] 476 Hz (unresolved); ^{2}J[^{13}*C*-^{117,119}*Sn*] 75.4 Hz (unresolved).

^{119}Sn NMR [δ(ppm), DMSO-d^6 solution]: -53.5.

IR [(cm^{-1}), KBr disk]: 3387, 2957, 2924, 2872, 2856, 1655, 1589, 1464, 1400, 1377, 1342, 1292, 1251, 1226, 1080, 1049, 1026, 962, 879, 771, 748, 679, 611, 515, 453.

^{119m}Sn Mössbauer (mms^{-1}): I.S. = 1.47; Q.S. = 3.59.

Preparation of 1,3,3,5-tetra-(triethylstannyltetrazole) pentane (**6**)

A mixture of triethyltin azide (1.72g, 6.9mmol) and 1,3,3,5 tetracyanopentane (0.25g, 1.5mmol) was heated under N_2 at 160°C for 30 mins. The resultant yellow glass was dissolved in hot methanol. Hot filtration afforded a yellow solution which, on cooling, gave a yellow gummy substance. The gummy solid, when washed with hexanes, gave **6** as a yellow powder (1.17g, 68%) (m.p. 206°C dec.).

Analysis: Found (Calc. for $C_{33}H_{68}N_{16}Sn_4$): C 33.3 (34.0); H 5.78 (5.84); N 19.0 (19.2)%.

^{1}H NMR [δ(ppm), DMSO-d^6 solution]: 1.04-1.50 [m, 60H, *CH$_2$CH$_3$*]; 2.48-2.55 [m, 4H, C*(CH$_2$CH$_2$)$_2$*].

^{13}C NMR [δ(ppm), DMSO-d^6 solution]: 161.5 [*C*N$_4$]; 121.9 [(CN$_4$)$_2$*C*]; 38.2 [(CN$_4$)$_2$C(CH$_2$)$_2$*(CH$_2$)$_2$*]; 21.9 [(CN$_4$)$_2$C*(CH$_2$)$_2$*(CH$_2$)$_2$]; 10.9 [*CH$_2$*CH$_3$]; 10.8 [CH$_2$*CH$_3$*]; ^{1}J[^{13}*C*-^{117,119}*Sn*] 482 Hz (unresolved).

^{119}Sn NMR [δ(ppm), DMSO-d^6 solution]: -51.8.

IR [(cm^{-1}), KBr disk]: 2949, 2850, 1637, 1458, 1400,1196, 1130, 1016, 962, 682.

^{119m}Sn Mössbauer (mms^{-1}): I.S. = 1.43; Q.S. = 3.63.

Preparation of 1,4-bis-(tributylstannyl tetrazole) benzene.H_2O (**7**)

A mixture of tributylstannyl azide (17.9g, 54.0 mmol) and 1,4-dicyanobenzene (3.46g, 27.0 mmol) was taken and heated under N_2 to 130°C for 30mins during which time the reaction mixture solidified. After cooling, the white solid was dissolved in hot methanol. Hot filtration afforded a clear yellow solution, which on cooling at -20°C afforded **7** as white crystals (11.3g, 53%) (m.p. 215°C).

Analysis: Found (Calc. for $C_{32}H_{58}N_8Sn_2.H_2O$): C 47.3 (47.4); H 7.48 (7.41); N 13.8 (13.8)%.

^{1}H NMR [δ(ppm), DMSO-d^6 solution]: 8.19 [s, 4H, *2,3,5,6-C_6*H_4]; 1.61 [m, 24H, Sn*CH_2*$CH_2CH_2CH_3$]; 1.28-1.37 [m, 48H, $SnCH_2$*CH_2CH_2*CH_3]; 0.86 [m, 36H, $(CH_2)_3$*CH_3*].

^{13}C NMR [δ(ppm), DMSO-d^6 solution]: 161.9 [*C*N_4]; 130.2 [*1,4-C_6*H_4]; 126.5 [*2,3,5,6-C_6*H_4]; 27.7 [$SnCH_2CH_2$*CH_2*CH_2]; 26.5 [$SnCH_2$*CH_2*CH_2CH_2]; 18.4 [Sn*CH_2*$(CH_2)_2CH_3$]; 13.6 [$Sn(CH_2)_3$*CH_3*]; ^{1}J[^{13}*C*-^{117,119}*Sn*] 470 Hz (unresolved); ^{2}J[^{13}*C*-^{117,119}*Sn*] 29.4 Hz (unresolved); ^{3}J[^{13}*C*-^{117,119}*Sn*] 75.4 Hz (unresolved).

^{119}Sn NMR [δ(ppm), DMSO-d^6 solution]: -54.4.

IR [(cm^{-1}), KBr disk]: 3412, 2959, 2924, 2855, 1618, 1464, 1442, 1427, 1365, 1377, 1342, 1159, 1082, 1010, 852, 752, 680, 615, 478, 465.

^{119m}Sn Mössbauer (mms^{-1}): I.S. = 1.48; Q.S. = 3.84.

Chapter 3

The Synthesis And Characterisation Of Organotin-Substituted Functionalised-tetrazoles

3.1 INTRODUCTION

In Chapter 2, the successful extention of cycloaddition chemistry to prepare a series of triorganotin-substituted tetra-tetrazoles was described. This chapter extends the study further to triorganotin-substituted functionalised tetrazoles especially pyridyl-tetrazoles.

Organotin-substituted pyridyl tetrazoles could have a wide range of applications in intercalation (host-guest) chemistry. The phenomenon of intercalation was first discovered by the Chinese in 600-700 A.D.[112] when they produced porcelain from the intercalation of alkali metal ions into commonly found naturally occurring minerals such as feldspar and kaolin[113]. Interest in intercalation in modern times dates back to 1926 when Karl Fredenhagen and Gustav Cadenbach described the uptake of potassium vapour by graphite.[114] Since then this field has rapidly grown with more than 6000 scientific papers published describing the synthesis, reactivity and physical characterisation of inorganic intercalation compounds.[115] Intercalation compounds have a wide variety of applications in materials chemistry, e.g. as superconductors, liquid crystals and as agents for extraction of precious metals from metal ores.[115] Modern host-guest chemistry can be broadly classified into two categories. The first category includes intercalation of guests into known species. A wide range of host lattices are available including framework (three-dimensional), layer (two-dimensional), linear chain (one-dimensional) and molecular (zero-dimensional) lattices as shown in Fig.3.1.[115] A typical example of intercalation of a guest species into a layered inorganic lattice is the reaction of lithium with the layered

metal dichalcogenide TiS_2.[116] The product of the reaction is $LiTiS_2$ which has a structure slightly expanded in the direction perpendicular to the layers.

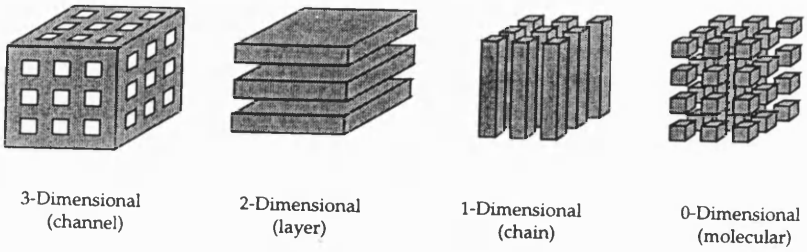

Fig.3.1: Schematic representation of host lattices with different structural dimensionality[115]

The second category includes design of molecules which yield cavities which can incorporate a guest. Typical examples of such ligands are crown ethers[117] (Fig.3.2a), cryptands[117] (Fig.3.2b), and podands[118-120] (Fig.3.2c).

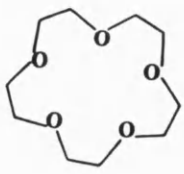

Fig.3.2a

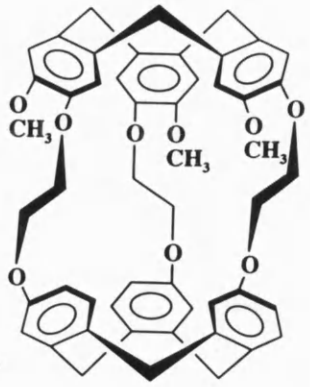

Fig.3.2b

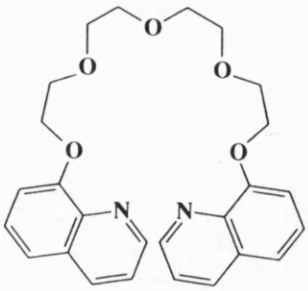

Fig.3.2c

Functionalised organotin-substituted tetrazoles have the potential of being used as host lattices in two possible ways. It has been established that organotin-substituted tetrazoles form extended structures in the solid-state.[24,80] By functionalising the organotin moiety, additional groups can be incorporated in these extended structures which can 'trap' guests. In addition, functionalised organotin tetrazoles can also serve as precursors to new, polydentate N-donor ligands. Precedents for such precursors include the synthesis of bis-tetrazole units linked with durable alkyl chains.[24]

Indeed, examples of tri-, di- and mono-organotin(IV) derivatives of pyridine carboxylic acids have been reported in the literature, where the carboxylate group competes with the pyridine nitrogen to chelate to the tin. The 2-, 3- and 4-pyridine carboxylate groups exhibit mono-, bi- or tri-dentate behaviour towards organotin(IV) depending upon the Lewis acidity of tin.[121] In complexes where the pyridine carboxylate group behaves as mono- or bi-dentate, N- or O- donor sites are available to trap 'guest' molecules.

3.2 SYNTHESIS OF ORGANOTIN-SUBSTITUTED FUNCTIONALISED-TETRAZOLES

Six triorganotin-substituted pyridyl tetrazoles and bis-{[2-(tributylstannyltetrazole)-phenoxy] ethyl}ether **(8-14)** have been synthesised (equations 3.1-3.4) using the well-established cycloaddition route of Sisido *et al*[103] and Molloy *et al*[53]. Typically, the functionalised organo-nitrile was heated with a slight excess of the appropriate organotin azide under N_2 neat. Reactions had to be heated over a temperature range of 100-140°C over 30 to 60 mins to attain completion. The disappearance of the IR bands due to the $\nu(N_3)$ at ~2060cm^{-1} and ν(CN) at ~2250cm^{-1} usually marked the end of the reactions. Characteristic aromatic bands between 1500-1600cm^{-1} in compounds **8-14** confirmed the presence of the phenylene ring. The functionalised-tetrazolyl compounds listed in this chapter exhibited the expected strong CH stretches and deformations at 2900cm^{-1} and 1460cm^{-1} respectively. Another feature of the IR spectra of the compounds

listed in this chapter are medium strength bands at 1000-1100cm^{-1} characteristic of tetrazole rings.

The crude solid products for **8-14** were recrystallised from methanol. Cooling the methanolic solution gave **8, 10-13** as a white crystalline solids and **9** and **14** as white powders. Compounds **8-10, 12** and **14** were obtained as anhydrous solids and characterised accordingly. However, **11** was obtained as a hydrate and **13** was obtained as a methanolate. Crystallographic characterisation of **8, 9** and **11** was performed. Dihydrated crystals of **8** were obtained from methanol, anhydrous crystals of **9** were grown from dichloromethane and monohydrated crystals of **11** were procured from methanol.

Section 3.5 gives detailed synthetic procedures and work-up of compounds **8-14**.

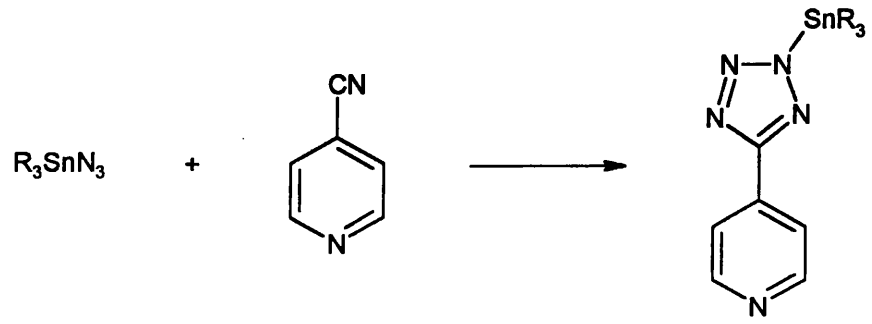

Eq.3.1

R = Bu (8), Et (9)

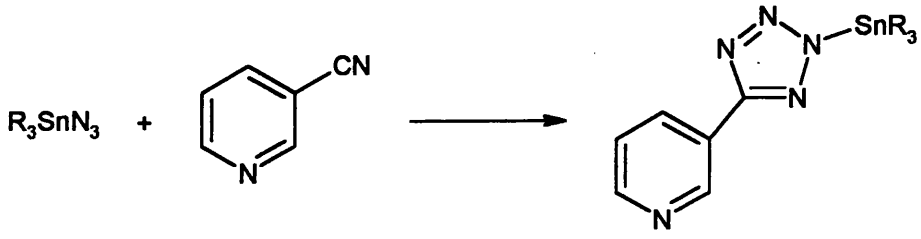

Eq.3.2

R = Bu (10), Et (11)

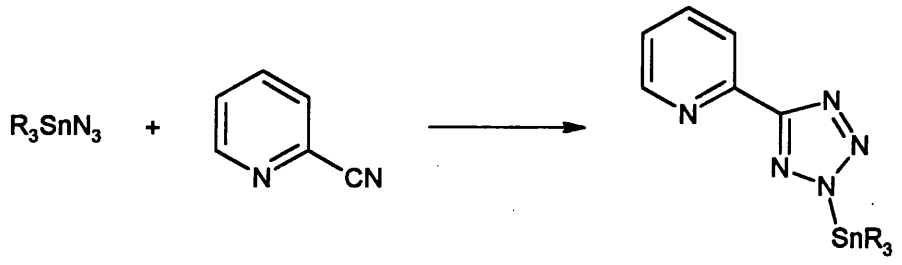

Eq.3.3

R = Bu (**12**), Et (**13**)

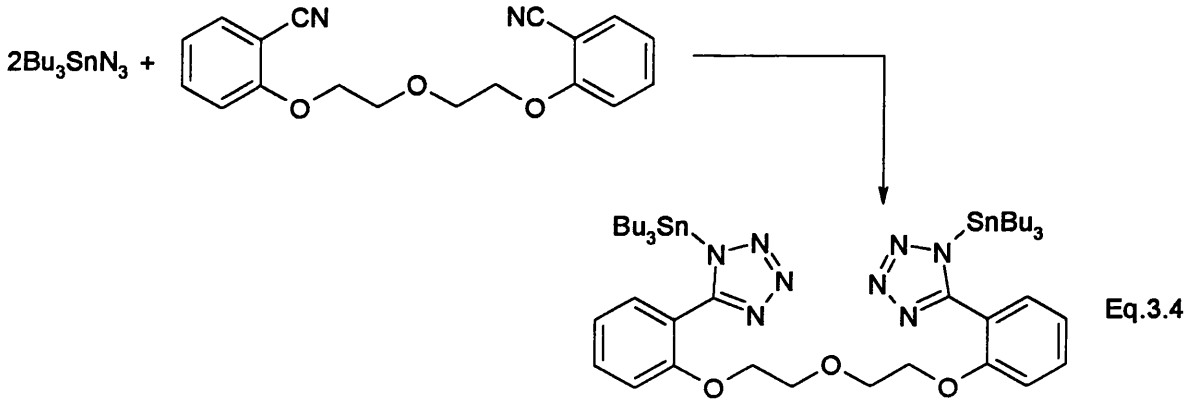

Eq.3.4

(**14**)

3.3 SPECTROSCOPY

3.3.1 Mössbauer Spectroscopy

The Mössbauer data for triorganotin-substituted functionalised tetrazoles are given in Table 3.1. The isomer shifts fall within the range 1.40-1.50 mms^{-1} and quadrupole splittings (q.s.) fall within the range 3.4-3.5 mms^{-1}. The former confirms the +4 oxidation state of tin while the latter points towards a *trans*-trigonal bipyramidal geometry about tin. The q.s. value of a related compound 2-(tributylstannyl)-5-(2′-pyridyl-6′-Me) tetrazole is 3.69 mms^{-1}.[80] *Trans*-trigonal bipyramidal geometry about tin is consistent with all

published organotin tetrazole structures.[24,80] The *trans*-trigonal bipyramidal geometry is achieved via *trans*-N_2SnC_3 type coordination which is also consistent with all organotin tetrazole structures known to date. Possible exceptions may arise in the case of **11**, **13** and **14**. In these three cases, both *trans*-N_2SnC_3 and *trans*-$NOSnC_3$ type coordinations are consistent with the Mössbauer data as discussed in Section 2.3.1. *Trans*-$NOSnC_3$ coordination arises if intermolecular N→Sn interaction is replaced by H_2O→Sn or by Me(H)O→Sn interaction and in the case of **14** by attainment of a structure of type **XXXIII**. As pointed out in Section 2.3.1, Mössbauer spectroscopy is not capable of distinguishing between the two environments. Narrow linewidths for **11** (Γ = 0.93, 0.93), **13** (Γ = 0.87, 0.99) and **14** (Γ = 0.82, 0.84) rule out the presence of a mixture of both environments.

This five coordinate *trans*-N_2SnC_3 geometry for compounds **8-14** can be attained via intermolecular coordination through the tetrazole nitrogen (**XXX**). For the pyridyl compounds (**8-13**), an additional possibility of intermolecular coordination through the pyridyl nitrogen exists (**XXXII**). The pK_b of pyridine is 8.6 while the pK_b of tetrazoles falls in the range of 9-12 with the aliphatic tetrazoles being at the lower end and the aromatic tetrazole at the higher end of the range.[10] In the competition to coordinate to tin between the pyridyl nitrogen and the tetrazole nitrogen, the former has a marginal preference due to its lower pK_b. A precedent for an analogous pyridine→Sn coordination has been observed for [2-(2′-pyridyl)ethyl]diphenyl tin(IV) N,N-dimethyldithiocarbamate.[122] Parallels can also be drawn with di-organotin(IV) derivatives of pyridine carboxylic acids.[121] Whereas ν_{as}(CO) and Mössbauer data for dimethyltin bis(3-pyridine carboxylate) suggest a polymeric structure with bridging carboxylate groups (**XXXIV**), the presence of an uncoordinated ν_{as}(CO) band in diphenyltin bis(2-pyridine carboxylate) suggests coordination to the tin through nitrogen (**XXXV**). It must be noted here that tetrazoles are considered to be nitrogen analogues of carboxylic acids (see Section 1.1). This makes the comparison between organotin(IV) derivatives of pyridine carboxylic acids and pyridyl tetrazoles more sound.

Table 3.1: ^{119}Sn NMR[a] and Mössbauer Studies[b] of Organotin-Substituted Fuctionalised-(tetrazoles)

Compound	$\delta(^{119}Sn)$[c]	$^{1}J(^{117,119}Sn-^{13}C)$ (Hz)	(δ)	ΔEq	Γ_1, Γ_2[d]
8	-49.4	466	1.43	3.48	0.95, 0.97
9	-50.9	-	1.48	3.58	0.88, 0.93
10	-52.1	478	1.46	3.53	0.82, 0.85
11	-48.3	496	1.45	3.63	0.93, 0.93
12	-47.1	461	1.47	3.75	0.81, 0.83
13	-42.0	478, 500	1.48	3.77	0.87, 0.99
14[e]	-46.7	463	1.47	3.72	0.82, 0.84

[a] All spectra run as DMSO-d^6 solutions at 25°C except **14**

[b] Mössbauer data recorded at 78K and data given as mms^{-1}

[c] Values given in ppm

[d] Refers to full width at half height of the high and low velocity resonances

[e] Spectra run at 50°C

IIIXXX

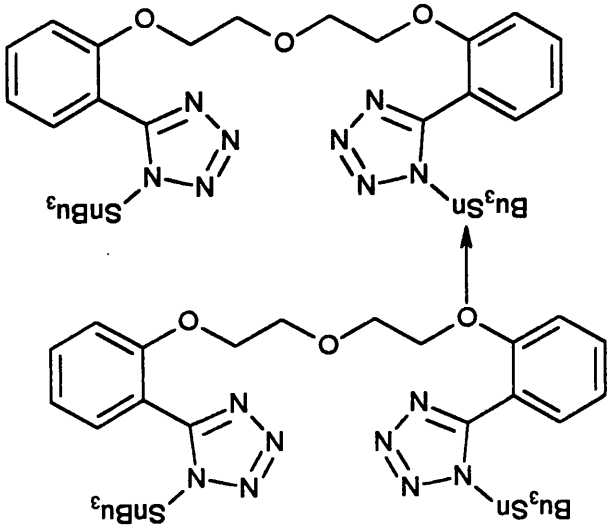

IIXXX

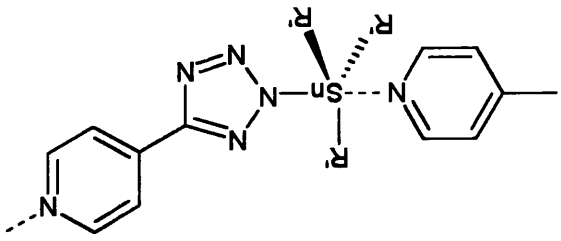

XXX

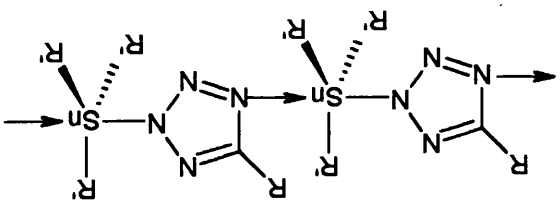

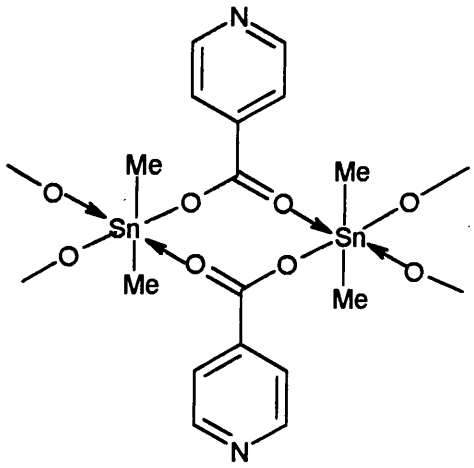

XXXIV

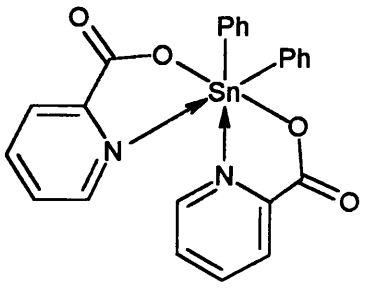

XXXV

3.3.2 Multinuclear NMR Spectroscopy

For all the organotin-substituted tetrazoles, ^{1}H, ^{13}C and ^{119}Sn NMR data were collected in d^{6}-DMSO. Table 3.1 gives the ^{119}Sn NMR data for all the compounds discussed in this chapter. ^{1}H and ^{13}C NMR data confirm the proposed structures.

The ^{1}H NMR spectra for all the tributyltin-substituted compounds show butyl resonances as multiplets at 0.8 ppm corresponding to the δ-CH_3 protons, at 1.3 ppm corresponding to β-CH_2 and γ-CH_2 protons and at 1.5 ppm corresponding to α-CH_2

protons. The triethyltin-substituted compounds show ethyl resonances as a multiplet at 0.8-1.5 ppm. In **8** and **9**, the aromatic protons in the 2,6 positions are equivalent as are those in positions 3,5. In **10** and **11**, the four aromatic protons of the 3-pyridyl ring are non-equivalent. Similarly in **12** and **13**, the four aromatic protons of the 2-pyridyl ring are non-equivalent. The ^{1}H NMR spectrum of **14** clearly shows the aromatic protons of the two phenyl rings and the ethyl protons of the ether groups appear as triplets.

The ^{13}C NMR spectra of all the compounds included in this chapter clearly show the quaternary carbon of the tetrazole ring at approximately 160 ppm. For **8**, **10**, **12** and **14**, butyl resonances appear between 13 and 27 ppm. Resonances for C_β and C_γ are reversed reasons for which have been discussed in Section 2.3.2. The $^{2}J(Sn\text{-}C_\beta)$ coupling constant is ~28 Hz while the $^{3}J(Sn\text{-}C_\gamma)$ coupling constant is ~78 Hz. For **9**, **11** and **13**, ethyl resonances appear between 10.0-10.1 ppm. The $^{1}J(Sn\text{-}C_\alpha)$ for the organotin-substituted functionalised tetrazoles listed in this chapter wherever observed is ~480 Hz. This value falls within the range for *trans*-trigonal bipyramidal geometry about tin (see Section 1.5.2). The semi-empirical relationship derived by Holecek and Lycka [77] for correlating ^{1}J and C-Sn-C angle suggests a range of 122-124° for compounds **8**, **10**, **12** and **14** consistent with this geometry. As discussed in Section 2.3.2, this information is also indicative of the geometry of the tin centre for the ethyl analogues (**9**, **11** and **13**).

For compounds **8-13**, the aromatic protons of the pyridyl ring can be clearly seen. The ^{13}C NMR spectrum of **14** shows the aromatic carbons of the two phenyl rings and the ethyl carbons.

^{119}Sn NMR resonances appear in the range of -40 to -80 ppm. This range of values indicates a five coordinate tin in comparison with organotin-substituted tetrazoles reported previously and those listed in Chapter 2. Attainment of structures of the type **XXX**, **XXXII**, **XXXIII** or **XXXI** (the tin centre is coordinated to a DMSO molecule) enables the formation of a five coordinate tin. However, in a coordinating solvent like DMSO, any of these structures could be formed and all that can be inferred is that the tin is five coordinate.

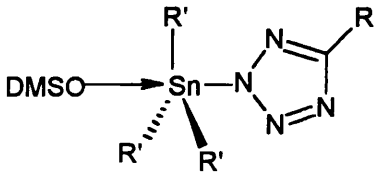

XXXI

The ^{119}Sn NMR signals obtained for compounds **8-14** have broad linewidths. This was also observed for compounds **1-7**. As discussed in Section 2.3.2, this is probably due to the fluxionality of the tin around the tetrazole ring.

3.4 X-RAY CRYSTALLOGRAPHY

The following sections describe the crystallographic analysis of 4-pyridyl-(triethyltin tetrazole) (**9**), 3-pyridyl-(triethylstannyltetrazole).H_2O (**11**), and 4-pyridyl-(tributylstannyl tetrazole).$2H_2O$ (**8**).

3.4.1 Crystal Structure Of 4-Pyridyl-(Triethyltin Tetrazole) (9)

Crystals of 4-pyridyl-(triethyltin tetrazole) (**9**) were grown from a dichloromethane solution at room temperature. Crystallographic analysis, atomic coordinates and thermal parameters for **9** are included in Appendix IV. The asymmetric unit of **9** is illustrated in Fig.3.3 and selected bond lengths and bond angles are given in Tables 3.2 and 3.3 respectively.

The asymmetric unit contains one trigonal bipyramidal *trans*-N_2SnC_3 tin centre. The trigonal bipyramidal tin centre is found in all previously examined organotin tetrazoles and is confirmed by spectroscopic evidence (see Sections 3.3.1 and 3.3.2) although in **9**, this geometry is obtained in a unique way. Whereas in the previous cases (see reference 24 and Sections 2.4.1 and 2.4.2), the two nitrogens came from two tetrazole moieties, in **9** one nitrogen comes from a tetrazole moiety and another one from the pyridyl group. Examination of Fig.3.3 reveals that **9** is anhydrous. The axial positions of tin are occupied

by N(1) atom of the tetrazole ring and the pyridine nitrogen. The N(1)-Sn(1)-N(5′) bond angle is close to 180° [N(1)-Sn(1)-N(5′) 178.2(2)°] and the two individual Sn-N bond lengths are equivalent within experimental error. Both with respect to itself and the tin, the tetrazole moiety is monodentate and exhibits coordination through N^2 (see numbering scheme discussed in Section 1.4). N^2 coordination is driven by steric factors and has also been seen in **7** (see Section 2.4.1).

The supramolecular structure is dominated by one-dimensional helical polymers which develop as a consequence of the six-fold screw axis intrinsic in the space group symmetry. Typically, N(5) in the asymmetric unit interacts with Sn(1) of the lattice neighbour generated by *x-y+1, x+1, z+1/6* and Sn(1) in the asymmetric unit interacts with N(5) of the lattice neighbour generated by *y-1, -x+y, z-1/6*. The bond length for this Sn-N interaction [Sn(1)-N(5′) 2.437(5)Å] is comparable to that of the Sn-N interaction in [2-(2′-pyridyl)ethyl]diphenyltin(IV) N,N-dimethyldithiocarbamate [Sn(1)-N(2) 2.486(7)Å].[122] Figs.3.4 and 3.5 show a view of the helical strand along the *c*-axis and the *a*-axis respectively. The long 'pitch' of the helix is due to the linear nature of the pyridyl-tetrazole moiety as a result of which only mild bending is possible. The torsion angle between the planes of the pyridyl ring and the tetrazole ring as shown in Fig.3.5 is 20.0(4)°. A similar helical structure of **XXXVI** but with a much shorter pitch has been reported by Lehn *et al* (Fig.3.6).[123] The pyridine-pyrimidine torsional angles are between 8.0° and 14.0°, whereas the two terminal pyridines are offset by only 3.5Å. The structure possesses an interior void of 2.6Å diameter and a helical pitch of 3.75Å.

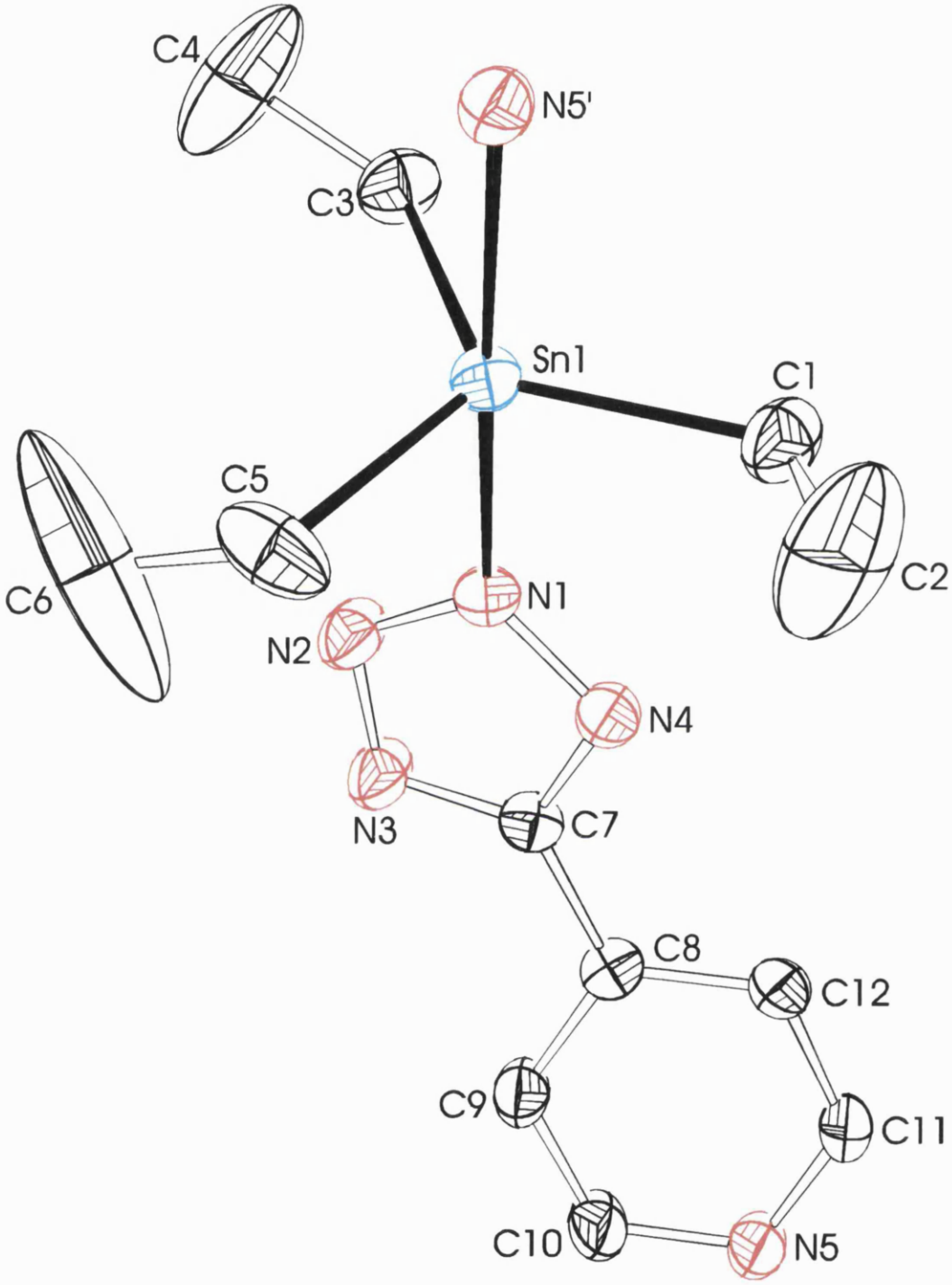

Fig.3.3: The asymmetric unit of **9** showing the atomic labeling scheme used in the text and tables. Hydrogen atoms omitted for clarity.

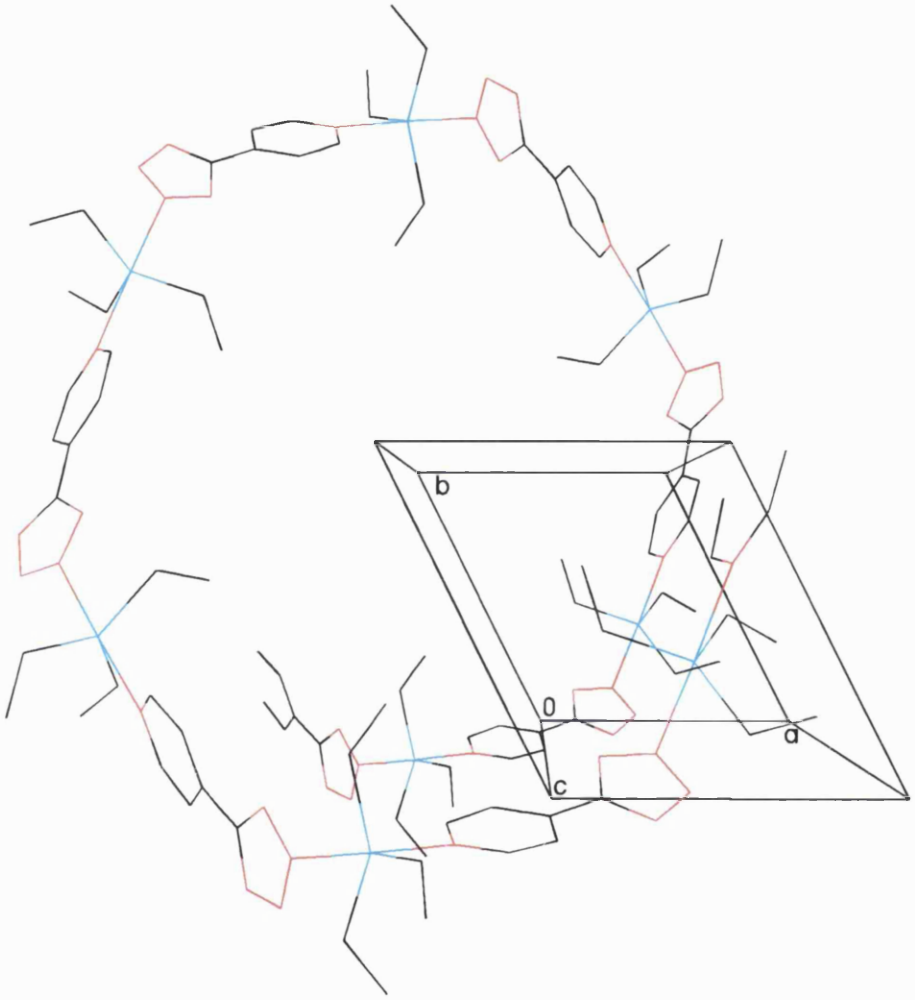

Fig.3.4: View of a helical strand of **9** along the *c*-axis.

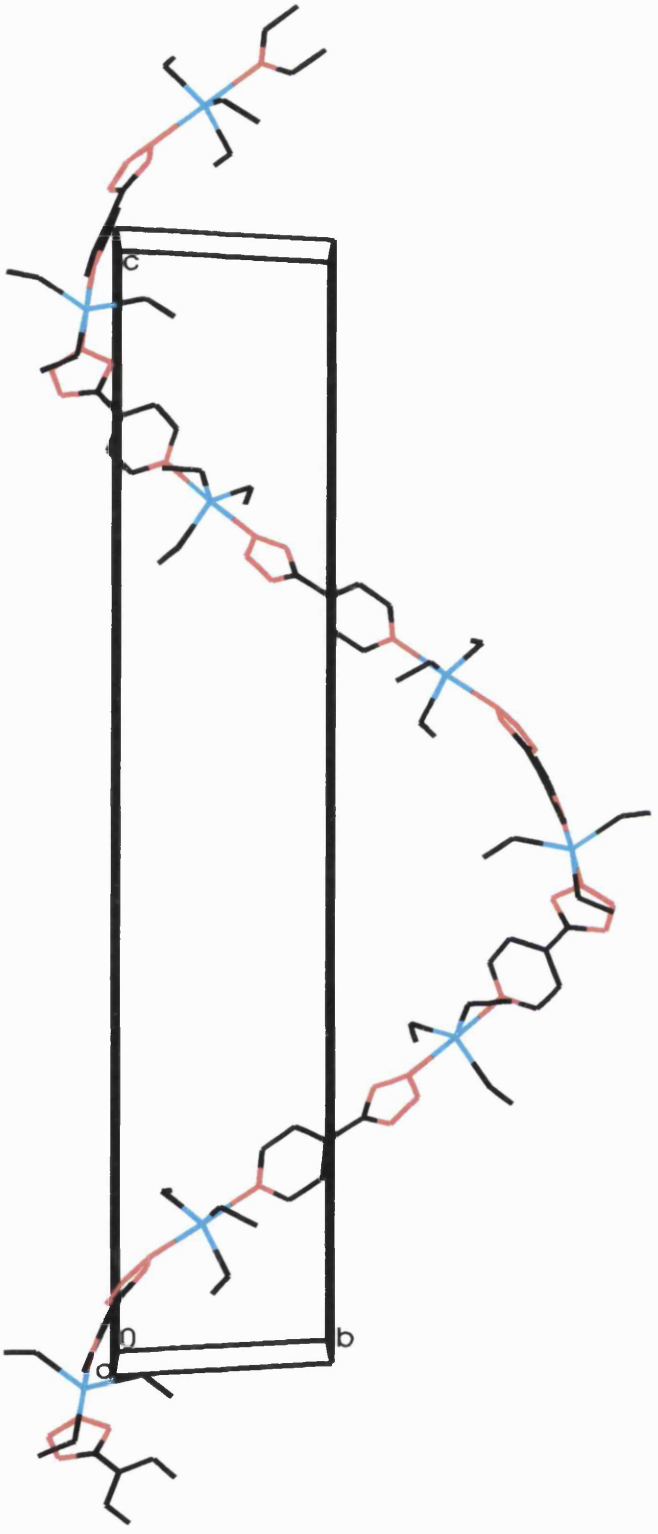

Fig.3.5: View of a helical strand of **9** along the *a*-axis

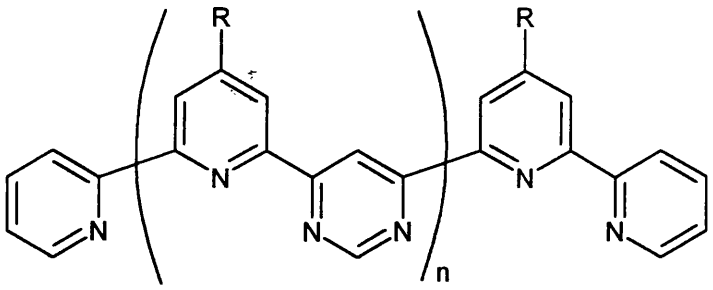

n = 5; R = S-^{n}Pr

XXXVI

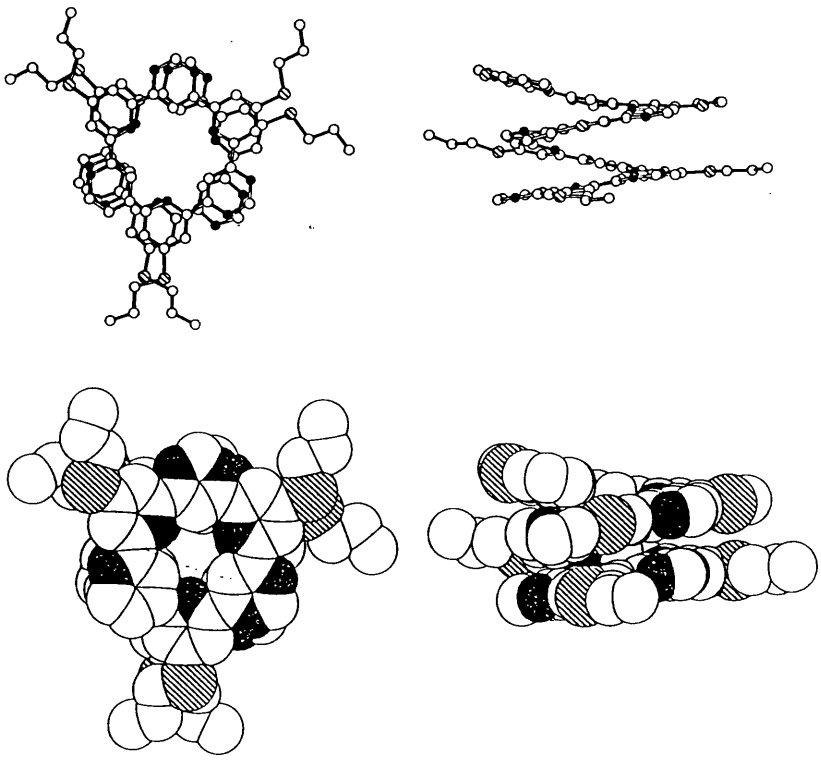

Fig3.6: Ball-and-stick (top) and space-filling (bottom) representation of the crystal structure of **XXXVI** viewed along the axis (left) and from the side (right); hydrogen atoms omitted for clarity.[123]

Table 3.2: Selected Bond Lengths (Å) For **9** With Their Estimated Standard Deviations In Parentheses.

Sn(1)-C(5)	2.129(7)	N(5)-C(10)	1.344(8)
Sn(1)-C(3)	2.133(7)	N(5)-C(11)	1.320(8)
Sn(1)-C(1)	2.141(6)	C(1)-C(2)	1.47(1)
Sn(1)-N(1)	2.344(5)	C(3)-C(4)	1.45(1)
Sn(1)-N(5)#1	2.437(5)	C(5)-C(6)	1.29(2)
N(1)-N(2)	1.310(7)	C(7)-C(8)	1.465(7)
N(1)-N(4)	1.333(7)	C(8)-C(12)	1.374(8)
N(2)-N(3)	1.323(7)	C(8)-C(9)	1.391(8)
N(3)-C(7)	1.326(7)	C(9)-C(10)	1.363(8)
N(4)-C(7)	1.335(7)	C(11)-C(12)	1.386(9)

Symmetry transformations used to generate equivalent atoms:

#1 x-y+1,x+1,z+1/6; #2 y-1,-x+y,z-1/6.

Table 3.3: Selected Bond Angles(°) For **9** With Their Estimated Standard Deviations In Parentheses.

C(5)-Sn(1)-C(3)	120.2(3)	N(2)-N(1)-Sn(1)	122.9(4)
C(5)-Sn(1)-C(1)	114.8(3)	N(4)-N(1)-Sn(1)	123.0(4)
C(3)-Sn(1)-C(1)	125.0(3)	N(1)-N(2)-N(3)	108.4(4)
C(5)-Sn(1)-N(1)	89.6(3)	N(2)-N(3)-C(7)	105.4(5)
C(3)-Sn(1)-N(1)	91.1(2)	N(1)-N(4)-C(7)	103.1(5)
C(1)-Sn(1)-N(1)	90.1(2)	C(11)-N(5)-C(10)	116.5(5)
C(5)-Sn(1)-N(5)#1	91.7(3)	C(11)-N(5)-Sn(1)#2	117.3(4)
C(3)-Sn(1)-N(5)#1	89.2(2)	C(10)-N(5)-Sn(1)#2	125.9(4)
C(1)-Sn(1)-N(5)#1	88.3(2)	C(2)-C(1)-Sn(1)	114.7(6)
N(1)-Sn(1)-N(5)#1	178.2(2)	C(4)-C(3)-Sn(1)	116.4(7)
N(2)-N(1)-N(4)	111.0(5)	C(6)-C(5)-Sn(1)	124.4(9)
C(12)-C(8)-C(9)	116.9(5)	N(3)-C(7)-N(4)	112.0(5)
N(5)-C(10)-C(9)	123.8(6)	N(3)-C(7)-C(8)	125.2(5)
N(5)-C(11)-C(12)	123.6(6)	N(4)-C(7)-C(8)	122.8(5)

Symmetry transformations used to generate equivalent atoms:

#1 x-y+1,x+1,z+1/6; #2 y-1,-x+y,z-1/6.

.3.4.2 Crystal Structure Of 3-Pyridyl-(Triethylstannyltetrazole).H_2O (11)

This is one of the few monohydrated organotin-substituted tetrazoles known to date.

Crystals of **11** were grown from a methanolic solution at room temperature. Full details of the crystallographic analysis, atomic coordinates and isotropic thermal parameters are included in Appendix V. Fig.3.7 shows the asymmetric unit of **11** and selected bond lengths and bond angles are given in Tables 3.4 and 3.5.

The asymmetric unit contains a trigonal bipyramidal *trans*-$NOSnC_3$ centre which is confirmed by spectroscopic evidence (see Section 3.3.1 and 3.3.2). All previously characterised organotin tetrazoles exhibit the trigonal bipyramidal geometry. Examination of the asymmetric unit reveals that **11** crystallises from methanol as a monohydrate. The axial positions of Sn(1) are occupied by N(1) nitrogen of the tetrazole and oxygen of the water molecule. The N-Sn-O bond angle is close to 180° [N(1)-Sn(1)-O(1) 177.0(2)°]. Thus, with respect to the tin centre, the tetrazole is monodentate via N^2 position of the tetrazole. Steric crowding leads to preference of the N^2 coordination site as discussed in Section 1.4.

Intermolecular interactions in **11** occur via hydrogen bonding. In the molecule as shown in Fig.3.6, H(1A) bonds to N(3) of the lattice neighbour generated by the transformation *-x, 0.5 + y, z* [O(1)-N(3) 2.57(3)Å; O(1)-H(1A)-N(3) 172(6)°] and H(1B) bonds to the pyridine nitrogen N(5) [O(1)-N(5) 2.60(3)Å; O(1)-H(1B)-N(5) 178(3)°]. The O-N distances are comparable with those observed in **2** [O(1)-N(3) 2.65(2)Å] (see Section 2.4.2). Fig.3.8 depicts the overall view of the structure. Hydrogen bonding interaction involving H(1A) of the water and N(3) of the tetrazole results in the formation of a polymeric chain running parallel to *b* with pendant pyridine moieties. The hydrogen bonding interactions between the water molecule attached to the tin H(1B) and the pyridyl nitrogen N(5) further links up these chains along *c* into sheets.

Taking into account the hydrogen bonding, the tetrazole is bidentate and exhibits the commonly occurring $N^1 + N^3$ mode of coordination.

The crystal structure of 1,3-phenylene-bis-5,5′-(tributylstannyltetrazole).bis methanolate (**XXV**) also shows intermolecular interactions through hydrogen-bonding (Fig.3.9).[24] Typically H(1) and H(2) of the molecule (the methanolic hydroxyl protons) interact with N(4) and N(8) of neighbouring molecules. The net result of these intermolecular bonds is an array of linear polymers along the *b*-axis as a result of N(8)-H(2) linkages. The linear polymers are cemented together along the *a*-axis as a consequence of infinite linear crosslinks through N(1) and H(1). The net result of these two interactions is a sheet-like array as shown in Fig.3.9.

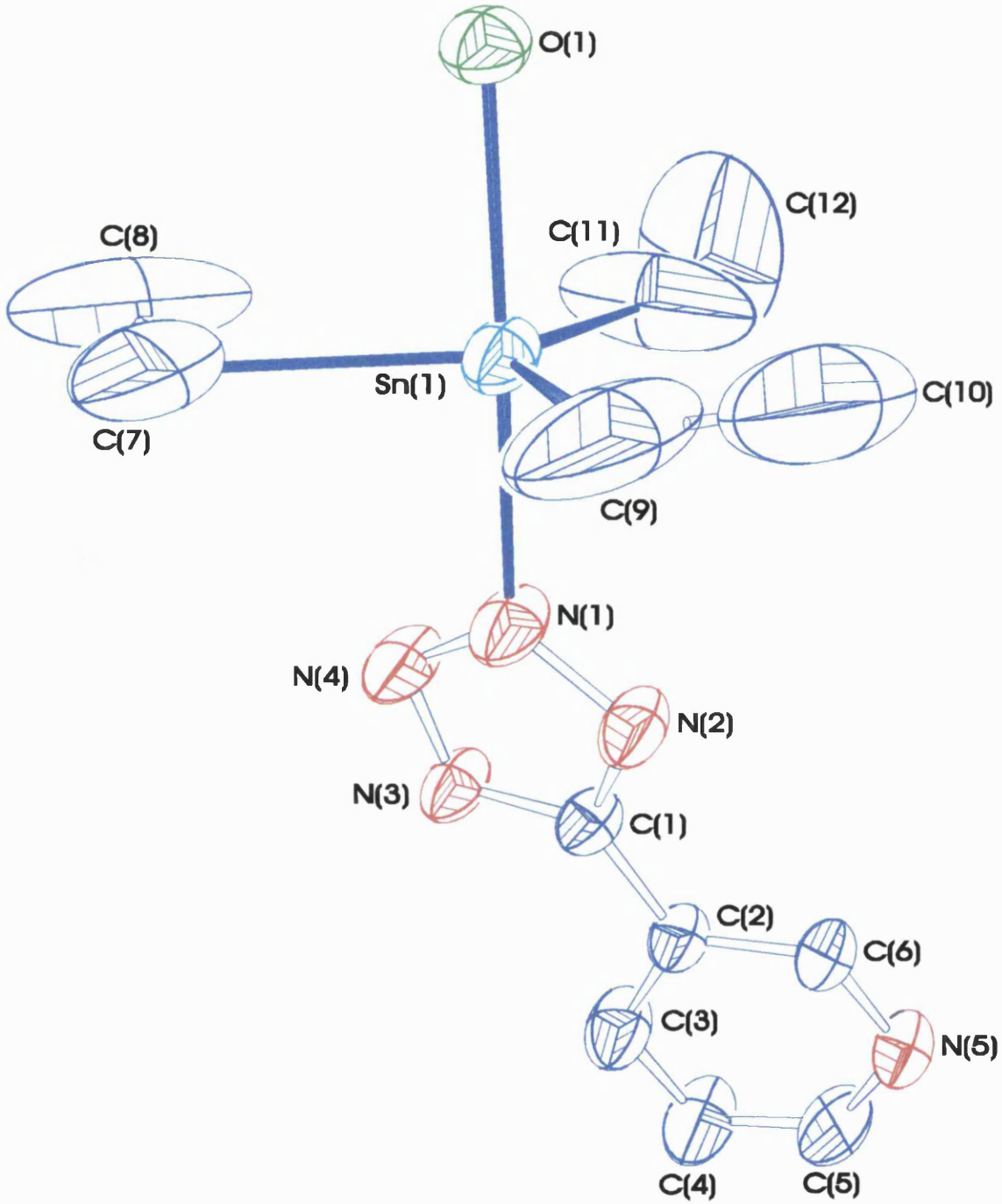

Fig.3.7: The asymmetric unit of **11** showing the atomic labeling scheme used in the text and tables. Hydrogen atoms omitted for clarity.

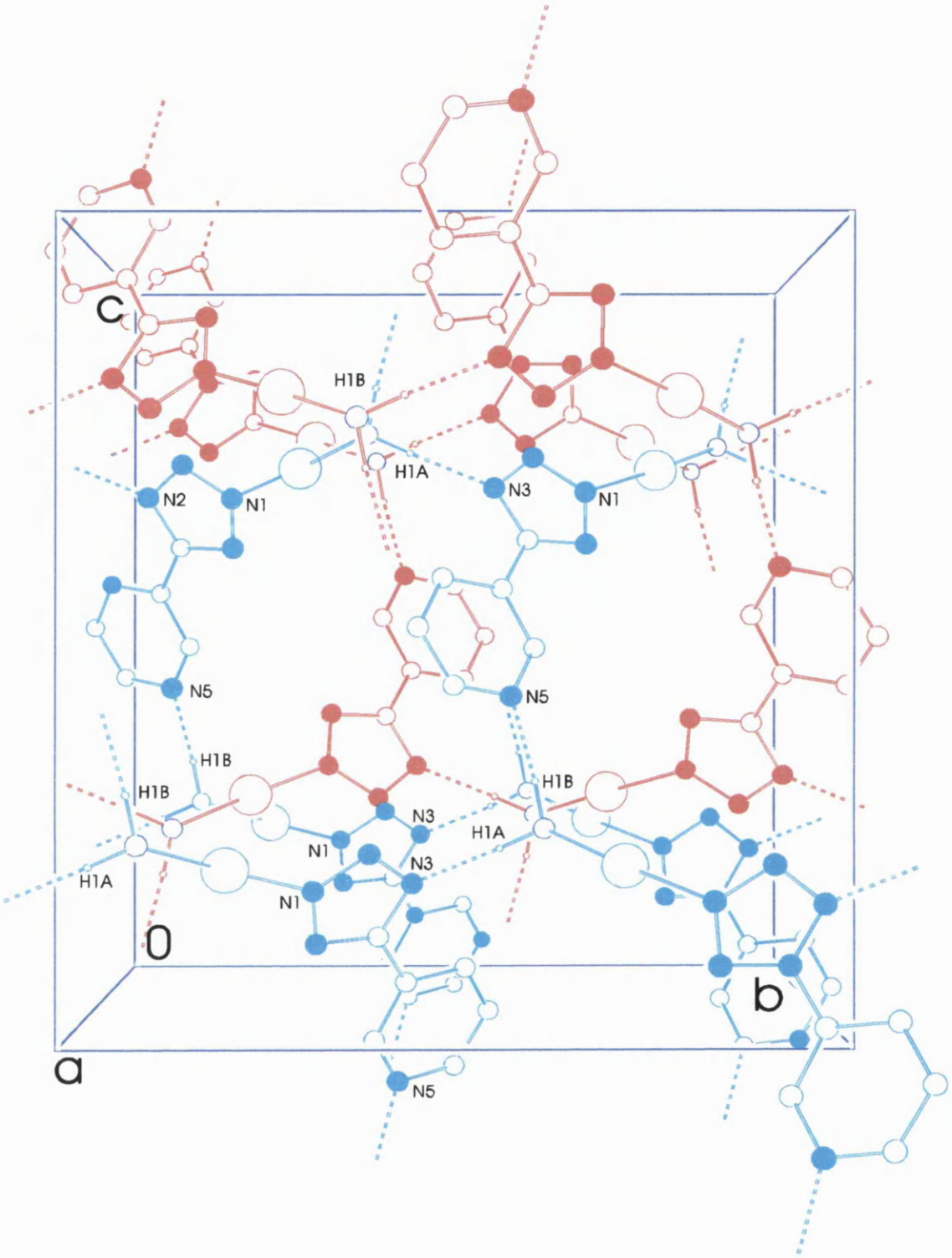

Fig.3.8: Overall view of the structure of **11**.

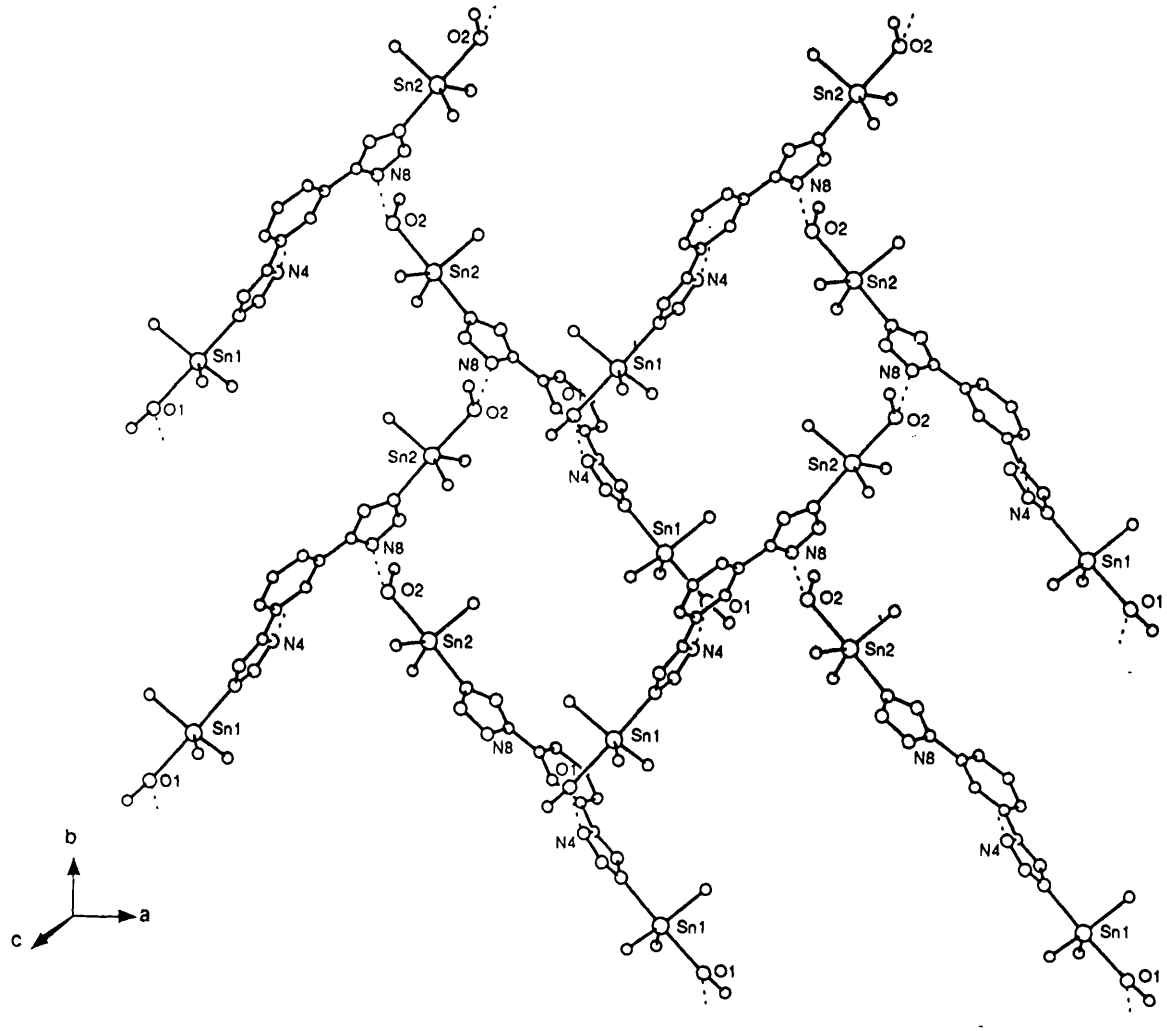

Fig.3.9: The sheet-like array of 1,3-phenylene-bis-5,5′-(tributylstannyltetrazole).bis methanolate (**XXV**) viewed perpendicular to the *ab*-plane.

Table 3.4: Selected Bond Lengths (Å) For **11** With Their Estimated Standard Deviations In Parentheses.

Sn(1)-C(11)	2.02(2)	N(5)-C(5)	1.325(9)
Sn(1)-C(9)	2.23(2)	N(5)-C(6)	1.331(7)
Sn(1)-C(7)	2.24(1)	C(1)-C(2)	1.463(8)
Sn(1)-N(1)	2.333(6)	C(2)-C(6)	1.379(8)
Sn(1)-O(1)	2.342(4)	C(2)-C(3)	1.390(9)
N(1)-N(4)	1.303(7)	C(3)-C(4)	1.371(9)
N(1)-N(2)	1.335(7)	C(4)-C(5)	1.36(1)
N(2)-C(1)	1.331(7)	C(7)-C(8)	1.34(2)
N(3)-C(1)	1.334(7)	C(9)-C(10)	1.39(3)
N(3)-N(4)	1.338(7)		

Table 3.5: Selected Bond Angles(°) For **11** With Their Estimated Standard Deviations In Parentheses.

C(11)-Sn(1)-C(9)	124(1)	C(1)-N(3)-N(4)	105.8(5)
C(11)-Sn(1)-C(7)	128(1)	N(1)-N(4)-N(3)	107.2(5)
C(9)-Sn(1)-C(7)	108.0(8)	C(5)-N(5)-C(6)	116.9(6)
C(11)-Sn(1)-N(1)	89.9(5)	N(2)-C(1)-N(3)	111.6(5)
C(9)-Sn(1)-N(1)	92.6(4)	N(2)-C(1)-C(2)	124.4(5)
C(7)-Sn(1)-N(1)	88.8(3)	N(3)-C(1)-C(2)	123.9(5)
C(11)-Sn(1)-O(1)	88.6(5)	C(6)-C(2)-C(3)	117.2(6)
C(9)-Sn(1)-O(1)	90.5(4)	C(6)-C(2)-C(1)	121.5(5)
C(7)-Sn(1)-O(1)	90.0(3)	C(3)-C(2)-C(1)	121.2(5)
N(1)-Sn(1)-O(1)	177.0(2)	N(5)-C(5)-C(4)	124.4(7)
N(4)-N(1)-N(2)	112.2(5)	N(5)-C(6)-C(2)	123.7(6)
N(4)-N(1)-Sn(1)	120.1(4)	C(8)-C(7)-Sn(1)	105(1)
N(2)-N(1)-Sn(1)	127.0(4)	C(10)-C(9)-Sn(1)	107(2)
C(1)-N(2)-N(1)	103.1(5)		

3.4.3 Crystal Structure Of 4-Pyridyl-(Tributylstannyltetrazole).2H_2O (8)

This is the second dihydrated organotin tetrazole structure known to date. The first water molecule is bonded to the tin. However, it is debatable whether the second water molecule is interstitial (as it is in **2**, see Section 2.4.2) or part of the lattice structure.

On slow evaporation of a methanolic solution of **8** at room temperature, crystals were obtained. Appendix VI includes crystallographic analysis, atomic coordinates and isotropic thermal parameters. The asymmetric unit of **8** is shown in Fig.3.10 and selected bond lengths and bond angles are given in Tables 3.6 and 3.7. As evidenced by thermal parameters, the largest smearing of electron density surrounds the butyl groups.

As implied by the spectroscopic evidence (see Section 3.3.1 and 3.3.2), the asymmetric unit contains a trigonal bipyramidal *trans*-$NOSnC_3$ centre. A trigonal bipyramidal tin centre is a consistent feature in the history of hydrated organotin-substituted tetrazoles. The axial positions of Sn(1) are occupied by N(1) nitrogen of the tetrazole and oxygen of the water molecule. The N-Sn-O bond angle is close to 180° [N(1)-Sn(1)-O(1) 176.9(2)°]. The monodentate, sterically-induced N^2 coordination of the tetrazole with respect to the tin has also been seen in **9** and **11**.

As in **11**, hydrogen bonding predominates intermolecular interactions. However, while in **11** polymeric chains are interlinked to form sheet-like structures, in **8** sheets formed as a result of hydrogen-bonding are interlinked to form a three-dimensional array. Typically, O(1) (the coordinated water molecule) hydrogen bonds with N(5) of the pyridine group generated by the symmetry operator *-1+x, 0.5-y, -0.5+z*; O(2) (the free water molecule) interacts with O(1) as presented in the asymmetric unit and N(4) of the molecule generated by the *x, 0.5-y, -0.5+z* symmetry operator. The net result of these three interactions is the formation of molecular sheets parallel to the *ac*-plane as shown in Fig.3.11. These sheets are interlinked by hydrogen-bonding linkages between the free water O(2) and N(3) of the lattice neighbour generated via the operator *1-x, -0.5+y, 1.5-z*. The net result of all these three interactions is a three-dimensional array as shown in Fig.3.12. Bond lengths for the O-N interactions [O(1)-N(5′) 2.760(8)Å; O(1)-O(2)

2.694(7)Å; O(2)-N(4′) 2.831(8)Å; O(2)-N(3′) 2.923(8)Å] are similar to the ones seen in **11** [O(1)-N(3) 2.65(2)Å; O(1)-N(5) 2.60(3)Å].

If hydrogen bonding is included, the tetrazole ring is tridentate with respect to itself and exhibits $N^1 + N^2 + N^3$ mode of coordination. This mode of coordination is unique and has not been previously reported. Tridentate coordination is, however, known in the literature and is of the type $N^1 + N^2 + N^4$ (see Table 1.1 and Section 2.4.1).

The seemingly empty cavities (Fig.3.10) are filled up with butyl groups. It is in this respect that the status of the free water molecule is in contention. In **2**, the second water molecule is clearly interstitial (see section 2.4.2). However, in **8** the second water molecule seems to have been picked up in order to expand the cavities to accommodate the butyl groups.

In the history of organotin-substituted tetrazoles, several of them have been known to exhibit three-dimensional arrays, e.g. **XXVII** (see Table 2.1), **2** and **7** (see Sections 2.4.2 and 2.4.1). However, this is the first example of one where the array is held together solely by hydrogen bonds. Hydrogen bonds also provide the 'cement' in **XXV** (see Table 2.1) and **11** although the net structure in these two cases is a two-dimensional array.

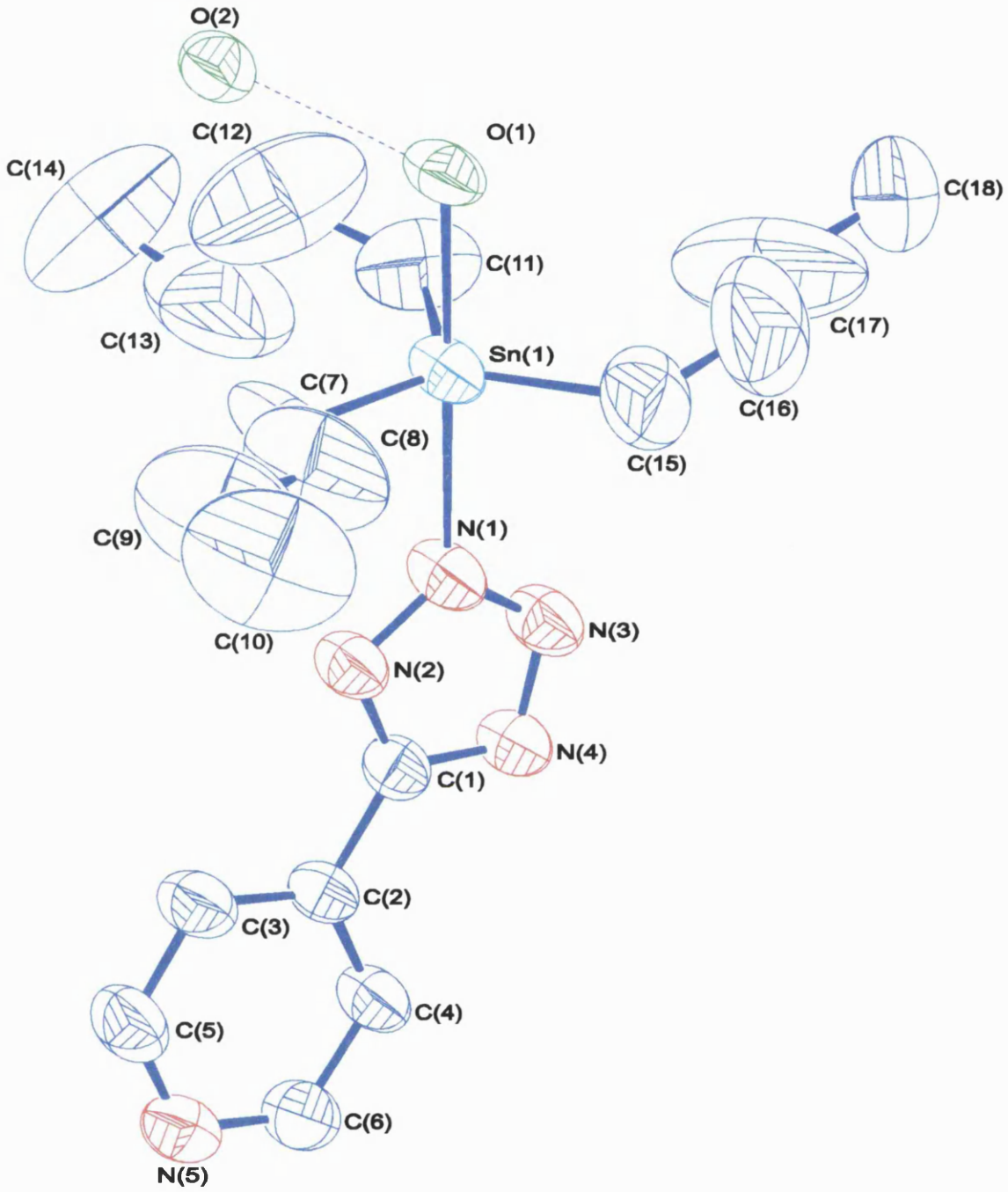

Fig.3.10: The asymmetric unit of **8** showing the atomic labeling scheme used in the text and tables. Hydrogen atoms omitted for clarity.

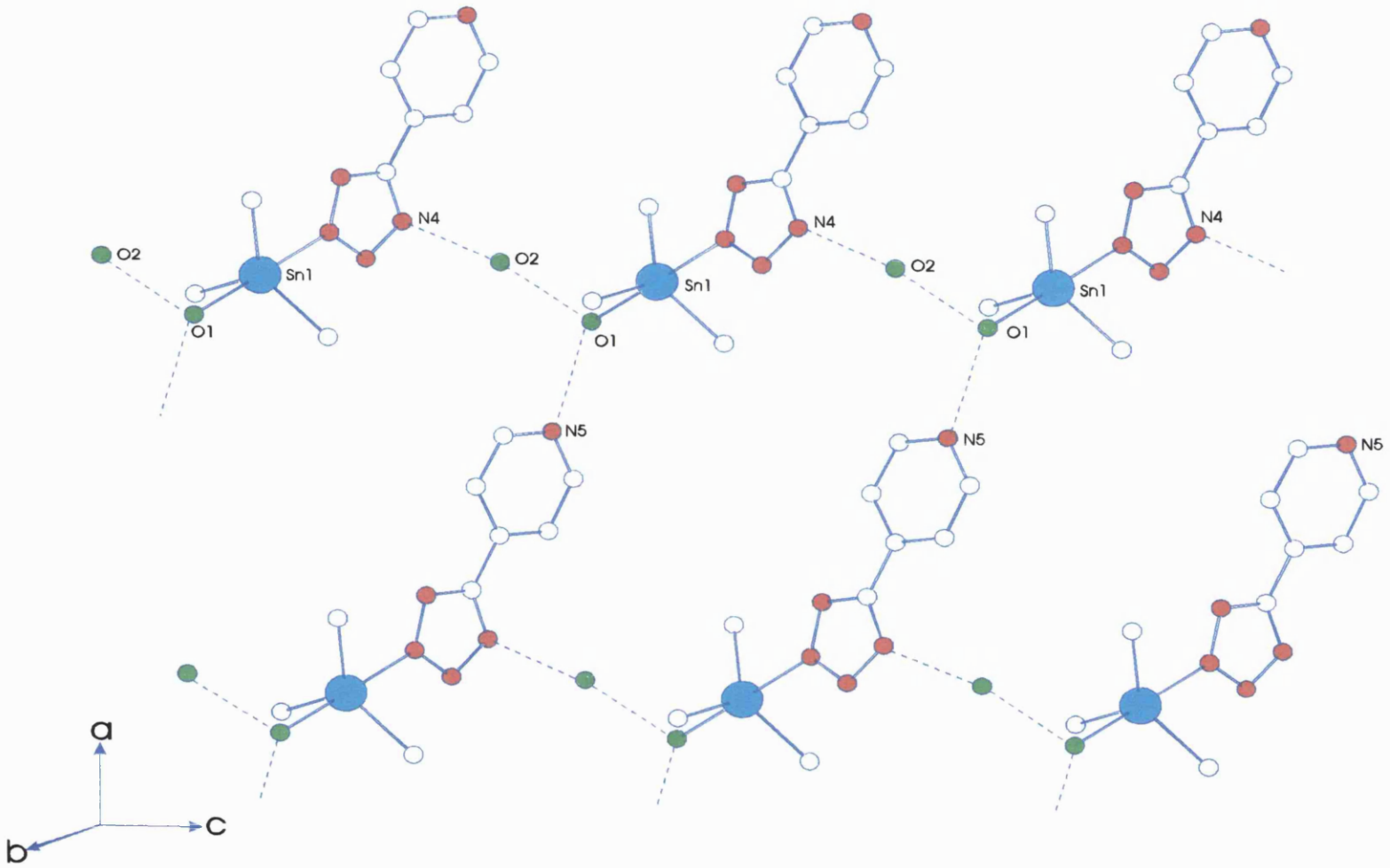

Fig.3.11: Molecular sheets of **8** parallel to the *ac*-plane

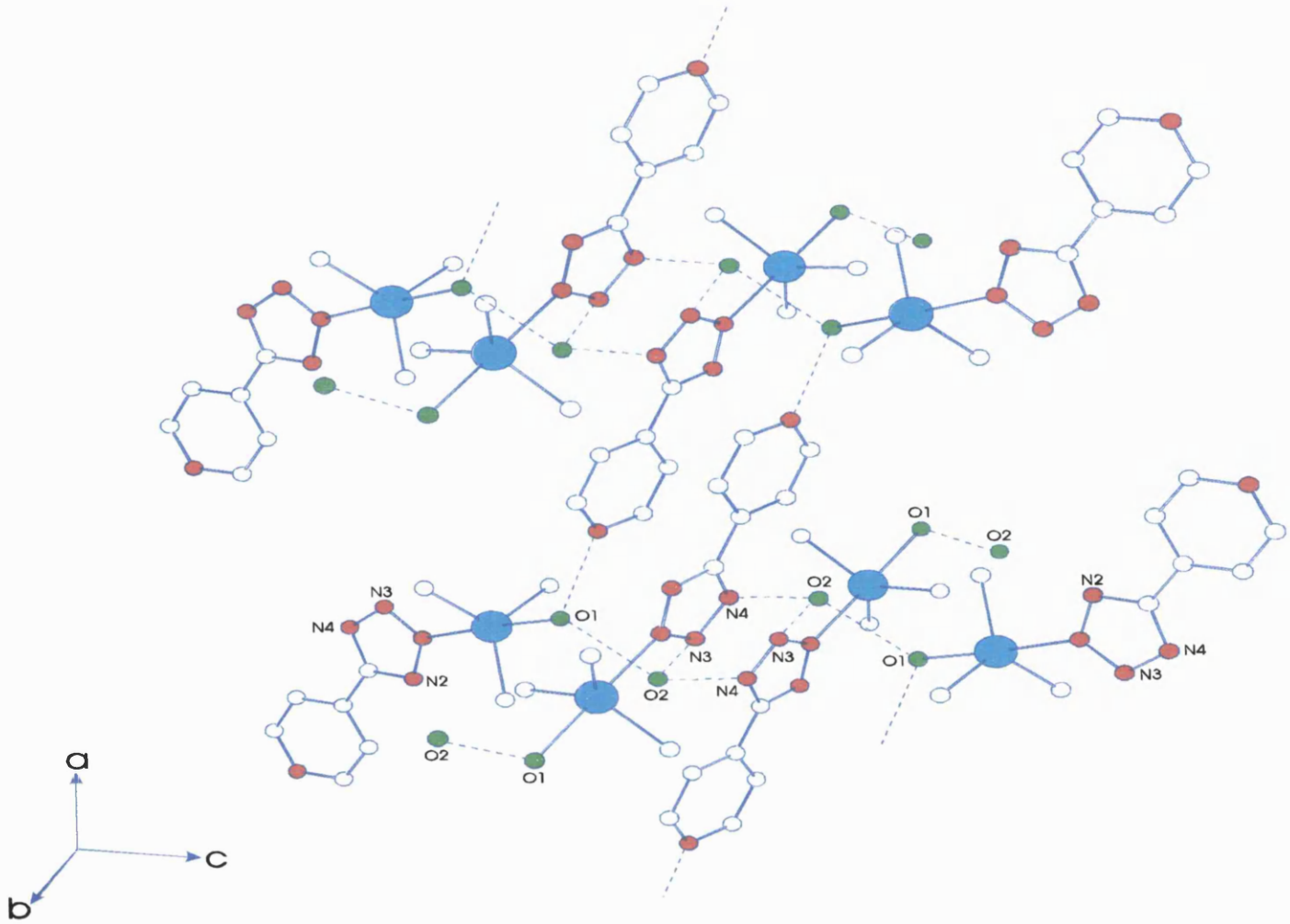

Fig.3.12: Three-dimensional array of **8**.

Table 3.6: Selected Bond Lengths (Å) For **8** With Their Estimated Standard Deviations In Parentheses.

Sn(1)-C(15)	2.09(1)	N(4)-C(1)	1.327(8)
Sn(1)-C(7)	2.103(9)	N(5)-C(5)	1.31(1)
Sn(1)-C(11)	2.11(1)	N(5)-C(6)	1.315(9)
Sn(1)-O(1)	2.340(5)	C(1)-C(2)	1.468(9)
Sn(1)-N(1)	2.360(6)	O(1)-O(2)	2.694(7)
N(1)-N(3)	1.319(8)	O(1)-N(5)#1	2.760(8)
N(1)-N(2)	1.331(8)	O(2)-N(4)#2	2.831(8)
N(2)-C(1)	1.332(8)	O(2)-N(3)#3	2.923(8)
N(3)-N(4)	1.330(7)		

Symmetry transformations used to generate equivalent atoms:

#1 x-1,-y+1/2,z-1/2; #2 x,-y+1/2,z-1/2; #3 -x+1,y-1/2,-z+3/2.

Table 3.7: Selected Bond Angles (°) For **8** With Their Estimated Standard Deviations In Parentheses.

C(15)-Sn(1)-C(7)	124.0(7)	N(4)-C(1)-N(2)	112.1(6)
C(15)-Sn(1)-C(11)	115.2(7)	N(4)-C(1)-C(2)	124.7(7)
C(7)-Sn(1)-C(11)	120.8(7)	N(2)-C(1)-C(2)	123.2(6)
C(15)-Sn(1)-O(1)	89.3(4)	C(4)-C(2)-C(1)	122.9(6)
C(7)-Sn(1)-O(1)	86.1(3)	C(3)-C(2)-C(1)	120.3(7)
C(11)-Sn(1)-O(1)	92.1(5)	N(5)-C(5)-C(3)	124.0(8)
C(15)-Sn(1)-N(1)	90.5(4)	N(5)-C(6)-C(4)	123.0(8)
C(7)-Sn(1)-N(1)	91.4(3)	C(8)-C(7)-Sn(1)	116(1)
C(11)-Sn(1)-N(1)	90.8(5)	C(12)-C(11)-Sn(1)	118(2)
O(1)-Sn(1)-N(1)	176.9(2)	C(16)-C(15)-Sn(1)	127(1)
N(3)-N(1)-N(2)	110.4(6)	Sn(1)-O(1)-O(2)	121.7(2)
N(3)-N(1)-Sn(1)	125.6(5)	Sn(1)-O(1)-N(5)#1	125.1(2)

Table 3.7: Selected Bond Angles (°) For **8** With Their Estimated Standard Deviations In Parentheses (contd.).

N(2)-N(1)-Sn(1)	123.7(5)	O(2)-O(1)-N(5)#1	106.0(2)
N(1)-N(2)-C(1)	103.9(6)	O(1)-O(2)-N(4)#2	116.2(2)
N(1)-N(3)-N(4)	108.6(6)	O(1)-O(2)-N(3)#3	93.5(2)
C(1)-N(4)-N(3)	105.1(6)	N(4)#2-O(2)-N(3)#3	118.4(2)
C(5)-N(5)-C(6)	116.4(7)		

Symmetry transformations used to generate equivalent atoms: #1 x-1,-y+1/2,z-1/2; #2 x,-y+1/2,z-1/2; #3 -x+1,y-1/2,-z+3/2.

3.5 SUMMARY

In conclusion, the cycloaddition route of Sisido *et al* [103] and Molloy *et al* [53] was successfully used to synthesise eight functionalised organotin-substituted tetrazoles. Structural analyses of three organotin-substituted pyridyl-tetrazoles- an anhydrous (**9**), a monohydrate (**11**) and a dihydrate (**8**) were obtained.

3.6 EXPERIMENTAL

Tributyltin azide, triethyltin azide and trimethyl azide were prepared by the literature procedures.[110] Bis[(2-cyanophenoxy)ethyl]ether was supplied by Dr.C.Frost (University of Bath). All other chemicals were obtained commercially (e.g. Aldrich) and used without further purification.

Preparation of 1-pyridyl-4-(tributylstannyl)tetrazole (**8**)

A mixture of tributyltin azide (2.30g, 6.93mmol) and 4-cyanopyridine (0.64g, 6.15mmol) in a three-necked flask under N_2 was heated together while stirring at 80°C for half an hour. The reaction mixture solidified at this temperature into a white solid, which was dissolved in boiling methanol. Hot filtration afforded a colourless solution, which, on cooling, gave **8** as a white crystalline solid. Yield: 1.42g (47%) (m.p. 134-136°C).

Analysis: Found (Calc. for $C_{18}H_{31}N_5Sn$): C 49.5 (48.6); H 7.11 (7.30); N 16.1 (14.1)%.

^{1}H NMR [δ(ppm), DMSO-d^6 solution]: 8.7 [dd, 2H, *2,6*-C_6H_4]; 7.9 [dd, 2H, *3,5*-C_6H_4]; 1.58 [m, 6H, $SnCH_2CH_2CH_2CH_3$]; 1.31 [m, 12H, $SnCH_2CH_2CH_2CH_3$]; 0.84 [m, 9H, $(CH_2)_3CH_3$]; ^{3}J[*2*-C_6H_4-*3*-C_6H_4] 6Hz.

^{13}C NMR [δ(ppm), DMSO-d^6 solution]: 160.4 [CN_4]; 150.3 [*3,5*-C_6H_4]; 137.2 [*4*-C_6H_4]; 120.2 [*2,6*-C_6H_4]; 27.7 [$SnCH_2CH_2CH_2CH_3$]; 26.4 [$Sn(CH_2)_2CH_2CH_3$]; 18.5

[Sn$CH_2$$(CH_2)_2CH_3$]; 13.5 [$(CH_2)_3CH_3$]; ^{1}J[$^{13}C$-$^{117,119}Sn$] 466 Hz. (unresolved); ^{2}J[^{13}C-$^{117,119}Sn$] 74 Hz. (unresolved).

^{15}N NMR [δ(ppm), DMSO-d^6 solution]: -61.5.

^{119}Sn NMR [δ(ppm), DMSO-d^6 solution]: -49.4.

IR [(cm^{-1}), KBr disk]: 2957, 2067, 1614, 1427, 1416, 1375, 1217, 1167, 1080, 1003, 962, 879, 841, 754, 706.

^{119m}Sn Mössbauer (mms^{-1}): I.S. = 1.43; Q.S. = 3.48.

Preparation of 1-pyridyl-4-(triethylstannyl)tetrazole, (**9**).

A mixture of triethyltin azide (3.33g, 13.4mmol) and 4-cyanopyridine (1.38g, 13.3mmol) was taken in a three-necked flask under N_2 and heated at 105°C for one hour. The resultant white cake was dissolved in hot methanol. Hot filtration afforded a colourless solution, which on cooling gave a white powder (4.1g, 88%) [(m.p. 178°C(dec.)].

Analysis: Found (Calc. for $C_{12}H_{19}N_5Sn$): C 40.7 (40.9); H 5.43 (5.39); N 19.9 (19.9)%.

^{1}H NMR [δ(ppm), DMSO-d^6 solution]: 0.8-1.5 [m, 15H, CH_2CH_3]; 8.0 [dd, 2H, *3,5*-C_6H_4]; 8.7 [dd, m, *2,6*-C_6H_4]; ^{3}J[*2*-$C_6{}^1H_4$-*3*-$C_6{}^1H_4$] 6Hz.

^{13}C NMR [δ(ppm), DMSO-d^6 solution]: 160.5 [CN_4]; 150.2 [*2,6*-C_6H_4]; 137.2 [*4*-C_6H_4]; 120.4 [*3,5*-C_6H_4]; 10.1 [CH_2CH_3]; 10.1 [CH_2CH_3].

^{119}Sn NMR [δ(ppm), DMSO-d^6 solution]: -50.9.

IR [(cm^{-1}), KBr disk]: 2947, 2866, 1618, 1558, 1446, 1429, 1377, 1215, 1194, 1165, 1128, 1043, 1005, 956, 848, 758, 711, 682, 534.

^{119m}Sn Mössbauer (mms^{-1}): I.S. = 1.48; Q.S. = 3.58.

Preparation of 1-pyridyl-3-(tributylstannyltetrazole), (**10**).

A mixture of tributyltin azide (2.41g, 7.25mmol) and 3-cyano pyridine (0.75g, 7.21mmol) was heated at 110°C for 30 mins in a flask under N_2 at which point a clear solution was obtained. As the reaction mixture was cooled to room temperature, it solidified into a white cake. This was dissolved in hot methanol. Hot filtration afforded a colourless solution, which on cooling gave colourless crystals of **10** (1.92g, 61%) (m.p. 91-93°C).

Analysis: Found (Calc. for $C_{18}H_{31}N_5Sn$): C 49.1 (49.5); H 7.19 (7.11); N 15.5 (16.1)%.

^{1}H NMR [δ(ppm), DMSO-d^6 solution]: 9.19 [d, 1H, *2*-C_6H_4]; 8.63 [dd, 1H, *6*-C_6H_4]; 8.32 [ddd, 1H, *4*-C_6H_4]; 7.53 [dd, 1H, *5*-C_6H_4]; 1.56 [m, 6H, $SnCH_2CH_2CH_2CH_3$]; 1.29 [m, 12H, $SnCH_2CH_2CH_2CH_3$]; 0.81 [m, 9H, $(CH_2)_3CH_3$]; ^{4}J[*2*-$C_6{}^1H_4$-*4*-$C_6{}^1H_4$] 1.22Hz; ^{4}J[*4*-$C_6{}^1H_4$-*6*-$C_6{}^1H_4$] 1.83Hz; ^{3}J[*5*-$C_6{}^1H_4$-*6*-$C_6{}^1H_4$] 4.73Hz; ^{3}J[*4*-$C_6{}^1H_4$-*5*-$C_6{}^1H_4$] 7.93Hz.

^{13}C NMR [δ(ppm), DMSO-d^6 solution]: 160.0 [CN_4]; 149.5 [*2*-C_6H_4]; 147.0 [*6*-C_6H_4]; 133.3 [*4*-C_6H_4]; 126.0 [*3*-C_6H_4]; 124.2 [*5*-C_6H_4]; 27.6 [$SnCH_2CH_2CH_2CH_3$]; 26.3 [$Sn(CH_2)_2CH_2CH_3$]; 18.3 [$SnCH_2(CH_2)_2CH_3$]; 13.5 [$(CH_2)_3CH_3$]; ^{1}J[^{13}C-$^{117,119}Sn$] 478 Hz. (unresolved); ^{2}J[^{13}C-$^{117,119}Sn$] 29.4 Hz. (unresolved); ^{3}J[^{13}C-$^{117,119}Sn$] 77.2 Hz. (unresolved).

^{119}Sn NMR [δ(ppm), DMSO-d^6 solution]: -52.1.

IR [(cm^{-1}), KBr disk]: 3080, 2922, 2955, 2870, 2863, 1583, 1464, 1427, 1186, 1082, 1055, 1008, 752, 709, 682, 640.

^{119m}Sn Mössbauer (mms^{-1}): I.S. = 1.46; Q.S. = 3.53.

Preparation of 1-pyridyl-3-(triethylstannyltetrazole).H_2O, (**11**).

A mixture of triethyltin azide (2.22g, 8.95mmol) and 3-cyanopyridine (0.93g, 8.94mmol) was taken in a flask under N_2 and heated at 140°C for 30 mins. The reaction mixture was cooled to room temperature at which point it solidified into a colourless glass. This was dissolved in hot methanol. Hot filtration afforded a colourless solution, which on cooling afforded colourless crystals (2.64g, 84%) [m.p. 181°C(dec.)].

Analysis: Found (Calc. for $C_{12}H_{19}N_5Sn.H_2O$): C 38.6 (38.9); H 5.56 (5.67); N 18.0 (18.9)%.

^{1}H NMR [δ(ppm), DMSO-d^6 solution]: 9.21 [d, 1H, *2*-C_6H_4]; 8.59 [dd, 1H, *6*-C_6H_4]; 8.34 [m, 1H, *4*-C_6H_4]; 7.49 [ddd, 1H, *5*-C_6H_4]; 0.9-1.4 [m, 15H, CH_2CH_3]; ^{4}J[*2*-$C_6{}^1H_4$-*4*-$C_6{}^1H_4$] 1.52Hz; ^{4}J[*4*-$C_6{}^1H_4$-*6*-$C_6{}^1H_4$] 1.84Hz; ^{3}J[*5*-$C_6{}^1H_4$-*6*-$C_6{}^1H_4$] 4.73Hz; ^{3}J[*4*-$C_6{}^1H_4$-*5*-$C_6{}^1H_4$] 7.93Hz.

^{13}C NMR [δ(ppm), DMSO-d^6 solution]: 160.0 [CN_4]; 149.5 [*2*-C_6H_4]; 147.0 [*6*-C_6H_4]; 133.3 [*4*-C_6H_4]; 126.0 [*3*-C_6H_4]; 124.2 [*5*-C_6H_4]; 10.2 [CH_2CH_3]; 10.2 [CH_2CH_3]; ^{1}J[^{13}C-$^{117,119}Sn$] 496.4Hz (unresolved).

^{119}Sn NMR [δ(ppm), DMSO-d^6 solution]: -48.3.

IR [(cm^{-1}), KBr disk]: 2966, 2870, 1604, 1581, 1454, 1429, 1377, 1363, 1192, 1159, 1142, 1012, 962, 815, 752, 707, 636, 688, 530.

^{119m}Sn Mössbauer (mms^{-1}): I.S. = 1.45; Q.S. = 3.63.

Preparation of 1-pyridyl-2-(tributylstannyltetrazole), (**12**).

Tributyltin azide (4.66g, 14 mmol) and 2-cyanopyridine (1.46g, 14 mmol) were heated at 110°C in a flask under N_2 for 30 mins at which point a clear solution was obtained. As the reaction mixture was cooled down to room temperature, it solidified into

a white cake. The white cake was dissolved in hot methanol and filtered hot. The resultant colourless solution on cooling gave colourless crystals of **12** (4.91g, 80%) (m.p. 106-108°C).

Analysis: Found (Calc. for $C_{18}H_{31}N_5Sn$): C 49.1 (49.5); H 7.00 (7.11); N 15.8 (16.1)%.

^{1}H NMR [δ(ppm), DMSO-d^6 solution]: 8.65 [d, 1H, *6*-C_6H_4]; 8.08 [d, 1H, *3*-C_6H_4]; 7.91 [m, 1H, *4*-C_6H_4]; 7.42 [ddd, 1H, *5*-C_6H_4]; 1.45 [m, 6H, $SnCH_2CH_2CH_2CH_3$]; 1.16-1.36 [m, 12H, $SnCH_2CH_2CH_2CH_3$]; 0.79 [m, 9H, $(CH_2)_3CH_3$]; ^{3}J[*3*-$C_6^1H_4$-*4*-$C_6^1H_4$] 7.78 Hz; ^{3}J[*4*-$C_6^1H_4$-*5*-$C_6^1H_4$] 7.78 Hz; ^{3}J[*5*-$C_6^1H_4$-*6*-$C_6^1H_4$] 4.43 Hz; ^{4}J[*4*-$C_6^1H_4$-*6*-$C_6^1H_4$] 1.83 Hz; ^{4}J[*3*-$C_6^1H_4$-*5*-$C_6^1H_4$] 1.2 Hz.

^{13}C NMR [δ(ppm), DMSO-d^6 solution]: 160.9 [CN_4]; 149.2 [*6*-C_6H_4]; 148.2 [*2*-C_6H_4]; 137.2 [*3*-C_6H_4]; 123.9 [*4*-C_6H_4]; 121.9 [*5*-C_6H_4]; 27.7 [$SnCH_2CH_2CH_2CH_3$]; 26.3 [$Sn(CH_2)_2CH_2CH_3$]; 18.9 [$SnCH_2(CH_2)_2CH_3$]; 13.5 [$(CH_2)_3CH_3$]; ^{1}J[^{13}C-$^{117,119}Sn$] 461.4 Hz, 484 Hz; ^{2}J[^{13}C-$^{117,119}Sn$] 27.6 Hz (unresolved); ^{3}J[^{13}C-$^{117,119}Sn$] 79 Hz (unresolved).

^{119}Sn NMR [δ(ppm), DMSO-d^6 solution]: -46.1.

IR [(cm^{-1}), KBr disk]: 3053, 2955, 2922, 2870, 2853, 1979, 1948, 1919, 1595, 1572, 1482, 1454, 1425, 1375, 1278, 1149, 742, 733, 679.

^{119m}Sn Mössbauer (mms^{-1}): I.S. = 1.47; Q.S. = 3.75.

Preparation of 1-pyridyl-2-(triethylstannyltetrazole).MeOH, (**13**).

A mixture of triethyltin azide (2.25g, 9.07mmol) and 2-cyanopyridine (0.94g, 9.038mmol) was heated at 140°C for 30 mins under N_2. The reaction mixture was, subsequently, cooled to room temperature at which point it solidified into a colourless glass. The work-up of the reaction was similar to **12.** Product **13** was obtained as colourless crystals (2.39g, 75%).

Analysis: Found (Calc. for $C_{12}H_{19}N_5Sn.CH_3OH$): C 39.8(40.6); H 5.39(5.98); N 18.9(18.2)%.

^{1}H NMR [δ(ppm), DMSO-d^6 solution]: 8.70 [d, 1H, *6*-C_6H_4]; 8.13 [d, 1H, *3*-C_6H_4]; 7.93 [m, 1H, *4*-C_6H_4]; 7.44 [ddd, 1H, *5*-C_6H_4]; 0.8-1.4 [m, 15H, CH_2CH_3]; ^{3}J[*3*-$C_6{}^1H_4$-*4*-$C_6{}^1H_4$] 7.93 Hz; ^{3}J[*4*-$C_6{}^1H_4$-*5*-$C_6{}^1H_4$] 7.78 Hz; ^{3}J[*5*-$C_6{}^1H_4$-*6*-$C_6{}^1H_4$] 3.97 Hz; 3.49 [s, 3H, CH_3OH].

^{13}C NMR [δ(ppm), DMSO-d^6 solution]: 160.7 [CN_4]; 149.2 [*6*-C_6H_4]; 148.0 [*2*-C_6H_4]; 137.4 [*3*-C_6H_4]; 124.0 [*4*-C_6H_4]; 121.9 [*5*-C_6H_4]; 10.9 [CH_2CH_3]; 10.2 [CH_2CH_3]; ^{1}J[^{13}C-$^{117,119}Sn$] 478, 500 Hz; ^{2}J[^{13}C-$^{117,119}Sn$] 33 Hz (unresolved).

^{119}Sn NMR [δ(ppm), DMSO-d^6 solution]: -42.0.

IR [(cm^{-1}), KBr disk]: 3049, 2972, 2945, 2866, 1595, 1452, 1425, 1375, 1149, 1020, 995, 958, 800, 744, 734, 717, 679, 528, 515.

^{119m}Sn Mössbauer (mms^{-1}): I.S. = 1.48; Q.S. = 3.77.

Preparation of Bis[(2-tributylstannyltetrazolephenoxy)ethyl]ether (**14**)

A mixture of tributyltin azide (1.60g, 4.82mmol) and bis[(2-cyanophenoxy)ethyl]ether (0.50g, 1.62mmol) was heated at 130°C for 30 mins under N_2. On cooling to room temperature, the reaction mixture solidified into a colourless glass. The reaction was worked up similarly to **12**. The product was collected as a white powder (1.0g, 98%) (m.p. 160-163°C).

Analysis: Found (Calc. for $C_{18}H_{16}N_8O_3Sn_2$): C 52.8(51.9); H 7.36(7.20); N 11.5(11.5)%.

^{1}H NMR [δ(ppm), DMSO-d^6 solution]: 7.54 [1H, dd, *3*-C_6H_4]; 7.38 [1H, m, *5*-C_6H_4]; 7.06 [2H, m, *4*-C_6H_4 & *6*-C_6H_4]; 4.08 [t, 4H, -OCH_2CH_2O-]; 3.70 [t, 4H, -OCH_2CH_2O-];

1.50 [Sn*CH*$_2$CH$_2$CH$_2$CH$_3$]; 1.25 [SnCH$_2$*CH*$_2$*CH*$_2$CH$_3$]; 0.80 [(CH$_2$)$_3$*CH*$_3$]; ^{3}J[*3*-C$_6$^{1}*H*$_4$-*4*-C$_6$^{1}*H*$_4$] 7.51Hz; ^{4}J[*3*-C$_6$^{1}*H*$_4$-*5*-C$_6$^{1}*H*$_4$] 1.65Hz; ^{3}J[-O*C*^{1}*H*$_2$-*C*^{1}*H*$_2$O-] 4.76Hz.

^{13}C NMR [δ(ppm), DMSO-d^6 solution]: 159.33 [*C*N$_4$]; 156.43 [*1*-*C*$_6$H$_4$]; 130.59 [*3*-*C*$_6$H$_4$]; 130.19 [*5*-*C*$_6$H$_4$]; 120.77 [*4*-*C*$_6$H$_4$]; 120.20 [*6*-*C*$_6$H$_4$]; 114.12 [*2*-*C*$_6$H$_4$]; 69.18 [-O*CH*$_2$CH$_2$O-]; 68.57 [-OCH$_2$*CH*$_2$O-]; 27.71 [SnCH$_2$CH$_2$*CH*$_2$CH$_2$]; 26.45 [SnCH$_2$*CH*$_2$CH$_2$CH$_2$]; 18.31 [Sn*CH*$_2$(CH$_2$)$_2$CH$_3$]; 13.59 [(CH$_2$)$_3$*CH*$_3$]; ^{1}J[^{13}*C*-^{117,119}*Sn*] Hz (unresolved); ^{2}J[^{13}*C*-^{117,119}*Sn*] 28.6Hz (unresolved); ^{3}J[^{13}*C*-^{117,119}*Sn*] 77.2Hz (unresolved).

^{119}Sn NMR [δ(ppm), DMSO-d^6 solution]: -53.0.

IR [(cm^{-1}), KBr disk]: 3414, 2959, 2670, 2229, 2066, 1612, 1522, 1466, 1450, 1433, 1342, 1284, 1255, 1223, 1147, 1126, 1103, 1057, 1026, 1014, 752, 680.

^{119m}Sn Mössbauer (mms^{-1}): I.S. = 1.47; Q.S. = 3.72.

Chapter 4

The Synthesis and Characterisation of Organolead-Substituted Mono-, Bis-, and Tris-Tetrazoles

4.1 INTRODUCTION

Lead is the heaviest element in Group 14 and its chemistry is very similar to the other members of the Group, especially tin.[124] Bonds involving lead are weaker and organolead compounds are much less thermally and photochemically stable than the corresponding organotin compounds. They show a marked tendency of decomposing via free radical pathways. Lead, like tin, has two oxidation states - II and IV. While the divalent state is more stable among inorganic lead compounds[124,125], the organolead compounds prefer the tetravalent state. The divalent derivatives of organolead compounds are very unstable and decompose via disproportionation to tetravalent lead and lead metal.

The single most important commercial application of organolead compounds is their use as anti-knock agents, a discovery by Midgley and Boyd.[126] Anti-knock agents (tetraethyllead), when added to aviation and motor gasolines, suppress the reactions that produce the undesirable phenomenon of knock in the internal combustion engine. Other applications of organolead compounds include polymerization catalysts, polymer stabilizers and biocidal agents.[124,125]

By way of introducing the syntheses and characterisation of organolead-substituted tetrazoles, organolead-substituted azoles known to date will be discussed. The structural chemistry of such species is very scant.

4.1.1 Syntheses And Characterisation Of Organolead-Substituted Azoles

Several organolead-substituted azoles were prepared by Willemsens and van der Kerk by mixing a triphenyllead hydroxide with the appropriate heterocycle in an organic solvent, e.g. ether (equation 4.1).[127,128]

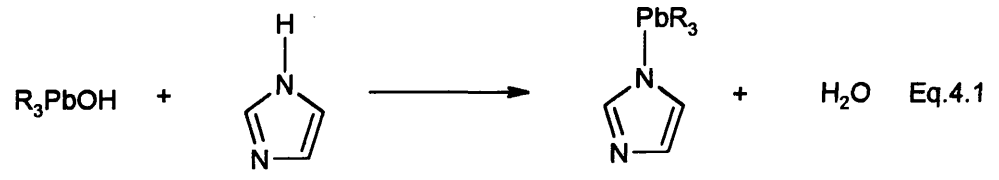

The organolead triazole (**XXXVII**) has been obtained by a [2 + 3] cycloaddition reaction of dimethylacetylene dicarboxylate with triphenyllead azide (equation 4.2).[129]

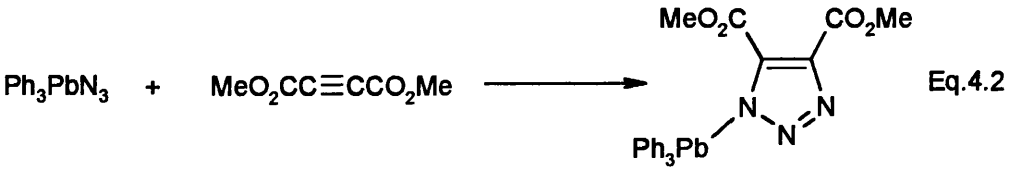

XXXVII

A Cambridge Crystal Structure Database search only revealed structures of two organolead-substituted imidazoles[129,130] and a series of Pb(II)pyrazoles[131,132]. This limited number of lead azoles available in the literature points towards a relatively unexplored area of chemistry. The following figures summarise some of the organolead-substituted azoles reported in the literature.

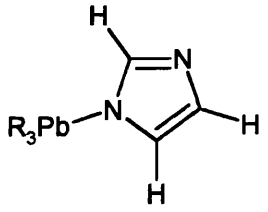

XXXVIII[128]

R = Et, Bu, ^{i}Pr, Ph

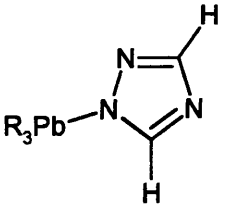

XXXIX[128]

R = Et, Ph

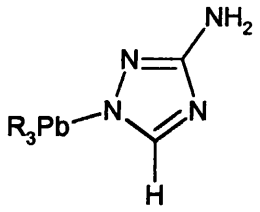

XL[128]

R = Et, Bu, Ph

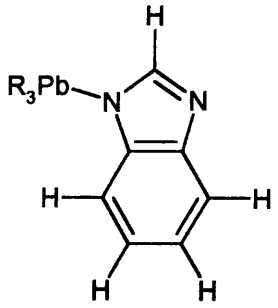

XLI[128]

R = Et, Bu, Ph

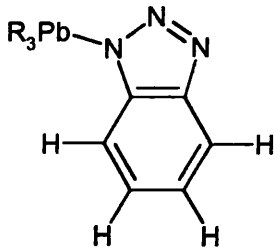

XLII[128]

R = Bu, Ph

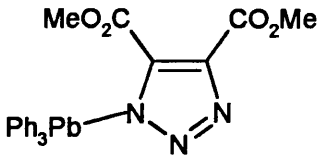

XLIII[129]

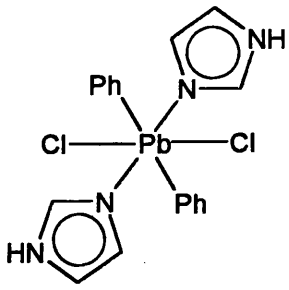

XLIV[130]

In addition to the compounds listed above, Pb(II) complexes of the poly(pyrazolyl)borate ligand have been reported.[131,132] These were prepared in an attempt to synthesise complexes with bulky poly(pyrazolyl)borate ligands in which the lone pair on the Group 14 metal(II) is stereochemically inactive. Fig.4.1 illustrates the crystal structure of bis[hydrotris(3,5-dimethylpyrazolyl)borato]lead(II).[131]

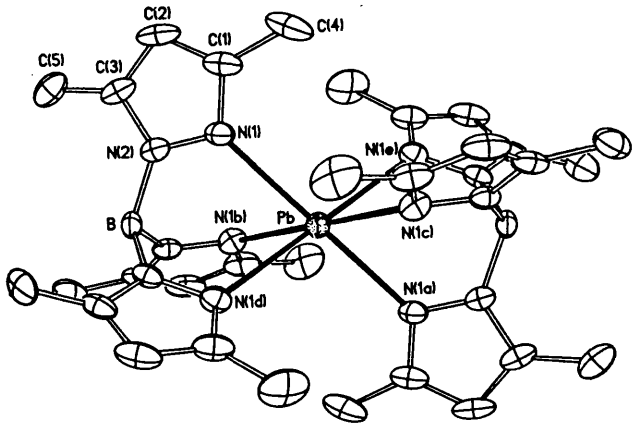

Fig.4.1: ORTEP drawing and labeling scheme for $[HB(3,5\text{-}Me_2pz)_3]_2Pb$. Ellipsoids are at 30% probability. Hydrogen atoms are omitted for clarity.[131]

CHN analysis, multinuclear NMR (^1H, ^{13}C, ^{207}Pb) spectroscopy, IR spectroscopy, mass spectrometry and X-ray diffraction are the main physical methods which have been used to characterise organolead-substituted azoles.[124,125] ^{207}Pb NMR chemical shifts have been measured for a variety of organolead derivatives and span a range of ±5000 ppm.[125,74] The factors affecting ^{207}Pb chemical shift values have been discussed in Section 1.5.2. The large range of values they cover make even minor differences in solvent and concentration cause large changes in chemical shifts. Similarly, seemingly innocuous changes in structure can also bring large changes in chemical shifts. Even when comparing data on similar compounds from different sources, care must be exercised. Very little information is available in the literature about the ^{207}Pb NMR values of organolead-substituted azoles.

4.2 SYNTHESIS OF ORGANOLEAD-SUBSTITUTED MONO-, BIS- AND TRIS-TETRAZOLES

Tris-[2-(5-hydrotetrazolyl)ethyl]nitromethane (**15**) was prepared by the procedure of Molloy *et al* (equation 4.3).[24] Typically, a methanolic solution of tris-[2-(5-tributylstannyltetrazolyl)ethyl]nitromethane was refluxed with concentrated hydrochloric acid for three hours. After cooling the reaction mixture to room temperature, the solvent was removed under reduced pressure. Subsequently, the product was washed with hexanes and collected by filtration.

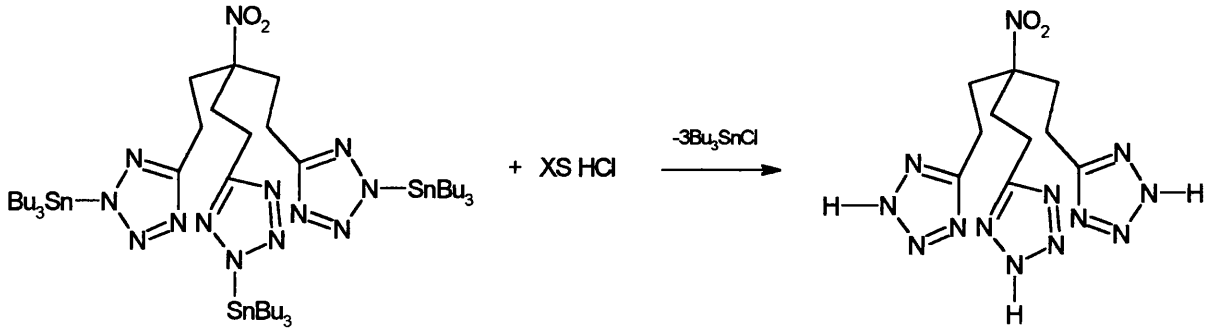

Eq.4.3

(15)

One triphenyllead-substituted mono-tetrazole has been synthesised via the well-established cycloaddition route of Molloy *et al*[103] and Sisido *et al*[53] (equation 4.4). A mixture of triphenyllead azide and excess benzonitrile was heated neat under N_2 to 160°C for one hour. After cooling, hexanes were added to the resultant yellow solution which precipitated the product (**16**) as a white solid. Recrystallization from methanol resulted in a white crystalline solid which was characterised as the methanol adduct of 2-triphenyllead-5-phenyltetrazole. IR spectroscopy was used to follow the course of the reaction. The disappearance of ν(CN) and $\nu(N_3)$ at 2250 cm^{-1} and 2053 cm^{-1} respectively in the starting materials indicated the completion of the reaction. However, reaction of Ph_3PbN_3 with other cyanobenzene compounds gave mixtures of compounds which could not be separated.

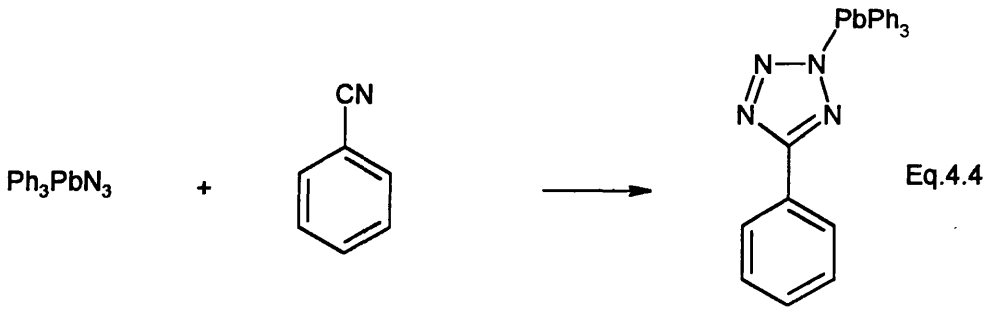

Eq.4.4

(16)

Five triphenyllead-substituted bis- and tris-tetrazoles have been synthesised (equations 4.5-4.7) using the condensation route of Sisido *et al*[25] (see Section 1.3.2.2) and Willemsens *et al.*[127,128] Typically, the free hydro-tetrazole was refluxed with triphenyllead hydroxide for 10 hours in ether. After removal of ether *in vacuo*, the white solid left behind was recrystallised from hot methanol. Products **17** and **18** were obtained from their respective methanolic solutions as white crystalline solids and were found to contain two methanol molecules as adducts. Broad bands in their IR spectra at 3410 and 3426 cm^{-1} respectively confirm the presence of the hydroxyl group of the methanol. **19** was not soluble in any commonly available solvent except DMSO. It was obtained from ether as a white powder, microanalysis of which suggests that it is a dihydrate. A broad band at 3449 cm^{-1} confirms the presence of water. **20** and **21** were collected from their respective methanolic solutions as white powders. **20** was determined to be a trihydrate and **21** a hexahydrate from microanalysis and infra-red spectroscopic data (where broad bands at 3420 and 3414 cm^{-1} were obtained respectively). A precedent for the formation of a hexahydrate can be found is reference 24. 1,3,5-phenylene-tris-5-(trimethyl stannyl)tetrazole was crystallised from methanol as a hexahydrate. Medium strength bands characteristic of tetrazole rings for **16-21** appeared at 1000-1100 cm^{-1}. In addition, these compounds also showed bands between 1500 and 1600 cm^{-1} corresponding to the phenyl rings.

A common feature of compounds **16-20** is that the number of solvent molecules (water or methanol) found in the respective products is the same as the number of metal centres. In organotin chemistry, solvent molecules may or may not be present in the

organotin-substituted products. However, crystallographic evidence suggests that if solvent molecules are a part of the lattice structure, they tend to coordinate to the metal centre (see Sections 2.4 and 3.4). In organothallium-substituted tetrazoles (see Section 5.4), the metal centres coordinate methanol molecules indiscriminately. Taking into account the evidence from tin and thallium chemistry and considering the fact that the number of solvent molecules is the same as the number of metal centres in **16-20**, it can be deduced that the solvent molecules are probably coordinated to the metal centres (also see Section 4.4).

Detailed synthetic procedures and work-up of compounds **15-21** are given in Section 4.5.

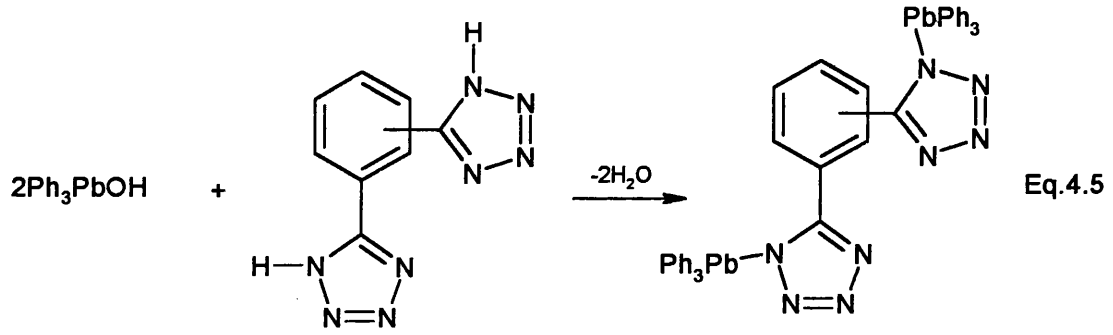

Eq.4.5

1,2 isomer (**17**), 1,3 isomer (**18**),

1,4 isomer (**19**)

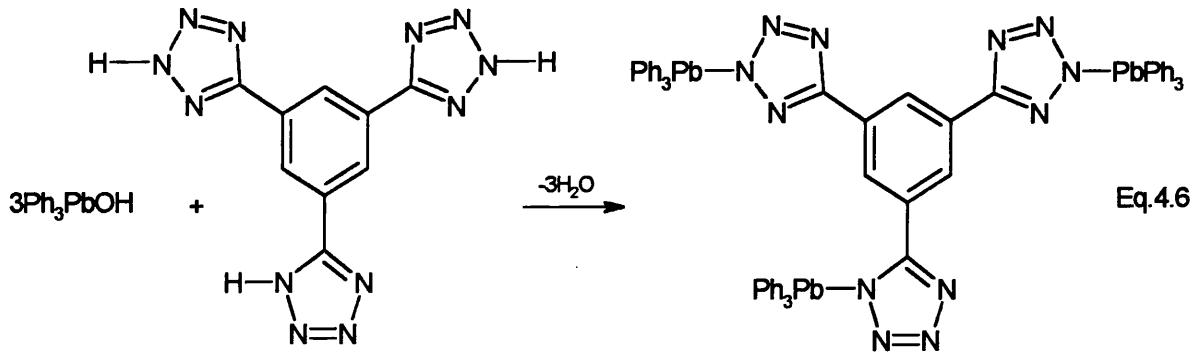

Eq.4.6

(**20**)

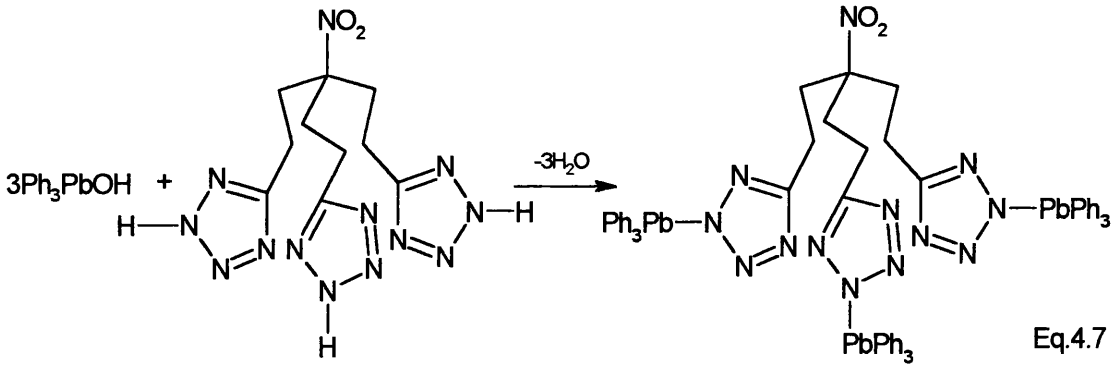

(21)

Attempts to synthesise organolead compounds were made using various other synthetic routes, but with little success. For instance, triphenyllead chloride was refluxed with methylene-5,5′-bis(hydrotetrazole) in a mixture of methanol and toluene in the presence of triethylamine. No reaction was observed (equation 4.8).

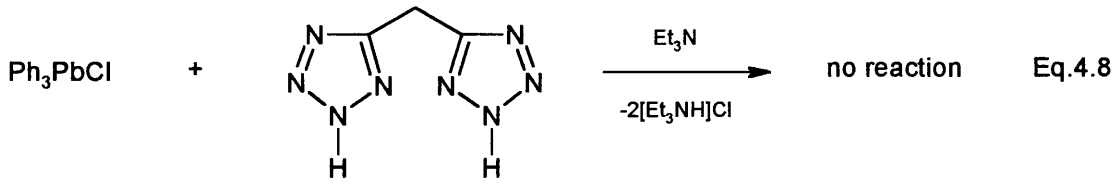

In another instance, sodium methoxide was refluxed with methylene-5,5′-bis-(hydrotetrazole) in methanol to form the sodium salt of the methylene-5,5′-bis(hydrotetrazole). This was then refluxed with triphenyllead chloride in a mixture of dichloromethane and methanol. CHN showed partial incorporation of nitrogen but the pure products could not be isolated (equation 4.9).

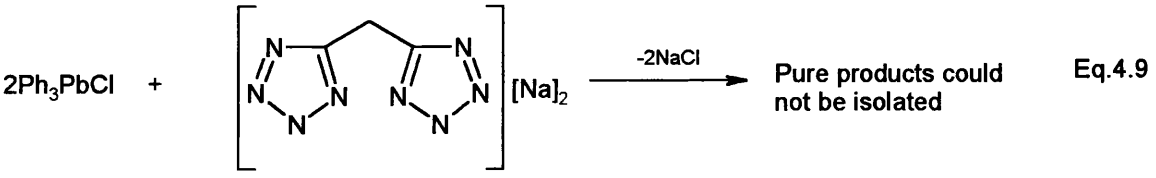

In another attempt to synthesise an organolead tetrazole, the thallium salt of the tetrazole was refluxed with two equivalents of triphenyllead chloride. CHN showed

partial incorporation of nitrogen but again the pure product could not be isolated (equation 4.10).

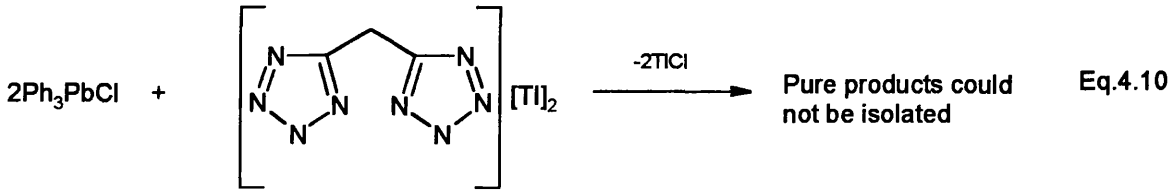

The following Table summarises the various routes - successful and unsuccessful used to synthesise organolead-substituted tetrazoles.

Table 4.1: Summary Of The Various Attempts To Synthesize Organolead Tetrazoles

Reactants	**Result of reaction**	**Bonds broken**	**Bonds formed**
Na_2(5,5′-methylene-hydrotetrazole) and Ph_3PbCl	Partial reaction	N-Na, Pb-Cl	Na-Cl, Pb-N
Tl_2(5,5′-methylene-hydrotetrazole) and Ph_3PbCl	Partial reaction	N-Tl, Pb-Cl	Tl-Cl, Pb-N
5,5′-methylene(hydrotetrazole), triphenyllead chloride, and triethylamine	Partial reaction	N-H, Pb-Cl	H-Cl, Pb-N
1,3-phenylene-bis-(hydro-tetrazole) and triphenyl-lead hydroxide	1,3-phenylene-bis-(triphenyl-lead-tetrazole) and water	N-H, Pb-OH	H-OH, Pb-N

The failure of the reaction with the thallium salt of the tetrazole can be explained on the basis of the partial solubility of thallium chloride and the thallium salt of the tetrazole in methanol making the thallium chloride difficult to remove. In the third reaction, triethylammonium chloride is a potential by-product and is very difficult to remove from the reaction mixture. The failure of the first reaction came as a surprise, especially since formation of organotin tetrazoles from sodium salts of tetrazoles is an established procedure.[27]

4.3 SPECTROSCOPY

4.3.1 Multinuclear NMR Spectroscopy

^{1}H, ^{13}C and ^{207}Pb NMR data were collected for all the organolead-substituted tetrazoles in d^{6}-DMSO. ^{207}Pb NMR data for all the compounds included in this chapter are summarised in Table 4.2. ^{1}H and ^{13}C NMR data are consistent with proposed structures.

The ^{1}H NMR spectrum of **15** reveals the ethyl protons at 3.02 ppm and 2.61 ppm. In addition, the tetrazole proton was also visible at 7.28 ppm. The CH_3 protons of the coordinated methanol were visible at 3.62 ppm. The ^{13}C NMR of **15** revealed the tetrazole quaternary carbon at 155.9 ppm, the quaternary nitromethane carbon at 92.7 ppm and the ethyl carbons at 32.1 and 17.9 ppm. The ^{1}H NMR spectra for all the compounds **16-21** show aromatic protons corresponding to the phenyl rings. **16**, **17** and **18** also show peaks corresponding to methanol. In **21**, ethyl protons are also visible at 2.35 and 2.08 ppm. The ^{13}C NMR spectra of all the triphenyllead-substituted tetrazole compounds listed in this chapter clearly show the quaternary carbon of the tetrazole at approximately 160 ppm. Aromatic carbons corresponding to the phenyl rings are also visible. In **21**, the quaternary nitromethane carbon appears at 93.0 ppm and the ethyl carbons at 33.3 and 19.1 ppm.

^{207}Pb NMR resonances appear between -250 ppm and -380 ppm. For purposes of comparison, these values were recorded at room temperature and at 100°C. However, **17** and **18** decompose at 100°C and **18** and **19** are insoluble in DMSO at room temperature. This makes a realistic comparison between these compounds very difficult. However, some inferences can be made based on $\delta(^{207}Pb)$ of known compounds. For instance, $\delta(^{207}Pb)$ for Ph_3PbO_2CMe is -93.0 ppm while $\delta(^{119}Sn)$ for Ph_3SnO_2CMe is -121.0 ppm.[133] The proximity of the chemical shift values of the two compounds indicate similar coordination. The latter compound is almost certainly four coordinate in dilute solution[72], which strongly suggests that the former is as well. The $\delta(^{207}Pb)$ for $Ph_2Pb(O_2CMe)_2$ is -688.0 ppm, which points towards a six coordinate lead brought about by the bidentate nature of the acetate groups. The range of -250 ppm to -400 ppm obtained for **16-21** suggests an intermediate coordination value of five between the two extremes of -93.0 ppm and -688.0 ppm.

In comparison with the solution-state structures of organotin-substituted tetrazoles in Chapters 2 and 3, the lead in compounds **16-21** is likely to be five coordinate in solution. Pentacoordination at lead could be achieved by coordination of a solvent molecule to the lead centre (**XLV**). The microanalysis and spectroscopic data indeed point towards molecules of crystallisation (water or methanol) being coordinated to the metal centre as pointed out in Sections 4.2 and 4.5 (also see Section 4.4). As for the organotin-substituted tetrazoles reported in Chapters 2 and 3, in a coordinating solvent like DMSO the NMR solvent may also be attached to the metal centre. Due to the lack of specific spectroscopic data confirming the coordination number at the metal centre or the nature of the coordinated molecule, no conclusive deductions can be made.

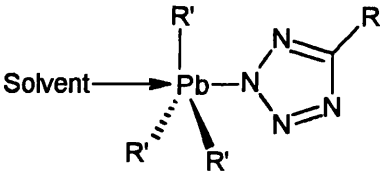

Solvent = H_2O, MeOH or DMSO

XLV

Table 4.2: ^{207}Pb NMR Studies of Organolead-Substituted Mono-, Bis-, and Tris-(tetrazoles)

Compound	δ(^{207}Pb)-Room temperature[a]	δ(^{207}Pb)-100°C[a]
16	-263.2	-251.3
17	-361.7	decomposes
18	insoluble	decomposes
19	insoluble	-257.1
20	-263.9	-250.4
21	-378.1	-360.2

[a] All spectra run as DMSO-d^6 solutions

4.4 X-RAY CRYSTALLOGRAPHY

It was very difficult to grow good quality single crystals for structure determination of the organolead-substituted tetrazoles as they crystallise from solution as twins. A data set was collected for 1,2-phenylene-bis-(triphenyllead tetrazole). However, satisfactory refinement of the structure set was not possible due to the low fraction of observed reflections and the twinned nature of the crystals. Only 8% of the observed reflections had $I \geq 2\sigma(I)$ i.e. only 8% of the reflections were not buried in the noise. The twinned nature of the crystals is reflected in the presence of an abnormal number of symmetry elements in the data set possibly due to the presence of 'anti-phase domains'.[134] Anti-phase domains can be explained by considering a set of horizontal planes of the type (001), which could be seen edge on as horizontal rows as shown in Fig.4.2. Assuming that the total volumes for the two kinds of twin orientations shown in the figure are equal, it is clearly evident that the (001) reflection has zero intensity. This is because the atoms in one twin scatter exactly out of phase with those in the other twin. This condition is strictly true only if the reflecting planes are perfectly parallel to each other throughout the crystal. Since real crystals are not perfect, the same kind of planes can be expected to be slightly tilted with respect to each other. This in turn gives rise to constructive interference at the two extremes of the reflection curve (Fig.4.3). The best that could be obtained was a partial structure of 1,3-phenylene-bis-(triphenyllead tetrazole) (Fig 4.4). However, at the very outset of data collection, indexation problems in succeeding peak search routines were encountered. When a cell was obtained, it had a very long *b*-axis (57Å). Although very little can be deduced about the structure itself, it appears that the methanol molecules coordinate to the two metal centres as suggested earlier (see Section 4.2). This also explains why the number of solvent molecules in **16-20** is the same as the number of metal centres (**21** is an exception with six coordinated water molecules).

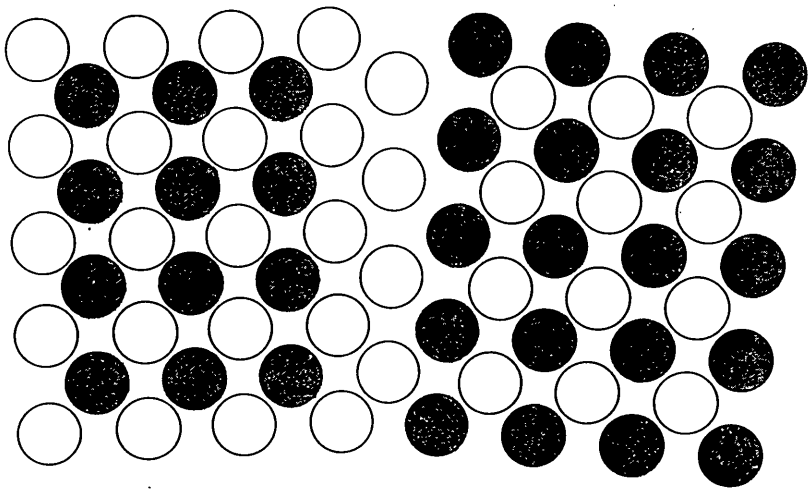

Fig.4.2: Planes of the type (001) slightly tilted with respect to each other.[134]

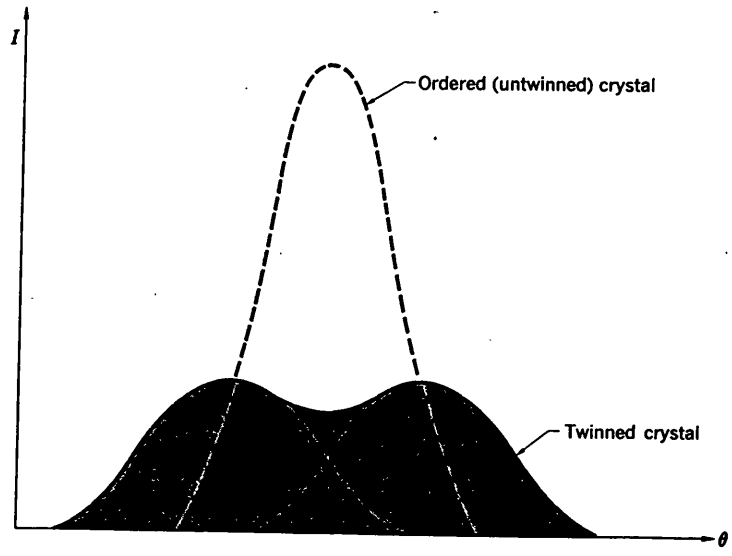

Fig.4.3: Constructive interference at the two extremes of the reflection curve.[134]

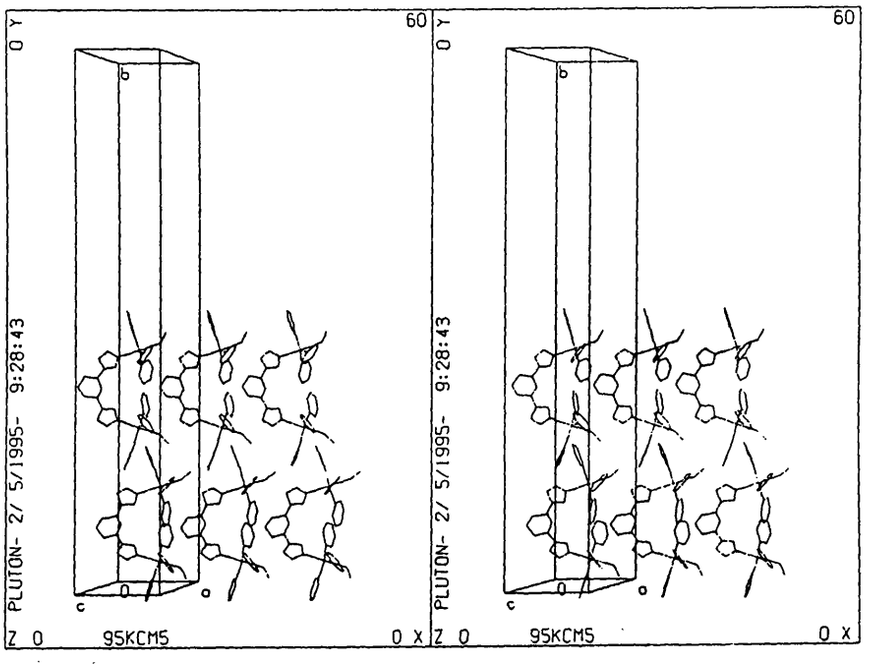

Fig.4.4: Partial structure of 1,3-phenylene-bis-(triphenyllead tetrazole).

4.5 SUMMARY

To summarise, a mono-triorganolead-substituted tetrazole has been synthesised via the cycloaddition route of Molloy *et al*[103] and a series of bis- and tris-triorganolead-substituted tetrazoles have been synthesised using the route of Willemsens *et al*[127,128]. These were characterised by ^{1}H, ^{13}C, ^{207}Pb NMR spectroscopies, IR spectroscopy and CHN analysis. All of these compounds (**16-21**) had coordinated solvent molecules (water or methanol). A partial structure of 1,3-phenylene-(triphenyllead tetrazole) (Fig.4.4), which shows two methanol molecules coordinated to the two lead centres, was obtained.

4.6 EXPERIMENTAL

Triphenyllead hydroxide[135] and triphenyllead azide[110] were prepared by the literature methods. All the mono-, bis- and tris-(hydro-tetrazoles) were prepared by refluxing the parent organotin-tetrazoles with concentrated hydrochloric acid[24]. All other reagents were of commercial origin (e.g. Aldrich) and used without further purification.

Preparation of Tris-[2-(5-hydrotetrazolyl)ethyl]nitromethane.MeOH (**15**)

To a well stirred solution of tris-[2-(5-tributylstannyl-tetrazolyl)ethyl] nitromethane (17.8g, 14.6 mmol), concentrated hydrochloric acid (96 mmol) was added dropwise. The resultant clear solution was refluxed for 3 hours. After cooling to room temperature, methanol was removed *in vacuo* and the remaining white solid was washed with hexanes and collected by filtration. The product was obtained as a methanol solvate (3.42g, 67%) (m.p. 194-198°C).

Analysis: Found (Calc. for $C_{10}H_{15}N_{13}O_2.CH_3OH$): C 34.4(34.6); H 4.57(4.99); N 48.2(47.8)%.

Preparation of 1,2-phenylene-bis-5,5′-(triphenylleadtetrazole).2MeOH (**17**)

A mixture of triphenyllead hydroxide (0.24g, 0.5mmol) and 1,2-phenylene-bis-(hydrotetrazole) (0.058, 0.3mmol) was refluxed in ether for 10 hours. After *in vacuo* removal of ether, the white powder was dissolved in refluxing methanol. Hot filtration afforded a colourless solution, which on cooling at room temperature afforded a white powder (0.05g, 17%) [m.p. 204°C(dec.)].

Analysis: Found (Calc. For $C_{44}H_{34}N_8Pb_2.2CH_3OH$): C 48.1 (47.9); H 3.63 (3.65); N 9.3 (9.7)%.

^{1}H NMR [δ(ppm), DMSO-d^6 solution]: 7.70-7.76, 7.55-7.60, 7.30-7.50 [complex, 34H, phenyl protons]; 3.43 [s, 3H, CH_3OH].

^{13}C NMR [δ(ppm), DMSO-d^6 solution]: 158.8 [CN_4]; 162.2, 136.4, 130.0, 129.4, 129.8, 128.0 [phenyl carbons].

^{207}Pb NMR [δ(ppm), DMSO-d^6 solution]: -361.7 (room temperature); decomposed at 100°C.

IR [(cm^{-1}), KBr disk]: 3414, 3049, 1637, 1618, 1568, 1475, 1431, 1385, 1363, 1327, 1300, 1261, 1099, 1068, 1016, 995, 729, 721, 690, 619.

Preparation of 1,3-phenylene-bis-5,5′-(triphenylleadtetrazole).2MeOH (**18**)

A mixture of triphenyllead hydroxide (0.75g, 1.7mmol) and 1,3-phenylene-bis-(hydrotetrazole) (0.17g, 0.8mmol) was refluxed in ether for 10 hours. The reaction mixture was worked-up similar to **17**. The product was collected as colourless cubic crystals (0.42g, 47%) [m.p. 272°C(dec.)].

Analysis: Found (Calc. for $C_{44}H_{34}N_8Pb_2.2CH_3OH$): C 47.6 (47.9); H 3.19 (3.65); N 10.1 (9.7)%.

^{1}H NMR [δ(ppm), DMSO-d^6 solution (80°C)]: 8.56, 7.93, 7.89, 7.61, 7.45 [complex, 34H, phenyl protons]; 3.50 [s, 3H, CH_3OH]; ^{3}J [^{1}H-^{1}H] 7.57 Hz; ^{3}J [^{1}H-^{1}H] 7.33 Hz.

^{13}C NMR [δ(ppm), DMSO-d^6 solution (80°C)]: 158.7 [CN_4]; 161.9, 136.5, 130.2, 129.8, 129.1, 126.2, 123.9 [phenyl carbons].

^{207}Pb NMR [δ(ppm), DMSO-d^6 solution]: insoluble at room temperature; decomposed at 100°C.

IR [(cm^{-1}), KBr disk]: 3377, 1628, 1568, 1473, 1431, 1327, 1298, 1261, 1192, 1155, 1128, 1084, 1059, 1039, 1014, 995, 908, 839, 804, 767, 744, 721, 688, 437.

Preparation of 1,4-phenylene-bis-5,5'-(triphenylleadtetrazole).2H_2O (**19**)

A mixture of triphenyllead hydroxide (0.61g, 1.3mmol) and 1,4-phenylene-bis-(hydrotetrazole) (0.15g, 0.7mmol) was refluxed in ether for 10 hours. After *in vacuo* removal of ether, the remaining product was found to be insoluble in methanol and in any other polar solvent except dimethyl sulphoxide. The product was obtained as a dihydrated white powder (0.57g, 71%) [m.p. 288°C(dec.)].

Analysis: Found (Calc. For $C_{44}H_{34}N_8Pb_2.2H_2O$): C 48.0 (48.5); H 3.15 (3.13); N 9.6 (9.7)%

^{1}H NMR [δ(ppm), DMSO-d^6 solution (80°C)]: 7.95, 7.90, 7.35-7.8 [complex, 34H, phenyl protons].

^{13}C NMR [δ(ppm), DMSO-d^6 solution (80°C)]: 158.8 [CN_4]; 136.5, 130.3, 129.8, 126.4 [phenyl carbons].

^{207}Pb NMR [δ(ppm), DMSO-d^6 solution]: insoluble at room temperature; -257.1 (100°C).

IR [(cm^{-1}), KBr disk]: 3449, 3063, 3049, 2986, 2963, 2926, 2855, 2583, 1570, 1475, 1431, 1421, 1261, 1107, 1060, 1037, 1016, 995, 802, 727, 690, 439.

Preparation of 1,3,5-phenylene-tris-5,5′,5′′-(triphenylleadtetrazole).3H_2O (**20**)

A mixture of triphenyllead hydroxide (0.29g, 0.6 mmol) and 1,3,5-phenylene-tris-(hydrotetrazole) (0.07g, 0.3 mmol) was refluxed in ether for 10 hours. After *in vacuo* removal of ether, the white powder was dissolved in hot methanol. Hot filtration afforded a colourless solution, which on cooling to room temperature gave a white powder (0.25g, 61%).

Analysis: Found (Calc. for $C_{63}H_{48}N_{12}Pb_3.3H_2O$): C 45.2 (45.9); H 3.47 (3.27); N 10.5 (10.2)%.

^{1}H NMR [δ(ppm), DMSO-d^6 solution]: 8.58, 7.94, 7.35-7.65 [complex, 48H, phenyl protons].

^{13}C NMR [δ(ppm), DMSO-d^6 solution]: 159.2 [*C*N_4]; 160.7, 135.9, 130.4, 129.5, 130.0, 123.8 [phenyl carbons]; ^{2}J[*2,6*-Pb^{13}*C*$_6$H$_5$-^{207}*Pb*] 44.1Hz.

^{207}Pb NMR [δ(ppm), DMSO-d^6 solution]: -263.9 (room temperature); -250.4 (100°C).

IR [(cm^{-1}), KBr disk]: 3420, 3049, 2957, 1635, 1570, 1477, 1433, 1417, 1385, 1329, 1157, 1060, 1016, 995, 788, 727, 690.

Preparation of Tris-[2-(5-triphenylplumbyltetrazolyl)ethyl]nitromethane.6H_2O (**21**)

A mixture of triphenyllead hydroxide (0.47g, 1.0 mmol) and tris-[2-(5-hydrotetrazolyl)ethyl]nitromethane (0.12g, 0.3 mmol) was refluxed in ether for 10 hours. After *in vacuo* removal of ether, the resultant white powder was washed with hot toluene and recrystallised from hot methanol (0.16g, 27%) [m.p. 206°C(dec.)].

Analysis: Found (Calc. for $C_{64}H_{57}N_{13}Pb_3.6H_2O$): C 42.9 (43.4); H 3.31 (3.90); N 10.9 (10.3)%.

^{1}H NMR [δ(ppm), DMSO-d^{6} solution]: 7.87, 7.32-7.60 [complex, 45H, phenyl protons]; 2.35 [m, 6H, $NO_2C(CH_2\text{-})_3$]; 2.08 [m, 6H, $\text{-}CH_2CN_4$].

^{13}C NMR [δ(ppm), DMSO-d^{6} solution]: 159.9 [CN_4]; 158.9, 135.9, 129.3 [phenyl carbons]; 93.0 [NO_2C]; 33.3 [$NO_2C(CH_2\text{-})_3$]; 19.1 [$\text{-}CH_2CN_4$]; ^{2}J[*2,6*-Pb$^{13}C_6H_5$-^{207}Pb] 42.3Hz.

^{207}Pb NMR [δ(ppm), DMSO-d^{6} solution]: -378.1(room temperature); -360.2 (100°C).

IR [(cm^{-1}), KBr disk]: 3414, 3057, 1637, 1616, 1570, 1541, 1475, 1435, 1385, 1325, 1259, 1060, 1016, 995, 727, 696, 682, 619, 476, 445.

Chapter 5

The Synthesis and Characterisation of Thallium(I) and Organothallium(III)-Substituted Mono-, Bis-, and Tris-Tetrazoles

5.1 INTRODUCTION

Thallium is the heaviest element of Group13 and can have oxidation states of I and III in its organometallic derivatives.[136] Among inorganic thallium compounds, the monovalent oxidation state is more stable and among organothallium compounds the trivalent oxidation state is more stable. Chemistry of diorganothallium(III) compounds has been known since the 19th century when the earliest organometallic chemistry was documented.[137] Investigations on mono- and tri-organothallium(III) derivatives began as late as 1930.[138,139] The first organothallium(I) compound, cyclopentadienylthallium, was reported five years after the discovery of the new type of chemical bonding in ferrocene.[140] There has been a steady progress in organometallic chemistry since the 1960's with emphasis on bonding, coordination, structure and spectroscopy.[141]

The dominant application of thallium is in the form of Tl_2SO_4 as rat and ant killer.[142,143] The lack of colour and odour of thallium makes it an active ingredient in rodenticides. Thallium is very toxic to living species and the human lethal dose is 1.75g.[144-146] The toxic effects have been observed in the neurological system, cardiovascular system, liver, kidneys and intestinal tract. The physiological mode of action of thallium(I) is by replacement of potassium ions in the activation of various enzymes.[147-149] Moreover, thallium(I) has an affinity approximately ten times greater than potassium for the potassium activating site. This property of thallium(I) ions has been exploited to study the binding of thallium(I) enzymes by thallium NMR.[150]

Thallium also has significant use in the electronics industry for production of thallium-activated NaI crystals for use in photomultiplier tubes and for the production of

'thallofide' cells which contain thallium(I) sulphide and are particularly sensitive to infrared radiation.[151] Thallium also finds uses in low melting alloys and in optical glasses.[151]

Cyclopentadienylthallium(I) has been very important in the development of cyclopentadienyl chemistry. This is because it can be readily formed in high yields, is extremely reactive with metal halides and is a convenient source of the cyclopentadienyl ligand.[152-154] Since the tetrazole moiety is isoelectronic with cyclopentadiene and is similar to it in its acidity,[155] it was interesting to investigate whether studies concerning cyclopentadienylthallium could be extended to tetrazoles. Unlike in cyclopentadienyls, the the tetrazolate ligands do not show η^5 coordination and this has been commented on in Section 1.5.

By way of introduction, the syntheses and characterisation of organothallium-substituted azoles known to date have been discussed in Section 5.1.1. This discussion also includes the few examples of thallium azole structures available in the literature.

5.1.1 Synthesis And Characterisation Of Organothallium-Substituted Azoles

5.1.1.1 Thallium(I) Derivatives Of Azoles

A number of thallium(I) *N*-heterocyclic derivatives have been synthesised from thallium(I) hydroxide in aqueous solution typified by the one shown in equation 5.1.[136]

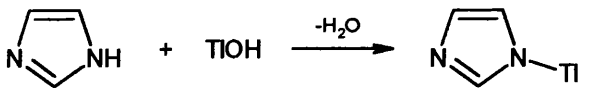

Eq. 5.1

The following figures list some of the known thallium(I) salts of nitrogen heterocycles.

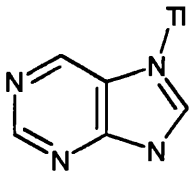

XLVI[156]

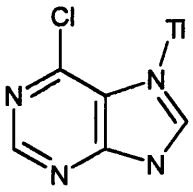

XLVII[156]

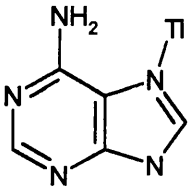

XLVIII[156]

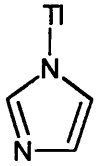

XLIX[136]

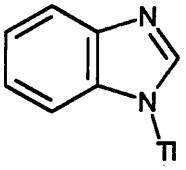

L[136]

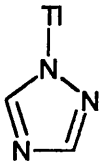

LI[136]

Besides the complexes listed above, crystallographic characterisation of a series of thallium(I) complexes of poly(pyrazolyl)borate ligands with a stereochemically inactive lone pair have been performed.[157-164] Fig.5.1 illustrates the crystal structure of $\{[HC(3,5\text{-}Me_2pz)_3]_2Tl\}^+$.[157]

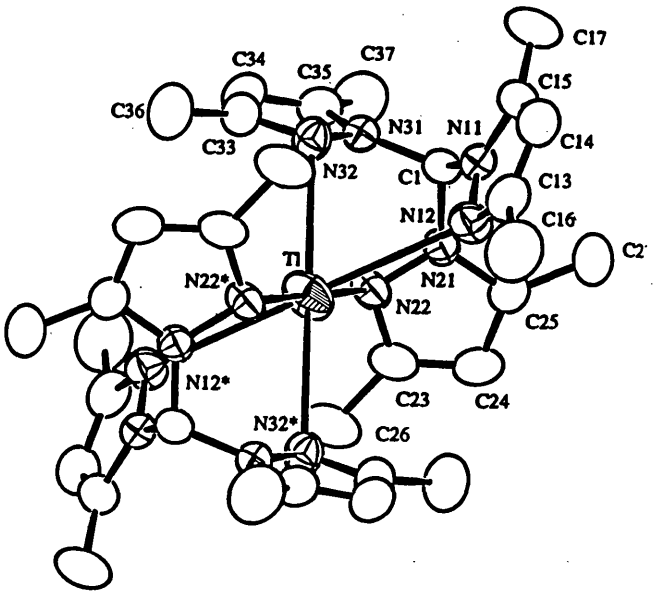

Fig.5.1: ORTEP diagram of $\{[HC(3,5\text{-}Me_2pz)_3]_2Tl\}^+$.[157]

5.1.1.2 Thallium(III) Derivatives Of Azoles

Mixing aqueous solutions of dimethylthallium(III) hydroxide with the appropriate heterocycle has yielded the dimethylthallium(III) derivatives of azoles (equation 5.2). Preparation of dimethylthallium(III) derivatives of imidazole, 1,2,4-triazole and benzimidazole have been reported.[165] These were characterised by mass spectra, infra-red, Raman, ultra-violet and NMR spectroscopies.

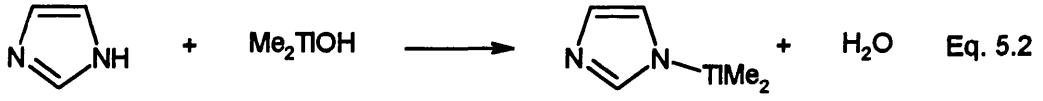

Eq. 5.2

There is only one organothallium(III) azole structure reported in the literature-dimethyl (4-amino-5-mercapto-3-trifluoromethyl-1,2,4-triazolato) thallium(III)[166]. This was prepared by the reaction of dimethylthallium hydroxide with the ligand (HL), where L = 4-amino-5-mercapto-3-trifluoromethyl-1,2,4-triazole.

5.1.3 Coordination Geometries Of Diorganothallium Compounds

Diorganothallium compounds can act as Lewis acids in the formation of intra and intermolecular coordination bonds.[167] This can lead to coordination numbers in the range

of 4-7 and a wide variety of coordination geometries as revealed by X-ray crystallography. In this respect, diorganothallium compounds are similar to organotin compounds. References 24, 68, and 80 comprehensively cover the coordination chemistry of organotin compounds. Table 5.2 illustrates typical coordination geometries of diorganothallium compounds.

Table 5.1: Coordination Geometry In Diorganothallium Compounds

Compound	Geometry[a]	Coordination Number	Reference
$Ph_2TlS_2CNEt_2$	Tetrahedral	4	168
Me_2TlOPh	*pseudo*-Trigonal bipyramidal [b]	4	169
$(C_6F_5)_2TlOH$	Trigonal bipyramidal	5	170
Me_2Tl(tryptophanate)	*pseudo*-Octahedral[b]	5	171
Me_2TlCN	Octahedral	6	172
Me_2TlO_2CMe	*pseudo*-Pentagonal bipyramidal[b]	6	173
Me_2TlS_2COMe	Pentagonal bipyramidal	7	174

[a] Most approximate geometry for thallium

[b] *Pseudo* geometries refer to that particular geometry with a bond missing. This is a unique observation made for diorganothallium compounds.

5.2 SYNTHESIS OF THALLIUM(I) AND ORGANOTHALLIUM(III)-SUBSTITUTED MONO-, BIS-, AND TRIS-TETRAZOLES

Two aliphatic hydro-tetrazoles, **22** and **23**, were synthesised by the established route of Molloy *et al*[24] (equation 5.3). After cooling to room temperature, the solvent was removed under reduced pressure and the respective products **22** and **23** were collected by filtration and washing with hexanes.

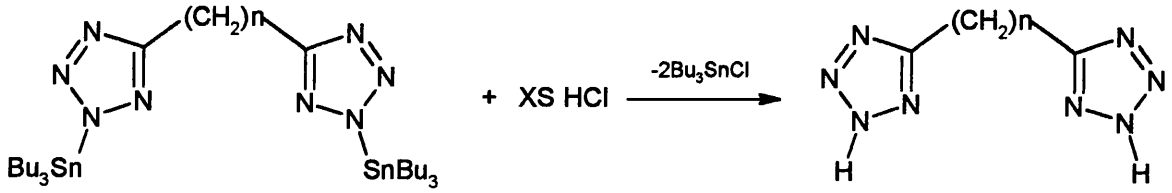

Eq.5.3

n = 2 (**22**), n = 4 (**23**)

Five thallium(I) tetrazolates were subsequently synthesised following the method of McKillop *et al* (equations 5.4-5.6).[175] Typically, a solution of thallium ethoxide in absolute ethanol was added dropwise to a solution of the appropriate hydro-tetrazole in absolute ethanol. A white precipitate resulted almost instantaneously in all cases. The reaction mixture was allowed to settle for 4-5 hours in each case, filtered and dried *in vacuo*. Products **24-27** were insoluble in commonly available solvents except dimethyl sulfoxide and water. However, product **28** was not even soluble in these solvents. Microanalysis revealed products **24**, **25** and **27** to be anhydrous, **26** to be a dihydrate and **28** to be a trihydrate. Broad bands in the IR spectra of the two compounds at 3352cm^{-1} and 3414cm^{-1} respectively confirmed the presence of water. All compounds showed bands at 1000-1100cm^{-1} typical of tetrazoles. In addition, products **26-28** also showed bands between 1500-1600cm^{-1} corresponding to aromatic rings. The insolubility of these compounds in most solvents made crystallographic characterisation very difficult.

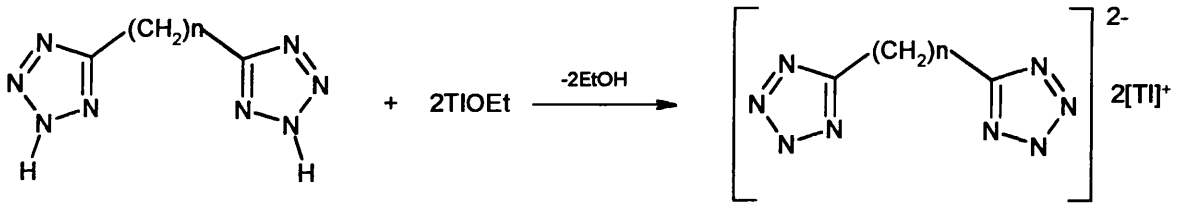

Eq.5.4

n = 1 (**24**), n = 4 (**25**)

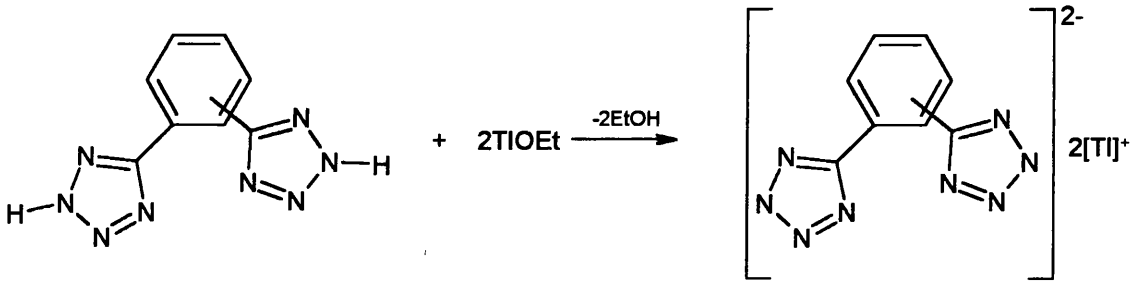

Eq.5.5

1,3 isomer (**26**), 1,4 isomer (**27**)

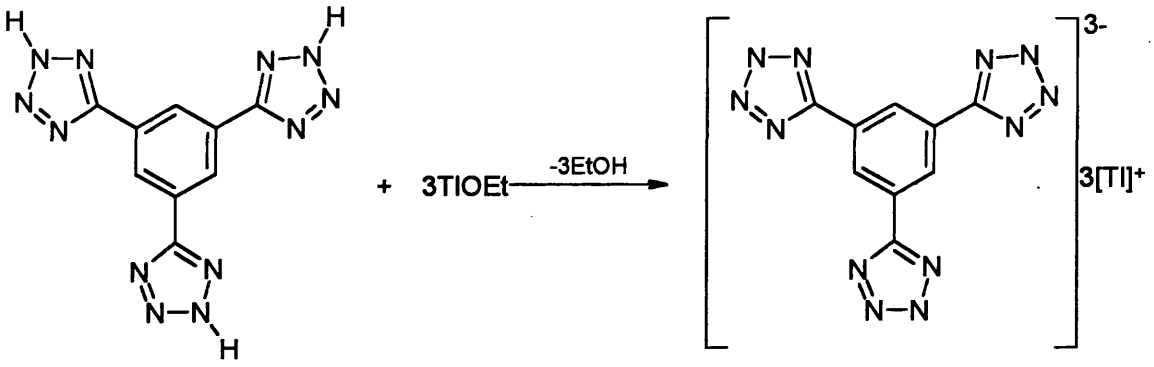

Eq.5.6

(**28**)

The cycloaddition route used in chapters 2 and 3 to prepare organotin-substituted tetrazoles[53,103] was used to synthesise one diphenylthallium-substituted mono-tetrazole (equation 5.7). Diphenylthallium azide was added to excess benzonitrile and was slowly stirred under N_2 for 10 hours at 150°C. The reaction was monitored by IR spectroscopy. The completion of the reaction was marked by the loss of ν(CN) and $\nu(N_3)$ at 2228cm^{-1}

and 1989cm^{-1}, respectively, in the starting materials. After cooling, the solid obtained at the end of the reaction was collected by filtration, washed with hexanes and recrystallized from hot methanol to yield the product in two forms- powder and crystalline. Microanalysis on both products suggested that the powder form was anhydrous and the crystalline form was methanol solvated. However, this route involves heating diphenylthallium azide at high temperatures for prolonged periods of time. This is particularly unsafe due to the high toxicity of thallium. Safety considerations led to the search of a more convenient synthetic procedure for the preparation of organothallium tetrazoles.

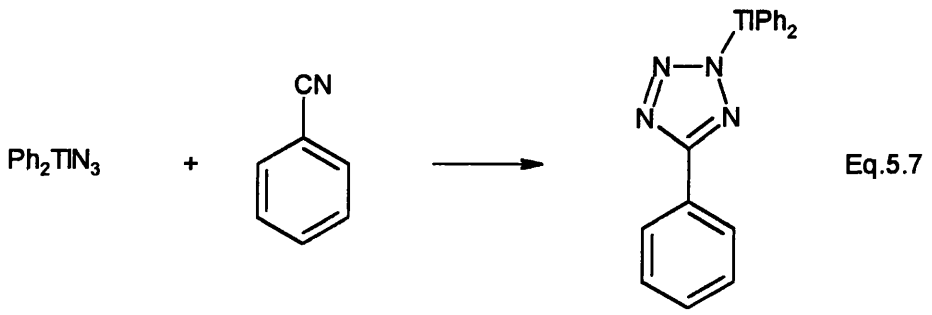

Eq.5.7

(29)

Seven diphenylthallium-substituted mono-, bis- and tris-tetrazoles, including **29**, have been prepared following the condensation route of Lee *et al*[165] (equations 5.8-5.10). Typically, a methanolic solution of the appropriate hydro-tetrazole was added to a refluxing methanolic solution of diphenylthallium hydroxide. The resultant colourless solution was refluxed for three hours. Cooling at room temperature for several days yielded **29** and **31-33** as white powders and **30, 34** and **35** as brown crystals. Some difficulty was encountered in generating analytically pure products. The anomaly was solved by the crystallographic analysis of 1,2-phenylene-bis-(diphenylthallium tetrazole) **(30)**, which revealed two methanol molecules, two water molecules and a molecule of diphenylthallium chloride, in addition to the organothallium bis-tetrazole, incorporated in the lattice structure (see Section 5.4.2). Two inferences can be made from this observation. Firstly, compounds **29-35** contain various permutations of water, methanol and diphenylthallium chloride molecules, the exact amount of which can only be

determined with certainty by crystallographic analysis. While the methanol/water incorporation is a consequence of the crystallisation process, the controlling factor in obtaining a pure organothallium-substituted tetrazole is the purity of the starting material, i.e. diphenylthallium hydroxide. The literature procedure of Casas *et al*[176] was used to prepare diphenylthallium hydroxide. This involved mixing a methanolic solution of diphenylthallium chloride with an aqueous solution of potassium hydroxide for two days at room temperature, cooling the reaction mixture to 0°C, filtering the resultant white solid, washing with methanol and then drying *in vacuo*. However, the conversion of the chloride to the hydroxide is variable and cannot be easily determined by available laboratory techniques.

IR spectra of all compounds (**29-35**) revealed medium strength bands at 1000-1100cm^{-1} typifying the presence of tetrazole rings. Compounds **29-31** also showed bands in the range of 1500-1600cm^{-1} confirming the presence of aromatic rings. Broad bands between 3000-3500cm^{-1} in the IR spectra of compounds **29-35** indicate the presence of water/methanol in them.

Preparative routes and work-up of compounds **22-35** are described in detail in Section 5.6.

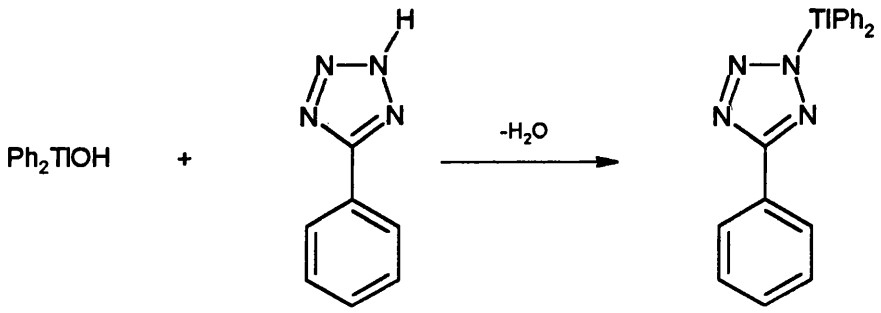

Eq.5.8

(29)

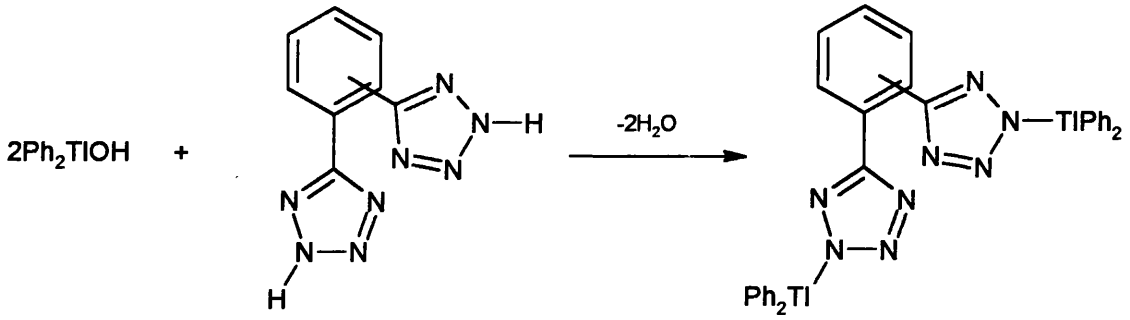

Eq.5.9

1,2 isomer (**30**), 1,3 isomer (**31**), 1,4 isomer (**32**)

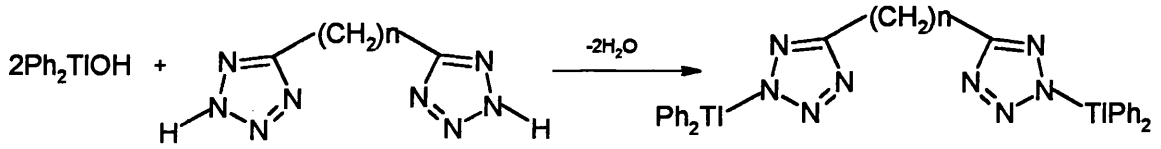

Eq.5.10

n = 1 (**33**), n = 2 (**34**), n = 4 (**35**)

5.3 SPECTROSCOPY

5.3.1 Multinuclear NMR Spectroscopy

^{1}H and ^{13}C NMR data for **22**, **23**, **27** and all the organothallium-substituted tetrazoles **29-35** were collected in d^{6}-DMSO, for **24-26** were taken in d^{2}-D_2O and **28** was not soluble in either solvent. The formation of the proposed products is confirmed by ^{1}H and ^{13}C NMR data. The ^{1}H NMR spectra for **22** and **23** exhibit the respective ethyl and butyl protons, while their ^{13}C NMR spectra reveal the tetrazole quaternary carbon and the central aliphatic carbons. The ^{1}H NMR spectra for **24** and **25** reveal the aliphatic methylene and butylene protons. The low solubility of these two compounds even in D_2O made it difficult to obtain clear ^{13}C NMR spectra. The ^{1}H NMR spectra for **26** and **27** reveal the aromatic protons of the central phenylene ring. The ^{13}C NMR spectra for **26** and **27** clearly show the quaternary tetrazole carbon at ~160 ppm. In addition, aromatic carbons are also visible. In the ^{1}H NMR spectra of **29-32**, aromatic protons of the central

phenylene ring and the diphenylthallium moiety are observed and for **33-35**, the protons of the respective central aliphatic moieties and the aromatic protons of the diphenylthallium are present. The ^{13}C NMR spectra of all the diphenylthallium-substituted tetrazole compounds listed in this chapter, except **34** and **35**, clearly show the quaternary carbon of the tetrazole at ~160ppm. The long relaxation time of the quaternary carbon coupled with the low solubility of **34** and **35** in DMSO and the high signal to noise ratio prevented the identification of the quaternary tetrazole carbon for these two compounds. The aromatic carbons corresponding to the central phenylene ring and the diphenylthallium moiety are visible for **29-32** and the central aliphatic carbons and the aromatic carbons corresponding to the diphenylthallium moiety are visible for **33-35.** However, due to the number and density of the aromatic peaks, an accurate assignment of them is difficult.

Unlike for tin, there are no easily available NMR handles available to indicate the coordination number of the thallium in solution-state. Thallium NMR spectroscopy is rare and expensive inspite of the fact that it has two stable isotopes, ^{203}Tl (29.5% natural abundance) and ^{205}Tl (70.5% natural abundance), both of which have nuclear spin 1/2.[177] For instance, on a 400MHz spectrometer, the ^{1}H nucleus resonates at 399 MHz and most other nuclei resonate between 0 and 160MHz. However, ^{205}Tl nucleus resonates at 230MHz which is a region that requires a special tunable oscillator. Nevertheless in comparison with organotin- and organolead-substituted tetrazoles, the thallium centre in the organothallium-substituted analogues probably achieves higher coordination in the solution-state. Preference by the thallium for higher coordination numbers must also be due to its large size. Besides, the extreme stablity of the organothallium-substituted tetrazoles (they are only soluble in MeOH and DMSO) also suggest polymerisation involving the thallium atom. Higher coordination can be achieved in various ways- either by coordinating to neighbouring tetrazole moieties (**LII**) or by coordinating to solvent molecules (**LIII**) or by a combination and permutation of the above two factors (**LIV**).

In a coordinating solvent like DMSO, either methanol or water (if present in the solid-state) or DMSO could coordinate to the metal centre.

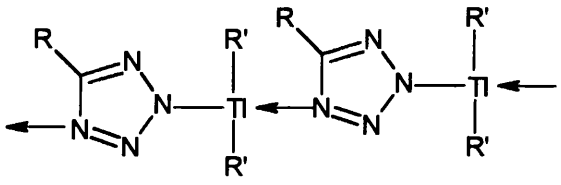

LII

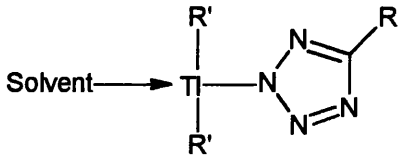

Solvent = MeOH, H_2O or DMSO

LIII

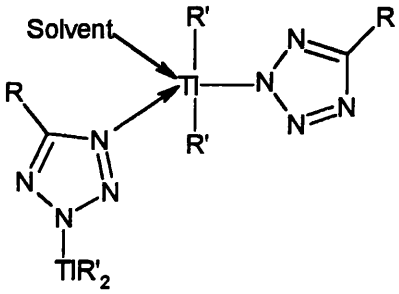

Solvent = MeOH, H_2O or DMSO

LIV

5.4 X-RAY CRYSTALLOGRAPHY

X-ray crystallography is of vital importance in characterising organothallium tetrazoles, even more so than organotin tetrazoles. In the case of the latter compounds, complementary techniques such as Mössbauer and ^{119}Sn NMR spectroscopies are

available to identify the local geometry about tin. However, these techniques are not easily available for thallium (see Section 5.3), which leads to heavy reliance on X-ray crystallography for ultimate characterisation. The following sections describe the crystallographic analysis of 1-diphenylthallium-5-phenyl tetrazole.MeOH (**29**), 1,2-phenylene-bis-(diphenylthallium tetrazole).2MeOH.$2H_2O$.Ph_2TlCl (**30**) and 1,4-butylene-bis-(diphenylthallium tetrazole).2MeOH (**35**).

5.4.1 Structure Of 2-Diphenylthallium-5-Phenyltetrazole.MeOH (29)

Crystals of 2-diphenylthallium-5-phenyltetrazole.MeOH (**29**) were grown from a methanolic solution at room temperature by slow evaporation. Full details of the crystallographic analysis, atomic coordinates and isotropic thermal parameters are included in Appendix VII. The asymmetric unit of **29** is half of a centrosymmetric dimer and is illustrated in Fig.5.2. Selected bond lengths and selected bond angles are given in Tables 5.2 and 5.3 respectively. The asymmetric unit contains two distorted trigonal bipyramidal *trans*-C_2TlN_2O thallium centres. This is similar to organotin-substituted tetrazoles known to date where the tin centre is *trans*-trigonal bipyramidal (see Section 2.5 and 3.5). The obvious difference between the two metal centres is that the tin is *trans* with respect to nitrogens and the thallium centre is *trans* with respect to the phenyl carbons. The axial positions of Tl(1) are occupied by the two phenyl groups and equatorial positions are occupied by a methanol molecule and two tetrazole N^1 and N^2 atoms (see numbering scheme discussed in Section 1.4). The $N^1 + N^2$ coordination mode of the metal atom has been seen in **XXVII**, **XXVIII** and **XXIX** (see Table 2.1). The C-Tl-C bond angle is close to 180° [C(8)-Tl(1)-C(14) 173.9(4)°]. In an ideal trigonal bipyramidal geometry, the equatorial bond angles are 120°, however this is not the case in **29**. This is probably due to the formation of the dimer containing a six-membered ring made up of two thallium atoms and four tetrazole nitrogen atoms. Ring formation puts a constraint on the equatorial bond angles and makes them deviate from 120°. Thus, [N(1)-Tl(1)-O(1) 106.8(2)°, N(2′)-Tl(1)-O(1) 159.3(3)° and N(1)-Tl(1)-N(2′) 93.9(3)°]. An alternative, more plausible description of the thallium centres and one which is used in the

literature without any explanation is as *pseudo*-octahedral. An example of such a centre is given in Table 5.1.

The six-membered ring contained in the dimer is a slight chair with a dihedral angle of 18(1)° and the two thallium atoms are displaced 0.26(2)Å above and below the plane formed by the four nitrogens. The Tl-Tl distance within the six-membered ring is 4.825(2)Å. This discounts the possibility of a Tl-Tl bond as the ionic radius of Tl^{3+} (0.95Å) is much shorter.[136] Since a search of the Cambridge Crystallographic Database revealed no precedent for a dative bond between a methanolic oxygen and a thallium centre in an organothallium(III) azole structure in the literature, the Tl(1)-O(1) bond length of 2.691(7)Å cannot really be compared with any such structure. A similar interaction i.e. dative bond between methanolic oxygen and metal centre has been reported in the structure of 1,3-phenylene-bis-(tributylstannyltetrazole).bis methanolate.[24] The Sn-O bond length of 2.393(9)Å, however, is much shorter than the Tl-O distance in **29**. The bridging Tl(1)-N(2′) 2.680(9)Å is only slightly longer than the covalent Tl(1)-N(1) 2.512(9)Å and is comparable with the bridging Tl-N bond length of 2.61(2)Å in dimethyl (4-amino-5-mercapto-3-trifluoromethyl-1,2,4-triazolato) thallium(III)[166].

Analysis of the supramolecular structure reveals that the dimers formed as a result of inversion centres further interact to generate one-dimensional polymers along *a* due to intermolecular hydrogen bonding (Fig.5.3). Hydrogen bonding is brought about by H(1A) bonding to N(4) of the residue generated by the transformation *x-1, y, z* [H(1A)-N(4) 1.9(2)Å]. The view of **29** in the *ac*-plane consists of alternating six-membered and twelve-membered rings. The twelve-membered rings consist of two thallium atoms, six nitrogen atoms, two oxygen atoms and two hydrogen atoms.

If hydrogen bonding in included, the tetrazole unit is tridentate with respect to itself and exhibits $N^1 + N^2 + N^4$ coordination. N^1 and N^2 are each coordinated to two thallium atoms in the dimeric unit and N^4 is hydrogen bonded to the oxygen of the methanol of the lattice neighbour. Tridentate coordination of the tetrazole moiety has been observed in $\{M[H_2B(CHN_4)_2]_2(H_2O)_2\}.(H_2O)_2$[48] (M = Co, Zn, Cd) (see Table 1.1),

where N^1 and N^4 are coordinated to a boron and a metal atom respectively and N^2 is hydrogen bonded to a water of crystallization.

The dominant feature of **29** is the six-membered ring in the dimeric unit and in the literature of thallium azole structures the closest analogy of this ring can be drawn with the eight-membered ring seen in the crystal structure of dimethyl (4-amino-5-mercapto-3-trifluoromethyl-1,2,4-triazolato) thallium(III)[166] (Fig.5.4). However, unlike in **29**, the eight-membered ring is a result of a tetrameric unit. Within the tetrameric unit, the molecules are interconnected by Tl-N(1) and Tl....S interactions and by hydrogen bonds between the NH_2 group and the N(2) atom of neighbouring molecules along the *c*-axis. The Tl-N(1) and Tl....S interactions result in the formation of an eight-membered ring similar to the six-membered ring seen in **29** and the hydrogen bonding between the NH_2 group N(7) and N(2) atoms result in eight-membered rings flanking the tetrameric eight-membered ring. In addition, there is also another hydrogen bond between two neighbouring NH_2 [N(7)-N(7)] groups. The Tl-Tl distance within the eight-membered ring is 4.14Å, which is shorter than the metal-metal distance in the six-membered ring of **29**.

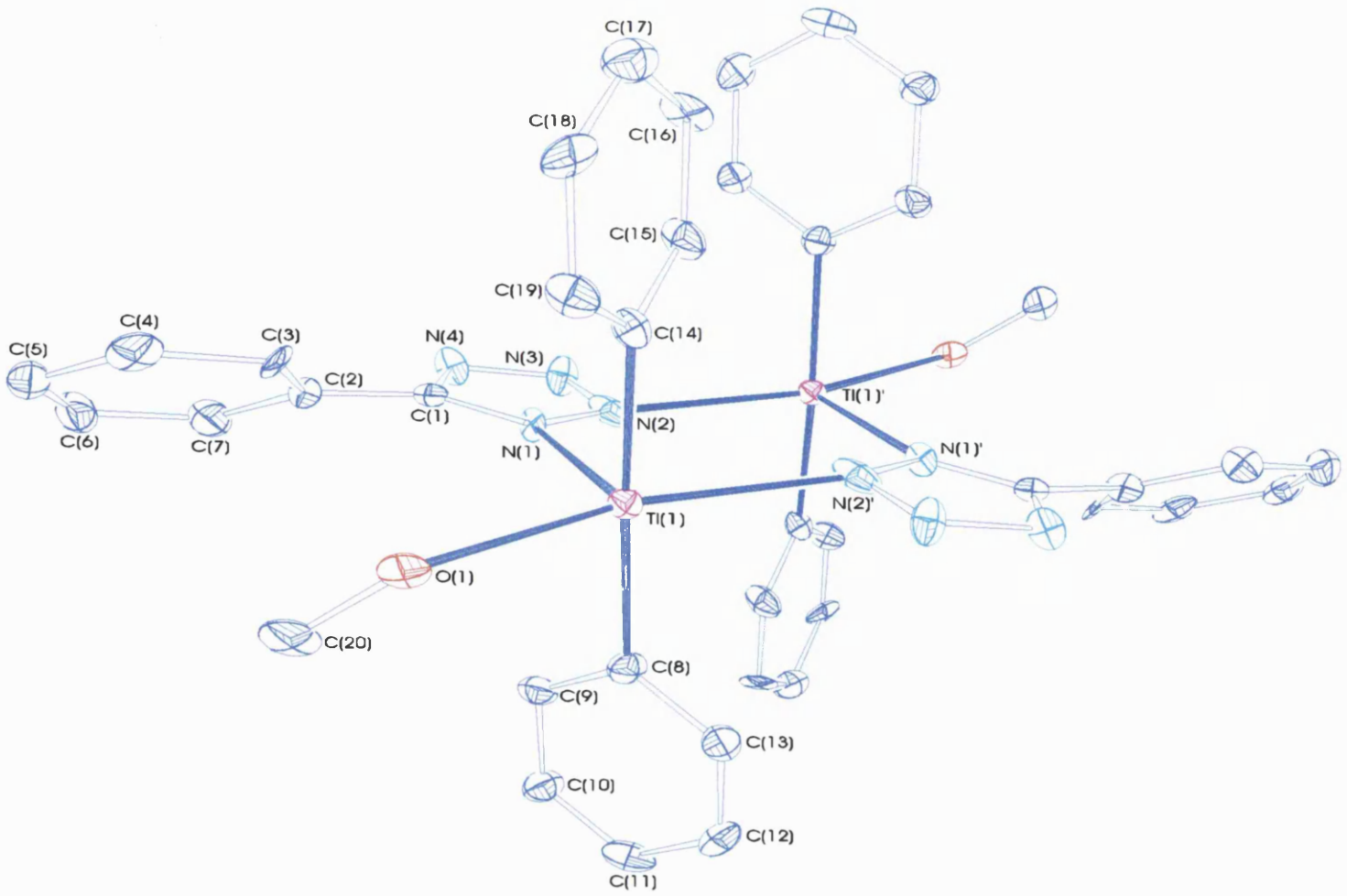

Fig.5.2: The asymmetric unit of **29** showing the atomic labelling scheme used in the text and tables. Hydrogen atoms are omitted for clarity.

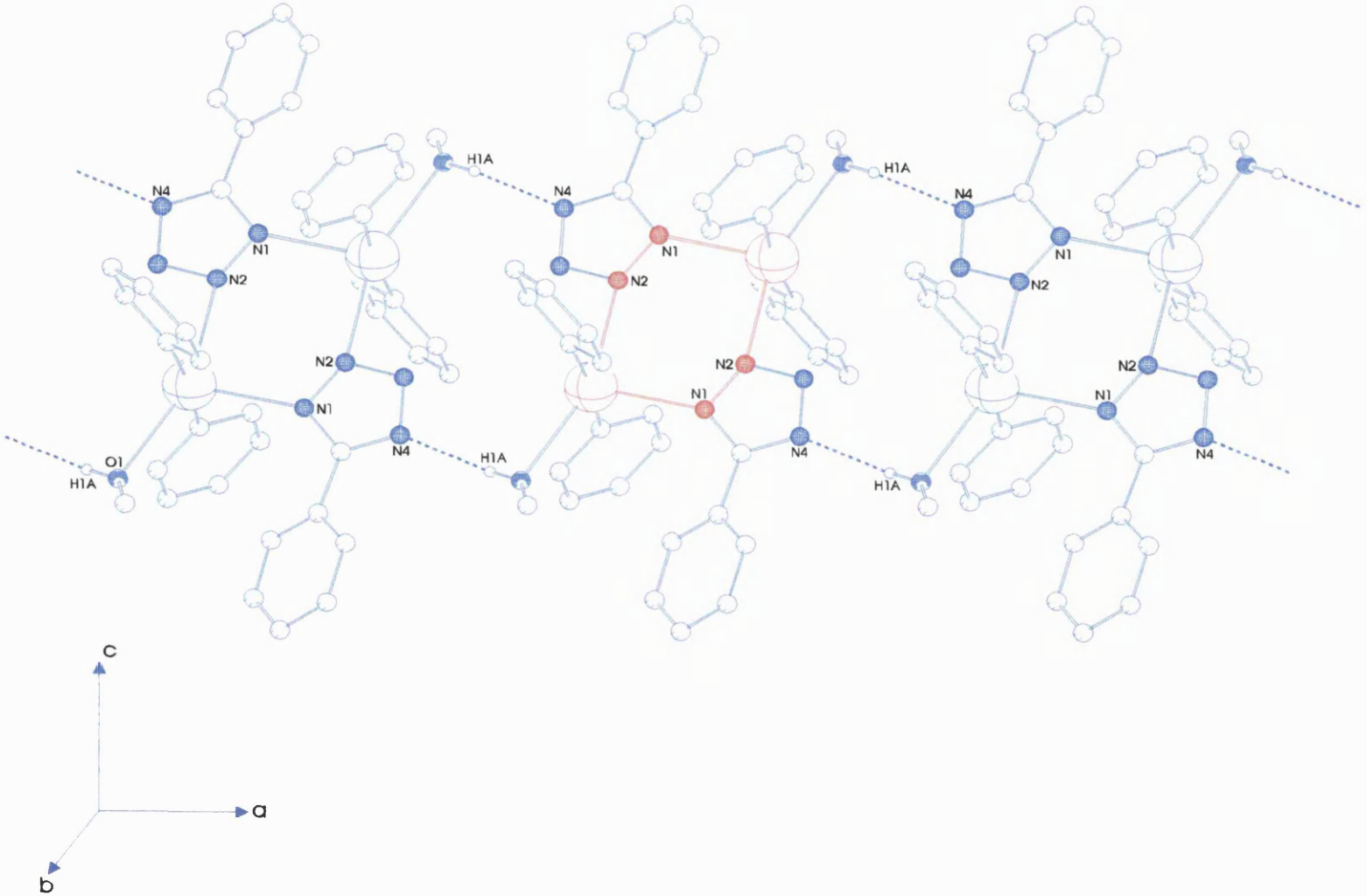

Fig.5.3: One-dimensional polymers of **29** propagating along the *a*-axis.

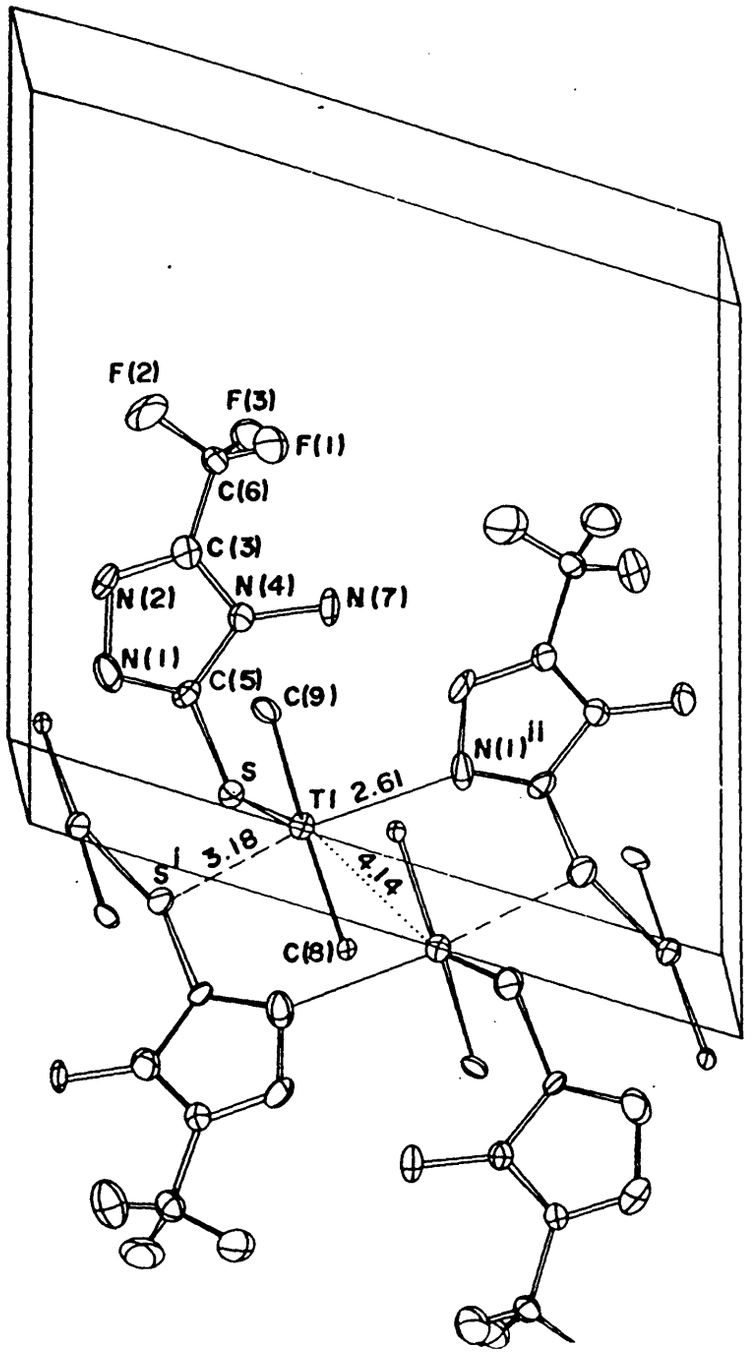

Fig.5.4: An ORTEP view of the crystal packing of dimethyl (4-amino-5-mercapto-3-trifluoromethyl-1,2,4-triazolato)thallium(III) with atomic labeling.[166]

Table 5.2: Selected Bond Lengths (Å) For **29** With Their Estimated Standard Deviations In Parentheses.

Tl(1)-C(8)	2.13(1)	N(1)-N(2)	1.33(1)
Tl(1)-C(14)	2.12(1)	N(2)-N(3)	1.32(1)
Tl(1)-N(1)	2.512(9)	N(2)-Tl(1)#1	2.680(9)
Tl(1)-N(2)#1	2.680(9)	N(3)-N(4)	1.36(1)
Tl(1)-O(1)	2.691(7)	N(4)-C(1)	1.31(1)
N(1)-C(1)	1.33(1)	C(1)-C(2)	1.48(2)
O(1)-C(20)	1.42(1)		

Symmetry transformations used to generate equivalent atoms: #1 1-x,-y,-z.

Table 5.3: Selected Bond Angles (°) For **29** With Their Estimated Standard Deviations In Parentheses

C(8)-Tl(1)-C(14)	173.9(4)	N(1)-N(2)-Tl(1)#1	150.5(8)
C(8)-Tl(1)-N(1)	94.1(3)	N(2)-N(3)-N(4)	105.4(8)
C(14)-Tl(1)-N(1)	92.0(3)	C(1)-N(4)-N(3)	107.4(8)
C(8)-Tl(1)-N(2)#1	90.1(4)	C(6)-C(7)-C(2)	119.0(1)
C(14)-Tl(1)-N(2)#1	89.9(3)	C(13)-C(8)-C(9)	121(1)
N(1)-Tl(1)-N(2)#1	93.9(3)	C(13)-C(8)-Tl(1)	120.4(8)
C(8)-Tl(1)-O(1)	88.6(3)	C(9)-C(8)-Tl(1)	118.9(8)
C(14)-Tl(1)-O(1)	89.2(3)	C(19)-C(14)-Tl(1)	121.2(8)
N(1)-Tl(1)-O(1)	106.8(2)	C(15)-C(14)-Tl(1)	119.8(8)
N(2)#1-Tl(1)-O(1)	159.3(3)	C(20)-O(1)-Tl(1)	121.9(7)
C(1)-N(1)-N(2)	104.9(9)	N(4)-C(1)-N(1)	111(1)
C(1)-N(1)-Tl(1)	140.8(7)	N(4)-C(1)-C(2)	124(1)
N(2)-N(1)-Tl(1)	114.3(7)	N(1)-C(1)-C(2)	125(1)
N(3)-N(2)-N(1)	111.4(9)	C(3)-C(2)-C(1)	121(1)
N(3)-N(2)-Tl(1)#1	96.6(6)	C(7)-C(2)-C(1)	118.7(9)

Symmetry transformations used to generate equivalent atoms: #1 1-x,-y,-z.

5.4.2 Structure Of 1,4-Butylene-Bis-(Diphenylthallium Tetrazole).2MeOH (35)

From a methanolic solution, crystals of 1,4-butylene-bis(diphenylthallium tetrazole).MeOH were grown slowly at room temperature. Appendix VIII contains full details of the crystallographic analysis, atomic coordinates and isotropic thermal parameters. The asymmetric unit of **35** is one half of the molecule as presented in Fig.5.5. The dimer is generated by an inversion centre lying halfway along C15-C15′. Selected bond lengths and bond angles are given in Tables 5.4 and 5.5 respectively. The thallium centre contained in the asymmetric unit is in a distorted octahedral (*trans*-C_2TlN_3O) environment. The two phenyl groups are axial and the equatorial positions are occupied by three tetrazolic nitrogens [N(1), N(3), N(4)] and oxygen of the methanol [O(1)]. The $N^1 + N^2 + N^3$ mode of coordination of the tetrazole ring with respect to the metal centre is unique. The axial C-Tl-C bond angle is approximately 180° [C(1)-Tl(1)-C(7) 175.8(4)°]. The four equatorial bond angles are close to 90° [N(1)-Tl(1)-N(3′) 93.2(3)°, N(3′)-Tl(1)-N(4′) 98.7(3)°, N(4′)-Tl(1)-O(1) 70.2(3)°, O(1)-Tl(1)-N(1) 97.6(3)°]. The dative Me(H)O→Tl bond [Tl(1)-O(1) 2.970(8)Å] is longer than that of **29** [Tl(1)-O(1) 2.691(7)Å]. The covalent Tl(1)-N(1) bond length of 2.535(9)Å and the bridging Tl(1)-N(3′) bond length of 2.568(9)Å are similar to the covalent Tl-N bond length seen in **29** [2.512(9)Å]. However, the bridging Tl(1)-N(4′) is 3.074(9)Å and is distinctly longer than any other Tl-N bond length in either **29**or **35**.

The supramolecular structure reveals polymeric sheets of molecules at unit cell intervals along *b*, where all nitrogens play a role in bonding (Fig.5.6). Viewed in the *ac*-plane, each polymeric sheet consists of stacks of six-membered rings, each containing two thallium atoms and four nitrogen atoms, connected by butylene moieties. There are two kinds of these rings in these stacks and these alternate with each other. The formation of the first ring is brought about by Tl(1) bonding to N(3) of the tetrazole generated by the symmetry operator *1-x, -y, 1-z* and it resembles the Tl_2N_4 rings in **29**. Like the latter, the rings in **35** are also chair-shaped. The two thallium atoms are displaced 0.89(2)Å above and below the plane of the four nitrogens and the dihedral angle of the chair is 51(1)°. The Tl-Tl distance is 4.731(1)Å, which is comparable to that in **29** [4.825(2)]Å. Whereas

in **29** the Tl_2N_4 rings further interact to form one-dimensional polymers via intermolecular hydrogen bonding, in **35** the Tl_2N_4 rings are held together by an additional Tl-N bond. Thus, Tl(1) bonds to N(4) in the lattice neighbour generated by *x-1, y, z* and this leads to the formation of a second six-membered Tl_2N_4 ring. As noted before, the Tl(1)-N(4′) bond is much longer than the Tl(1)-N(3′) bond. This ring has a dihedral angle of 19(1)° and the thallium atoms are displaced 0.31(2)Å above and below the plane of the four nitrogens. Thus, it also forms a slight chair but it is not as pronounced as in the first ring. The Tl-Tl distance of 4.953(1)Å within the ring is slightly longer than for the first ring or for the one **29**. Hydrogen bonding between N(2) and the oxygen of the methanol attached to Tl(1) generated via the operator *x-1, y, z* merely stabilises the long Tl-N bond. These ribbons of alternating six-membered rings are further connected by butylene bridges to form sheets.

The structure is unique in the literature of organometallic tetrazoles in containing tetradentate tetrazoles. The tetrazole moiety is tetradentate and exhibits $N^1 + N^2 + N^3 + N^4$ mode of coordination. N^1 is coordinated to Tl(1); N^2 is coordinated to Tl(1) generated by the symmetry operator *1-x, -y, 1-z*; N^3 is coordinated to Tl(1) generated by the symmetry operator *-1+x, y, z*; and N^4 is hydrogen bonded to the oxygen of the methanol of the lattice neighbour generated via the symmetry operator *x-1, y, z* [O(1).....N(2) 2.81(1)Å, H(1)....N(2) 2.02(3)Å]. The hydrogen bond is comparable to that of **29** [H(1A)....N(4) 1.9(2)Å].

Parallels can be drawn with the bilayer structure of 1,6-hexylene-bis-(tributylstannyl tetrazole) (Fig.5.7a and b).[19] Fig.5.7a reveals that half of the hexyl groups [C(41)-C(48)] are used to form the polymer strands into sheets, while the other half [C(38)-C(40) and their symmetry-related partners are used to join centrosymmetrically related sheet structures into a bilayer array. Fig.5.7b gives an orthogonal view of the bilayer along *a* and reveals the non-planar nature of the layer structure. The formation of hexagonal-looking channels within the bilayer is also illustrated in this figure.

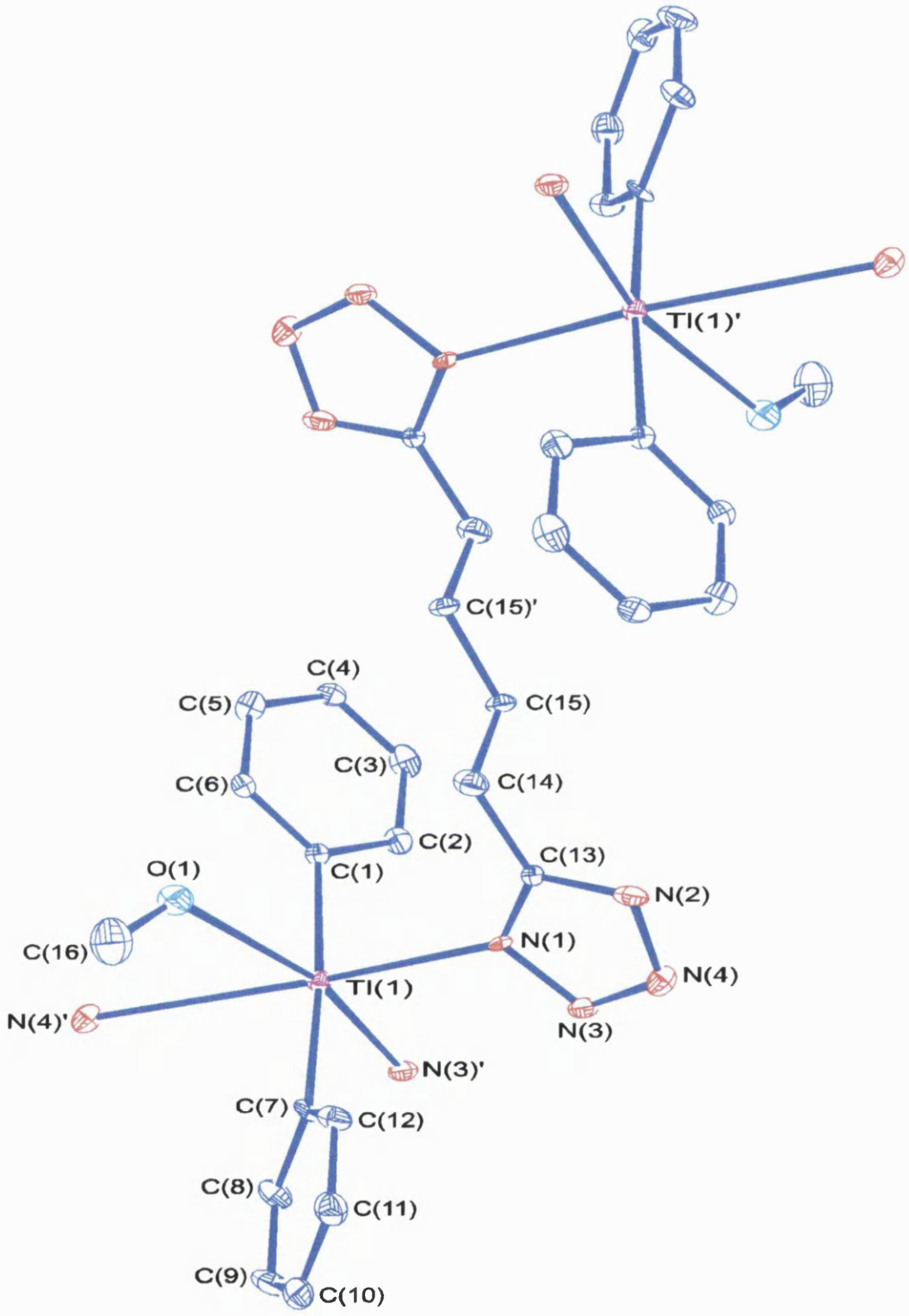

Fig.5.5: The asymmetric unit of **35** showing the atomic labeling scheme used in the text and tables. Hydrogen atoms are omitted for clarity.

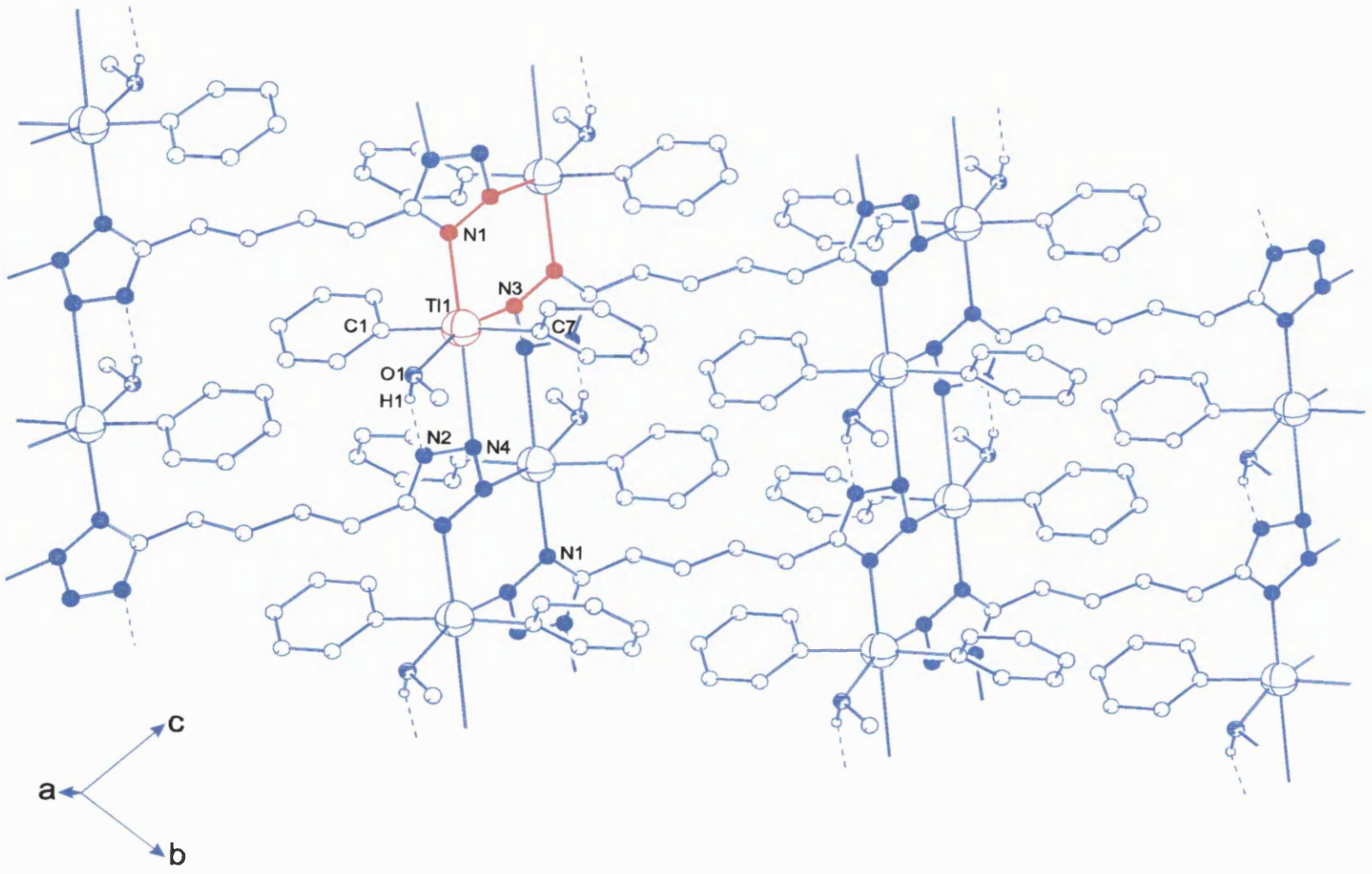

Fig.5.6: View of **35** in the *ac*-plane.

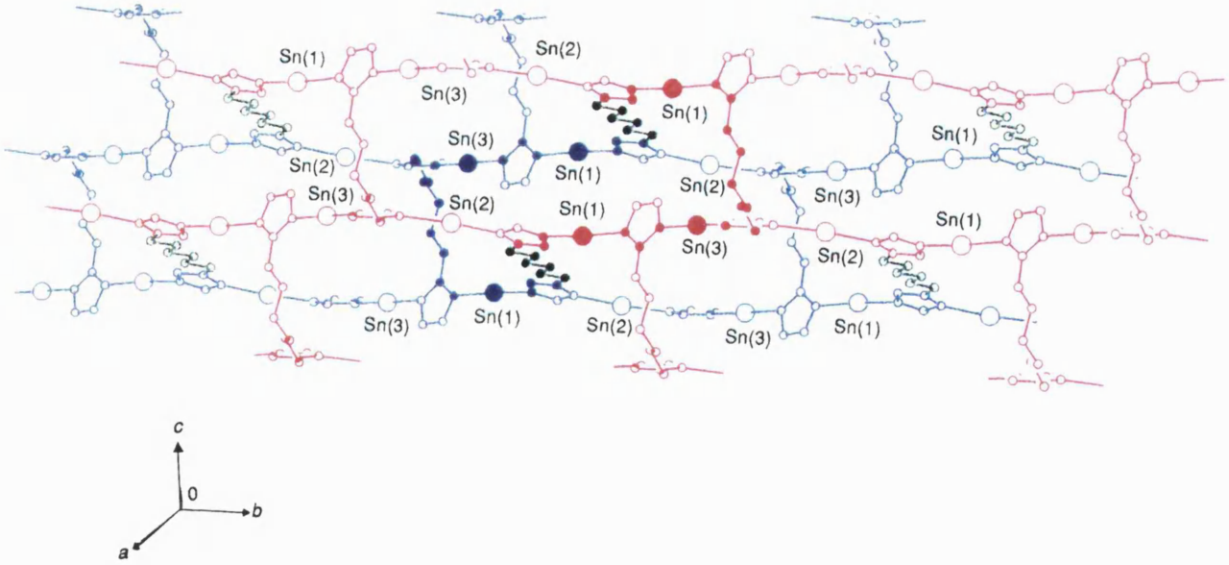

Fig.5.7a: The bilayer nature of 1,6-hexylene-bis-(tributylstannyl tetrazole). Only the α-carbon atoms of the n-butyl groups are shown for clarity. Atoms coloured red and blue belong to separate layers and are linked into the bilayer arrangement by the hexyl groups (green).[19]

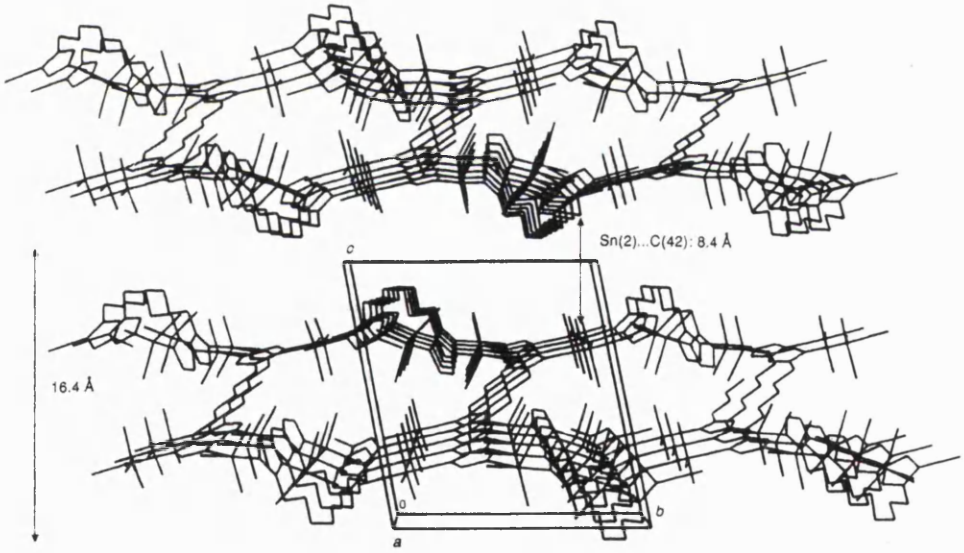

Fig.5.7b: View of 1,6-hexylene-bis-(tributylstannyl tetrazole) orthogonal to the bilayer (along *a*) which shows the formation of hexagonal channels.[19]

Table 5.4: : Selected Bond Lengths (Å) For **35** With Their Estimated Standard Deviations In Parentheses.

Tl(1)-C(7)	2.11(1)	N(2)-N(4)	1.35(1)
Tl(1)-C(1)	2.12(1)	N(1)-N(3)	1.36(1)
Tl(1)-N(1)	2.535(9)	N(2)-C(13)	1.31(1)
Tl(1)-N(3)#1	2.568(9)	N(3)-N(4)	1.30(1)
Tl(1)-N(4)#2	3.074(9)	C(13)-C(14)	1.49(1)
O(1)-C(16)	1.44(2)	C(14)-C(15)	1.51(1)
N(1)-C(13)	1.34(1)	C(15)-C(15)#3	1.53(2)

Symmetry transformations used to generate equivalent atoms: #1 1-x,-y,1-z; #2 x-1,y,z; #3 1-x,-y,-z.

Table 5.5: Selected Bond Lengths (°) For **35** With Their Estimated Standard Deviations In Parentheses.

C(7)-Tl(1)-C(1)	175.8(4)	N(4)-N(3)-N(1)	109.7(8)
C(7)-Tl(1)-N(1)	90.5(3)	N(4)-N(3)-Tl(1)#1	110.3(6)
C(1)-Tl(1)-N(1)	92.9(3)	N(2)-C(13)-N(1)	110.6(8)
C(7)-Tl(1)-N(3)#1	88.5(3)	N(1)-N(3)-Tl(1)#1	130.7(6)
C(1)-Tl(1)-N(3)#1	93.8(3)	N(3)-N(4)-N(2)	108.0(8)
N(1)-Tl(1)-N(3)#1	93.2(3)	C(6)-C(1)-Tl(1)	123.7(8)
C(7)-Tl(1)-N(4)#2	84.4(3)	C(2)-C(1)-Tl(1)	117.2(8)
C(1)-Tl(1)-N(4)#2	91.8(3)	C(12)-C(7)-Tl(1)	121.5(7)
N(1)-Tl(1)-N(4)#2	166.9(3)	C(8)-C(7)-Tl(1)	119.5(8)
N(3)#1-Tl(1)-N(4)#2	98.7(3)	C(13)-C(14)-C(15)	113.4(9)
C(13)-N(1)-N(3)	104.5(8)	C(14)-C(15)-C(15)#3	114(1)
C(13)-N(1)-Tl(1)	131.9(7)	N(1)-C(13)-C(14)	124.6(9)
N(3)-N(1)-Tl(1)	121.9(6)	N(2)-C(13)-C(14)	124.6(9)
C(13)-N(2)-N(4)	107.2(9)		

Symmetry transformations used to generate equivalent atoms: #1 1-x,-y,1-z; #2 x-1,y,z; #3 1-x,-y,-z.

5.4.3 Structure Of 1,2-Phenylene-Bis-(Diphenylthallium Tetrazole).2MeOH.2H_2O. Ph_2TlCl (30)

X-ray quality crystals of 1,2-phenylene-bis(diphenylthallium tetrazole). 2MeOH. 2H_2O. Ph_2TlCl were grown slowly from a methanolic solution at room temperature. Detailed crystallographic analysis, atomic coordinates and isotropic thermal parameters are included in Appendix IX. The asymmetric unit of **30** is shown in Fig.5.8 and selected bond lengths and bond angles are given in Tables 5.6 and 5.7 respectively. The structure as presented in Fig.5.8 consists of 1,2-$C_6H_4[Ph_2Tl(CN_4)]_2$, a coordinated Ph_2TlCl, two water molecules and two methanols. The asymmetric unit consists of half this collective, the half of the assembly being generated from the other by a mirror plane containing Tl(2) and Cl(1) and bisecting C(24)-C(24′), C(26)-C(26′). The mirror plane also consists of the phenyl ring C(14-19) and it bisects the phenyl ring C(20-23). The Ph_2TlCl is a unique feature of this crystal structure and was probably coordinated for crystallisation purposes. It was probably present in the reaction mixture due to the partial conversion of Ph_2TlCl to the starting material Ph_2TlOH. There are two distorted octahedral thallium centres in the asymmetric unit- *trans*-$C_2TlO_2N_2$ and *trans*-C_2TlN_2OCl. In both cases, the phenyl groups are in axial positions. The axial bond angles are close to 180° [C(14)-Tl(2)-C(20) 171.4(8)°, C(8)-Tl(1)-C(2) 168.0(6)°]. The equatorial positions of Tl(1) are occupied by two tetrazolic nitrogens, the bridging chlorine atom and an oxygen of a neighbouring water. The four equatorial bond angles deviate from 90° [N(1)-Tl(1)-Cl(1) 86.7(3)°, N(1)-Tl(1)-N(2′) 89.7(4)°, N(2′)-Tl(1)-O(2′) 100.5(3)°, Cl(1)-Tl(1)-O(2′) 83.1(3)°]. The Tl(1)-N(2′) [2.87(1)Å] bond is longer than the Tl(1)-N(1) bond length of 2.60(1)Å. The latter Tl-N bond length is equivalent with the covalent Tl-N bond lengths of **29** [Tl(1)-N(1) 2.512(9)Å] and **35** [Tl(1)-N(1) 2.535(9)Å]. The Tl(1)-O(2′) bond length of 2.95(1)Å is only marginally longer than the Tl-O bond lengths of the Tl←OH_2 bond in $(Me_3SiCH_2)_2TlN(SO_2Me)_2.H_2O$ [Tl-O 2.799(3)Å, 2.813(3)Å].[178] The bridging chlorine is equidistant from both the thallium atoms rendering the Tl-Cl bond lengths equivalent [Tl(1)-Cl(1) 2.777(1)Å, Tl(1′)-Cl(1) 2.777(1)Å]. This bond length lies between terminal Tl-Cl and bridging Tl-Cl bond distances reported in the literature. In $TlCl_3.3C_6H_5N$, the

terminal Tl-Cl(1) and Tl-Cl(2) bond lengths are 2.520(6)Å and 2.498(4)Å respectively.[179] The bridging Tl-Cl(2) bond length in $[(p\text{-}HC_6F_4)_2TlCl(OPPh_3)]_2$ is 2.936(3)Å.[180] The equatorial positions of Tl(2) are occupied by two tetrazolic nitrogens and oxygens of two water molecules. The four equatorial bond angles show major deviations from 90° [O(2)-Tl(2)-N(4) 83.4(4)°, N(4)-Tl(2)-N(4′) 73.4(6)°, N(4′)-Tl(2)-O(2′) 83.4(4)°, O(2′)-Tl(2)-O(2) 119.4(4)°]. The Tl-N bond lengths [Tl(2)-N(4) 2.61(1)Å and Tl(2)-N(4′) 2.61(1)Å] are equivalent with the Tl(1)-N(1) bond length of 2.60(1)Å. The Tl(2)-O(2) bond length of 2.95(1)Å is exactly the same as the Tl(1)-O(2′) by symmetry. It must be noted here that unlike in **29** and **35** which have methanol molecules coordinated to the thallium atoms, the metal centres in **30** have coordinated water molecules. The Tl-O bond lengths in **30** are close to the Tl-O bond lengths resulting from a dative Tl←O(H)Me coordination in **35** [Tl(1)-O(1) 2.970(8)Å in **35**]. With respect to the thallium centres, Tl(2) is coordinated to two N^1 atoms (see numbering scheme in Section 1.4). The $N^1 + N^1$ coordination has been observed in **XXIV** and **XXVI** (see Table 2.1). The Tl(1) atom is coordinated to tetrazole N^1 and N^2 atoms. The $N^1 + N^2$ coordination has been seen in the thallium centres in **29** and also in **XXVIII** and **XXIX** (see Table 2.1).

The supramolecular structure consists of polymeric sheets of molecules parallel to the *ab*-plane as follows (Fig.5.9). Firstly, the water molecule acts as a bridge between the thallium centres along the *a* direction. O(2) bonds to Tl(2) as presented and also to Tl(1′) of the lattice neighbour. The sheet is propagated in the *b*-direction by Tl(1) bonding to N(2′) generated by the symmetry operator *-x, -y, -z*. Methanol cements these sheets by hydrogen bonding to the tetrazolic nitrogen N(3) and O(2) of the water [N(3)-O(1) 2.77(2), O(1)-O(2) 2.82(2)Å]. The hydrogen bond between the tetrazolic nitrogen and the methanol oxygen is similar in length to the one seen in **35** [O(1)-N(2) 2.81(1)Å]. The sum total of all these interactions render the oxygens of the water molecules four coordinate.

Each tetrazole is tetradentate with N^1 being coordinated to Tl(1), N^2 being coordinated to Tl(1) of the lattice neighbour generated by the inversion centre at 0,0,0 [Tl(1)-N(2) 2.867(14)Å], N^3 being hydrogen bonded to O(2) of the methanol molecule

generated by the transformation *-1-x, -y, -z* [N(3)-O(1) 2.77(2)Å] and N^4 being coordinated to Tl(2).

The most striking feature of this complex is the presence of the six-membered ring in its intricate mesh of interactions, which has been previously seen in **29** and **35**. As in the previous two cases, this ring consists of two thallium atoms and four tetrazole nitrogens. The formation of this ring is brought about by the intermolecular bond formation between Tl(1) and N(2′) generated by the symmetry operator *-x, -y, -z*. Tl(2) is not involved in ring formation. As in the previous two structures, this ring is also a chair with a dihedral angle of 73(1)° and the two thallium atoms displaced 1.41(3)Å above and below the plane of the four nitrogens. The following table summarises the dihedral angle, displacement of the metal atoms above and below the plane of the nitrogens and the thallium-thallium distance for the unique six-membered ring seen in **29**, **35** and **30**.

Table 5.8: Summary of parameters for the six-membered rings seen in **29**, **35** and **30**.

Compound	**Dihedral Angle(°)**	**Displacement of metal atoms above and below the 4×N plane (Å)**	**Tl-Tl distance(Å)**
29	18(1)	0.26(2)	4.825
35	51(1)	0.89(2)	4.731
30	73(1)	1.41(3)	4.921

As is apparent from the above table, there is a steady increase in the dihedral angle of the six-membered ring and displacement of the thallium atoms from the plane of the four nitrogens from **29** to **30**. This suggests that the chair becomes more and more pronounced as we move down the series **29**, **35**, **30**. Interestingly enough, the dihedral angle in cyclohexane is 58°.

30 is the second organometallic tetrazole structure with tetradentate tetrazoles. This structure is different from the previous two in not only being very complex but also coordinating an additional metal (Ph_2TlCl). Attempts were made to direct the coordination of Ph_2TlCl in the lattice structure of an organothallium-substituted tetrazole by refluxing 1,3-phenylene-bis-5,5′-(diphenylthallium tetrazole) with Ph_2TlCl. However, this gave products which could not be identified.

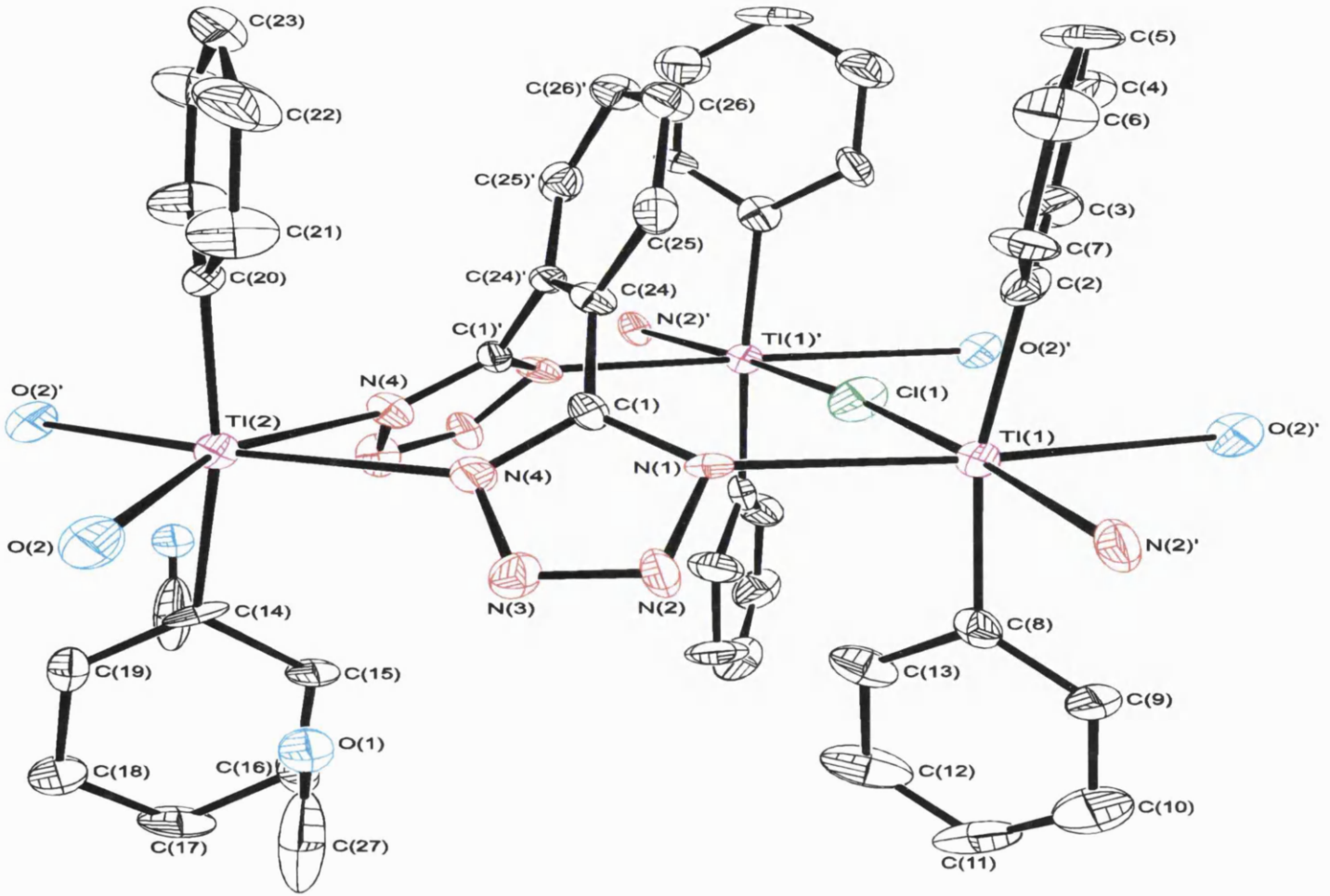

Fig.5.8: The asymmetric unit of **30** showing the atomic labelling scheme used in the text and tables. Hydrogen atoms are omitted for clarity.

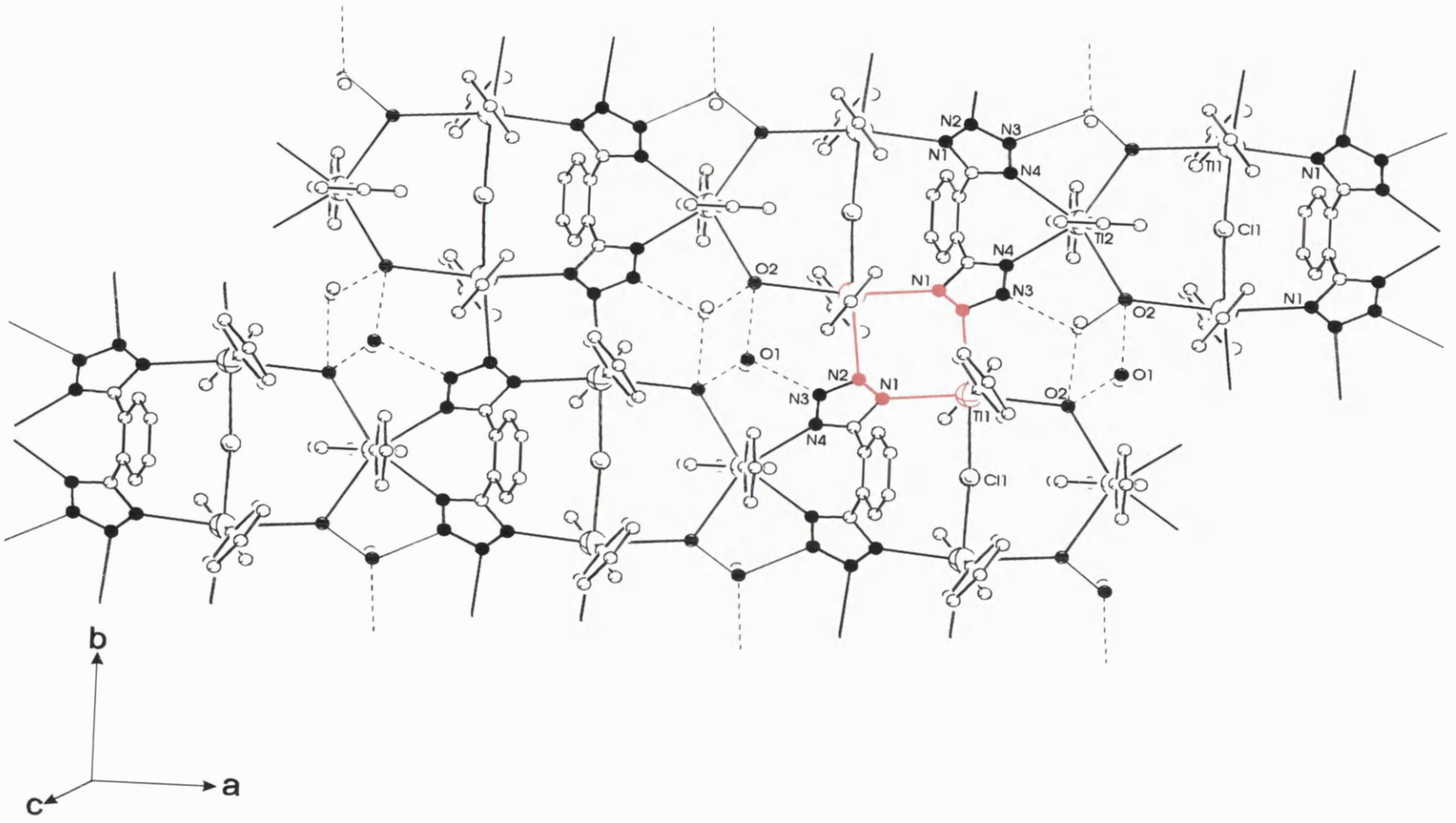

Fig.5.9: Polymeric sheet of **30** parallel to the *ab*-plane.

Table 5.6: Selected Bond Lengths (Å) For **30** With Their Estimated Standard Deviations In Parentheses.

Tl(1)-C(8)	2.11(2)	O(1)-C(27)	0.97(4)
Tl(1)-C(2)	2.12(2)	N(1)-N(2)	1.38(2)
Tl(1)-N(1)	2.60(1)	N(1)-C(1)	1.37(2)
Tl(1)-Cl(1)	2.777(1)	N(2)-N(3)	1.30(2)
Tl(2)-C(14)	2.08(2)	N(3)-N(4)	1.35(2)
Tl(2)-C(20)	2.10(2)	N(4)-C(1)	1.32(2)
Tl(2)-N(4)	2.61(1)	C(1)-C(24)	1.47(2)

Symmetry transformations used to generate equivalent atoms: #1 x,-y+1/2,z.

Table 5.7: Selected Bond Lengths (Å) For **30** With Their Estimated Standard Deviations In Parentheses.

C(8)-Tl(1)-C(2)	168.0(6)	C(15)-C(14)-Tl(2)	122(2)
C(8)-Tl(1)-N(1)	94.2(5)	C(25)-C(24)-C(1)	116(1)
C(2)-Tl(1)-N(1)	94.9(5)	N(2)-N(3)-N(4)	110(1)
C(8)-Tl(1)-Cl(1)	93.7(5)	C(1)-N(4)-N(3)	108(1)
C(2)-Tl(1)-Cl(1)	94.6(5)	C(1)-N(4)-Tl(2)	131(1)
N(1)-Tl(1)-Cl(1)	86.7(3)	N(3)-N(4)-Tl(2)	120.6(9)
C(14)-Tl(2)-C(20)	171.4(8)	N(4)-C(1)-N(1)	109(1)
C(14)-Tl(2)-N(4)#1	95.4(6)	N(4)-C(1)-C(24)	128(1)
C(20)-Tl(2)-N(4)#1	91.5(5)	N(1)-C(1)-C(24)	123(1)
C(14)-Tl(2)-N(4)	95.4(6)	C(7)-C(2)-Tl(1)	120(1)
C(20)-Tl(2)-N(4)	91.5(5)	C(3)-C(2)-Tl(1)	122(1)
N(4)#1-Tl(2)-N(4)	73.4(6)	C(9)-C(8)-Tl(1)	121(1)
Tl(1)#1-Cl(1)-Tl(1)	174.8(3)	C(13)-C(8)-Tl(1)	121(1)
N(2)-N(1)-C(1)	106(1)	C(19)-C(14)-Tl(2)	123(2)
N(2)-N(1)-Tl(1)	116.0(9)	C(21)#1-C(20)-Tl(2)	121(1)
C(1)-N(1)-Tl(1)	132.4(9)	C(21)-C(20)-Tl(2)	121(1)
N(3)-N(2)-N(1)	108(1)	C(24)#1-C(24)-C(1)	124.0(8)

Symmetry transformations used to generate equivalent atoms: #1 x,-y+1/2,z.

5.5 SUMMARY

To summarise, five thallium(I) tetrazolates have been prepared. Diphenylthallium-substituted phenyl tetrazole was synthesised by the traditional cycloaddition route used to synthesise the organotin derivatives (see chapters 2 and 3). However, safety considerations led to the quest of other preparative methods. The condensation route involving the reaction of diphenylthallium hydroxide with aromatic and aliphatic hydro-tetrazoles was used to synthesise seven diphenylthallium-substituted tetrazoles. Three of these tetrazoles have been crystallographically characterised-1-diphenylthallium-5-phenyltetrazole (**29**), 1,4-butylene-bis-(diphenylthallium tetrazole). 2MeOH (**35**), 1,2-phenylene-bis-(diphenylthallium tetrazole). 2MeOH. $2H_2O$. Ph_2TlCl (**30**).

5.6 EXPERIMENTAL

Diphenylthallium azide and diphenylthallium hydroxide were prepared by the methods of Srivastava *et al*[181] and Casas *et al*[176], respectively. All the other chemicals were purchased commercially and used without further purification.

Preparation of 1,2-ethylene-bis-(hydrotetrazole), (**22**).

Concentrated hydrochloric acid (60 mmol) was added dropwise to a well stirred solution of 1,2-ethylene-bis-(tributylstannyl tetrazole) (8.13g, 10.9 mmol). The resultant clear solution was refluxed for 3 hours. Subsequently, methanol was removed *in vacuo* and the remaining white solid was collected by filtration and washing with hexanes. The white solid was recrystallised twice from methanol. The product was obtained as a mixture of brown crystals (**22a**) (1.0g, 6%) and a white powder (**22b**) (0.63g, 34%) [m.p. of crystalline product 232-234°C; m.p. of powder product 212°C (dec.)].

Analysis: **22a**-Found (Calc. for $C_4H_6N_8$): C 29.2 (28.9); H 3.43 (3.61); N 67.6 (67.5)%.

^{1}H NMR [δ(ppm), DMSO-d^6 solution]: 2.50 [s, 4H, CH_2CH_2].

^{13}C NMR [δ(ppm), DMSO-d^6 solution]: 155.2 [CN$_4$]; 21.2 [CH_2CH_2].

IR [(cm^{-1}), KBr disk]: 3420[ν(NH)], 2635, 1585, 1454, 1414, 1261, 1228, 1113, 1060, 1003, 870, 788, 696, 621.

22b- Found (Calc. for $C_4H_6N_8.H_2O$): C 28.8 (26.1); H 3.48 (4.34); N 61.3 (60.9)%.

^{1}H NMR [δ(ppm), DMSO-d^6 solution]: 2.50 [s 4H, CH_2CH_2].

^{13}C NMR [δ(ppm), DMSO-d^6 solution]: 155.0 [CN$_4$]; 21.0 [CH_2CH_2].

IR [(cm^{-1}), KBr disk]: 3418[ν(NH) and ν(H_2O)], 1633, 1550, 1414, 1259, 1221, 1153, 1113, 1093, 1066, 999, 897, 808, 698, 621, 518.

Preparation of 1,4-butylene-bis-(hydro tetrazole), (**23**).

Concentrated hydrochloric acid (2.5 mL, 29 mmol) was added dropwise to a well stirred solution of 1,4-butylene-bis-(tributylstannyl tetrazole) (10.89g, 14 mmol) in hot methanol and the reaction mixture was refluxed for 3 hours. Subsequently, methanol was removed *in vacuo*. The resultant white solid was washed with hexanes and dried *in vacuo* and recrystallised from methanol to give white crystals of the product (1.08g, 39%) (m.p. 202-204°C).

Analysis: Found (Calc. for $C_6H_{10}N_8$): C 37.4 (37.1); H 5.14 (5.20); N 56.7 (57.7)%.

^{1}H NMR [δ(ppm), DMSO-d^6 solution]: 1.74 [m, 4H, $CH_2CH_2CH_2CH_2$]; 2.92 [m, 4H, $CH_2CH_2CH_2CH_2$].

^{13}C NMR [δ(ppm), DMSO-d^6 solution]: 155.7 [CN$_4$]; 26.4 [$CH_2CH_2CH_2CH_2$]; 22.4 [$CH_2CH_2CH_2CH_2$].

IR [(cm^{-1}), Nujol, KBr disk]: 3430, 3131, 2961, 2853, 2730, 2614, 2469, 2363, 2943, 1578, 1456, 1424, 1377, 1321, 1304, 1262, 1109, 1086, 1053, 918.

Preparation of the [thallium]$_2$[methylene-5,5′-bis-(tetrazolate)] (**24**)

A solution of thallium(I) ethoxide (0.44g, 1.77 mmol) in absolute ethanol (15mL) was added dropwise to a solution of 5,5′-methylene bis-(hydrotetrazole) (0.13g, 0.855mmol) in absolute ethanol (20mL). A white precipitate was formed immediately, which was collected by filtration, washed with methanol and dried *in vacuo*. Yield: (0.30g, 63%) [m.p. 290°C(dec.)].

Analysis: Found (Calc. for $C_3H_2N_8Tl_2$): C 6.5 (6.4); H 0.36 (0.32); N 20.1 (20.2)%.

^{1}H NMR [δ(ppm), D_2O-d^2 solution]: 4.38 [s, 2H, CH_2].

IR [(cm^{-1}), KBr disk]: 2966, 2947, 2905, 2874, 1483, 1469, 1454, 1379, 1271, 1182, 1118, 1113, 1099, 1089, 1049, 1018, 767, 665.

Preparation of the [thallium]$_2$[1,4-butylene-bis-5,5′-(tetrazolate)], (**25**)

A solution of thallium(I) ethoxide (1.01g, 4mmol) in absolute ethanol (35mL) was added dropwise to a solution of 1,4-butylene-bis-5,5′-(hydrotetrazole) (0.39g, 2mmol) in absolute ethanol (70mL). A fine white precipitate formed almost instantaneously. This precipitate was collected by filtration, washed with methanol and dried *in vacuo* (0.90g, 75%) (m.p. 242°C).

Analysis: Found (Calc. for $C_8H_4N_8Tl_2$): C 12.1 (12.0); H 1.28 (1.34); N 18.5 (18.7)%.

^{1}H NMR [δ(ppm), D_2O-d^2 solution]: 1.55 [m, 4H, $CH_2CH_2CH_2CH_2$]; 2.71 [m, 4H, $CH_2CH_2CH_2CH_2$].

^{13}C NMR [δ(ppm), D_2O-d^2 solution]: 23.4 [$CH_2CH_2CH_2CH_2$]; 27.1 [$CH_2CH_2CH_2CH_2$].

IR [(cm^{-1}), Nujol, KBr disk]: 3405, 2955, 2855, 2726, 1734, 1601, 1460, 1377, 1310, 1146, 1127, 1061.

Preparation of the [thallium]$_2$[1,3-phenylene-bis-5,5′-(tetrazolate)].2H_2O, (**26**)

A solution of thallium(I) ethoxide (0.51g, 2.05mmol) absolute ethanol (20mL) was added dropwise to a solution of 1,3-phenylene-bis-(hydrotetrazole) (0.19g, 0.88mmol) in absolute ethanol (10mL). A white precipitate was formed immediately, which was collected by filtration and dried *in vacuo*. Yield: (0.89g, 70%) [m.p. 300°C(dec.)].

Analysis: Found (Calc. for $C_8H_4N_8Tl_2.2H_2O$): C 14.5 (14.6); H 1.21 (1.22); N 16.5 (17.1)%.

^1H NMR [δ(ppm), D_2O-d^2 solution]: 8.44 [t, 1H, *2*-C_6H_4]; 7.95 [dd, 2H, *4,6*-C_6H_4]; 7.53 [t, 1H, *5*-C_6H_4]; ^3J 7.6 Hz; ^4J 1.8Hz.

^{13}C NMR [δ(ppm), D_2O-d^2 solution]: 163.5 [*C*N_4]; 131.2 [*2*-C_6H_4]; 130.4 [*1,3*-C_6H_4]; 128.8 [*4,6*-C_6H_4]; 125.9 [*5*-C_6H_4].

IR [(cm^{-1}), KBr disk]: 3352, 2959, 1653, 1427, 1375, 1331, 1194, 1128, 1082, 1028, 900, 804, 767, 744, 690, 426.

Preparation of the [thallium]$_2$[1,4-phenylene-bis-5,5′-(tetrazolate)], (**27**)

1,4-phenylene-bis-5,5′-(hydrotetrazole) (0.21g, 1mmol) was dissolved in a 1:1 mixture of absolute ethanol and methanol (200mL) with heating. To this solution was added a solution of thallium(I) ethoxide (0.49g, 2mmol) in absolute ethanol (30mL) in a dropwise fashion and with stirring. A very fine precipitate formed almost immediately.

^{13}C NMR [δ(ppm), D_2O-d^2 solution]: 23.4 [$CH_2CH_2CH_2CH_2$]; 27.1 [$CH_2CH_2CH_2CH_2$].

IR [(cm^{-1}), Nujol, KBr disk]: 3405, 2955, 2855, 2726, 1734, 1601, 1460, 1377, 1310, 1146, 1127, 1061.

Preparation of the [thallium]$_2$[1,3-phenylene-bis-5,5′-(tetrazolate)].2H_2O, (**26**)

A solution of thallium(I) ethoxide (0.51g, 2.05mmol) in minimum absolute ethanol was added dropwise to a solution of 1,3-phenylene-bis-(hydrotetrazole) (0.19g, 0.88mmol) in minimum absolute ethanol. A white precipitate was formed immediately, which was collected by filtration and dried *in vacuo*. Yield: (0.89g, 70%) [m.p. 300°C(dec.)].

Analysis: Found (Calc. for $C_8H_4N_8Tl_2.2H_2O$): C 14.5 (14.6); H 1.21 (1.22); N 16.5 (17.1)%.

^1H NMR [δ(ppm), D_2O-d^2 solution]: 8.44 [t, 1H, *2*-C_6H_4]; 7.95 [dd, 2H, *4,6*-C_6H_4]; 7.53 [t, 1H, *5*-C_6H_4]; ^3J 7.6 Hz; ^4J 1.8Hz.

^{13}C NMR [δ(ppm), D_2O-d^2 solution]: 163.5 [CN_4]; 131.2 [*2*-C_6H_4]; 130.4 [*1,3*-C_6H_4]; 128.8 [*4,6*-C_6H_4]; 125.9 [*5*-C_6H_4].

IR [(cm^{-1}), KBr disk]: 3352, 2959, 1653, 1427, 1375, 1331, 1194, 1128, 1082, 1028, 900, 804, 767, 744, 690, 426.

Preparation of the [thallium]$_2$[1,4-phenylene-bis-5,5′-(tetrazolate)], (**27**)

1,4-phenylene-bis-5,5′-(hydrotetrazole) (0.21g, 1mmol) was dissolved in a 1:1 mixture of absolute ethanol and methanol (200mL) with heating. To this solution was added a solution of thallium(I) ethoxide (0.49g, 2mmol) in absolute ethanol (30mL) in a dropwise fashion and with stirring. A very fine precipitate formed almost immediately.

This precipitate was collected by filtration, washed with methanol and dried *in vacuo* (0.43g, 71%) [m.p. 235°C(dec.)].

Analysis: Found (Calc. for $C_8H_4N_8Tl_2$): C 15.8 (15.5); H 0.62 (0.65); N 17.7 (18.1)%.

^{1}H NMR [δ(ppm), DMSO-d^6 solution]: 7.98 [s, 4H, *2,3,5,6*-C_6H_4].

^{13}C NMR [δ(ppm), DMSO-d^6 solution]: 160.5 [CN_4]; 131.0 [*1,4*-C_6H_4]; 130.7 [*2,6*-C_6H_4]; 127.5 [*3,5*-C_6H_4].

IR [(cm^{-1}), Nujol, KBr disk]: 2926, 2855, 1464,1426, 1377, 1335, 1267, 1194, 1105, 1060, 1026, 851, 741, 725, 532, 482, 422.

Preparation of the [thallium]$_3$[1,3,5-phenylene-tris-5,5′,5′′-(tetrazolate)].3H_2O, (**28**)

1,3,5-phenylene-tris-5,5′,5′′-(hydrotetrazole) (0.18g, 0.60mmol) was dissolved in absolute ethanol (40mL) with heating. To this solution was added a solution of thallium(I) ethoxide (0.52g, 2mmol) in absolute ethanol (20mL) in a dropwise fashion and with stirring. A very fine white precipitate was obtained almost immediately. This precipitate was collected by filtration, washed with methanol and dried with *in vacuo*. (0.55g, 97%) [m.p. 241°C(dec.)]. The product is not soluble in commonly available solvents.

Analysis: Found (Calc. for $C_9H_3N_{12}Tl_3.3H_2O$): C 11.5 (11.4); H 0.64 (0.96), N 16.6 (17.8)%.

IR [(cm^{-1}), KBr disk]: 3414, 1616, 1414, 1190, 1128, 1032, 889, 787, 748, 682, 621, 449.

Preparation of 1-diphenylthallium-5-phenyltetrazole, (**29**)

Method 1:

Diphenylthallium azide (0.42g, 1mmol) was added to excess benzonitrile (20mL) and the mixture was stirred at a temperature of 150°C for 10 hours under N_2. The initial suspension became a clear solution and then after two hours turned yellow. On cooling to room temperature after 10 hours, a white solid was obtained. The solid was collected by filtration, washed with hexanes and recrystallised from hot methanol to yield the product in two off-white forms (powder and crystalline) [m.p. of powder 244°C (dec)]. While the crystals were used to obtain crystallographic data, the powder was fully characterised.

Analysis: Powder product-Found (Calc. for $C_{19}H_{15}N_4Tl$): C 45.1 (45.3); H 2.92 (3.01); N 11.0 (11.1) %; Crystalline product- Found (Calc. for $C_{19}H_{15}N_4Tl.CH_3OH$): C 43.8 (44.8); H 2.96 (3.58); N 10.8 (10.5)%.

^1H NMR [δ(ppm), DMSO-d^6 solution; (100°C)]: 8.24, 8.0, 7.55, 7.34, 7.22, 7.21 [phenyl protons].

^{13}C NMR [δ(ppm), DMSO-d^6 solution; (100°C)]: 161.0 [CN_4]; 137.5, 135.5, 133.4, 132.3, 132.1, 130.0, 129.6, 128.5, 127.3, 126.0, 119.0, 111.4 [phenyl carbons].

IR [(cm^{-1}), KBr disk]: 3414, 3065, 1637, 1616, 1576, 1479, 1458, 1442, 1433, 1385, 1359, 1142, 1074, 1018, 1008, 997, 725, 688, 619, 447.

Method 2:

A solution of 1-phenyl-tetrazole (0.05g, 0.35 mmol) in methanol (50mL) was added dropwise to a well stirred solution of diphenylthallium hydroxide (0.13g, 0.35 mmol) in hot methanol (200mL). The resultant clear solution was refluxed for 3 hours. Hot filtration afforded a clear solution, which on cooling gave the product as a white solid (0.14g, 80%) [m.p. 206°C (dec.)].

Analysis: Found (Calc. for $C_{19}H_{15}N_4Tl.CH_3OH$): C 44.4 (44.9); H 2.96 (3.58); N 10.9 (10.5)%.

^1H NMR [δ(ppm), DMSO-d^6 solution; (80°C)]: 7.20-8.39 (m) [phenyl protons]; 3.24 [s, 3H, CH_3OH].

^{13}C NMR [δ(ppm), DMSO-d^6 solution; (80°C)]: 160.6 [CN_4]; 137.6, 134.6, 132.2, 130.5, 127.9, 126.7, 125.7 [phenyl carbons].

IR [(cm^{-1}), KBr disk]: 3408, 3042, 1616, 1576, 1479, 1458, 1442, 1431, 1385, 1359, 1261, 1142, 1099, 1074, 1022, 1008, 997, 729, 690, 449.

Preparation of 1,2-phenylene-bis-5,5′-(diphenylthallium tetrazole). $2H_2O$. 2MeOH. Ph_2TlCl, (**30**)

A solution of 1,2-phenylene-bis-5,5′-(hydrotetrazole) (0.02g, 0.06 mmol) in methanol (20mL) was added dropwise to a well stirred solution of diphenylthallium hydroxide (0.04g, 0.12 mmol) in hot methanol (200mL) and the resultant clear solution was refluxed for 3 hours. The reaction was worked up similarly to **29** (method 2). The product was collected as brown crystals(0.07g, 82%).

Analysis: Found (Calc. for $C_{32}H_{24}N_8Tl_2.Ph_2TlCl.2H_2O.2CH_3OH$): C 38.1 (38.8); H 3.11 (3.24); N 8.0 (7.9)%.

^1H NMR [δ(ppm), DMSO-d^6 solution]: 7.20-7.42 [m, 34H, phenyl protons]; 3.39 [s, 6H, CH_3OH].

^{13}C NMR [δ(ppm), DMSO-d^6 solution]: 160.5 [CN_4]; 138.1, 135.3, 131.0, 129.9, 128.2, 127.8, 126.3 [phenyl carbons].

IR [(cm^{-1}), KBr disk]: 3412, 3045, 1637, 1616, 1479, 1431, 1385, 1350, 1261, 1118, 1022, 999, 952, 910, 802, 754, 725, 690, 486, 447.

Analysis: Found (Calc. for $C_{19}H_{15}N_4Tl.CH_3OH$): C 44.4 (44.9); H 2.96 (3.58); N 10.9 (10.5)%.

^1H NMR [δ(ppm), DMSO-d^6 solution; (80°C)]: 7.20-8.39 (m) [phenyl protons]; 3.24 [s, 3H, CH_3OH].

^{13}C NMR [δ(ppm), DMSO-d^6 solution; (80°C)]: 160.6 [CN_4]; 137.6, 134.6, 132.2, 130.5, 127.9, 126.7, 125.7 [phenyl carbons].

IR [(cm^{-1}), KBr disk]: 3408, 3042, 1616, 1576, 1479, 1458, 1442, 1431, 1385, 1359, 1261, 1142, 1099, 1074, 1022, 1008, 997, 729, 690, 449.

Preparation of 1,2-phenylene-bis-5,5′-(diphenylthallium tetrazole). $2H_2O$. 2MeOH. Ph_2TlCl, (**30**)

A solution of 1,2-phenylene-bis-5,5′-(hydrotetrazole) (0.02g, 0.06 mmol) in methanol (20mL) was added dropwise to a well stirred solution of diphenylthallium hydroxide (0.04g, 0.12 mmol) in hot methanol (200mL) and the resultant clear solution was refluxed for 3 hours. The reaction was worked up similarly to **29** (method 2). The product was collected as brown crystals(0.07g, 82%) [m.p. 34°C (dec.)].

Analysis: Found (Calc. for $C_{32}H_{24}N_8Tl_2.Ph_2TlCl.2H_2O.2CH_3OH$): C 38.1 (38.8); H 3.11 (3.24); N 8.0 (7.9)%.

^1H NMR [δ(ppm), DMSO-d^6 solution]: 7.20-7.42 [m, 34H, phenyl protons]; 3.39 [s, 6H, CH_3OH].

^{13}C NMR [δ(ppm), DMSO-d^6 solution]: 160.5 [CN_4]; 138.1, 135.3, 131.0, 129.9, 128.2, 127.8, 126.3 [phenyl carbons].

IR [(cm^{-1}), KBr disk]: 3412, 3045, 1637, 1616, 1479, 1431, 1385, 1350, 1261, 1118, 1022, 999, 952, 910, 802, 754, 725, 690, 486, 447.

Preparation of 1,3-phenylene-bis-5,5′-(diphenylthallium tetrazole).2H_2O, (**31**)

A solution of 1,3-phenylene-bis-5,5′-(hydro tetrazole) (0.032g, 0.150 mmol) in methanol (80 mL) was added dropwise to a well stirred solution of diphenylthallium hydroxide (0.11g, 0.29 mmol) in hot methanol (220 mL) and the resultant clear solution was refluxed for 3 hours. The reaction was worked up similarly to **29** (method 2). The product was collected as a white powder (0.18g, 85%) [m.p. 228°C (dec.)].

Analysis: Found (Calc. for $C_{32}H_{24}N_8Tl_2.2H_2O$): C 40.0 (39.8); H 2.70 (2.90); N 11.5 (11.6)%.

^{1}H NMR [δ(ppm), DMSO-d^6 solution (80°C)]: 8.70 (s), 8.34 (s), 7.88-7.90 (m), 7.20-7.60 (m) [phenyl protons].

^{13}C NMR [δ(ppm), DMSO-d^6 solution (80°C)]: 160.9 [*C*N_4]; 132.8, 134.8, 132.3, 130.3, 127.9, 126.0, 124.4, 123.7 [phenyl carbons].

IR [(cm^{-1}), KBr disk]: 3414, 1637, 1616, 1574, 1516, 1479, 1433, 1385, 1309, 1261, 1217, 1136, 1018, 997, 804, 767, 742, 727, 690, 619.

Preparation of 1,4-phenylene-bis-5,5′-(diphenylthallium tetrazole).0.5$Ph_2TlCl.2H_2O$, (**32**)

A solution of 1,4-phenylene-bis-5,5′-(hydrotetrazole) (0.029g, 0.134mmol) in methanol (90mL) was added dropwise to a well stirred solution of diphenylthallium hydroxide (0.100g, 0.267mmol) in hot methanol (150mL) and the resultant clear solution was refluxed for 3 hours. The reaction was worked up similarly to **29** (method 2). The product was collected as a white powder (0.09g, 58%) [m.p. 218°C (dec.)].

Analysis: Found (Calc. for $C_{32}H_{24}N_8Tl_2.0.5Ph_2TlCl.2H_2O$): C 39.0 (39.3); H 2.99 (2.84); N 10.4 (9.7)%.

^{1}H NMR [δ(ppm), DMSO-d^{6} solution (80°C)]: 7.0-8.5 [m, 24H, phenyl protons].

^{13}C NMR [δ(ppm), DMSO-d^{6} solution (80°C)]: 160.7 [*C*N$_4$]; 137.6, 134.6, 131.0, 130.5, 128.7, 125.6 [phenyl carbons].

IR [(cm^{-1}), KBr disk]: 3414, 1637, 1618, 1574, 1477, 1433, 1385, 1338, 1265, 1151, 1136, 1103, 1020, 1006, 997, 744, 727, 690, 482, 453.

Preparation of methylene-bis-5,5′-(diphenylthallium tetrazole).2H$_2$O, (**33**)

A solution of 1,3-phenylene-bis-5,5′-(hydrotetrazole) (0.021g, 0.139mmol) in methanol (40mL) was added dropwise to a well stirred solution of diphenylthallium hydroxide (0.100g, 0.267mmol) in hot methanol (200mL) and the resultant clear solution was refluxed for 3 hours. The reaction was worked up similarly to **29** (method 2). The product was collected as a white powder (0.06g, 47%) [m.p. 225°C (dec.)].

Analysis: Found (Calc. for $C_{27}H_{22}N_8Tl_2.2H_2O$): C 36.7(35.9); H 2.47(2.88); N 11.8(12.4)%.

^{1}H NMR [δ(ppm), DMSO-d^{6} solution]: 7.26-8.19 [10H, m, phenyl protons].

^{13}C NMR [δ(ppm), DMSO-d^{6} solution]: 157.6 [*C*N$_4$]; 138.1, 135.2, 128.4 [phenyl carbons].

IR [(cm^{-1}), KBr disk]: 3047, 1952, 1576, 1481, 1471, 1433, 1383, 1300, 1192, 1130, 1091, 1057, 1030, 1020, 997, 760, 727, 692, 461, 451.

Preparation of ethylene-bis-5,5′-(diphenylthallium tetrazole).2H$_2$O, (**34**)

A solution of 1,2-ethylene-bis-5,5′-(hydrotetrazole) (0.03g, 0.16mmol) in methanol (70mL) was added dropwise to a well stirred solution of diphenylthallium

hydroxide (0.11g, 0.29mmol) in hot methanol (170mL) and the resultant clear solution was refluxed for 3 hours. The reaction was worked up similarly to **29** (method 2) and **34** was collected as brown crystals (0.06g, 35%).

Analysis: Found (Calc. for $C_{28}H_{24}N_8Tl_2.2H_2O$): C 36.2 (36.7); H 3.33 (3.05); N 11.1 (12.2)%.

^{1}H NMR [δ(ppm), DMSO-d^6 solution (100°C)]: 7.30-8.54 [phenyl protons]; 2.50 [s, 4H, CH_2CH_2].

^{13}C NMR [δ(ppm), DMSO-d^6 solution (100°C)]: 138.1, 134.9, 130.6, 129.4, 128.4, 128.0, 127.5, 125.9 [phenyl carbons].

IR [(cm^{-1}), KBr disk]: 3410,1618, 1574, 1479, 1433, 1408, 1329, 1203, 1143, 1070, 1018, 997, 729, 688.

Preparation of 1,4-butylene-bis-5,5′-(diphenylthallium tetrazole).2MeOH, (**35**)

A solution of 1,4-butylene-bis-5,5′-(hydrotetrazole) (0.02g, 0.11mmol) in methanol (20mL) was added dropwise to a well stirred solution of diphenylthallium hydroxide (0.08g, 0.21 mmol) in hot methanol (200mL) and the resultant clear solution was refluxed for 3 hours. The reaction was worked up similarly to **29** (method 2) and **35** was collected as brown crystals (0.08, 41%) [m.p.192°C (dec.)].

Analysis: Found (Calc. for $C_{30}H_{28}N_8Tl_2.2CH_3OH$): C 38.9 (39.5); H 3.36 (3.70); N 11.4 (11.5)%.

^{1}H NMR [δ(ppm), DMSO-d^6 solution (100°C)]: 7.26-8.30 [phenyl protons]; 2.50 [m, 4H, $CH_2CH_2CH_2CH_2$]; 1.62 [m, 4H, $CH_2CH_2CH_2CH_2$]; 3.19 [s, 3H, CH_3OH].

^{13}C NMR [δ(ppm), DMSO-d^6 solution (100°C)]: 137.7, 134.4, 130.5, 127.8, 125.8 [phenyl carbons]; 26.4 [$CH_2CH_2CH_2CH_2$]; 22.9 [$CH_2CH_2CH_2CH_2$].

IR [(cm^{-1}), KBr disk]: 3412, 3049, 2924, 1637, 1616, 1576, 1479, 1450, 1433, 1394, 1315, 1203, 1143, 1126, 1066, 1020, 997, 727, 690, 449.

Chapter 6

The Synthesis, Characterisation And Synthetic Applications Of Organotin-Substituted Thio-Tetrazoles

6.1 INTRODUCTION

The major application of organotin sulphur compounds is as heat stabilisers for poly(vinyl chloride),[68,182] a versatile polymer used in a wide range of applications. In the absence of a stabiliser, halogenated polymers rapidly degrade by heat, light, or oxygen to form discoloured, brittle products.[183] Stabilisers must be incorporated into the polymer to make it commercially useful.[68,182] Two principal processes occur during degradation: loss of hydrogen chloride and autooxidation resulting in the discolouration of the PVC. The functions of the stabiliser are to remove free HCl before it can catalyse dehydrochlorination and to inhibit the onset of dehydrochlorination by exchanging its anionic groups X with reactive chlorine atoms in the polymer. The most important organotin derivatives used as stabilisers are the dialkyltin dithiolates $R_2Sn(SR')_2$, e.g. dialkyltin "diisooctylthioglycolates", $R_2Sn\ [SCH_2CO_2CH_2CH(Et)Bu]_2$ (R = Me, Bu or Oct), "di-(estertin) di-(iso-octyl thio-glycollate)" $(BuOCOCH_2CH_2)_2Sn\ [SCH_2CO_2CH_2CH(Et)Bu]_2$.[182] These are used in synergistic mixture with the corresponding monoorganotin trithiolates $RSn(SR')_3$.[182]

Due to the wide use of organotin compounds as biocides and pesticides, it is important to consider their toxicity and biological action in relationship to the thiophilic nature of tin.[68,182] Biocidal activity of diorganotin compounds arises from binding to enzymes or coenzymes possessing dithiol groups. Binding to reduced lipoic acid is an example of this phenomenon and it results in the inhibition of α-ketoacid oxidation.[184]

Chapter 6

The Synthesis, Characterisation And Synthetic Applications Of Organotin-Substituted Thio-Tetrazoles

6.1 INTRODUCTION

The major application of organotin sulphur compounds is as heat stabilisers for poly(vinyl chloride),[68,182] a versatile polymer used in a wide range of applications. In the absence of a stabiliser, halogenated polymers rapidly degrade by heat, light, or oxygen to form discoloured, brittle products.[183] Stabilisers must be incorporated into the polymer to make it commercially useful.[68,182] Two principle processes occur during degradation: loss of hydrogen chloride and autooxidation resulting in the discolouration of the PVC. The functions of the stabiliser are to remove free HCl before it can catalyse dehydrochlorination and to inhibit the onset of dehydrochlorination by exchanging its anionic groups X with reactive chlorine atoms in the polymer. The most important organotin derivatives used as stabilisers are the dialkyltin dithiolates $R_2Sn(SR')_2$, e.g. dialkyltin "diisooctylthioglycolates", $R_2Sn\ [SCH_2CO_2CH_2CH(Et)Bu]_2$ (R = Me, Bu or Oct), "di-(estertin) di-(iso-octyl thio-glycollate)" $(BuOCOCH_2CH_2)_2Sn\ [SCH_2CO_2CH_2CH(Et)Bu]_2$.[182] These are used in synergistic mixture with the corresponding monoorganotin trithiolates $RSn(SR')_3$.[182]

Due to the wide use of organotin compounds as biocides and pesticides, it is important to consider their toxicity and biological action in relationship to the thiophilic nature of tin.[68,182] Biocidal activity of diorganotin compounds arises from binding to enzymes or coenzymes possessing dithiol groups. Binding to reduced lipoic acid is an example of this phenomenon and it results in the inhibition of α-ketoacid oxidation.[184]

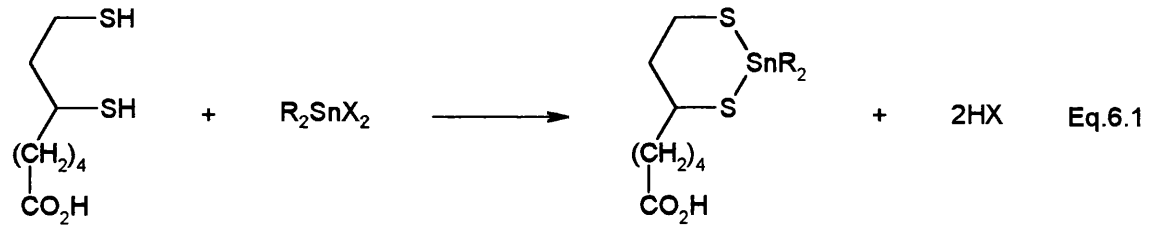

Eq.6.1

Triorganotin compounds have a tendency to increase their coordination number to more than four by interacting with donor molecules such as, S, O or N. Cysteine is a sulphur containing amino acid which binds to the organotin preferentially via the sulphur illustrating the thiophilic nature of tin.[69]

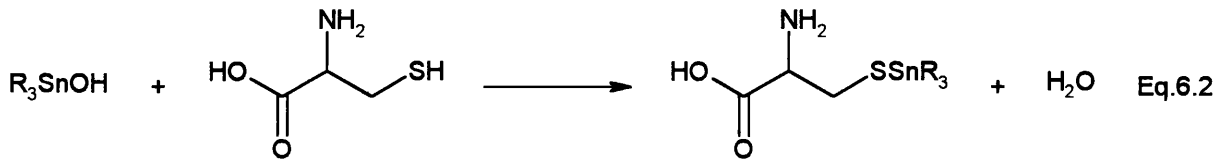

Eq.6.2

6.1.1 Synthesis Of Organotin-Substituted Thio-Tetrazoles

Three major routes have been used to date to synthesise organotin-substituted thio-tetrazoles. The first route involves cycloaddition of an organotin azide with organoisothiocyanate (equation 6.3).[26]

Eq.6.3

The second route employed is the simple metathesis between an organotin chloride and the sodium or ammonium salt of the preformed tetrazole (equation 6.4).[27] Diorganotin bis(thiotetrazoles) have also been synthesised by this route.

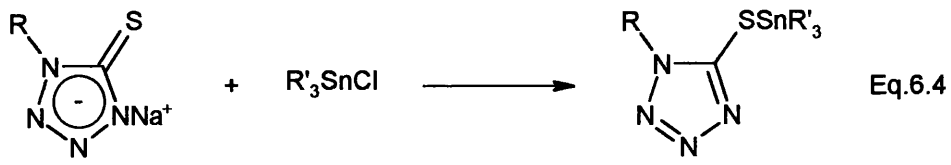

Eq.6.4

Casas *et al* have reported a third route involving condensation of preformed tetrazoles with organotin oxides and hydroxides (equation 6.5).[185]

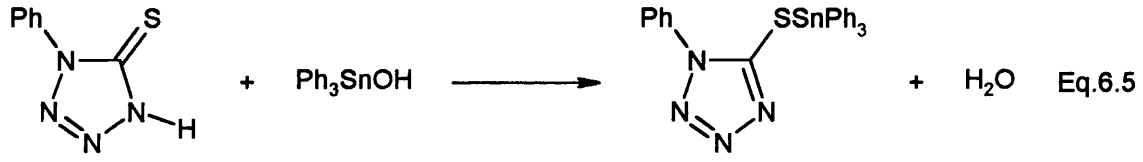

6.1.2 Structural Chemistry Of Organotin Thio-Tetrazoles

The synthesis and spectroscopic characterisation of some triorganotin(IV) derivatives of 1-organyl-(5-thiolato-tetrazoles) (**LV**) were reported as early as 1971 and the metal-ligand bonding was assumed to take place solely through nitrogen.[26]

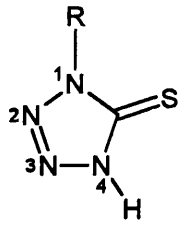

LV

However, the thiophilicity of tin is well known and the products initially formulated in the thione form (**LVIa**) could equally exist in the tautomeric thiol form (**LVIb**) as shown in equilibrium 6.1.[26] Spectroscopic evidence distinguishing the thiol and thione isomers is limited. However, the absence of the ν(C=S) stretch at 1110cm^{-1} indicates the formation of the thiol isomer.

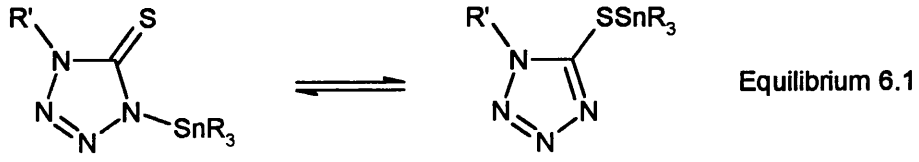

Equilibrium 6.1

LVIa **LVIb**

In fact, Molloy *et al* [26] and subsequently, Cea-Olivares *et al* [27] crystallographically demonstrated for di- and tri-organotin(IV) derivatives respectively that the primary metal-ligand bonding actually occurs through sulphur. Table 6.1 summarises some examples of organotin-substituted thio-tetrazoles, their modes of coordination and their lattice types (see page 200).

This chapter extends the study of thio-tetrazoles to the syntheses of 1,4-phenylene-bis-(triorganotin thio-tetrazoles) via various synthetic routes and their use as precursors for other inorganic and organometallic thio-tetrazoles.

6.2 SYNTHESES OF ORGANOTIN-SUBSTITUTED THIO-TETRAZOLES AND THEIR USE AS PRECURSORS TO THE SYNTHESIS OF ORGANOMETALLIC THIO-TETRAZOLES

The traditional cycloaddition route used to synthesise organotin-substituted tetra-tetrazoles and organotin-substituted functionalised tetrazoles (see chapters 2 and 3) was used to synthesise 1,4-phenylene-bis-[(5′-thiolato-tributylstannyl)-1′-tetrazole] (**36**) and 1,4-phenylene-bis-[(5′-thiolato-triethylstannyl)-1′-tetrazole] (**37**) (equation 6.6). The triorganotin azide was heated with 1,4-phenylene-diisothiocyanate under N_2 at high temperatures (80-100°C) for 30 mins. IR spectroscopy was the tool used to monitor the course of these cycloaddition reactions. As the reaction proceeded, the $\nu(N_3)$ band at 2076 cm^{-1} and ν(NCS) band at 2112 cm^{-1} reduce in size and their eventual disappearance marked the end of the reactions. Bands corresponding to the phenyl rings appeared at 1500-1600 cm^{-1}. The IR stretches of 1080cm^{-1} and 1082cm^{-1} in **36** and **37** respectively were characteristic of tetrazole rings. The lack of the ν(C=S) band at 1110cm^{-1} suggests that formation of the thiol isomer is most likely. Unfortunately, the characteristic Sn-S[68] stretches appear between 300-400cm^{-1} which makes it difficult to observe them as they are below the cut-off for the IR plates (NaCl) used. **36** was recrystallised from hot methanol and collected as a white microcrystalline solid. However, **37** surprisingly was not soluble

Table 6.1: Modes Of Coordination And Lattice Types Of Organotin-Substituted Thio-tetrazoles

	Compound	Metal-Tetrazole Coordination with respect to Tin	Lattice Type; CN	Reference
LVII	(dibutylstannyl)-bis-(1-phenyl-5-thiotetrazole)	*trans*-$R_2SnS_2N_2$, distorted tetrahedral with two secondary N-Sn interactions	Monomeric; 6	26
LVIII	1/∞{1-phenyl-[(5′-thiolato-tribenzylstannyl)-1′-tetrazole]}	*trans*-$SNSnC_3$, distorted trigonal bipyramidal with weak intramolecular Sn-N interaction	Polymeric chain; 6	27
LIX	1-phenyl-[(5′-thiolato-triphenylstannyl)-1′-tetrazole]	*trans*-R_3SnSN, distorted tetrahedral with one intramolecular Sn-N bond	Monomeric; 5	185
LX	1-phenyl-[(5′-thiolato-trimethylstannyl)-1′-tetrazole]	*trans*-R_3SnN_2S, distorted trigonal bipyramidal with weak intramolecular secondary Sn-N interaction	Trimeric; 6	186

in either methanol or ethanol. It was washed with hexanes to remove the excess azide and collected as a white powder.

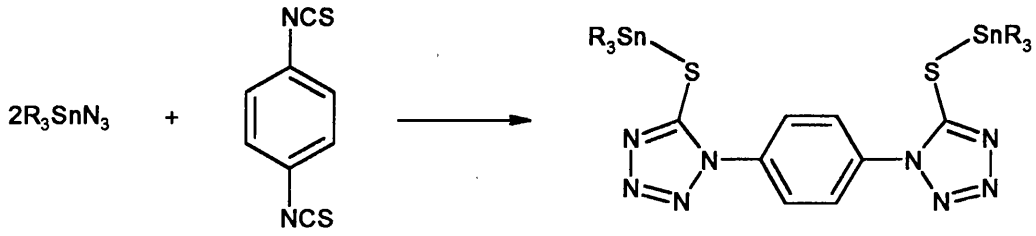

Eq.6.6

R = Bu (**36**), Et (**37**)

1,4-phenylene-bis-[(5′-thiolato-trimethylstannyl)-1′-tetrazole] (**40**) and 1,4-phenylene-bis-[(5′-thiolato-triphenylstannyl)-1′-tetrazole] (**41**) were prepared by a salt elimination route, which required the conversion of **36** to the corresponding ammonium salt (**39**) via the dithiol (**38**) (equations 6.7 and 6.8). The thiol (**38**) was prepared by refluxing a solution of **36** with concentrated hydrochloric acid in methanol for three hours. After cooling, methanol was removed *in vacuo* and the product was collected by washing with hexanes to remove the tributyltin chloride. **38** was obtained as a white solid in quantitative yield. In the IR spectra, no band corresponding to the S-H stretch (usually between 2550-2600 cm^{-1}) was observed. This suggests that the thio-tetrazole may have tautomerised to give the thione. Indeed, a band was observed at 1050cm^{-1} corresponding to the C=S fragment and a band at 3275 cm^{-1} corresponding to the -NH group.

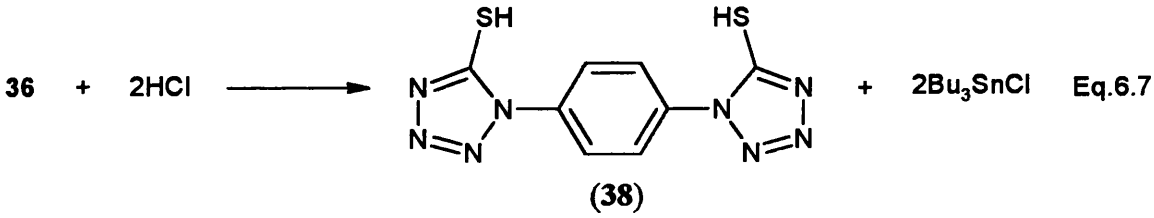

Eq.6.7

(**38**)

The ammonium salt (**39**) was synthesised by bubbling ammonia through a solution of the **38** for 30 mins. After *in vacuo* concentration of the solution, the ammonium salt was collected as a white precipitate.

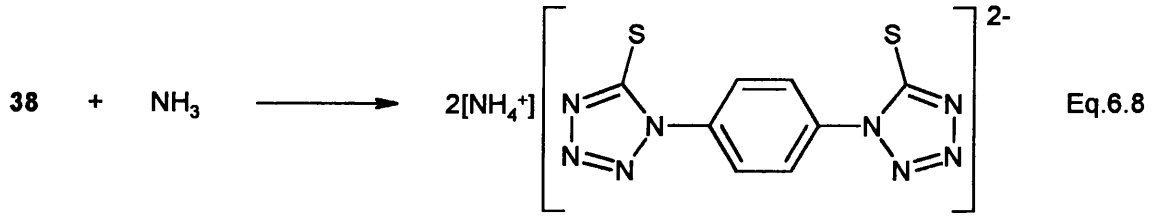

Eq.6.8

(39)

To prepare **40** and **41**, a methanolic solution of the appropriate triorganotin chloride was added to a solution of **39** in methanol in a 2:1 ratio and refluxed. After cooling, methanol was removed *in vacuo*. Extraction from the by-product NH_4Cl was performed by refluxing the crude reaction mixtures with acetone followed by hot filtration. Acetone was then removed under reduced pressure yielding **40** as a yellow/white solid and **41** as a white solid. Both products were recrystallised from methanol and characterised. **40** contains two molecules of methanol as is evident from its CHN analysis while **41** is anhydrous. In the IR spectra, the products contain bands in the range of 1500-1600 cm^{-1} indicating the presence of aromatic rings. The IR stretch observed at 1098cm^{-1} for **40** and at 1091cm^{-1} for **41** is characteristic of the tetrazole. The absence of the ν(C=S) stretch at 1110cm^{-1} indicates the presence of the thiol isomer.

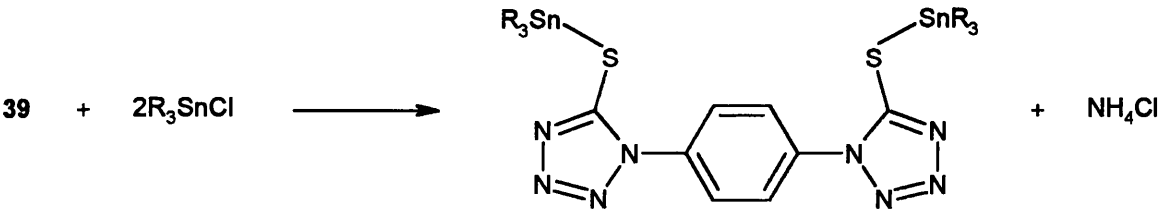

Eq.6.9

R = Me (**40**), R = Ph (**41**)

Crystallographic analyses of **36** and **40** are presented in Sections 6.4.1 and 6.4.2, respectively.

Three inorganic derivatives of 1,4-phenylene-bis-(5′-thiolato-1′-tetrazole) have been prepared (equations 6.10-6.12). In each case, a methanolic solution of the metal chloride was added dropwise to a solution of **36** in methanol. The products were obtained as precipitates almost instantaneously in all cases and were collected by filtration. For **42**

and **44**, the by-product tributyltin chloride was removed by washing with hexanes. The by-products for **43** were tributyltin fluoride (removed by washing with methanol) and trifluoroborane. While **42** was obtained as a grey powder, **43** was a brown precipitate and **44** was a white powder. All three products were characterised by CHN analysis and IR spectroscopy. It must be noted that **42** and **43** are not analytically pure and they could not be recrystallised due to their insolubility in most commonly available solvents. All three compounds showed IR bands typical of the tetrazole unit (1084-1092cm^{-1}). In each case CHN analysis indicated the presence of water of hydration [**42**.6H_2O; **43** .2H_2O; **44** .2H_2O] and this is supported by IR bands at 3428, 3436, 3420 cm^{-1} respectively.

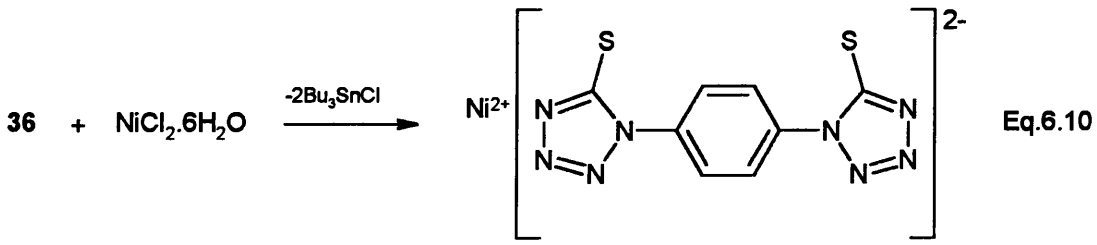

Eq.6.10

(42)

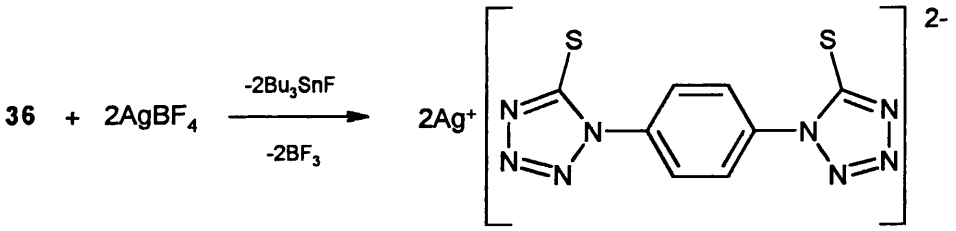

Eq.6.11

(43)

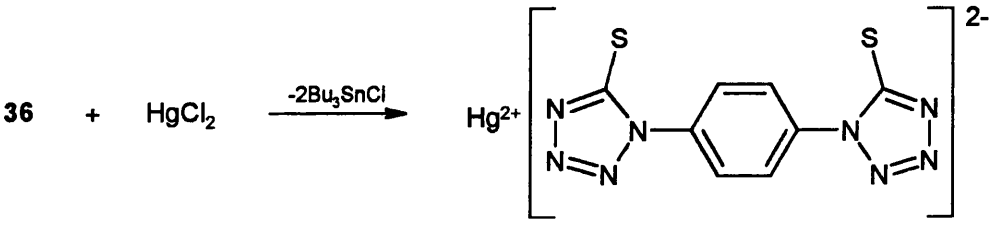

Eq.6.12

(44)

1,4-phenylene-bis-[(5′-thiolato-triphenyllead)-1′-tetrazole] (**45**) was prepared by refluxing a methanolic solution of the triphenyllead chloride with a solution of **36** in

methanol for 10 hours (equation 6.13). After cooling, methanol was removed *in vacuo* and the resulting white product was washed with hexanes and collected by filtration. It was then recrystallised from toluene, which resulted in a white crystalline solid. CHN analysis of the product revealed half a molecule of coordinated toluene. The IR stretch observed at 1098cm^{-1} confirmed the presence of the tetrazole ring. Typical aromatic bands corresponding to the phenyl rings between 1500-1600cm^{-1} were also present. In the case of **46**, the dropwise addition of a methanolic solution of phenylmercuric chloride to a solution of **36** in methanol resulted in a white precipitate (equation 6.14). This precipitate was collected by filtration and washed with hexanes to remove the by-product, tributyltin chloride. The presence of the tetrazole ring was confirmed by an IR stretch at 1094 cm^{-1}. Recrystallisation or NMR characterisation of **49** was not possible due to its insolubility in commonly occurring solvents.

Addition of a methanolic solution of diphenylthallium hydroxide to a methanolic solution of **38** resulted in a cloudy solution which was refluxed for three hours (equation 6.15). Subsequently, the reaction mixture was cooled to room temperature and the volume of the solvent decreased under reduced pressure. This resulted in more fine white solid (**47**) coming out of solution which was collected by filtration and dried *in vacuo*. Presence of the tetrazole ring was confirmed by band at 1093cm^{-1} in the IR spectrum. Other features of the IR spectrum were aromatic bands between 1500 and 1600cm^{-1} and a broad band at 3414cm^{-1} corresponding to the two waters of hydration.

The absence of the ν(C=S) stretches in **45-47** points towards formation of the thiol isomer. The M-S (M = Pb, Hg, Tl) stretches[124,167,187] cannot be observed as they occur in the region between 300-400cm^{-1}.

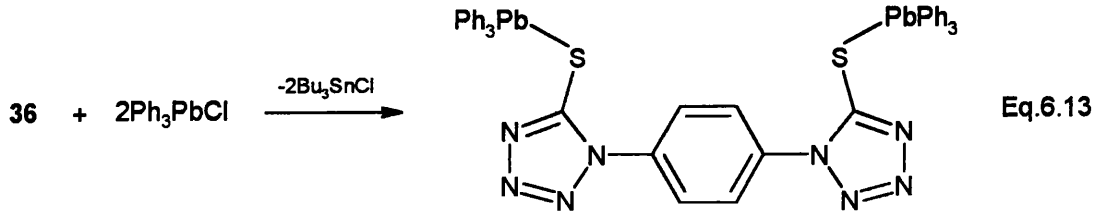

Eq.6.13

(45)

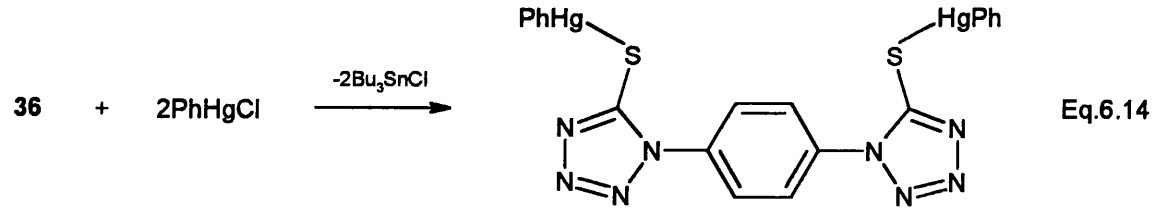

Eq.6.14

(46)

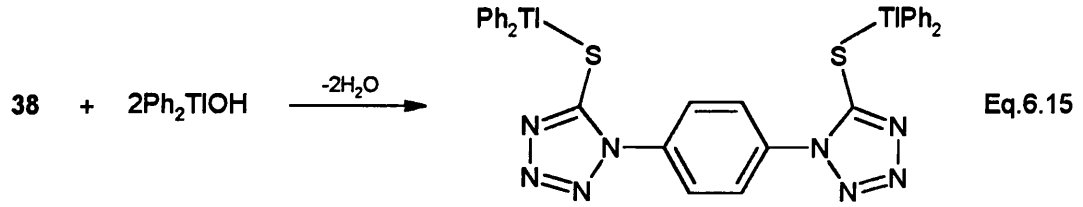

Eq.6.15

(47)

The syntheses and isolation of compounds **36-47** are comprehensively described in Section 6.6.

6.3 SPECTROSOCOPY

6.3.1 Mössbauer Spectroscopy

Table 6.2 gives the Mössbauer data for triorganotin-substituted thio-tetrazoles. The range of the isomer shifts for **36, 37, 40** and **41** is 1.35-1.55 mms^{-1} and that of the quadrupole splittings (q.s.) is 3.0-3.5 mms^{-1}. The former indicates a +4 oxidation state while the latter suggests a five coordinate *trans*-trigonal bipyramidal geometry in the solid-state. A *trans*-trigonal bipyramidal geometry is also seen in (dibutylstannyl)-bis-1-(phenyl-5-thiotetrazole) (see Table 6.2) and its q.s. is 3.32 mms^{-1}.[26] The most probable way of attaining this geometry is via formation of structures of type **LXI** which involves a *trans*-$SNSnC_3$ type of coordination through intermolecular interactions between the tin centre and nitrogen of a neighbouring tetrazole or **LXII** where a solvent molecule is coordinated to the metal centre.

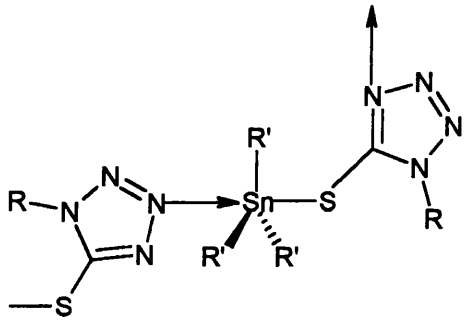

LXI

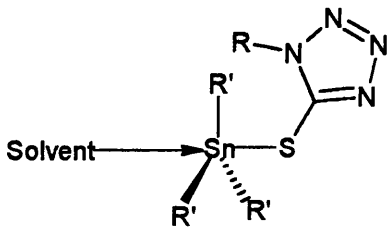

Solvent = MeOH, DMSO

LXII

In **40**, both *trans*-$NSSnC_3$ and *trans*-$SOSnC_3$ coordinations are possible, brought about by the presence of Me(H)O→Sn coordination. However, there is no literature precedent for a *trans*-$SOSnC_3$ type tin centre where the oxygen comes from a solvent molecule and the axial unit is S-Sn-O. Mössbauer spectroscopy by itself is not sufficient to distinguish between the two environments. However, narrow linewidths for **40** (Γ = 0.97, 0.96) rule out the presence of a mixture of both *trans*-$NSSnC_3$ and *trans*-$SOSnC_3$ environments and in fact X-ray crystallography confirms a *trans*-R_3SnSO centre (see Section 6.4.1).

The isomer shift for **41** is 1.22 mms^{-1} and the q.s. is 2.29 mms^{-1}. The former suggests a +4 oxidation state, while the latter points towards a tetrahedral geometry in the solid-state. This is comparable with the q.s. value 2.38 mms^{-1} for tetrahedral 1-phenyl-[(5′-thiolato-triphenylstannyl)-1′-tetrazole],[26] (see Table 6.2) and also parallels the

structure of 1-phenyl-[(5′-thiolato-tricyclohexylstannyl)-1′-tetrazole],[188] (q.s. 1.91 mms^{-1}) which is also tetrahedral at tin.

6.3.2 Multinuclear NMR Spectroscopy

The compounds listed in this chapter, wherever possible, have been characterised by multinuclear NMR spectroscopies (^{1}H, ^{13}C, ^{119}Sn and ^{207}Pb). The spectra confirm the structures proposed in Section 6.2. All spectra were taken in d^{6}-DMSO.

The ^{1}H NMRs of the four organotin compounds (**36**, **37**, **40** and **41**) reveal the characteristic aromatic protons corresponding to the central phenylene ring at ~8.0 ppm. Other features of these ^{1}H NMRs are the hydrocarbon groups on the tin. For **36**, butyl protons appear at 1.62 ppm (α-CH_2), 1.48 ppm (β-CH_2), 1.54 ppm (γ-CH_2) and 0.91 ppm (δ-CH_2); for **37**, ethyl protons at 1.20-1.30 ppm; for **40**, methyl protons at 0.64 ppm and for **41**, phenyl protons at 7.42-7.89 ppm.

The quaternary tetrazole carbon can be clearly seen in the ^{13}C NMR spectra of **36**, **37** and **40** at ~160 ppm. Resonances for the butyl groups in **36** appear between 13 and 27 ppm. The ethyl carbons are clearly visible in **37** and appear between 11.5 and 10.5 ppm. The methyl carbons on the tin in **40** appear at 0.9 ppm. For **41**, the phenyl carbons are visible in the aromatic region, however, an accurate assignment is difficult due to the number and proximity of the peaks. The long relaxation time for a quaternary carbon coupled with the low insolubility of **41** in DMSO made it difficult to detect the quaternary tetrazole carbon.

The ^{119}Sn NMR chemical shift for **36** is 122.8 ppm. The downfield chemical shift value indicates a tetrahedral monomer in solution, which is comparable to that of 1-methyl-[(5′-thiolato-tributylstannyl)-1′-tetrazole] (112.5 ppm).[26] The semi-empirical Holecek and Lycka relationship correlating ^{1}J and C-Sn-C angle gives a value of 109° confirming tetrahedral geometry about the tin centre.[77]

The upfield chemical shift of **37** (-10.3 ppm) suggests a five coordinate tin in the solution-state. Tetrahedral monomers exhibit more downfield shifts, e.g. $\delta(^{119}Sn)$ for

Table 6.2: ^{119}Sn NMR[a] And Mössbauer Studies[b] Of Organotin-Substituted Thio-(tetrazoles)

Compound	$\delta(^{119}Sn)$[c]	$^{1}J(^{117,119}Sn\text{-}^{13}C)$; $^{2}J(^{117,119}Sn\text{-}^{1}H)$ (Hz)	(δ)	ΔEq	Γ_1, Γ_2[d]
(S-tributylstannyl)-1-methyl-5-thiotetrazole[26]	112.5	328	1.48	3.32	
(S-triphenylstannyl)-1-phenyl-5-thiotetrazole[26]	-69.4		1.33	2.38	
36	122.8	327	1.50	3.32	0.80, 0.79
37	-10.3	474	1.52	3.39	0.94, 0.93
40[e]	-23.7	491, 515; 68.5	1.38	3.35	0.97, 0.96
41	-65.0[f]	-	1.22	2.29	0.97, 0.91

[a] All spectra run as d^6-DMSO solutions at 25°C except **41**

[b] Mössbauer data recorded at 78K and data given as mms^{-1}

[c] Values given in ppm

[d] Refers to full width at half height of the high and low velocity

[e] **40** has two coordinated molecules of methanol

[f] Spectra run at 100°C

Et_3SnCl in CH_2Cl_2 is 153.4 ppm.[72] Due to lack of triethyltin-substituted thio-tetrazoles in the literature, a comparison of ^{119}Sn chemical shifts is not possible. However, five coordinate tins in triethyltin-substituted tetrazoles give upfield chemical shifts between -40 and -80 ppm (see Sections 2.3 and 3.3). A value of -10 ppm suggests that the tin centre in **37** is probably not strongly five coordinate.

The upfield ^{119}Sn NMR chemical shift of **40** (-23.7 ppm) suggests that it is clearly trigonal bipyramidal in solution. Comparison with chloroform and dimethyl sulphoxide solutions of Me_3SnCl[(72)] [$\delta(^{119}Sn)$ 164 ppm, 3 ppm respectively] serves to endorse this interpretation. The $^1J(^{119}Sn\text{-}^{13}C)$ and $^2J(^{119}Sn\text{-}^1H)$ values of 515 and 68.5 Hz respectively confirm a trigonal bipyramidal geometry.[68] Using the semi-empirical relationship correlating $^2J(^{119}Sn\text{-}^1H)$ with the C-Sn-C bond angle[78], a bond angle of 119° was obtained, thus providing more evidence towards the above analysis.

A comparison of ^{119}Sn chemical shift values of **36**, **37** and **40** indicates that the tin becomes increasingly monomeric tetrahedral as the alkyl chain increases in length.

The most likely way of attaining the five coordination is via structures of the type **LXI** (see Section 6.3.1) or **LXII** where a solvent molecule is coordinated to the tin. In a coordinating solvent like DMSO, either structure could be formed and nothing can be unambiguously inferred.

The ^{119}Sn NMR chemical shift of **41** (-65.0 ppm) implies it retains its tetrahedral nature in the solution-state. This conclusion can be endorsed by the chemical shift values in $CHCl_3$ and DMSO of Ph_3SnCl[72] [$\delta(^{119}Sn)$ -44.7ppm, -226.8ppm respectively] and Ph_3SnBr[72] [$\delta(^{119}Sn)$ -59.8ppm, -228.4ppm respectively].

38 and **39**, the precursors for **40** and **41** were also characterised by ^1H and ^{13}C NMR spectroscopies. The ^1H NMR for both compounds showed the aromatic protons of the central phenylene ring at ~8 ppm. The ammonium protons of **39** occurred at 7.30 ppm. The main features of the ^{13}C NMR spectra of **38** and **39** were the quaternary tetrazole

carbon at ~160 ppm, the quaternary *1,4* phenylene carbons at ~135 ppm and the *2,3,5,6* phenylene carbons at 124 ppm.

The ^{1}H NMR of **45** and **47** showed aromatic peaks corresponding to the central phenylene ring and the phenylmetal moiety. In the ^{1}H NMR spectrum of **45**, the $-CH_3$ protons of the coordinated toluene are also visible at 3.07 ppm. The ^{13}C NMR of both compounds showed the tetrazole carbon at ~160 ppm. Aromatic resonances due to the central phenylene ring and the diphenylthallium and triphenyllead moieties were also visible. The $\delta(^{207}Pb)$ NMR value of 235.5ppm for **45** falls in the same range as the $\delta(^{207}Pb)$ NMR values for **16-21** which indicates a five coordinate lead (see discussion in Section 4.3). Five coordination could be achieved by forming structures of the type **LXI** or **XLV** (see Section 4.3). To attain a structure of the type **XLV** for **45** in solution-state, the coordinated solvent molecule must be DMSO as there is no evidence for H_2O or MeOH in CHN or NMR data.

Since the inorganic derivatives of 1,4-phenylene-bis-(5′-thiolato-1′-tetrazole)-**42**, **43** and **44**-and the organomercury compound (**46**) were not soluble in DMSO, no NMR spectra could be obtained.

6.4 X-RAY CRYSTALLOGRAPHY

6.4.1 Crystal Structure Of 1,4-Phenylene-Bis-[(5′-Thiolato-Tributylstannyl)-1′-tetrazole], (36)

Crystals of **36** were grown from a methanolic solution at room temperature by slow evaporation. Appendix X includes all the crystallographic analysis, atomic coordinates and isotropic thermal parameters. Fig.6.1 shows the asymmetric unit of **36** and Tables 6.3, 6.4 contain selected bond lengths and bond angles, respectively.

The asymmetric unit contains two trigonal bipyramidal *trans*-$NSSnC_3$ centres as implied by Mössbauer data (see Section 6.3.1). Each tin is directly bonded to the sulphur

and the nitrogen from the tetrazole of a neighbouring molecule is bonded intermolecularly. This type of a tin centre is consistent with the previously known organotin thio-tetrazoles.[27,5] The main difference between this class of compounds and organotin tetrazoles is that in the latter compounds the tin centre is *trans*-N_2SnC_3 where one nitrogen comes from the tetrazole of the asymmetric unit and the other comes from a neighbouring tetrazole (see Sections 2.4.1 and 2.4.2).

For purposes of comparison, the Sn-S, Sn-N, C-S bond lengths, coordination number of the tin and the C-Sn-C bond angle of previously known organotin-substituted thio-tetrazoles are summarised in Table 6.5. In **36** the axial positions of Sn(1) are occupied by S(2) and N(6′) nitrogen of a neighbouring tetrazole. Similarly, the axial positions of Sn(2) are occupied by S(1) and N(2′) nitrogen of a neighbouring tetrazole. The N-Sn-S bond angles are close to 180° [N(6′)-Sn(1)-S(2) 172.6(2)°; S(1)-Sn(2)-N(2′) 169.4(2)°]. The two Sn-S distances [Sn(1)-S(2) 2.574(2)Å; Sn(2)-S(1) 2.554(3)Å] are comparable with the Sn-S bond lengths of previously known organotin thio-tetrazoles (see Table 6.5) although are at the longer end of the range. The intermolecular Sn-N bonds [Sn(1)-N(6′) 2.781(7)Å; Sn(2)-N(2′) 2.810(7)Å] are similar to the intermolecular Sn-N bond lengths of **LVIII** and **LX** (see Table 6.5) but longer than the intermolecular Sn-N bond length of 1,4-phenylene-bis-(tributylstannyl tetrazole) (7) [Sn(1)-N(6′) 2.573(6)Å]. The two Sn-S distances are slightly shorter than the two Sn-N distances. Metal-ligand bonding primarily takes place through the sulphur of the tetrazole rather than the nitrogen (see section 6.1.2). The C-S bond length [S(1)-C(1) 1.716(9)Å; S(2)-C(8) 1.726(9)Å] is similar to known organotin-substituted thio-tetrazoles (see Table 6.5).

The N^2 coordination of the tetrazole with respect to the tin is sterically induced (see Section 1.4). This mode of coordination has been reported in Bz_3SnSCN_4Ph.[27] With respect to itself, the tetrazole ring is bidentate and exhibits $N^1 + N^3$ mode of coordination, the N^1 site being occupied by sulphur. The $N^1 + N^3$ mode of coordination is the commonest for organotin tetrazole and organotin thio-tetrazoles (see Table 1.1) presumably because this is the least sterically hindered combination of ligation modes.

Table 6.5: Important Bond Lengths And Bond Angles For Previously Known Organotin Thio-(tetrazoles)

Compound	Sn-S(Å)	Sn-N(Å)	C-S(Å)	C-Sn-C(°)	CN[a]
36	2.574(2), 2.554(3)	2.781(7)[c], 2.810(7)[c]	1.716(9), 1.726(9)	110.8(8)-125.0(8)	5
40	2.607(2)	-	1.723(7)	115.2(3)-120.3(3)	5
LVII[26]	2.477(4)	2.99[b]	1.76(2)	130.7(4)	6
LVIII[27]	2.565(4)	3.204[b], 2.68(1)[c]	1.72(1)	111.4(4)-126.1(5)	6
LIX[185]	2.482(1)	3.275(3)[b]	1.728(4)	113.6(1)-122.7(1)	5
LX[186]	2.565(4)	3.29(1)[b], 2.75(1)[c]	1.73(2)	115.8(8)-120(1)	6

[a] coordination number

[b] intramolecular

[c] intermolecular

The supramolecular structure is dominated by two-dimensional sheets as shown in Fig.6.2. Sn(1) and Sn(2) in the asymmetric unit interact with N(6) and N(2) of the lattice neighbours generated via the symmetry operators *0.5-x, 0.5+y, -z* and *1.5-x, 0.5+y, 1-z* respectively. The axial nitrogens coordinated to the tin lie in the plane of the sheets polymers. The sheets are dominated by 32-membered rings containing four tins, four sulphurs, twelve tetrazole nitrogens, four tetrazole carbons and eight phenyl carbons as

shown in Fig.6.2. The interlayer region is packed by the equatorial n-butyl groups as shown Fig.6.3.

The supramolecular arrays of other organotin-tetrazoles have also shown planar and puckered two-dimensional arrays (see Table 2.1). The closest analogy for **36** can be drawn with tris-[2-(5-tributylstannyltetrazole) ethyl] nitromethane (**XXVIII**) which is a two-dimensional puckered sheet structure.[24] As is shown in Fig.6.4, the individual polymeric sheets lie parallel to one another. The interlamellar region is populated by tin-bonded butyl groups and the tripodal nitromethane units alternately project above and below the plane of polymer propagation. Each sheet is dominated by hexagonal rings as shown in Fig.6.5.

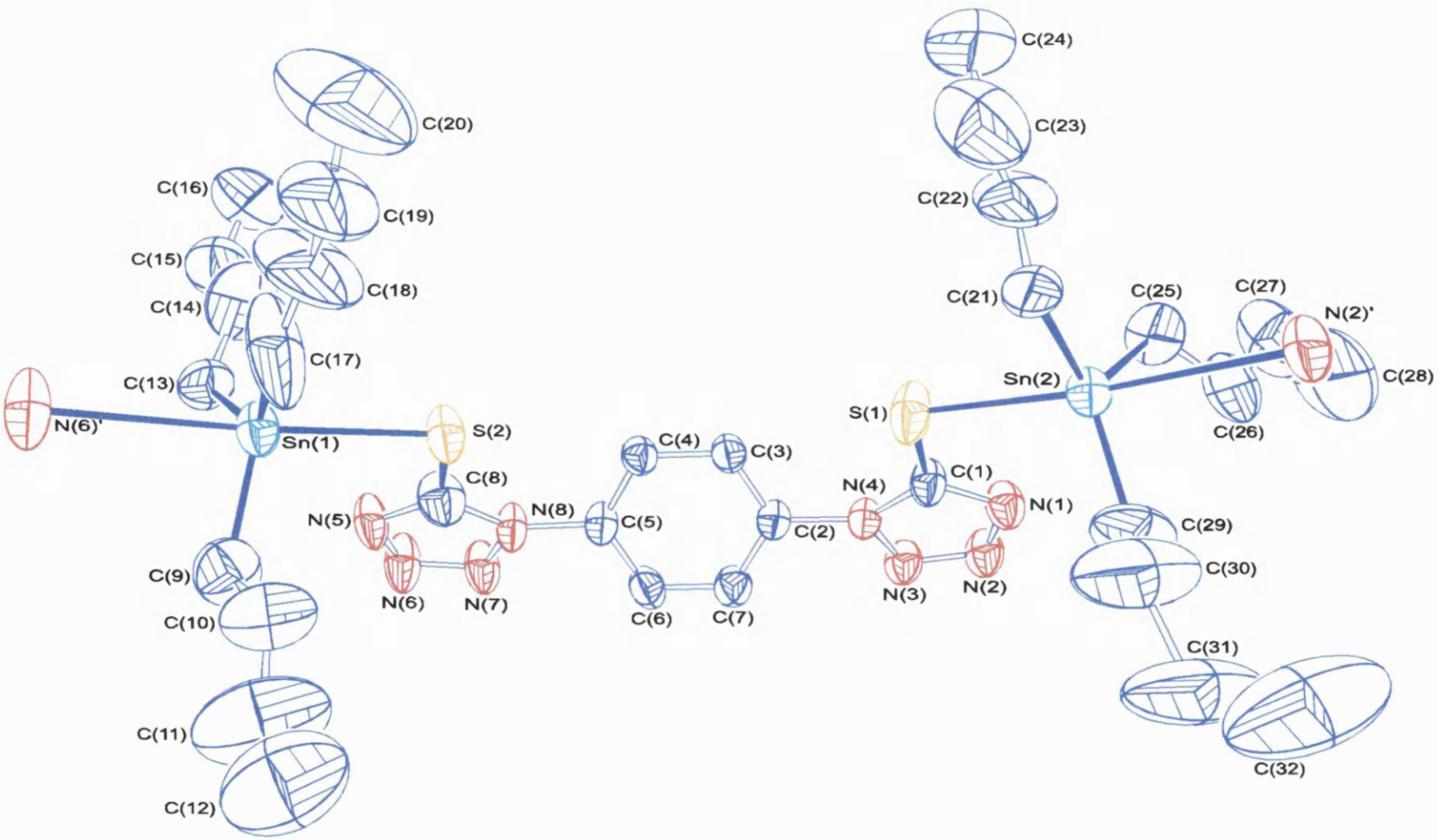

Fig.6.1: The asymmetric unit of **36** showing the atomic labelling scheme used in the text and tables. Hydrogen atoms are omitted for clarity.

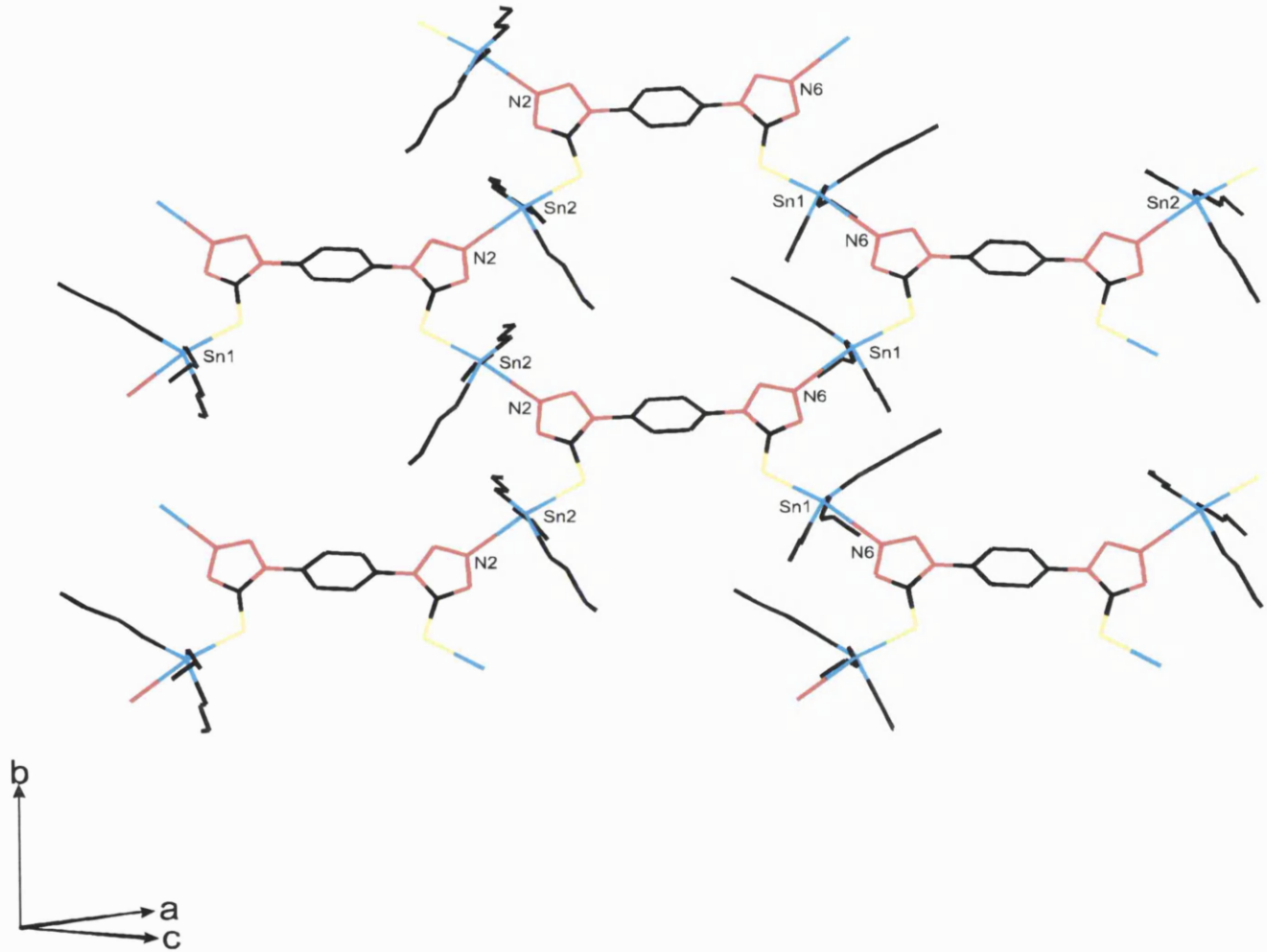

Fig.6.2: View of the two-dimensional sheets dominated by 32-membered rings of **36**.

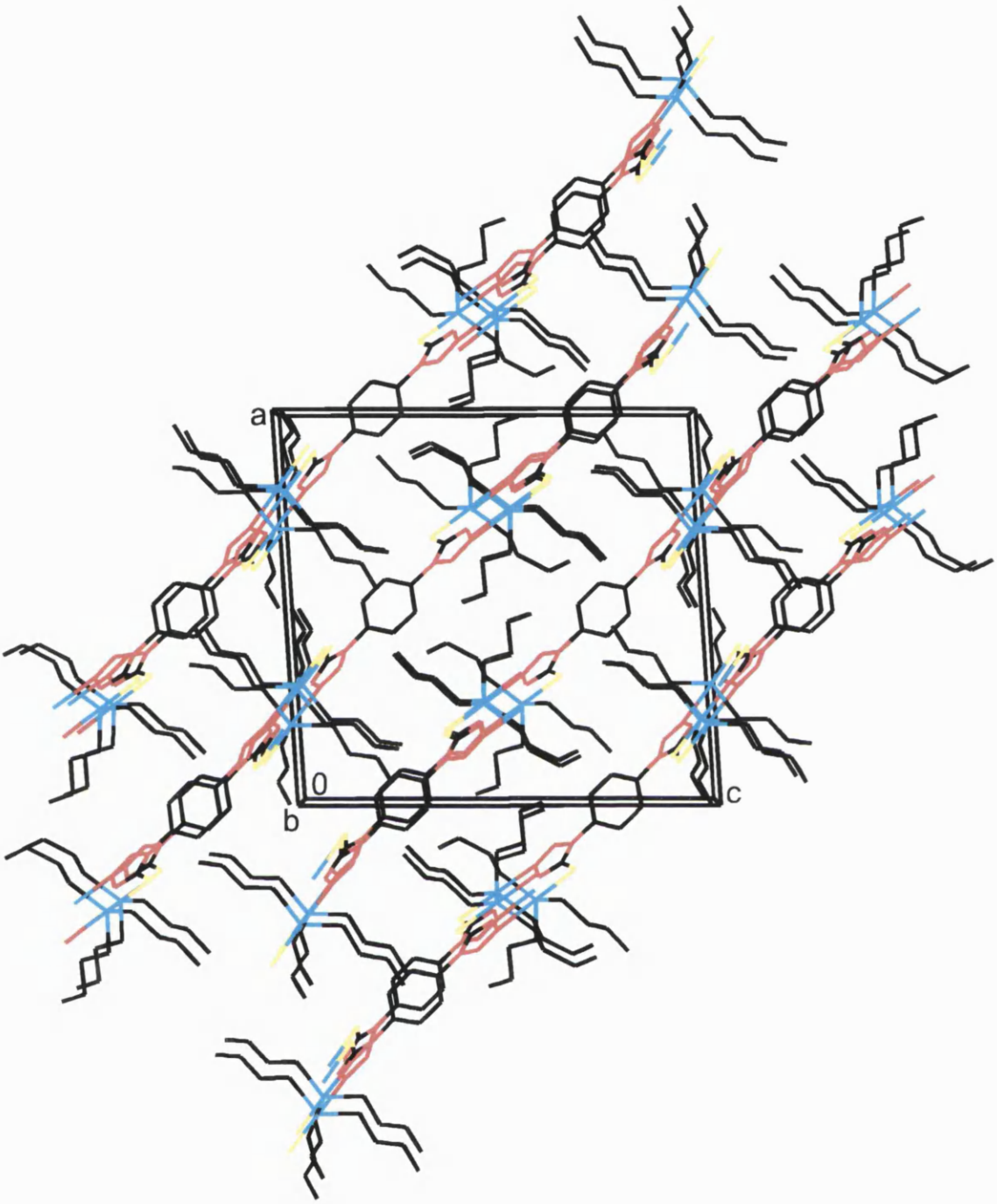

Fig.6.3: View of the interlayer region of **36** packed by equatorial n-butyl groups.

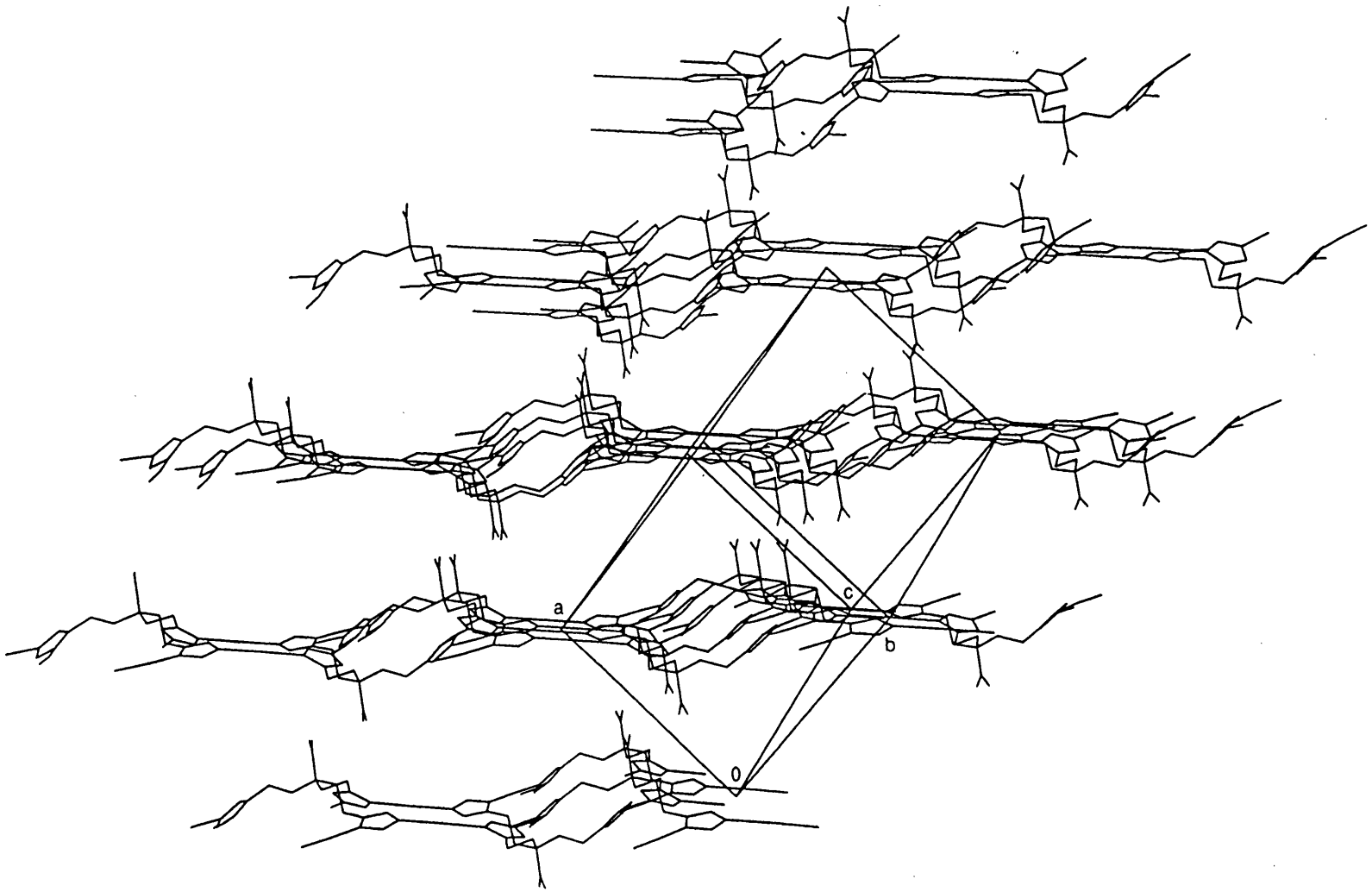

Fig.6.4: Side view of the sheet structure of Tris-[2-(5-tributylstannyl-tetrazolyl)-ethyl]-nitromethane (**XXVIII**). Tributyltin groups omitted for clarity.[24]

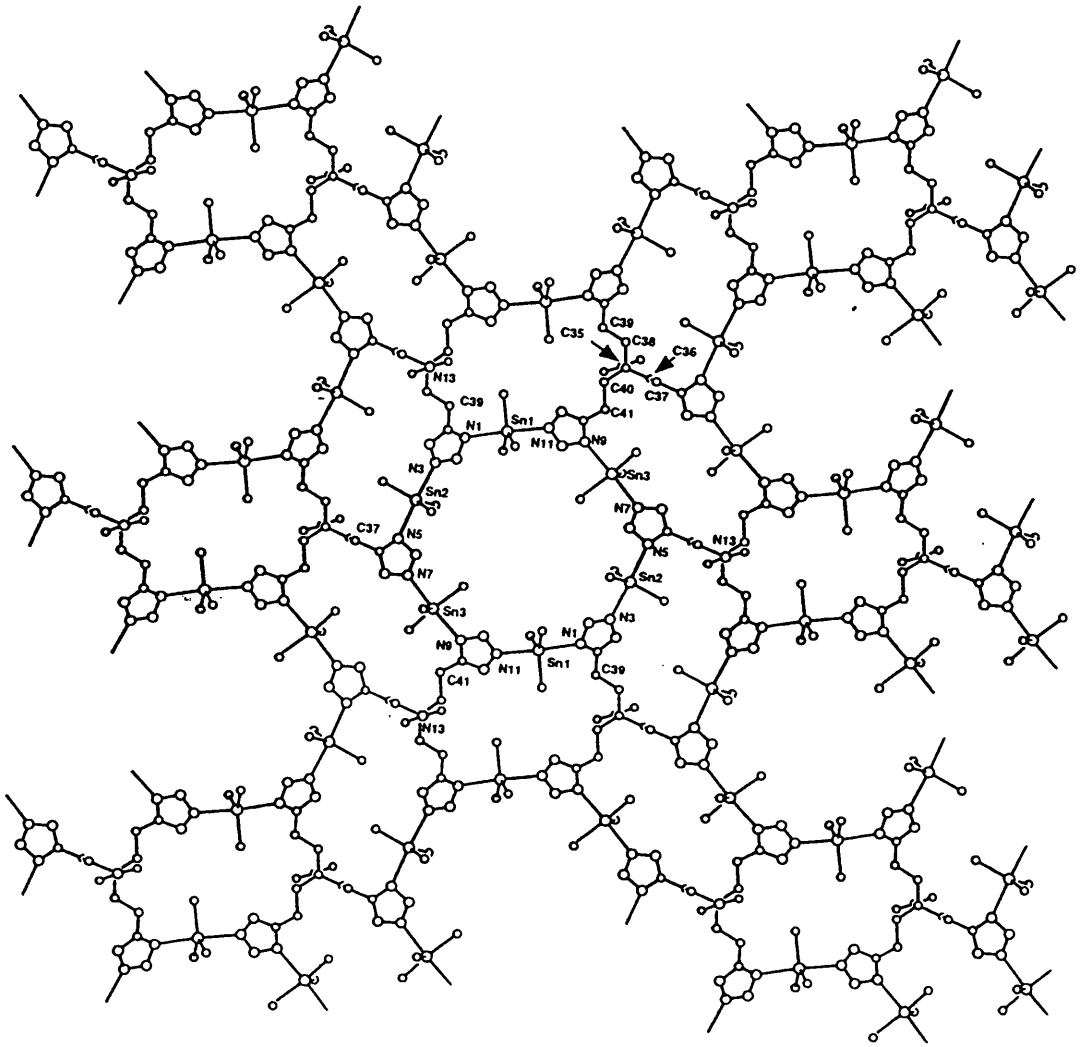

Fig.6.5: The sheet-like array of of Tris-[2-(5-tributylstannyl-tetrazolyl)-ethyl]-nitromethane (**XXVIII**) showing the N-Sn-N polymer propagation.[24]

Table 6.4: Selected Bond Lengths (Å) For **36** With Their Estimated Standard Deviations In Parentheses.

Sn(1)-C(17)	2.09(1)	N(1)-C(1)	1.32(1)
Sn(1)-C(13)	2.10(1)	N(1)-N(2)	1.34(1)
Sn(1)-C(9)	2.11(2)	N(2)-N(3)	1.300(9)
Sn(1)-S(2)	2.574(2)	N(3)-N(4)	1.364(9)
Sn(1)-N(6)#1	2.781(7)	N(4)-C(1)	1.36(1)
Sn(2)-C(29)	2.11(1)	N(4)-C(2)	1.427(9)
Sn(2)-C(21)	2.13(1)	N(5)-C(8)	1.31(1)
Sn(2)-C(25)	2.13(1)	N(5)-N(6)	1.341(1)
Sn(2)-S(1)	2.554(3)	N(6)-N(7)	1.29(1)
Sn(2)-N(2)#2	2.810(7)	N(7)-N(8)	1.356(9)
S(1)-C(1)	1.716(9)	N(8)-C(8)	1.35(1)
S(2)-C(8)	1.726(9)	N(8)-C(5)	1.45(1)

Symmetry transformations used to generate equivalent atoms:

#1 -x+1/2,y+1/2,-z; #2 -x+3/2,y+1/2,-z+1.

Table 6.5: Selected Bond Angles (°) For **36** With Their Standard Deviations In Parentheses.

C(17)-Sn(1)-C(13)	125.0(8)	C(1)-N(4)-N(3)	108.1(6)
C(17)-Sn(1)-C(9)	110.8(8)	C(1)-N(4)-C(2)	131.7(7)
C(13)-Sn(1)-C(9)	118.4(5)	C(30)-C(29)-Sn(2)	123(1)
C(17)-Sn(1)-S(2)	92.9(4)	N(3)-N(4)-C(2)	119.9(7)
C(13)-Sn(1)-S(2)	101.9(3)	C(8)-N(5)-N(6)	105.7(7)
C(9)-Sn(1)-S(2)	98.8(4)	N(7)-N(6)-N(5)	113.1(7)
C(17)-Sn(1)-N(6)#1	79.7(4)	N(6)-N(7)-N(8)	104.4(7)
C(13)-Sn(1)-N(6)#1	82.6(4)	C(8)-N(8)-N(7)	108.9(6)
C(9)-Sn(1)-N(6)#1	83.9(4)	C(8)-N(8)-C(5)	131.7(7)
S(2)-Sn(1)-N(6)#1	172.6(2)	N(7)-N(8)-C(5)	119.3(7)
C(29)-Sn(2)-C(21)	122.2(5)	N(1)-C(1)-N(4)	107.9(7)
C(29)-Sn(2)-C(25)	117.6(6)	N(1)-C(1)-S(1)	126.5(7)
C(21)-Sn(2)-C(25)	114.5(5)	N(4)-C(1)-S(1)	125.6(6)
C(29)-Sn(2)-S(1)	101.1(4)	C(3)-C(2)-N(4)	119.7(8)
C(21)-Sn(2)-S(1)	89.5(3)	C(7)-C(2)-N(4)	119.0(8)
C(25)-Sn(2)-S(1)	103.2(3)	C(6)-C(5)-N(8)	118.9(8)
C(29)-Sn(2)-N(2)#2	82.0(4)	C(4)-C(5)-N(8)	119.5(8)

Table 6.5: Selected Bond Angles (°) For **36** With Their Standard Deviations In Parentheses (contd.).

C(21)-Sn(2)-N(2)#2	80.4(3)	N(5)-C(8)-N(8)	107.8(7)
C(25)-Sn(2)-N(2)#2	84.0(4)	N(5)-C(8)-S(2)	127.1(7)
S(1)-Sn(2)-N(2)#2	169.4(2)	N(8)-C(8)-S(2)	125.1(6)
C(1)-S(1)-Sn(2)	104.0(3)	C(10)-C(9)-Sn(1)	118(1)
C(8)-S(2)-Sn(1)	101.8(3)	C(14)-C(13)-Sn(1)	114(1)
C(1)-N(1)-N(2)	106.6(7)	C(18)-C(17)-Sn(1)	136(2)
N(3)-N(2)-N(1)	112.2(6)	C(22)-C(21)-Sn(2)	109.0(9)
N(2)-N(3)-N(4)	105.1(7)	C(26)-C(25)-Sn(2)	115.7(9)

Symmetry transformations used to generate equivalent atoms:

#1 -x+1/2,y+1/2,-z; #2 -x+3/2,y+1/2,-z+1.

6.4.2 Crystal Structure Of 1,4-Phenylene-Bis-[(5′-Thiolato-Trimethylstannyl)-1′-Tetrazole].2MeOH, (40)

X-ray quality crystals of **40** were obtained by slow evaporation of a methanolic solution at room temperature. Crystal data had to be collected at low temperature as the crystals lost solvent at room temperature. All data, including crystallographic analysis, atomic coordinates and isotropic thermal parameters, are given in Appendix XI. The asymmetric unit of **40** is shown in Fig.6.6 and selected bond lengths and bond angles are contained in Tables 6.6 and 6.7 respectively.

The asymmetric unit in this structure was seen to consist of one half of the molecule, the remainder being generated by inversion through the centre of the C_6 ring. The tin in the asymmetric unit is trigonal bipyramidal *trans*-$SOSnC_3$ as is suggested by spectroscopic evidence (see Sections 6.3.1 and 6.3.2 respectively). The axial positions of Sn(1) are taken up by O(1) of the coordinated methanol molecule and S(1) as presented in the asymmetric unit. The O-Sn-S bond angle is close to 180° [O(1)-Sn(1)-S(1) 174.7(1)°]. The Sn(1)-S(1) bond length is 2.607(2)Å and the Sn(1)-O(1) bond length is 2.464(5)Å. The Sn-S distance is comparable with **36** [Sn(1)-S(2) 2.574(2)Å; Sn(2)-S(1) 2.554(3)Å] and with the previously known organotin-substituted thio-tetrazoles (see Table 6.5) although it is the longest Sn-S distance known yet. The Sn-O bond distance cannot be compared with any known organotin thio-tetrazole as there is no precedent for a *trans*-R_3SnSO centre in these systems. However, the Sn-O bond distance can be compared with that of $[Me_3SnOSPMe_2]_\infty$ which has a *trans*-R_3SnSO centre.[189] As in **40**, the methyl groups are equatorial and the axial positions are occupied by the S and the O. The S-Sn-O bond angle is 172.4(3)° and the Sn-O bond length is 2.267(6)Å. The latter is shorter than the Sn-O distance in **40**. Parallels can also be drawn with 1,3-phenylene-bis-(tributylstannyl tetrazole).2MeOH (**XXV**)which has two *trans*-R_3SnNO tin centres. The Sn-O bond length of 2.393(9)Å in **XXV** is marginally shorter than in **40**.

The salient feature of the supramolecular structure is one-dimensional polymers held together by hydrogen-bonding as shown in Fig.6.7. The coordinated methanol

hydrogen bonds to N(2) of a neighbouring tetrazole [O(1)-N(2) 2.801(8)Å; H(1)-N(2) 1.84(3)Å; O(1)-H(1)-N(2) 173(5)°] to generate one-dimensional polymers. The polymers are dominated by fourteen-membered rings generated by an inversion centre. These rings are reminiscent of the twelve-membered rings seen in the crystal structure of 1-phenyl-5-diphenylthallium tetrazole, (**29**) (see Fig.5.4). The ring size is increased in (**40**) by the two sulphur atoms.

As a final note, the tetrazole ring is effectively bidentate and exhibits $N^1 + N^3$ mode of coordination (sulphur occupying the N^1 site). As discussed in Section 6.4.1, this is also seen in **36** and is the commonest mode of coordination for organotin-substituted tetrazoles (see Table 2.1).

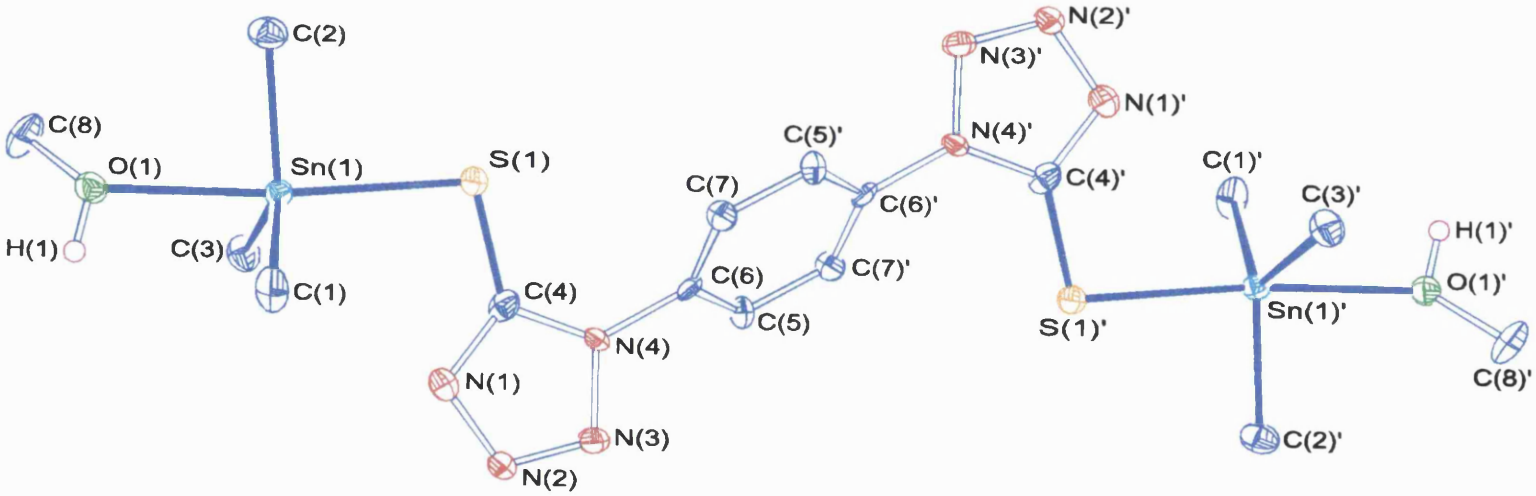

Fig.6.6: The asymmetric unit of **40** showing the atomic labelling scheme used in the text and tables. Hydrogen atoms are omitted for clarity.

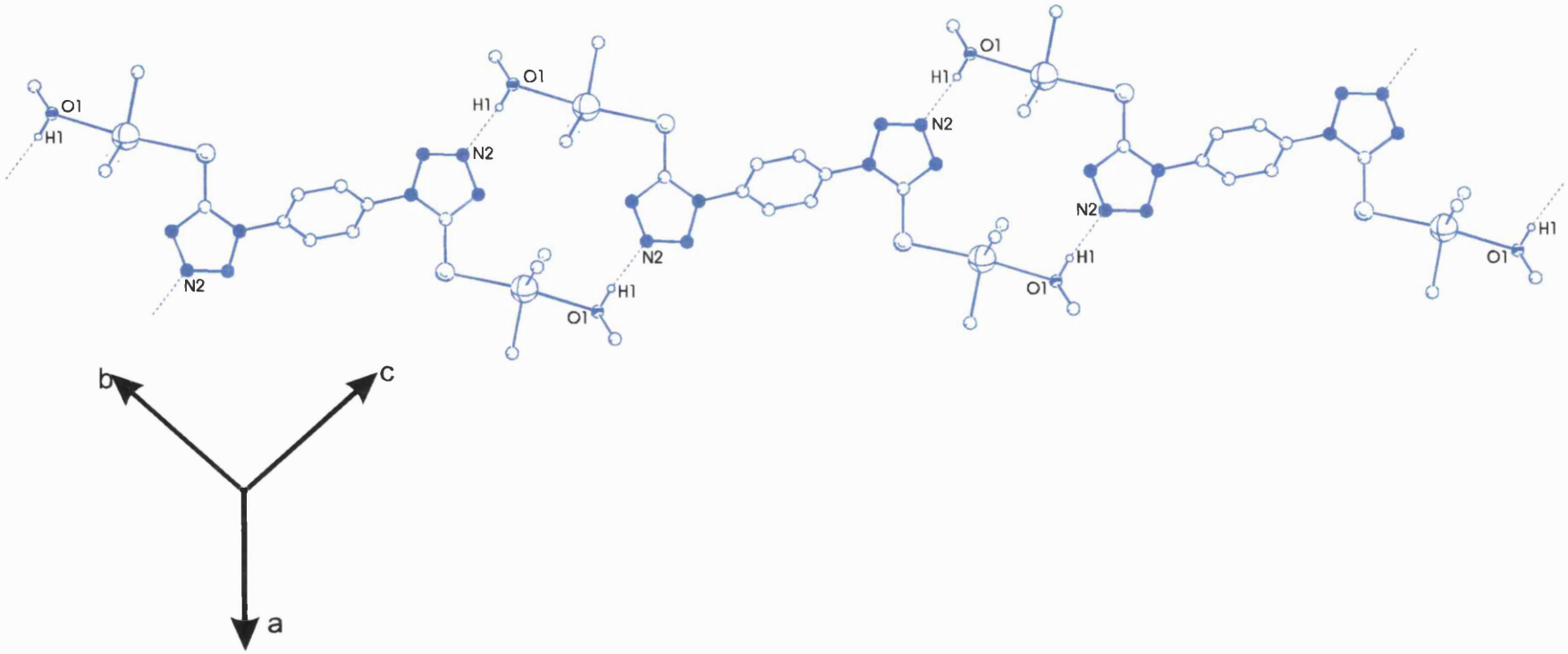

Fig.6.7: View of the one-dimensional polymers of **40** held together by hydrogen bonding.

Table 6.6: Selected Bond Lengths (Å) For **40** With Their Estimated Standard Deviations In Parentheses.

Sn(1)-C(2)	2.132(7)	N(3)-N(4)	1.367(8)
Sn(1)-C(1)	2.133(6)	N(4)-C(4)	1.356(9)
Sn(1)-C(3)	2.141(7)	N(4)-C(6)	1.440(8)
Sn(1)-O(1)	2.464(5)	O(1)-C(8)	1.427(8)
Sn(1)-S(1)	2.607(2)	C(5)-C(6)	1.385(9)
S(1)-C(4)	1.723(7)	C(5)-C(7)#1	1.396(9)
N(1)-C(4)	1.32(1)	C(6)-C(7)	1.39(1)
N(1)-N(2)	1.367(9)	C(7)-C(5)#1	1.396(9)
N(2)-N(3)	1.291(8)		

Symmetry transformations used to generate equivalent atoms:

#1 -x+1,-y+1,-z+1

Table 6.7: Selected Bond Angles (°) For **40** With Their Estimated Standard Deviations In Parentheses.

C(2)-Sn(1)-C(1)	115.2(3)	N(2)-N(3)-N(4)	105.6(5)
C(2)-Sn(1)-C(3)	120.9(3)	C(4)-N(4)-N(3)	108.9(5)
C(1)-Sn(1)-C(3)	120.3(3)	C(4)-N(4)-C(6)	132.1(6)
C(2)-Sn(1)-O(1)	83.7(2)	N(3)-N(4)-C(6)	119.0(5)
C(1)-Sn(1)-O(1)	82.2(2)	C(8)-O(1)-Sn(1)	123.7(4)
C(3)-Sn(1)-O(1)	85.0(2)	N(1)-C(4)-N(4)	107.6(6)
C(2)-Sn(1)-S(1)	91.1(2)	N(1)-C(4)-S(1)	127.8(5)
C(1)-Sn(1)-S(1)	99.3(2)	N(4)-C(4)-S(1)	124.6(5)
C(3)-Sn(1)-S(1)	98.5(2)	C(6)-C(5)-C(7)#1	119.2(6)
O(1)-Sn(1)-S(1)	174.7(1)	C(5)-C(6)-C(7)	122.6(6)
C(4)-S(1)-Sn(1)	101.1(2)	C(5)-C(6)-N(4)	117.9(6)
C(4)-N(1)-N(2)	106.3(5)	C(7)-C(6)-N(4)	119.4(6)
N(3)-N(2)-N(1)	111.7(6)	C(6)-C(7)-C(5)#1	118.2(6)

Symmetry transformations used to generate equivalent atoms:

#1 -x+1,-y+1,-z+1

6.6 SUMMARY

To summarise, the cycloaddition route used in chapters 2 and 3 to synthesise organotin tetra-tetrazoles and functionalised organotin-tetrazoles was used to synthesise 1,4-phenylene-bis-(5′-thiolato-tributylstannyl-1′-tetrazole) (**36**), 1,4-phenylene-bis-(5′-thiolato-triethylstannyl-1′-tetrazole) (**37**). Two other organotin-substituted thio-tetrazoles, 1,4-phenylene-bis-(5′-thiolato-trimethyl-1′-tetrazole) (**40**) and 1,4-phenylene-bis-(5′-thiolato-triphenylstannyl-1′-tetrazole) (**41**) were prepared by the reaction of the ammonium salt of 1,4-phenylene-bis-(5′-thiolato-tributylstannyl-1′-tetrazole) with the respective triorganotin chlorides. Crystallographic analyses of the anhydrous **36** and the bis-methanolated **40** were obtained. 1,4-phenylene-bis-(5′-thiolato-tributylstannyl-1′-tetrazole) (**36**) was used as a precursor for the syntheses of three inorganic thio-tetrazoles and three organometallic thio-tetrazoles.

6.7 EXPERIMENTAL

Literature procedures were used to synthesise tributyltin azide and triethyltin azide.[110] Diphenylthallium hydroxide was prepared by the method of Casas *et al.*[176] All other chemicals were commercially obtained and used without further purification.

Preparation of 1,4-phenylene-bis-(5′-thiolato-tributylstannyl-1′-tetrazole), (**36**)

A mixture of 6.96g (21.0 mmol) tributyltin azide and 2.04g (10.6 mmol) of 1,4-phenylene-diisothiocyanate were heated while stirring in a three-necked flask under N_2 at 100°C for half an hour. The resultant yellow/white solid was recrystallised from hexanes and the product was obtained as a white microcrystalline solid (5.02g, 55%) (m.p. 122°C).

Analysis: Found (Calc. for $C_{32}H_{58}N_8S_2Sn_2$): C 44.6 (44.9); H 6.81 (6.83); N 13.0 (13.1)%.

^{1}H NMR [δ(ppm), DMSO-d^{6} solution]: 8.01 [s, 4H, *2,3,5,6*-C_6H_4]; 1.62 [m, 12H, Sn$CH_2$$CH_2$$CH_2$$CH_3$]; 1.54 [m, 12H, Sn$CH_2$$CH_2$$CH_2$$CH_3$]; 1.48 [m, 12H, Sn$CH_2$$CH_2$$CH_2$$CH_3$]; 0.91 [t, 9H, $(CH_2)_3CH_3$].

^{13}C NMR [δ(ppm), DMSO-d^{6} solution]: 155.7 [CN_4]; 135.1 [*1,4*-C_6H_4]; 124.6 [*2,3,5,6*-C_6H_4]; 28.5 [Sn$CH_2$$CH_2$$CH_2$$CH_3$]; 27.0 [Sn$(CH_2)_2$$CH_2$$CH_3$]; 16.6 [Sn$CH_2$$(CH_2)_2CH_3$]; 13.6 [$(CH_2)_3CH_3$]; ^{1}J[^{13}*C*-^{117,119}*Sn*] 327 Hz (unresolved); ^{3}J[^{13}*C*-^{117,119}*Sn*] 66 Hz (unresolved).

^{119}Sn NMR [δ(ppm), DMSO-d^{6} solution]: 122.8.

IR [(cm^{-1}), Nujol]: 3457, 2924, 2855, 2363, 2340, 2168, 1653, 1601, 1509, 1464, 1418, 1375, 1300, 1277, 1219, 1080, 1039, 1011, 837.

^{119m}Sn Mössbauer (mms^{-1}): I.S. = 1.50; Q.S. = 3.32.

Preparation of 1,4-phenylene-bis-(5'-thiolato-triethylstannyl-1'-tetrazole), (**37**)

A mixture of 2.91g (11.73 mmol) triethyltin azide and 1.13g (5.87 mmol) of 1,4-phenylene-diisothiocyanate was heated while stirring in a three-necked flask under N_2 at 88°C for half an hour. The resultant yellow/white solid was washed with hexanes and the product was obtained as a white powder (2.12g, 53%) [m.p. 184°C(dec.)].

Analysis: Found (Calc. for $C_{20}H_{34}N_8S_2Sn_2$): C 34.9 (34.9); H 4.80 (4.94); N 16.7 (16.3)%.

^{1}H NMR [δ(ppm), DMSO-d^{6} solution]: 8.06 [s, 4H, *2,3,5,6*-C_6H_4]; 1.20-1.30 [m, 30H, CH_2CH_3]; ^{1}J[$C^{1}H_2CH_3$-^{117,119}*Sn*] 90 Hz (unresolved).

^{13}C NMR [δ(ppm), DMSO-d^{6} solution]: 163.0 [CN_4]; 135.1. [*1,4*-C_6H_4]; 124.7 [*2,3,5,6*-C_6H_4]; 11.5 [CH_2CH_3]; 10.5 [CH_2CH_3]; ^{1}J[$^{13}CH_2CH_3$-^{117,119}*Sn*] 237 Hz (unresolved).

^{119}Sn NMR [δ(ppm), DMSO-d^{6} solution]: -10.3.

IR [(cm^{-1}), KBr]: 2947, 1606, 1518, 1446, 1371, 1300, 1277, 1218, 1120, 1082, 1039, 1010, 952, 839, 715, 677.

^{119m}Sn Mössbauer (mms^{-1}): I.S. = 1.52; Q.S. = 3.39.

Preparation of 1,4-phenylene-bis-(5′-thiolato-hydro-1′-tetrazole).MeOH, (**38**)

To a well stirred solution of 1,4-phenylene-bis-(5′-thiolato-tributylstannyl-1′-tetrazole) (3.0g, 3.5 mmol) in hot methanol (300 mL), 1.50mL (18 mmol) of concentrated hydrochloric acid was added dropwise. The resultant colourless solution was refluxed for an hour. After cooling, methanol was removed *in vacuo* and the remaining white solid washed with hexanes and recrystallised from methanol to give the product as a white solid (0.96g, 99%) [m.p. 200°C(dec.)].

Analysis: Found (Calc. for $C_8H_6N_8S_2.CH_3OH$): C 34.9 (34.7); H 2.05 (2.74); N 38.5 (38.1)%.

^{1}H NMR [δ(ppm), DMSO-d^6 solution]: 8.17 [s, 4H, *2,3,5,6*-C_6H_4]; 3.18[s,CH_3OH].

^{13}C NMR [δ(ppm), DMSO-d^6 solution]: 162.5 [CN_4]; 134.5 [*1,4*-C_6H_4]; 125.4 [*2,3,5,6*-C_6H_4].

IR [(cm^{-1}), KBr disk]: 3553, 3414, 3069, 2937, 2750, 1637, 1616, 1522, 1477, 1385, 1350, 1296, 1275, 1217, 1049, 989, 841, 767, 657, 590.

Preparation of [ammonium]$_2$[1,4-phenylene-bis-(5′-thiolato-1′-tetrazolate)], (**39**)

Ammonia gas was bubbled through a solution of **38** in methanol (350 mL) for 30 mins. The methanol was removed *in vacuo* to yield a white solid in 100% yield [m.p. 190°C(dec.)].

Analysis: Found (Calc. for $C_8H_{12}N_{10}S_2$): C 31.4 (30.8); H 3.90 (3.85); N 44.2 (44.9)%.

^{1}H NMR [δ(ppm), DMSO-d^6 solution]: 8.16 [s, 4H, *2,3,5,6*-C_6H_4]; 7.30 [s, 8H, NH_4^+].

^{13}C NMR [δ(ppm), DMSO-d^6 solution]: 167.5 [CN_4]; 135.5 [*1,4*-C_6H_4]; 123.5 [*2,3,5,6*-C_6H_4].

IR [(cm^{-1}), Nujol]: 3443, 2955, 2924, 2855, 2363, 2342, 1734, 1653, 1559, 1516, 1458, 1420, 1375, 1358, 1292, 1283, 1219, 1089, 1040, 1013.

Preparation of 1,4-phenylene-bis-(5'-thiolato-trimethyl stannyl-1'-tetrazole). 2MeOH, **(40)**

A solution of trimethyltin chloride (0.62g, 3.12 mmol) in methanol (100 mL) was added dropwise to a well-stirred solution of **39** (0.50g, 1.56 mmol) in methanol (200 mL) and the reaction mixture was refluxed for 3 hours. Subsequently, the methanol was removed *in vacuo* and the white solid was refluxed in acetone (300mL) for 30 mins. Hot filtration resulted in a yellow solution. The acetone was removed *in vacuo* and the resulting yellow/white solid recrystallised from methanol to yield the product as a yellow crystalline solid (0.73g, 77%) [m.p. 175°C(dec.)].

Analysis: Found (Calc. for $C_{14}H_{22}N_8S_2Sn_2.2CH_3OH$): C 28.5 (28.7); H 4.32 (4.49); N 17.0 (16.8)%.

^{1}H NMR [δ(ppm), DMSO-d^6 solution]: 8.06 [s, 4H, *2,3,5,6*-C_6H_4]; 3.16 [s, 6H, CH_3OH]; 0.64 [s, 12H, -Sn-CH_3]; $^2J[^1H\text{-}^{117,119}Sn]$ 68.5 Hz (unresolved); 3.50 [s, CH_3OH].

^{13}C NMR [δ(ppm), DMSO-d^6 solution]: 164.7 [CN_4]; 135.1 [*1,4*-C_6H_4]; 124.5 [*2,3,5,6*-C_6H_4]; 48.7 [CH_3OH]; 0.9 [-CH_3];]; $^1J[^{13}C\text{-}^{117,119}Sn]$ 491, 515 Hz.

^{119}Sn NMR [δ(ppm), DMSO-d^6 solution]: -23.7.

IR [(cm^{-1}), KBr disk]: 3245, 2924, 2855, 2363, 2342, 1520, 1512, 1464, 1368, 1352, 1298, 1277, 1219 1117, 1098, 1082, 1020, 1010, 837, 789.

^{119m}Sn Mössbauer (mms^{-1}): I.S. = 1.37; Q.S. = 1.69.

Preparation of 1,4-phenylene-bis-(5'-thiolato-triphenylstannyl-1'-tetrazole), (**41**)

A solution of triphenyltin chloride (0.76g, 1.97 mmol) in methanol (100 mL) was added dropwise to a well-stirred solution of **39** (0.31g, 0.99 mmol) in methanol (250 mL) and the reaction mixture was refluxed for 3 hours. The reaction was worked up in the same way as **40** to yield **41** as a white powder (0.42g, 40%) [m.p. 160-162°C].

Analysis: Found (Calc. for $C_{44}H_{34}N_8S_2Sn_2$): C 53.2 (54.1); H 3.46 (3.48); N 11.5 (11.5)%.

^{1}H NMR [δ(ppm), DMSO-d^6 solution (100°C)]: 7.89-7.42 [m, 34H, phenyl protons].

^{13}C NMR [δ(ppm), DMSO-d^6 solution(100°C)]: 141.7, 135.7, 134.9, 129.0, 128.3, 125.2, 124.0, 118.0 [phenyl carbons].

^{119}Sn NMR [δ(ppm), DMSO-d^6 solution (100°C)]: -65.0

IR [(cm^{-1}), KBr disk]: 3414, 3067, 1637, 1618, 1522, 1479, 1429, 1379, 1238, 1226, 1091, 1074, 1016, 997, 837, 731, 696, 619, 574, 453.

^{119m}Sn Mössbauer (mms^{-1}): I.S. = 1.22; Q.S. = 2.29.

Preparation of Nickel(II) 1,4-phenylene-bis-(5'-thiolato-1'-tetrazolate).6H_2O, (**42**)

A solution of nickel dichloride.6H_2O (0.14g, 0.59 mmol) in methanol (20mL) was added dropwise to a well-stirred solution of **36** (0.50g, 0.58 mmol) in methanol (150mL). A grey precipitate was obtained immediately. The reaction mixture was refluxed for 1

hour. The grey product was collected by hot filtration and washed with hexanes (0.19g, 70%) [m.p. 200°C(dec.)].

Analysis: Found (Calc. for $C_8H_4N_8S_2Ni.6H_2O$): C 23.4 (21.7); H 3.27 (3.61); N 25.1 (25.3)%.

IR [(cm^{-1}), Nujol]: 3428, 2924, 2955, 2855, 2361, 2342, 1653, 1636, 1516, 1462, 1377, 1300, 1090, 1049, 1011, 833, 762, 721, 667.

Preparation of Silver(I) 1,4-phenylene-bis-(5'-thiolato-1'-tetrazolate).2H_2O, (**43**)

A solution of silver tetrafluoroborate (0.31g, 1.17 mmol) in methanol (20 mL) was added dropwise to a well-stirred solution of **36** (0.50g, 0.58 mmol) in methanol (150 mL). A yellow/brown precipitate was formed instantaneously. The reaction mixture was refluxed for 3 hours. Subsequently, the brown solid product was collected by hot filtration (0.19g, 67%) [m.p. 172-177°C (dec.)].

Analysis: Found (Calc. for $C_8H_4N_8S_2Ag.2H_2O$): C 19.3 (21.2); H 0.92 (1.51); N 19.3 (21.2)%.

IR [(cm^{-1}), Nujol]: 3420, 2924, 2855, 1636, 1512, 1462, 1377, 1306, 1233, 1084, 1044, 1013, 839, 721, 579.

Preparation of Mercury(II) 1,4-phenylene-bis-(5'-thiolato-1'-tetrazolate).2H_2O, (**44**)

To a well-stirred, refluxing solution of **36** (0.50g, 0.58 mmol) in methanol (150mL), a solution of mercury(II) chloride (0.16g, 0.60 mmol) in methanol (10 mL) was added dropwise. A white precipitate resulted immediately. Subsequently, methanol was partially removed *in vacuo* and the resultant white product was collected by filtration and washed with hexanes (0.22g, 74%) [m.p. 185-190°C(dec.)].

Analysis: Found (Calc. for $C_8H_4N_8S_2Hg.2H_2O$): C 19.2 (18.7); H 1.08 (1.55); N 21.8 (21.8)%.

IR [(cm^{-1}), Nujol]: 3436, 2926, 2855, 2361, 1653, 1636, 1510, 1464, 1377, 1302, 1273, 1225, 1092, 1044, 1009, 990, 839, 762, 721, 571.

Preparation of 1,4-phenylene-bis-(5'-thiolato-triphenyllead-1'-tetrazole).0.5$CH_3C_6H_5$, **(45)**

A solution of triphenyllead chloride (0.56g, 1.18 mmol) in methanol (200 mL) was added dropwise to a well stirred solution of **36** (0.50g, 0.58 mmol) in hot methanol (150mL). The resultant clear solution was refluxed for 10 hours. Subsequently, methanol was removed *in vacuo* and the resulting white product was washed with hexanes and recrystallised from toluene to give **45** as white crystalline product (0.22g, 33%) [m.p. 218-220°C(dec.)].

Analysis: Found (Calc. for $C_{44}H_{34}N_8S_2Pb_2.1/2CH_3C_6H_5$): C 47.7 (47.5); H 3.32 (3.17); N 9.48 (9.35)%.

^{1}H NMR [δ(ppm), DMSO-d^6 solution]: 7.84, 7.74, 7.32-7.60 [phenyl protons]; 3.07 [s, $CH_3C_6H_5$].

^{13}C NMR [δ(ppm), DMSO-d^6 solution]: 160.0 [CN_4]; 135.8, 134.5, 129.4, 128.7, 124.3 [phenyl carbons].

^{207}Pb NMR [δ(ppm), DMSO-d^6 solution]: -235.5 (100°C).

IR [cm^{-1}; Nujol]: 2926, 2855, 1933, 1836, 1715, 1633, 1603, 1568, 1435, 1377, 1335, 1298, 1233, 1098, 1026, 1011, 997, 857, 760, 741, 696.

Preparation of 1,4-phenylene-bis-(5′-thiolato-phenylmercury-1′-tetrazole), (**46**)

46 was prepared similarly to **45** from a methanolic solution (100mL) of **36** (0.53g, 0.61mmol) and a solution of phenylmercuric chloride (0.38g, 1.27mmol) in methanol (130mL). A white precipitate formed instantaneously, which was collected by washing with hexanes and filtering. The product was found to be insoluble in most commonly available solvents (0.40g, 80%) [m.p. 190-192°C(dec.)].

Analysis: Found (Calc. for $C_{20}H_{14}N_8S_2Hg_2$): C 28.2 (28.9); H 1.74 (1.68); N 13.0 (13.5)%.

IR [cm^{-1}; Nujol]: 3441, 2955, 2924, 2855, 1624, 1524, 1464, 1431, 1372, 1294, 1271, 1235, 1094, 1041, 1020, 997, 982, 843, 723, 629.

Preparation of 1,4-phenylene-bis-(5′-thiolato-diphenylthallium tetrazole).2H_2O, (**47**)

A solution of diphenylthallium hydroxide (0.100g, 0.267mmol) in methanol (200 mL) was added dropwise to a well stirred solution of 1,4-phenylene-bis-(5′-thiolato-hydro-1′-tetrazole) (**38**) (0.04g, 0.134mmol) in hot methanol (60mL). The resultant solution became cloudy. After refluxing for 3 hours, the solution still remained cloudy. The reaction mixture was then cooled to room temperature and the volume of solvent was decreased under reduced pressure. This resulted in more white solid precipitating from solution, which was collected by filtration and dried *in vacuo* (0.06g, 43%) [m.p. 202°C(dec.)].

Analysis: Found (Calc. for $C_{32}H_{24}N_8S_2Tl_2.2H_2O$): C 38.7 (37.3); H 2.42 (2.72); N 11.3 (10.9)%.

^{1}H NMR [δ(ppm), DMSO-d^6 solution]: 8.28-7.29 [m, 24H, phenyl protons].

^{13}C NMR [δ(ppm), DMSO-d^6 solution]: 164.0 [CN_4]; 137.3, 136.9, 135.6, 130.9, 128.8, 126.5, 123.9 [phenyl carbons].

IR [cm^{-1}; KBr]: 3414, 3044, 2924, 1616,1510, 1475, 1431, 1363, 1340, 1296, 1280, 1215, 1093, 1078, 1006, 997, 841, 723, 688, 451.

APPENDIX I

INSTRUMENTAL DETAILS

I) Infra-red Spectroscopy

Infra-red spectra were recorded either as KBr discs or nujol mulls on NaCl using a Nicolet 510P FT-IR spectrometer in the region 400-4000cm^{-1}.

II) NMR Spectroscopy

^{1}H and ^{13}C spectra were recorded either on a Jeol GX 270 MHz spectrometer or a Jeol EX 400 MHz spectrometer using a TMS as an internal standard. ^{119}Sn and ^{207}Pb spectra were recorded on a Jeol GX 400 MHz spectrometer. Chemical shifts [$\delta(^{119}Sn)$] for tin spectra are relative to Me_4Sn and [$\delta(^{207}Pb)$] for lead spectra are relative to Et_4Pb. $Pb(NO_3)_2$ is also a commonly used standard for obtaining ^{207}Pb NMR spectra.[74] However, for the organolead compounds included in this thesis, use of Et_4Pb was more convenient. This is because [$\delta(^{207}Pb)$] for Et_4Pb is +6.5 ppm while [$\delta(^{207}Pb)$] for $Pb(NO_3)_2$ in 1M H_2O is -2961.2 ppm.

III) Microanalysis

Carbon, hydrogen and nitrogen analyses were carried out using a Carlo Erba Strumentazione E.A. model 1106 analyser at the University of Bath.

IV) Mössbauer Spectroscopy

Mössbauer spectra were recorded on a constant acceleration Mössbauer spectrometer (Cryophysics) fitted with a 10 mCi calcium stannate-119m source (Amersham Int.) and operated in sawtooth mode. The sample temperature was controlled using a continuous flow liquid nitrogen cryostat linked to a DTC-2 digital variable temperature controller (Oxford Instruments). Temperature stability was ±0.1K of the set temperature (78K). The source was at room temperature. Samples were prepared as finely ground powders. Calibration was based on the spectrum of natural iron, with ^{119}Sn isomer shifts relative to SnO_2 (zero velocity). Spectra were

fitted to Standard Lorentzian line shapes, with a correction for parabolic background curvature using a conventional least squares fit technique.

APPENDIX II

CRYSTALLOGRAPHIC DATA FOR (7)

A crystal of approximate dimensions 0.15 x 0.15 x 0.2 mm was used for data collection. Crystal data and structure refinement are given in Table A.1. Final fractional atomic co-ordinates and isotropic thermal parameters are given in Table A.2. Tables of anisotropic temperature factors are available as supplementary data.

In the final least squares cycles all atoms except for the γ and δ butyl carbons were allowed to vibrate anisotropically. Attempts to refine these carbons anisotropically only served to destabilise the structural refinement, most probably a consequence of thermal vibration and smearing of the electron density at the termini of these functionalities. Hydrogen atoms were included at calculated positions where relevant except in the instance of H1 and H2 attached to the bound water ligand. These protons were located in an advanced difference Fourier and refined at a restrained distance of 0.82 Å from the parent oxygen in the final least squares run.

The solution of the structure (SHELX86)[190] and refinement (SHELX93)[191] converged to a conventional [i.e. based on 4125 reflections with $F_o>4\sigma(F_o)$] $R1$=0.0487 and $wR2$=0.1207. Goodness of fit = 1.069. The max. and min. residual densities were 0.77 and -0.46Å^{-3} respectively.

Table A.1: Crystal Data And Structure Refinement For (7).

Identification code	95KCM4
Diffractometer	CAD4 automatic four-circle
Empirical formula	$C_{32}H_{60}N_8OSn_2$
Formula weight	810.26
Temperature	293(2) K
Wavelength	0.70930 Å
Crystal system	Monoclinic
Space group	$P2_1/n$
Unit cell dimensions	a = 14.249(3)Å α= 90°
	b = 15.406(4)Å β= 109.71(2)°
	c = 19.252(4)Å γ= 90°
Volume	3979(2) $Å^3$
Z	4
Density (calculated)	1.353 Mg/m^3
Absorption coefficient	1.288 mm^{-1}
F(000)	1664
Crystal size	0.15 x 0.15 x 0.2 mm
Theta range for data collection	2.01 to 23.92 °.
Index ranges	-16<=h<=0; -17<=k<=0; -20<=l<=22
Reflections collected	6504
Independent reflections	6227 [R(int) = 0.0320]
Refinement method	Full-matrix least-squares on F^2
Data / restraints / parameters	6216 / 17 / 343
Data corrections	Lorentz, polarisation
Goodness-of-fit on F^2	1.069
Final R indices [I>2σ(I)]	R1 = 0.0487 wR2 = 0.1207
R indices (all data)	R1 = 0.0958 wR2 = 0.1544
Largest diff. peak and hole	0.773 and -0.464 $e.Å^{-3}$
Weighting scheme	calc $w=1/[\sigma^2(Fo^2)+(0.0740P)^2+10.6499P]$
	where $P=(Fo^2+2Fc^2)/3$
Extinction coefficient	0.0005(2)
Extinction expression	$Fc^*=kFc[1+0.001xFc^2\lambda^3/\sin(2\theta)]^{-1/4}$

Table A.2: Atomic Co-ordinates (X 10^4) And Equivalent Isotropic Displacement Parameters ($Å^2$ X 10^3) For (7). U(Eq) Is Defined As One Third Of The Trace Of The Orthogonalized Uij Tensor.

Atom	x	y	z	U(eq)
Sn(1)	456(1)	875(1)	6634(1)	63(1)
Sn(2)	7858(1)	2920(1)	8291(1)	58(1)
O(1)	7686(4)	4101(4)	9026(3)	66(1)
N(1)	2727(4)	908(5)	6631(4)	66(2)
N(2)	1763(4)	884(5)	6192(4)	70(2)
N(3)	1675(4)	874(5)	5496(4)	73(2)
N(4)	2579(4)	897(5)	5447(3)	66(2)
N(5)	8026(4)	692(4)	6744(4)	62(2)
N(6)	8971(4)	966(5)	7106(4)	67(2)
N(7)	8985(4)	1560(5)	7591(4)	66(2)
N(8)	8038(4)	1699(4)	7569(3)	60(2)
C(1)	3204(5)	918(5)	6148(4)	59(2)
C(2)	4311(5)	966(5)	6378(4)	54(2)
C(3)	4784(5)	936(6)	5859(4)	70(2)
C(4)	5806(5)	999(6)	6073(4)	66(2)
C(5)	6374(5)	1070(5)	6818(4)	54(2)
C(6)	5888(5)	1076(6)	7329(4)	69(2)
C(7)	4870(5)	1025(6)	7113(5)	72(2)
C(8)	7475(5)	1155(5)	7047(4)	52(2)
C(9)	1368(6)	1230(8)	7719(5)	95(3)
C(10)	1638(20)	531(14)	8246(8)	267(14)
C(11)	1908(16)	801(20)	9060(10)	334(17)
C(12)	2976(18)	825(20)	9033(18)	337(17)
C(13)	58(8)	-451(7)	6366(7)	114(4)
C(14)	868(15)	-1030(8)	6309(12)	242(13)
C(15)	848(18)	-1922(7)	6665(16)	485(30)
C(16)	1512(29)	-1889(23)	7483(15)	448(25)
C(17)	-306(10)	1893(9)	5898(7)	146(6)
C(18)	-139(17)	2788(10)	6278(9)	253(14)
C(19)	-655(23)	3639(15)	5935(19)	455(27)
C(20)	113(26)	4207(20)	6509(17)	343(18)
C(21)	9254(6)	3448(6)	8318(6)	81(3)
C(22)	10136(6)	3171(8)	8968(6)	106(4)
C(23)	11101(7)	3556(8)	8905(7)	120(4)
C(24)	12007(10)	3372(12)	9600(8)	178(7)
C(25)	6600(6)	3384(7)	7412(5)	82(3)
C(26)	6834(12)	3706(12)	6753(8)	170(7)
C(27)	6210(16)	4381(13)	6198(13)	281(13)
C(28)	5468(22)	3647(18)	5846(17)	328(16)
C(29)	7770(9)	2091(8)	9146(6)	101(3)
C(30)	6783(17)	2130(12)	9252(10)	205(10)
C(31)	6635(21)	1460(17)	9799(14)	333(17)
C(32)	7562(25)	1648(23)	10477(17)	399(21)

APPENDIX III

CRYSTALLOGRAPHIC DATA FOR (2)

A crystal of approximate dimensions 0.25 x 0.25 x 0.3 mm was used for data collection. Table A.3 gives crystal and structure refinement data. Final fractional atomic co-ordinates and isotropic thermal parameters, bond distances and angles are given in Table A.4. Tables of anisotropic temperature factors are available as supplementary data.

In the final least squares cycles all Sn, O and N atoms along with carbons 1-11 were allowed to vibrate anisotropically. Ethyl carbons were refined isotropically. Hydrogen atoms were included at calculated positions where relevant on non-disordered ethyl groups. The protons on the water molecules could not be located with any reliability and were not modelled.

Disorder of the ethyl groups as a consequence of the inherent symmetry associated with the equatorial ligands at both Sn1 and Sn3 precluded a clean refinement in these areas, and only two β-carbons could be reliably located and refined between these 2 centres. Given α-carbons were refined with half site-occupancies.

Table A.3: Crystal Data And Structure Refinement For (**2**).

Identification code	95KCM8
Diffractometer	CAD4 Automatic four-circle
Empirical formula	$C_{34}H_{66}N_{16}O_2Sn_4$
Formula weight	1205.79
Temperature	293(2)° K
Wavelength	0.70930 Å
Crystal system	Monoclinic
Space group	C2/c
Unit cell dimensions	a = 30.070(3)Å b = 14.241(2)Å beta = 105.28(1)° c = 25.259(2)Å
Volume	10434(2) $Å^3$
Z	8
Density (calculated)	1.535 Mg/m^3
Absorption coefficient	1.936 mm^{-1}
F(000)	4784
Crystal size	0.25 x 0.25 x 0.3 mm
Theta range for data collection	2.17 to 23.92°
Index ranges	-33<=h<=34; 0<=k<=16; -28<=l<=0
Reflections collected	8368
Independent reflections	8152 [R(int) = 0.0431]
Refinement method	Full-matrix least-squares on F^2
Data / restraints / parameters	8116 / 2 / 407
Data corrections	Lorentz, polarisation, linear decay of crystal during data collection
Goodness-of-fit on F2	1.043
Final R indices [I>2σ(I)]	R1 = 0.0628 wR2 = 0.1451
R indices (all data)	R1 = 0.1642 wR2 = 0.2295
Largest diff. peak and hole	0.944 and -1.086 $eÅ^{-3}$
Weighting scheme	calc $w=1/[\sigma^2(Fo^2)+(0.0801P)^2+247.5413P]$ where $P=(Fo^2+2Fc^2)/3$
Extinction coefficient	0.00009(2)

Table A.4: Atomic Co-ordinates (X 10^4) And Equivalent Isotropic Displacement Parameters (A^2 X 10^3) For (**2**). U(Eq) Is Defined As One Third Of The Trace Of The Orthogonalized Uij Tensor.

Atom	x	y	z	U(eq)
Sn(1)	2500	2500	10000	74(1)
Sn(2)	3316(1)	6151(1)	8694(1)	59(1)
Sn(3)	0	5000	5000	77(1)
Sn(4)	1229(1)	5138(1)	7543(1)	60(1)
Sn(5)	5430(1)	5044(1)	8777(1)	72(1)
N(1)	2745(5)	4082(8)	10053(6)	72(4)
N(2)	3145(5)	4326(9)	10358(6)	89(5)
N(3)	3164(4)	5264(7)	10385(5)	64(4)
N(4)	2483(4)	4839(8)	9880(5)	68(4)
N(5)	1801(3)	6238(8)	8736(5)	50(3)
N(6)	1838(4)	5726(8)	8297(4)	53(3)
N(7)	2272(4)	5569(9)	8317(5)	63(3)
N(8)	2530(3)	5992(8)	8774(4)	50(3)
N(9)	4062(4)	6320(10)	8554(6)	68(4)
N(10)	4401(5)	5722(11)	8692(6)	78(4)
N(11)	4749(4)	6017(9)	8480(5)	63(3)
N(12)	4171(4)	7016(9)	8259(5)	55(3)
N(13)	299(5)	4500(10)	5933(5)	77(4)
N(14)	618(5)	4953(10)	6297(5)	84(5)
N(15)	630(5)	4568(9)	6789(4)	70(4)
N(16)	99(4)	3834(9)	6161(4)	64(3)
O(1)	6032(4)	4037(9)	9057(7)	125(6)
O(2)	6070(6)	2128(12)	9062(8)	150(7)
C(1)	2619(4)	6555(7)	10033(5)	37(3)
C(2)	2755(4)	7126(8)	10491(5)	36(3)
C(3)	2367(4)	6938(8)	9531(5)	34(3)
C(4)	2755(4)	5559(9)	10092(5)	44(3)
C(5)	2238(4)	6377(8)	9019(4)	35(3)
C(6)	4589(4)	6832(10)	8222(5)	46(3)
C(7)	5000	6862(14)	7500	46(5)
C(8)	4824(4)	7362(9)	7873(5)	38(3)
C(9)	4834(4)	8346(9)	7883(5)	45(3)
C(10)	5000	8840(14)	7500	55(5)
C(11)	313(5)	3890(10)	6691(5)	50(3)
C(101)	2888(16)	2215(33)	10812(20)	117(15)
C(102)	2652(22)	2652(44)	11235(27)	165(22)
C(103)	2727(22)	2250(44)	9283(26)	165(22)
C(105)	1748(20)	2956(44)	9796(26)	160(21)

Table A.4: Atomic Co-ordinates (X 10^4) And Equivalent Isotropic Displacement Parameters (A^2 X 10^3) For (**2**). U(Eq) Is Defined As One Third Of The Trace Of The Orthogonalized Uij Tensor (contd.).

C(106)	1638(29)	2857(59)	10388(35)	228(33)
C(201)	3546(8)	7045(15)	9400(9)	109(7)
C(202)	3482(13)	8009(28)	9254(15)	230(17)
C(203)	3421(8)	4674(16)	8846(10)	120(8)
C(204)	3318(14)	4220(33)	8323(18)	267(21)
C(205)	3052(8)	6719(16)	7887(9)	113(7)
C(206)	2727(12)	7575(25)	7893(15)	221(16)
C(301)	115(20)	6520(45)	5250(24)	163(21)
C(303)	-768(23)	4404(52)	4967(28)	183(25)
C(305)	710(26)	4672(57)	4785(32)	203(29)
C(401)	805(10)	6263(21)	7609(13)	169(11)
C(402)	1051(18)	7189(38)	7496(21)	331(28)
C(403)	1290(10)	3836(19)	7974(11)	144(9)
C(404)	1115(12)	3998(27)	8454(15)	222(16)
C(405)	1743(12)	4959(23)	7046(14)	196(14)
C(406)	1742(14)	5930(28)	6834(16)	290(23)
C(501)	5433(11)	5261(22)	9599(12)	162(11)
C(502)	5548(15)	6194(31)	9776(18)	262(20)
C(503)	5883(7)	5956(15)	8494(9)	106(6)
C(504)	6041(12)	5446(26)	8038(14)	215(15)
C(505)	5042(10)	3968(21)	8265(12)	169(11)
C(506)	4883(15)	3393(31)	8657(17)	263(20)

APPENDIX IV

CRYSTALLOGRAPHIC DATA FOR (9)

A crystal of approximate dimensions 0.2 x 0.2 x 0.25 mm was used for data collection. Crystal and structure refinement data are summarised in Table A.5. Final fractional atomic co-ordinates and isotropic thermal parameters, bond distances and angles are given in Table A.6. Tables of anisotropic temperature factors are available as supplementary data.

In the final least squares cycles all atoms were allowed to vibrate anisotropically. Hydrogen atoms were included at calculated positions where relevant.

Table A.5: Crystal Data And Structure Refinement For (**9**).

Identification code	95KCM9
Diffractometer	CAD4 Automatic four-circle
Empirical formula	$C_{12}H_{19}N_5Sn$
Formula weight	352.01
Temperature	293(2)°K
Wavelength	0.70930 Å
Crystal system	Hexagonal
Space group	$P6_1$
Unit cell dimensions	a = 8.263(1)Å b = 8.263(1)Å c = 38.991(6)Å
Volume	2305.5(5) $Å^3$
Z	6
Density (calculated)	1.521 Mg/m^3
Absorption coefficient	1.655 mm^{-1}
F(000)	1056
Crystal size	0.2 x 0.2 x 0.25 mm
Theta range for data collection	2.84 to 23.92 °
Index ranges	-8<=h<=9; -9<=k<=0; 0<=l<=44
Reflections collected	3933
Independent reflections	1226 [R(int) = 0.0287]
Refinement method	Full-matrix least-squares on F^2
Data / restraints / parameters	1226 / 1 / 169
Data corrections	Lorentz, polarisation
Goodness-of-fit on F^2	1.132
Final R indices [$I>2\sigma(I)$]	R1 = 0.0188 wR2 = 0.0426
R indices (all data)	R1 = 0.0284 wR2 = 0.0467
Absolute structure parameter	-0.02(4)
Largest diff. peak and hole	0.276 and -0.253 e.A-3
Weighting scheme	calc $w=1/[\sigma 2(Fo^2)+(0.0273P)^2+0.2266P]$ where $P=(Fo^2+2Fc^2)/3$
Extinction coefficient	0.0012(3)
Extinction expression	$Fc^*=kFc[1+0.001xFc^2\lambda^3/\sin(2\theta)]^{-1/4}$

Table A.6: Atomic co-ordinates (x 10^4) and equivalent isotropic displacement parameters ($Å^2$ x 10^3) for (**9**). U(Eq) is defined as one third of the trace of the orthogonalized Uij tensor.

Atom	x	y	z	U(eq)
Sn(1)	5721(1)	4012(1)	1224(1)	45(1)
N(1)	3502(7)	1497(7)	897(1)	51(1)
N(2)	3903(7)	391(8)	721(2)	64(1)
N(3)	2601(7)	-465(8)	484(2)	66(2)
N(4)	1927(7)	1388(7)	784(1)	52(1)
N(5)	-3373(7)	-1324(7)	-94(1)	54(1)
C(1)	3706(9)	4853(9)	1330(2)	68(2)
C(2)	4042(19)	6562(18)	1153(5)	174(7)
C(3)	6201(10)	2171(10)	1535(2)	68(2)
C(4)	8133(17)	2628(20)	1573(5)	186(8)
C(5)	7339(13)	5205(11)	773(2)	87(2)
C(6)	8307(29)	4579(18)	620(6)	325(22)
C(7)	1422(8)	167(8)	526(2)	46(1)
C(8)	-250(7)	-382(7)	318(1)	45(2)
C(9)	-444(8)	-1179(9)	-5(2)	57(2)
C(10)	-1973(8)	-1588(10)	-199(2)	63(2)
C(11)	-3209(9)	-617(9)	216(2)	58(2)
C(12)	-1680(9)	-115(8)	427(2)	54(1)

APPENDIX V

CRYSTALLOGRAPHIC DATA FOR (11)

A crystal of approximate dimensions 0.2 x 0.2 x 0.2 mm was used for data collection. Table A.7 summarises crystal and structure refinement data. Final fractional atomic co-ordinates and isotropic thermal parameters, bond distances and angles are given in Table A.8. Tables of anisotropic temperature factors are available as supplementary data.

In the final least squares cycles all atoms were allowed to vibrate anisotropically. Hydrogen atoms were included at calculated positions where relevant except for H1A and H1B in the ligated water molecule. These protons were located and refined at a fixed distance of 0.98Å from the parent atom, O1.

Table A.7: Crystal Data And Structure Refinement For (**11**).

Identification code	96KCM1
Diffractometer	CAD4 Automatic four-circle
Empirical formula	$C_{12}H_{21}N_5OSn$
Formula weight	370.03
Temperature	293(2)°K
Wavelength	0.70930 Å
Crystal system	Orthorhombic
Space group	Pbna (No. 60)
Unit cell dimensions	a = 13.781(2)Å b = 14.764(2)Å c = 16.227(3)Å
Volume	3301.6(9) $Å^3$
Z	8
Density (calculated)	1.489 Mg/m^3
Absorption coefficient	1.549 mm^{-1}
F(000)	1488
Crystal size	0.2 x 0.2 x 0.2 mm
Theta range for data collection	2.37 to 23.91°
Index ranges	-15<=h<=0; 0<=k<=16; 0<=l<=18
Reflections collected	2589
Independent reflections	2589 [R(int) = 0.0000]
Refinement method	Full-matrix least-squares on F^2
Data / restraints / parameters	2582 / 2 / 184
Data corrections	Lorentz, polarisation
Goodness-of-fit on F^2	1.135
Final R indices [$I>2\sigma(I)$]	R1 = 0.0450 wR2 = 0.1097
R indices (all data)	R1 = 0.0797 wR2 = 0.1351
Largest diff. peak and hole	0.639 and -0.754 $eÅ^{-3}$
Weighting scheme	calc $w=1/[\sigma^2(Fo^2)+(0.0652P)^2+4.1402P]$ where $P=(Fo^2+2Fc^2)/3$
Extinction coefficient	0.0035(3)
Extinction expression	$Fc^*=kFc[1+0.001xFc^2\lambda^3/\sin(2\theta)]^{-1/4}$

Table A.8: Atomic Co-ordinates (X 10^4) And Equivalent Isotropic Displacement Parameters ($Å^2$ X 10Å) For (**11**). U(Eq) Is Defined As One Third Of The Trace Of The Orthogonalized Uij Tensor.

Atom	x	y	z	U(eq)
Sn(1)	339(1)	2157(1)	2173(1)	69(1)
O(1)	1599(4)	1176(3)	2549(3)	75(1)
N(1)	-870(5)	3196(4)	1828(3)	77(2)
N(2)	-1393(4)	3216(4)	1136(3)	74(2)
N(3)	-1612(4)	4458(3)	1867(3)	68(1)
N(4)	-996(5)	3920(4)	2275(3)	74(2)
N(5)	-3170(4)	4248(4)	-807(3)	72(1)
C(1)	-1846(4)	4011(4)	1180(4)	57(1)
C(2)	-2498(4)	4365(4)	547(3)	58(2)
C(3)	-3034(5)	5150(5)	677(4)	81(2)
C(4)	-3627(6)	5467(5)	62(5)	93(2)
C(5)	-3660(5)	5003(6)	-659(5)	85(2)
C(6)	-2604(5)	3940(4)	-204(3)	61(2)
C(7)	-27(10)	2365(10)	3504(8)	151(4)
C(8)	620(11)	2976(9)	3778(14)	222(10)
C(9)	-532(14)	987(11)	1711(13)	237(11)
C(10)	-229(16)	817(16)	911(19)	333(18)
C(11)	1299(14)	2853(17)	1475(18)	366(22)
C(12)	1880(21)	3018(26)	1204(18)	468(28)

APPENDIX VI

CRYSTALLOGRAPHIC DATA FOR (8)

A crystal of approximate dimensions 0.2 x 0.2 x 0.3 mm was used for data collection. The summary of crystal and structure refinement data is given in Table A.9. Final fractional atomic co-ordinates and isotropic thermal parameters, bond distances and angles are given in Table A.10. Tables of anisotropic temperature factors are available as supplementary data.

In the final least squares cycles all atoms were allowed to vibrate anisotropically. Hydrogen atoms were included at calculated positions where relevant on carbon atoms. The water molecule hydrogen could not be located and hence were not included in the refinement.

Table A.9: Crystal Data And Structure Refinement For (**8**).

Identification code	97KCM9
Diffractometer	CAD4 Automatic four-circle
Empirical formula	$C_{18}H_{35}N_5O_2Sn$
Formula weight	472.20
Temperature	293(2)°K
Wavelength	0.70930 Å
Crystal system	Monoclinic
Space group	$P2_1/c$
Unit cell dimensions	a = 10.120(2)Å b = 14.269(2)Å b = 101.31(2)° c = 16.788(3)Å
Volume	2377.1(7) $Å^3$
Z	4
Density (calculated)	1.319 Mg/m^3
Absorption coefficient	1.094 mm^{-1}
F(000)	976
Crystal size	0.2 x 0.2 x 0.3 mm
Theta range for data collection	2.05 to 23.93 °.
Index ranges	0<=h<=11; 0<=k<=16; -19<=l<=18
Reflections collected	3953
Independent reflections	3722 [R(int) = 0.0290]
Refinement method	Full-matrix least-squares on F^2
Data / restraints / parameters	3712 / 3 / 239
Data corrections	Lorentz, polarisation, 28% linear decay in the x-ray beam
Goodness-of-fit on F^2	1.134
Final R indices [I>2σ(I)]	R1 = 0.0492 wR2 = 0.1080
R indices (all data)	R1 = 0.1165 wR2 = 0.1420
Largest diff. peak and hole	0.480 and -0.306 $eÅ^{-3}$
Weighting scheme	calc $w=1/[s^2(Fo^2)+(0.0559P)^2+2.1686P]$ where $P=(Fo^2+2Fc^2)/3$
Extinction coefficient	0.0033(5)
Extinction expression	$Fc^*=kFc[1+0.001xFc^2l^3/\sin(2q)]^{-1/4}$

Table A.10: Atomic co-ordinates (x 10^4) and equivalent isotropic displacement parameters ($Å^2$ x 10^3) for (**8**). U(Eq) is defined as one third of the trace of the orthogonalized Uij tensor.

Atom	x	y	z	U(eq)
Sn(1)	5656(1)	1847(1)	8088(1)	92(1)
N(1)	6717(6)	2933(4)	9068(4)	97(2)
N(2)	8040(6)	2955(4)	9355(4)	92(2)
N(3)	6096(6)	3535(5)	9464(4)	98(2)
N(4)	7012(6)	3964(4)	10021(3)	88(2)
N(5)	12011(7)	4319(5)	11370(4)	96(2)
C(1)	8184(7)	3598(5)	9941(4)	76(2)
C(2)	9495(6)	3857(5)	10436(4)	75(2)
C(3)	10661(8)	3494(6)	10263(5)	105(3)
C(4)	9626(7)	4460(5)	11065(5)	92(2)
C(5)	11889(8)	3752(7)	10743(6)	112(3)
C(6)	10888(8)	4675(6)	11522(5)	102(2)
C(7)	7453(10)	1078(9)	8178(9)	196(7)
C(8)	7513(16)	203(12)	8629(11)	266(10)
C(9)	8649(23)	-323(17)	8728(15)	333(13)
C(10)	8588(24)	-1063(15)	9269(15)	351(15)
C(11)	5173(18)	2924(10)	7223(9)	203(6)
C(12)	5963(35)	2958(18)	6496(16)	380(20)
C(13)	6979(26)	3525(25)	6840(16)	427(29)
C(14)	7452(32)	3743(19)	6044(12)	360(17)
C(15)	4194(13)	1575(10)	8782(8)	196(6)
C(16)	2787(24)	1857(22)	8601(15)	335(18)
C(17)	2314(38)	2419(20)	8199(16)	382(25)
C(18)	804(15)	2671(17)	8024(11)	248(9)
O(1)	4675(4)	705(4)	7158(3)	106(2)
O(2)	6069(5)	-140(4)	6148(3)	101(2)

APPENDIX VII

CRYSTALLOGRAPHIC DATA FOR (29)

A crystal of approximate dimensions 0.5 x 0.4 x 0.4 mm was used for data collection. Table A.11 gives crystal and structure refinement data. Final fractional atomic co-ordinates and isotropic thermal parameters, bond distances and angles are given in Table A.12. Tables of anisotropic temperature factors are available as supplementary data.

In the final least squares cycles all atoms were allowed to vibrate anisotropically. Hydrogen atoms were included at calculated positions where relevant except in the case of the methanolic proton, H1A, (attached to O1) which was positionally located (although the esds on the fractional co-ordinates are large) and refined at a distance of 0.98(2) Å from the parent atom.

Table A.11. Crystal data and structure refinement for (**29**).

Identification code	96KCM2
Diffractometer	CAD4 Automatic four-circle
Empirical formula	$C_{20}H_{19}N_4OTl$
Formula weight	535.76
Temperature	293(2)°K
Wavelength	0.70930 Å
Crystal system	Triclinic
Space group	P-1(No.2)
Unit cell dimensions	a = 8.413(3)Å α= 81.02(3)°
	b = 9.509(3)Å β= 78.17(3)°
	c = 12.148(5)Å γ= 85.76(3)°
Volume	938.6(6) $Å^3$
Z	2
Density (calculated)	1.896 Mg/m^3
Absorption coefficient	8.619 mm^{-1}
F(000)	512
Crystal size	0.5 x 0.4 x 0.4 mm
Theta range for data collection	2.17 to 22.00 °.
Index ranges	-10<=h<=10; -11<=k<=11; 0<=l<=14
Reflections collected	2298
Independent reflections	2298 [R(int) = 0.0000]
Refinement method	Full-matrix least-squares on F^2
Data / restraints / parameters	2277 / 1 / 241
Data corrections	Lorentz, polarisation, absorption (Max. and Min. absorption corrections; 1.000, 0.379)
Goodness-of-fit on F^2	0.919
Final R indices [I>2σ(I)]	R1 = 0.0342 wR2 = 0.0978
R indices (all data)	R1 = 0.0433 wR2 = 0.1311
Largest diff. peak and hole	1.739 and -2.354 $eÅ^{-3}$
Weighting scheme	calc $w=1/[\sigma^2(Fo^2)+(0.0836P)^2+15.5963P]$ where $P=(Fo^2+2Fc^2)/3$
Extinction coefficient	0.0007(7)
Extinction expression	$Fc^*=kFc[1+0.001xFc^2\lambda^3/\sin(2\theta)]^{-1/4}$

Table A.12: Atomic Co-ordinates (X 10^4) And Equivalent Isotropic Displacement Parameters ($Å^2$ X 10^3) For (**29**). U(Eq) Is Defined As One Third Of The Trace Of The Orthogonalized Uij Tensor.

Atom	x	y	z	U(eq)
Tl(1)	2395(1)	429(1)	1192(1)	18(1)
N(1)	5132(11)	839(9)	1579(7)	21(2)
N(2)	6367(12)	642(9)	733(8)	30(2)
N(3)	7775(11)	849(10)	995(7)	26(2)
N(4)	7396(10)	1221(9)	2057(7)	23(2)
C(1)	5810(14)	1205(11)	2381(9)	22(3)
C(2)	4927(12)	1511(11)	3507(8)	17(2)
C(3)	3589(12)	756(12)	4071(8)	20(2)
C(4)	2851(14)	1006(13)	5141(10)	30(3)
C(5)	3364(14)	2045(13)	5666(10)	29(3)
C(6)	4690(15)	2821(13)	5084(10)	33(3)
C(7)	5484(15)	2565(12)	3991(10)	30(3)
C(8)	2170(13)	2486(12)	240(9)	23(3)
C(9)	2900(13)	3616(12)	509(10)	26(3)
C(10)	2739(14)	4967(12)	-131(10)	27(3)
C(11)	1938(14)	5157(12)	-1005(11)	31(3)
C(12)	1217(14)	4001(13)	-1264(10)	34(3)
C(13)	1359(14)	2681(12)	-647(9)	26(3)
C(14)	2364(13)	-1659(11)	2121(9)	20(2)
C(15)	3683(14)	-2579(12)	1913(9)	27(3)
C(16)	3697(14)	-3930(12)	2538(11)	30(3)
C(17)	2394(14)	-4350(13)	3401(10)	30(3)
C(18)	1094(13)	-3419(12)	3593(10)	27(3)
C(19)	1061(13)	-2092(12)	2966(10)	26(3)
O(1)	161(8)	1300(8)	2903(6)	25(2)
C(20)	238(15)	2637(14)	3276(12)	42(3)

APPENDIX VIII

CRYSTALLOGRAPHIC DATA FOR (35)

A crystal of approximate dimensions 0.18 x 0.10 x 0.10 mm was used for data collection. Crystal data and structure refinement are given in Table A.13. Final fractional atomic co-ordinates and isotropic thermal parameters, bond distances and angles are given in Tables A.14. Tables of anisotropic temperature factors are available as supplementary data.

In the final least squares cycles all atoms were allowed to vibrate anisotropically. Hydrogen atoms were included at calculated positions where relevant.

Table A.13: Crystal Data And Structure Refinement For (**35**).

Identification code	97kcm8
Diffractometer	EPSRC FAST system at Cardiff
Empirical formula	$C_{16}H_{18}N_4OTl$
Formula weight	486.71
Temperature	396(2)°K
Wavelength	0.71069 Å
Crystal system	Triclinic
Space group	P-1(No.2)
Unit cell dimensions	a = 7.596(2)Å a = 108.88(2)°
	b = 9.862(2)Å b = 97.69(3)°
	c = 11.388(1)Å g = 92.10(1)°
Volume	797.0(3) $Å^3$
Z	2
Density (calculated)	2.028 Mg/m^3
Absorption coefficient	10.139 mm^{-1}
F(000)	462
Crystal size	0.18 x 0.10 x 0.10 mm
Theta range for data collection	1.91 to 24.83 °.
Index ranges	-8<=h<=8; -11<=k<=10; 0<=l<=12
Reflections collected	2234
Independent reflections	2234 [R(int) = 0.0000]
Absorption correction	DIFABS
Max. and min. transmission	1.000 and 0.651
Refinement method	Full-matrix least-squares on F^2
Data / restraints / parameters	2234 / 1 / 202
Data corrections	Lorentz, polarisation, absorption (Max. and Min. absorption corrections; 1.000, 0.651 respectively)
Goodness-of-fit on F^2	1.138
Final R indices [I>2s(I)]	R1 = 0.0387 wR2 = 0.1042
R indices (all data)	R1 = 0.0414 wR2 = 0.1046
Largest diff. peak and hole	1.359 and -1.463 $eÅ^{-3}$
Weighting scheme	calc $w=1/[s^2(Fo^2)+(0.0576P)^2+0.0000P]$ where $P=(Fo^2+2Fc^2)/3$
Extinction coefficient	0.0002(8)
Extinction expression	$Fc^*=kFc[1+0.001xFc^2l^3/\sin(2q)]^{-1/4}$

Table A.14: Atomic Co-ordinates (X 10^4) And Equivalent Isotropic Displacement Parameters ($Å^2$ X 10^3) For (**35**). U(Eq) Is Defined As One Third Of The Trace Of The Orthogonalized Uij Tensor.

Atom	x	y	z	U(eq)
Tl(1)	2445(1)	796(1)	4073(1)	12(1)
O(1)	1256(11)	3009(9)	2959(7)	27(2)
N(1)	5676(11)	925(9)	3749(7)	14(2)
N(2)	8189(13)	1560(10)	3279(8)	18(2)
N(3)	7042(12)	920(10)	4656(8)	16(2)
N(4)	8540(12)	1310(10)	4379(8)	17(2)
C(1)	1672(13)	-893(11)	2343(9)	13(2)
C(2)	2478(15)	-2170(11)	2188(10)	18(2)
C(3)	2109(16)	-3302(12)	1055(11)	23(3)
C(4)	901(15)	-3173(13)	83(10)	20(3)
C(5)	91(15)	-1883(12)	254(10)	19(2)
C(6)	481(14)	-769(12)	1363(9)	18(2)
C(7)	3032(13)	2538(11)	5773(9)	13(2)
C(8)	2330(15)	2470(12)	6844(10)	20(3)
C(9)	2774(17)	3615(13)	7964(11)	27(3)
C(10)	3856(16)	4755(12)	8056(11)	23(3)
C(11)	4544(16)	4845(13)	6992(11)	23(3)
C(12)	4118(16)	3741(12)	5871(10)	20(3)
C(13)	6468(13)	1324(10)	2917(9)	10(2)
C(14)	5532(16)	1376(12)	1697(10)	21(3)
C(15)	5427(15)	-31(11)	638(9)	14(2)
C(16)	993(18)	4516(15)	3476(13)	39(3)

APPENDIX IX

CRYSTALLOGRAPHIC DATA FOR (30)

A crystal of approximate dimensions 0.32 x 0.32 x 0.2 mm was used for data collection. Table A.15 given crystal data and structure refinement. Final fractional atomic co-ordinates and isotropic thermal parameters, bond distances and angles are given in Table A.16. Tables of anisotropic temperature factors are available as supplementary data.

In the final least squares cycles all atoms were allowed to vibrate anisotropically except for O1, where anisotropic refinement resulted in unsatisfactory thermal parameters. Hydrogen atoms were included at calculated positions where relevant, except for the methanolic hydrogen (attached to O1) and the two water hydrogens (attached to O2) which could not be located, even by examining a difference electron density map based on low Bragg angle data. This is not altogether surprising given the size of the crystal and the large absorption coefficient of it's content.

Table A.15: Crystal Data And Structure Refinement For (**30**).

Identification code	97kcm3
Diffractometer	CAD4 Automatic four-circle
Empirical formula	$C_{46}H_{46}ClN_8O_4Tl_3$
Formula weight	1423.47
Temperature	293(2)°K
Wavelength	0.70930 Å
Crystal system	Monoclinic
Space group	$P2_1/m$
Unit cell dimensions	a = 11.041(2)Å b = 17.520(5)Å b = 105.21(2)° c = 12.406(2)Å
Volume	2315.7(9) $Å^3$
Z	2
Density (calculated)	2.041 Mg/m^3
Absorption coefficient	10.521 mm^{-1}
F(000)	1340
Crystal size	0.32 x 0.32 x 0.2 mm
Theta range for data collection	2.06 to 23.93°.
Index ranges	-12<=h<=12; 0<=k<=20; 0<=l<=14
Reflections collected	3751
Independent reflections	3751 [R(int) = 0.0000]
Absorption correction	DIFABS
Max. and min. transmission	1.000 and 0.182
Refinement method	Full-matrix least-squares on F^2
Data / restraints / parameters	3746 / 0 / 292
Data corrections	Lorentz, polarisation, crystal decay (32%) in the X-ray beam and absorption (Max. and Min. absorption corrections; 1.000, 0.182 respectively)
Goodness-of-fit on F^2	1.111
Final R indices [I>2s(I)]	R1 = 0.0563 wR2 = 0.1320
R indices (all data)	R1 = 0.1001 wR2 = 0.1590
Largest diff. peak and hole	2.455 and -2.383 $eÅ^{-3}$
Weighting scheme	calc $w=1/[s^2(Fo^2)+(0.1000P)^2+0.0000P]$ where $P=(Fo^2+2Fc^2)/3$
Extinction coefficient	0.0004(3)
Extinction expression	$Fc^*=kFc[1+0.001xFc^2l^3/\sin(2q)]^{-1/4}$

Table A.16: Atomic Co-ordinates (X 10^4) And Equivalent Isotropic Displacement Parameters ($Å^2$ X 10^3) For (**30**). U(Eq) Is Defined As One Third Of The Trace Of The Orthogonalized Uij Tensor.

Atom	x	y	z	U(eq)
Tl(1)	1751(1)	917(1)	397(1)	32(1)
Tl(2)	-4233(1)	2500	449(1)	33(1)
Cl(1)	1868(6)	2500	437(6)	54(2)
O(1)	-4828(9)	428(7)	-1470(9)	32(3)
O(2)	-5609(11)	1048(7)	333(11)	46(3)
N(1)	-553(11)	1064(8)	514(10)	35(3)
N(2)	-1452(10)	710(8)	-317(12)	41(3)
N(3)	-2522(12)	1043(7)	-380(13)	43(3)
N(4)	-2366(11)	1612(7)	373(12)	36(3)
C(1)	-1166(11)	1637(8)	911(13)	27(3)
C(2)	2515(14)	792(9)	2147(14)	38(4)
C(3)	3378(14)	1312(12)	2763(16)	54(5)
C(4)	3838(18)	1239(15)	3870(18)	66(6)
C(5)	3432(23)	649(16)	4429(16)	75(7)
C(6)	2569(19)	129(13)	3849(19)	65(5)
C(7)	2114(14)	207(11)	2713(13)	43(4)
C(8)	1260(12)	860(9)	-1364(15)	38(4)
C(9)	1706(16)	290(12)	-1914(15)	52(5)
C(10)	1371(21)	226(13)	-3062(20)	66(6)
C(11)	586(23)	777(14)	-3686(19)	71(7)
C(12)	110(24)	1361(14)	-3162(18)	79(7)
C(13)	412(18)	1396(13)	-2010(17)	62(5)
C(14)	-5042(21)	2500	-1270(17)	30(5)
C(15)	-4285(22)	2500	-2072(18)	44(6)
C(16)	-4822(21)	2500	-3189(24)	61(8)
C(17)	-6081(28)	2500	-3612(22)	64(8)
C(18)	-6860(25)	2500	-2903(22)	54(7)
C(19)	-6327(19)	2500	-1740(22)	39(5)
C(20)	-3697(18)	2500	2202(19)	36(5)
C(21)	-3435(21)	1818(10)	2800(18)	62(5)
C(22)	-2982(22)	1841(18)	3946(21)	88(8)
C(23)	-2728(26)	2500	4552(31)	91(14)
C(24)	-564(12)	2106(8)	1884(12)	27(3)
C(25)	65(13)	1717(10)	2831(15)	42(4)
C(26)	694(14)	2097(10)	3808(15)	42(4)
C(27)	-5111(21)	542(12)	-2265(38)	137(17)

APPENDIX X

CRYSTALLOGRAPHIC DATA FOR (36)

A crystal of approximate dimensions 0.4 x 0.4 x 0.4 mm was used for data collection. Table A.17 gives crystal data and structure refinement. Final fractional atomic co-ordinates and isotropic thermal parameters, bond distances and angles are given in Table A.18. Tables of anisotropic temperature factors are available as supplementary data.

In the final least squares cycles all atoms were allowed to vibrate anisotropically. Hydrogen atoms were included at calculated positions where relevant. C-C bond lengths in the butyl group containing carbons C17-20 were constrained to an ideal distance of 1.54 Å, as early refinement cycles indicated some instability in this region of the electron density map. This action was reflected in an improvement of residuals.

Table A.17: Crystal Data And Structure Refinement For (**36**).

Identification code	96KCM8
Diffractometer	CAD4 Automatic four-circle
Empirical formula	$C_{32}H_{58}N_8S_2Sn_2$
Formula weight	856.36
Temperature	293(2)°K
Wavelength	0.70930 Å
Crystal system	Monoclinic
Space group	$P2_1/a$
Unit cell dimensions	a = 17.602(2)Å b = 12.639(2)Å beta = 93.79(1)° c = 18.733(6)Å
Volume	4158(2) $Å^3$
Z	4
Density (calculated)	1.368 Mg/m^3
Absorption coefficient	1.332 mm^{-1}
F(000)	1752
Crystal size	0.4 x 0.4 x 0.4 mm
Theta range for data collection	2.17 to 23.00°
Index ranges	-20<=h<=20; -14<=k<=0; 0<=l<=21
Reflections collected	6015
Independent reflections	5814 [R(int) = 0.0260]
Refinement method	Full-matrix least-squares on F^2
Data / restraints / parameters	5624 / 3 / 405
Data corrections	Lorentz, polarisation
Goodness-of-fit on F^2	1.003
Final R indices [$I>2\sigma(I)$]	R1 = 0.0496 wR2 = 0.1059
R indices (all data)	R1 = 0.1341 wR2 = 0.1524
Largest diff. peak and hole	0.537 and -0.368 $eÅ^{-3}$
Weighting scheme	calc $w=1/[\sigma^2(Fo^2)+(0.0548P)^2+11.1369P]$ where $P=(Fo^2+2Fc^2)/3$
Extinction coefficient	0.00049(10)
Extinction expression	$Fc^*=kFc[1+0.001xFc^2\lambda^3/\sin(2\theta)]^{-1/4}$

Table A.18: Atomic Co-ordinates (X 10^4) And Equivalent Isotropic Displacement Parameters ($Å^2$ X 10^3) For (**36**). U(Eq) Is Defined As One Third Of The Trace Of The Orthogonalized Uij Tensor.

Atom	x	y	z	U(eq)
Sn(1)	3007(1)	206(1)	128(1)	81(1)
Sn(2)	7527(1)	-138(1)	4533(1)	74(1)
S(1)	6767(2)	-1097(2)	3520(2)	122(1)
S(2)	4028(2)	-820(2)	893(2)	97(1)
N(1)	7007(5)	-2765(6)	4418(4)	89(3)
N(2)	6729(5)	-3741(6)	4486(4)	89(2)
N(3)	6207(5)	-3964(5)	3986(4)	84(2)
N(4)	6149(4)	-3083(5)	3565(3)	68(2)
N(5)	3082(5)	-2437(6)	460(5)	96(3)
N(6)	2993(5)	-3452(6)	645(5)	113(3)
N(7)	3477(5)	-3757(6)	1149(5)	100(3)
N(8)	3910(4)	-2889(5)	1302(4)	79(2)
C(1)	6642(6)	-2346(7)	3851(5)	79(3)
C(2)	5587(5)	-3034(6)	2981(4)	63(2)
C(3)	5737(5)	-2491(6)	2373(5)	69(2)
C(4)	5173(5)	-2430(6)	1809(5)	68(2)
C(5)	4495(5)	-2935(6)	1880(5)	69(2)
C(6)	4360(5)	-3500(8)	2481(5)	88(3)
C(7)	4905(6)	-3555(7)	3036(5)	85(3)
C(8)	3653(5)	-2082(7)	878(5)	81(3)
C(9)	2072(8)	-50(12)	758(7)	143(5)
C(10)	2075(13)	486(20)	1446(12)	228(10)
C(11)	1512(18)	253(19)	1901(14)	265(15)
C(12)	1437(16)	863(20)	2477(14)	274(12)
C(13)	3021(8)	-575(11)	-863(6)	122(4)
C(14)	3759(11)	-461(15)	-1220(10)	177(7)
C(15)	3862(12)	-922(18)	-1869(10)	191(8)
C(16)	4525(10)	-865(15)	-2203(10)	183(7)
C(17)	3518(9)	1665(10)	366(12)	267(15)
C(18)	4092(10)	2081(14)	245(13)	255(12)
C(19)	4420(11)	3180(12)	480(12)	199(9)
C(20)	4996(14)	3503(26)	217(16)	359(20)
C(21)	7499(7)	1263(8)	3902(6)	103(4)
C(22)	8132(11)	1175(16)	3323(11)	212(11)
C(23)	8212(15)	1932(27)	2910(16)	318(18)

APPENDIX XI

CRYSTALLOGRAPHIC DATA FOR (40)

A crystal of approximate dimensions 0.5 x 0.4 x 0.25 mm was used for data collection. The summary of crystal data and structure refinement is given in Table A.19. Final fractional atomic co-ordinates and isotropic thermal parameters, bond distances and angles are given in Table A.20. Tables of anisotropic temperature factors are available as supplementary data.

In the final least squares cycles all atoms were allowed to vibrate anisotropically. Hydrogen atoms were included at calculated positions where relevant, except for the methanolic proton (H1) which was located and refined at a distance of 0.98Å from O1.

The asymmetric unit in this structure was seen to consist of one half of a dimer molecule, the remainder being generated by inversion through the centre at ½, ½, ½ in this space group.

Table A.19: Crystal Data And Structure Refinement For (**40**).

Identification code	97kcm1
Diffractometer	CAD4 automatic four-circle
Empirical formula	$C_8H_{15}N_4OSSn$
Formula weight	333.99
Temperature	170(2)°K
Wavelength	0.70930 Å
Crystal system	Triclinic
Space group	P-1(No.2)
Unit cell dimensions	a = 6.755(2)Å α= 70.44(4)°
	b = 10.253(4)Å β= 83.67(4)°
	c = 10.452(4)Å γ= 70.84(3)°
Volume	644.3(4) $Å^3$
Z	2
Density (calculated)	1.721 Mg/m^3
Absorption coefficient	2.128 mm^{-1}
F(000)	330
Crystal size	0.5 x 0.4 x 0.25 mm
Theta range for data collection	2.06 to 23.93 °.
Index ranges	-7<=h<=7; -10<=k<=11; 0<=l<=11
Reflections collected	2023
Independent reflections	2023 [R(int) = 0.0000]
Absorption correction	DIFABS
Max. and min. transmission	1.000 and 0.654
Refinement method	Full-matrix least-squares on F^2
Data / restraints / parameters	2023 / 1 / 145
Data corrections	Lorentz, polarisation, absorption (Max. and min. absorption corrections; 1.000, 0.654 respectively)
Goodness-of-fit on F2	1.165
Final R indices [I>2σ(I)]	R1 = 0.0347 wR2 = 0.0978
R indices (all data)	R1 = 0.0512 wR2 = 0.1051
Largest diff. peak and hole	0.892 and -1.705 $eÅ^{-3}$
Weighting scheme	calc $w=1/[\sigma^2(Fo^2)+(0.0422P)^2+3.2195P]$ where $P=(Fo^2+2Fc^2)/3$
Extinction coefficient	0.0002(12)
Extinction expression	$Fc^*=kFc[1+0.001xFc^2\lambda^3/\sin(2\theta)]^{-1/4}$

Table A.20: Atomic Co-ordinates (X 10^4) And Equivalent Isotropic Displacement Parameters ($Å^2$ X 10^3) For (**36**). U(Eq) Is Defined As One Third Of The Trace Of The Orthogonalized Uij Tensor.

Atom	x	y	z	U(eq)
Sn(1)	922(1)	2145(1)	11181(1)	17(1)
S(1)	2733(3)	3436(2)	9022(2)	22(1)
N(1)	1397(10)	1664(6)	8090(6)	26(1)
N(2)	1472(10)	1401(6)	6885(6)	28(1)
N(3)	2404(11)	2188(7)	5954(6)	29(1)
N(4)	2945(9)	3017(6)	6558(5)	18(1)
O(1)	-633(7)	1014(5)	13341(5)	24(1)
C(1)	2805(12)	-57(7)	11466(8)	32(2)
C(2)	1836(12)	3211(8)	12342(7)	28(2)
C(3)	-2195(11)	2915(8)	10397(7)	28(2)
C(4)	2326(11)	2673(7)	7875(7)	22(1)
C(5)	3228(10)	4926(7)	4491(6)	21(1)
C(6)	4012(11)	4032(7)	5767(6)	19(1)
C(7)	5756(10)	4089(7)	6304(7)	21(1)
C(8)	-2322(13)	1808(9)	14002(8)	37(2)

REFERENCES

1. R.N.Butler, *'Comprehensive Heterocyclic Chemistry'*, 1984, **5**, 791.

2. R.L.Kieft, W.M.Peterson, G.L.Blundell, S.Horton, R.A.Henry, H.B.Jonassen, *Inorg.Chem.*, 1976, **15**, 1721.

3. S.J.Wittenberger, *Organic Preparations and Procedures Int.*, 1994, **26**, 499.

4. H.Singh, *Prog. in Med.Chem.*, 1980, **17**, 151.

5. R.N.Butler, *'Advanced Heterocyclic Chemistry'*, 1977, **21**, 323.

6. W.R.Carpenter, U.S.Patent 3 386 968, 1968; *Chem.Abs.*, 1968, 69, 28.106, 5707.

7. J.C.Weiss, W.Beck, *Chem.Ber.*, 1972, **105**, 3203.

8. E.P.Ahern, K.J.Dignam, A.F.Hegarty, *J.Org.Chem.*, 1980, **45**, 4302; A.F.Hegarty, K.Brady, M.Mullane, *J.Chem.Soc., Perkin Trans.2*, 1980, 535.

9. E.Lippman, A.Könnecker, *Z. Chem.*, 1976, **16**, 90.

10. F.R.Benson, *'Heterocyclic Compounds'*, ed.R.C.Elderfield; Wiley, New York, 1967, vol. 8, 1.

11. P.K.Kadaba, *Synthesis*, 1973, 71.

12. L.A.Lee, R.Evans, J.W.Wheeler, *J.Org.Chem.*, 1972, **37**, 1454.

13. D.H.Zimmerman, R.A.Olofson, *Tetrahedron Lett.*, 1969, 5081.

14. G.L ábbé, *Chem.Rev.*, 1969, **69**, 359.

15. N.Jagerovic, J.M.Barbe, M.Farnier, R.Guilard, *J.Chem.Soc., Dalton Trans.*, 1988, 2569.

16. R.Guilard, N.Jagerovic, A.Tabard, P.Richard, L.Courthaudon, A.Louati, C.Lecomte, K.M.Kadish, *Inorg.Chem.*, 1991, **30**, 16.

17. R.Guilard, N.Jagerovic, A.Tabard, C.Naillon, K.M.Kadish, *J.Chem.Soc., Dalton Trans.*, 1992, 1957.

18. M.Hill, M.F.Mahon, J.McGinley, K.C.Molloy, *J.Chem.Soc., Dalton Trans.*, 1996, 835.

19. A.Goodger, M.Hill, M.F.Mahon, J.McGinley, K.C.Molloy, *J.Chem.Soc., Dalton Trans.*, 1996, 847.

20. I.Fleming, *'Frontier Orbitals and Organic Chemical Reactions'*, Wiley-Interscience, London, 1976.

21. P.Sykes, *'Mechanism in Organic Chemistry'*, John Wiley & Sons, Inc., New York, 1987.

22. E.Obed, R.D.Willett, B.Scott, R.L.Kirchmeier, J.M.Shreeve, *Inorg.Chem.*, 1989, **28**, 893.

23. S.J.Wittenberger, B.G.Donner, *J.Org.Chem.*, 1993, **58**, 4139.

24. M.Hill, *'Organotin Tetrazoles and Related Compounds'*, Ph.D Thesis, University Of Bath, 1994.

25. K.Sisido, K.Nabika, T.Isida, S.Kozima, *J.Orgmet.Chem.*, 1971, **33**, 337.

26. R.J.Deeth, K.C.Molloy, M.F.Mahon, S.Whittaker, *J.Orgmet.Chem.*, 1992, **430**, 25.

27. R.Cea-Olivares, O.J.Sandoval, G.Espinosa-Perez, C.Silvestru, *Polyhedron*, 1994, **13**, 2809.

28. D.S.Moore, S.D.Robinson, *Advances in Inorganic Chemistry*, 1988, **32**, 171.

16. R.Guilard, N.Jagerovic, A.Tabard, P.Richard, L.Courthaudon, A.Louati, C.Lecomte, K.M.Kadish, *Inorg.Chem.*, 1991, **30**, 16.

17. R.Guilard, N.Jagerovic, A.Tabard, C.Naillon, K.M.Kadish, *J.Chem.Soc., Dalton Trans.*, 1992, 1957.

18. M.Hill, M.F.Mahon, J.McGinley, K.C.Molloy, *J.Chem.Soc., Dalton Trans.*, 1996, 835.

19. A.Goodger, M.Hill, M.F.Mahon, J.McGinley, K.C.Molloy, *J.Chem.Soc., Dalton Trans.*, 1996, 847.

20. I.Fleming, *'Frontier Orbitals and Organic Chemical Reactions'*, Wiley-Interscience, London, 1976.

21. P.Sykes, *'Mechanism in Organic Chemistry'*, John Wiley & Sons, Inc., New York, 1987.

22. E.Obed, R.D.Willett, B.Scott, R.L.Kirchmeier, J.M.Shreeve, *Inorg.Chem.*, 1989, **28**, 893.

23. S.J.Wittenberger, B.G.Donner, *J.Org.Chem.*, 1993, **58**, 4139.

24. M.Hill, *'Organotin Tetrazoles and Related Compounds'*, Ph.D Thesis, University Of Bath, 1994.

25. K.Sisido, K.Nabika, T.Isida, S.Kozima, *J.Orgmet.Chem.*, 1971, **33**, 337.

26. R.J.Deeth, K.C.Molloy, M.F.Mahon, S.Whittaker, *J.Orgamet.Chem.*, 1992, **430**, 25.

27. R.Cea-Olivares, O.J.Sandoval, G.Espinosa-Perez, C.Silvestru, *Polyhedron*, 1994, **13**, 2809.

28. D.S.Moore, S.D.Robinson, *Advances in Inorganic Chemistry*, 1988, **32**, 171.

29. F.M.D'itri, A.I.Popov, *Inorg.Chem.*, 1966, **5**, 1670; P.L.Franke, W.L.Groeneveld, *Transition Metal Chem.*, 1981, **6**, 54.

30. J.C.Weiss, W.Beck, *Chem.Ber.*, 1972, **105**, 3203.

31. J.Reedijk, A.R.Siedle, R.A.Velapoldi, J.A.M.Van Hest, *Inorg.Chim.Acta.*, 1983, **74**, 109.

32. J.M.Nelson, D.L.Schmitt, R.A.Henry, D.W.Moore, H.B.Jonassen, *Inorg.Chem.*, 1970, **9**, 2678.

33. G.Minghetti, G.Banditelli, F.Bonati, *J.Chem.Soc., Dalton Trans.*, 1979, 1851.

34. W.Beck, W.P.Fehlhammer, H.Bock, M.Bauder, *Chem.Ber.*, 1969, **102**, 3637.

35. J.Erbe, W.Beck, *Chem.Ber.*, 1983, **116**, 3867.

36. W.Beck, K.Burger, W.P.Fehlhammer, *Chem.Ber.*, 1971, **104**, 1816.

37. A.D.Harris, R.H.Herber, H.B.Jonassen, G.K.Wertheim, *J.Am.Chem.Soc.*, 1968, **90**, 6588.

38. T.Kemmerich, J.H.Nelson, N.E.Takach, H.Boehme, B.Jablonski, W.Beck, *Inorg.Chem.*, 1982, **21**, 1226.

39. G.B.Ansell, *J.Chem.Soc., Dalton Trans.*, 1973, 371.

40. P.Kreutzer, C.Weiss, H.Boehme, T.Kemmerich, W.Beck, C.Spencer, R.Mason, *Z.Naturforsch*, 1972, **27B**, 745.

41. J.H.Nelson, D.L.Schmitt, R.A.Henry, D.W.Moore, H.B.Jonassen, *Inorg.Chem.*, 1970, **9**, 2678.

42. L.A.Oro, M.T.Pinillos, C.Tejel, M.C.Apreda, C.Foces-Foces, F.H.Cano, *J.Chem.Soc., Dalton Trans.*, 1988, 1927.

43. R.Guilard, I.Perrot, A.Tabard, P.Richard, C.Lecomte, Y.H.Liu, K.M.Kadish, *Inorg.Chem.*, 1991, **30**, 27.

44. R.Das, P.Paul, K.Nag, K.Venkatasubramanian, *Inorg. Chim.Acta*, 1991, **185**, 221.

45. W.P.Fehlhammer, L.F.Dahl, *J.Am.Chem.Soc.*, 1972, **94**, 3370.

46. E.J.Van den Heuvel, P.L.Franke, G.C.Verschoor, A.P.Zuur, *Acta.Cryst.*, 1983, **C39**, 337.

47. G.J.Palenik, *Acta.Cryst.*, 1963, **16**, 596.

48. C.Janiak, *J.Chem.Soc., Chem.Commun.*, 1994, 545; C.Janiak, T.G.Scharmann, K.Brzezinka, P.Reich, *Chem.Ber.*, 1995, **128**, 323.

49. R.Guilard, N.Jagerovic, A.Tabard, P.Richard, L. Courthaudon, A.Louati, C.Lecomte, K.M.Kadish, *Inorg.Chem.*, 1991, **30**,16; L.Wiehl, *Acta.Cryst.*, 1993, **B49**, 289.

50. A.Alvanipour, N.H.Buttrus, C.Eaborn, P.B.Hitchcock, A.I.Mansour, A.K.Saxena, *J.Orgmet.Chem.*, 1988, **349**, 29.

51. P.Dunn, D.Oldfield, *Aust.J.Chem.*, 1971, **24**, 645.

52. M.Hill, M.F.Mahon, K.C.Molloy, *J.Chem.,Soc., Dalton Trans.*, 1996, 1857.

53. S.J.Blunden, M.F.Mahon, K.C.Molloy, P.C.Waterfield, *J.Chem.Soc., Dalton Trans.*, 1994, 2135.

54. G.B.Ansell, *J.Chem.Soc., Dalton Trans.*, 1973, 371.

55. E.J.Graeber, B.Morosin, *Acta. Cryst.*, 1983, **C39**, 567.

56. N.C.Baezinger, R.J.Schultz, *Inorg.Chem.*, 1971, **10**, 661.

57. R.L.Bodner, A.I.Popov, *Inorg.Chem.*, 1972, **11**, 1410.

58. L.Wiehl, *Acta.Cryst.*, 1993, **B49**, 289.

59. E.O.John, R.D.Willet, B.Scott, R.L.Kirchmeir, J.M.Shreeve, *Inorg.Chem.*, 1989, **28**, 893.

60. J.J.Zuckerman, *Adv.Organometal.Chem.*, 1970, **9**, 21.

61. J.R.Ruddick, *Rev.Silicon, Germanium, Tin and Lead Compounds*, 1976, **2**, 115.

62. G.M.Bancroft, R.H.Platt, *Adv.Inorg.Radiochem.*, 1976, **15**, 59.

63. J.J.Zuckerman in *'Chemical Mössbauer Spectroscopy'*, ed.R.H.Herber, Plenum, New York, 1984.

64. N.N.Greenwood, T.C.Gibb, *'Mössbauer Spectroscopy'*, Chapman and Hall, London, 1971.

65. A.Vertes, L.Korecz, K.Berger, *'Mössbauer Spectroscopy'*, Elsevier, Amsterdam, 1979.

66. G.M.Bancroft, *'Mössbauer Spectroscopy-An Introduction for Chemists and Geochemists'*, McGraw-Hill, London, 1973.

67. R.V.Parish, *'NMR, NQR, EPR and Mössbauer Spectroscopy in Inorganic Chemistry'*, Ellis Horwood, London, 1990.

68. P.G.Harrison, *'Chemistry of Tin'*, Chapman and Hall, New York, 1989.

69. A.G.Davies, P.J.Smith, *'Comprehensive Organometallic Chemistry'*, eds. G.Wilkinson, F.G.A.Stone, E.W.Abel, Permagon, Oxford, 1982, **2**, 529.

70. P.J.Smith, A.P.Tupciauskas, *Ann.Rev.NMR Spec.*, 1978, **8**, 291.

71. V.S.Petrosyan, *Prog.NMR Spec.*, 1977, **11**, 115.

72. B.Wrackmeyer, *Ann.Rep.NMR Spec.*, 1985, **16**, 73.

73. J.D.Kennedy, W.M.McFarlane, *Rev.Si, Ge, Sn and Pb*, 1974, **1**, 235.

74. R.K.Harris, B.E.Mann, *'NMR and the Periodic Table'*, Academic Press, London, 1987.

75. J.Mason, *'Multinuclear NMR'*, Plenum Press, New York and London, 1987.

76. M.Nadvornik, J.Holecek, K.Handlir, A.Lycka, *J.Orgmet.Chem.*, 1984, **275**, 43.

77. J.Holecek, A.Lycka, *Inorg.Chim.Acta*, 1986, **118**, L15.

78. T.P.Lockhart, W.F.Manders, *Inorg.Chem.*, 1986, **25**, 892.

79. J.Holecek, M.Nadvornik, K.Handlir, A.Lycka, *J.Orgmet.Chem.*, 1983, **241**, 177.

80. P.C.Waterfield, *'Novel C-Organostannyl Heterocycles'*, Ph.D Thesis, University Of Bath, 1988.

81. R.K.Ingham, S.D.Rosenberg, H.Gilman, *Chem.Rev.*, 1960, **60**, 459.

82. A.G.Davies, P.J.Smith, *Adv.Inorg.Chem.Radiochem.*, 1980, **23**, 1.

83. M.Pereyre, J.C.Pommier, *J.Organometal.Chem.Library*, 1976, **1**, 161.

84. J.A.Zubieta, J.J.Zuckerman, *Prog.Inorg.Chem.*, 1978, **24**, 251.

85. *'Organotin Compounds'*, ed. A.K.Sawyer, Dekker, New York, 1971, vols.1,2,3.

86. 'G.Bähr, S.Pawlenko, in *'Methoden der Organischen Chemie (Houben Weyl)'*, , Stuttgart, 1978, **13/16** Thieme, 181.

87. *'Gmelin Handbuch der Anorganischen Chemie'*, 'Tin.Part 1: Tin Tetraorganyls SnR_4', Springer-Verlag, Berlin, 1975.

88. *'Gmelin Handbuch der Anorganischen Chemie'*, 'Tin.Part 2: Tin Tetraorganyls R_3SnR'', Springer-Verlag, Berlin, 1975.

89. *'Gmelin Handbuch der Anorganischen Chemie'*, 'Tin.Part 3: Tin Tetraorganyls $R_2SnR'_2$, $R_2SnR'R''$, $RR'SnR''R''''$, Heterocyclic and Spiranes', Springer-Verlag, Berlin, 1976.

90. *'Gmelin Handbuch der Anorganischen Chemie'*, 'Tin.Part 4: 'Organotin Hydrides', Springer-Verlag, Berlin, 1976.

91. *'Gmelin Handbuch der Anorganischen Chemie'*, 'Tin.Part 5: 'Organotin Fluorides. Triorganotin Chlorides', Springer-Verlag, Berlin, 1978.

92. *'Gmelin Handbuch der Anorganischen Chemie'*, 'Tin.Part 6: 'Diorganotin Dichlorides. Organotin Trichlorides', Springer-Verlag, Berlin, 1979.

93. P.A. Cusack, P.J.Smith, J.D.Donaldson, S.M.Grimes, *'A Bibliography of X-Ray Crystal structures of Tin Compounds'*, International tin research institute, London, 1981.

94. M.H.Gitliz, *Adv.Chem.Ser.*, 1976, **157**, 167.

95. V.G.Kumar Das, *Planter (Kuala Lumpur)*, 1975, **51**, 355.

96. B. Sugavanam, *Tin Its Uses*, 1980, **126**, 4.

97. G.H.Nöhler, *Gesund. Disinfekt.*, 1970, **62**, 10, 65, and 175.

98. P.Klimsch, *Plaste Kauc.*, 1977, **24**, 380.

99. D.Lanigan, *'Proceedings of the International Conference on PVC Processing'*, Plastics and Rubber Institute, Lodon, 1978, 4.1.

100. G.Ayrey, B.C.Head, R.C.Poller, *Macromol.Rev.*, 1974, **8**, 1.

101. C.J.Evans, *Glass*, 1974, **51**, 303.

102. T.Suzukawa, *Serramikkusu (Japan)*, 1969, **4**, 852.

103. S.Kozima, T.Itano, N.Mihara, K.Sisido, T.Isida, *J.Orgmet.Chem.*, 1972, **44**, 117.

104. D.H.Williams, I.Fleming, *'Spectroscopic Methods in Organic Chemistry'*, McGraw-Hill Book Company (UK) Ltd., 1989.

105. C.A.Kraus, W.N.Greer, *J.Am.Chem.Soc.*, 1923, **45**, 294.

106. J.Ensling, P.Gütlich, K.M.Hasselbach, B.W.Fitzsimmons, *J.Chem.Soc.(A)*, 1971, 1940.

107. S.W.Ng, A.J.Kuthubutheen, Z.Arifin, W.Chen, V.G.Kumar Das, *J.Orgmet.Chem.*, 1991, **403**, 102.

108. K.C.Molloy, S.F.Sayers, M.F.Mahon, University of Bath, Unpublished Results.

109. S.Kozima, T.Hitomi, T.Akiyama, T.Isida, *J.Orgmet.Chem.*, 1975, **32**, 303.

110. W.T.Reichle, *Inorg.Chem.*, 1964, **3**, 402.

111. I.Belsky, *J.Chem.Soc., Chem.Comm.*, 1977, 237.

112. B.Laufer, *Beginnings of Porcelain in China*, ARC Press, 1917.

113. A.Weiss, A.Weiss, *Angew.Chem.*, 1960, **72**, 413.

114. K.Fredenhagen, G.Cadenbach, *Z.Anorg.Allg.Chem.*, 1926, **158**, 249.

115. D.W.Bruce, D.O'Hare, *'Inorganic Materials'*, 2nd edition, John Wiley and sons, 1997.

116. R.Schöllhorn, *Angew.Chem.Int.Ed.Engl.*, 1980, **19**, 983.

117. R.T.Morrison, R.N.Boyd, *'Organic Chemistry'*, Allyn and Bacon Inc., 1987.

118. F.Vogtle, E.Weber, *'The Chemistry of the Ether Linkage'*, Suppl. E, Part 1.

119. G.W.Gockel, O.Murillo, *Comprehensive Supramolecular Chemistry*, 1996, **1**, 1.

120. F.Vogtle, E.Weber, *Tetrahedron Letters*, 1975, **29**, 2415.

121. A.J.Crowe, R.Hill, P.J.Smith, J.S.Brooks, R.Formstone, *J.Orgmet.Chem.*, 1981, **204**, 47.

122. M.F.Mahon, K.C.Molloy, P.C.Waterfield, *Organometallics*, 1993, **12**, 769.

123. D.M.Bassani, J.M.Lehn, G.Baum, D.Fenske, *Angew.Chem.Int.Ed.Engl.*, 1997, **36**, 1845.

124. P.G.Harrison, *'Comprehensive Organometallic Chemistry'*, eds. G.Wilkinson, F.G.A.Stone, E.W.Abel, Permagon, Oxford, 1982, **2**, 629.

125. H.Shapiro, F.W.Frey, *'The Organic Compounds of Lead'*, John Wiley and Sons, 1968, 5.

126. T.Midgley Jr., T.A.Boyd, *Ind.Eng.Chem.*, 1922, **14**, 894.

127. L.C.Willemsens, *'Organolead Chemistry'*, International Lead Zinc Research Organisation, New York, 1964, 54.

128. L.C.Willemsens, G.J.M.van der Kerk, *Investigations in the Field of Organolead Chemistry*, International Lead Zinc Research Organisation, New York, 1965.

129. H.Gorth, M.C.Henry, *J.Orgmet.Chem.*, 1967, **9**, 117.

130. A.V.Yatsenko, H.Schenk, L.A.Aslanov, *J.Orgmet.Chem.*, 1994, **474**, 107.

131. D.L.Reger, M.F.Huff, A.L.Rheigold, B.S.Haggerty, *J.Am.Chem.Soc.*, 1992, **114**, 579.

132. D.L.Reger, Y.Ding, A.L.Rheingold, R.L.Ostrander, *Inorg.Chem.*, 1994, **33**, 4226.

133. T.N.Mitchell, J.Gmehling, F.Huber, *J.Chem.Soc., Dalton Trans.*, 1978, 960.

134. L.V.Azaroff, *'Elements of X-ray Crystallography'*, McGraw-Hill Inc., U.S.A., 1968.

135. E.Lieber, C.N.R.Rao, F.M.Keane, *J.Inorg.Nucl.Chem.*, 1962, **25**, 631.

136. A.G.Lee, *'The Chemistry of Thallium'*, Elvesier Publishing Company, 1971.

137. C.Hansen, *Ber.*, 1870, **3**, 9.

138. H.P.A.Groll, *J.Am.Chem.Soc.*, 1930, **52**, 2998.

139. F.Challenger, B.Parker, *J.Chem.Soc.*, 1931, 1462.

140. E.O.Fischer, *Angew.Chem.*, 1957, **69**, 207.

141. A.G.Lee, *'Organometallic Reactions'*, ed. E.I.Becker and M.Tsutsui, Wiley, New York, 1975, **5**, 1; H.Kurosawa, R.Okawara, *Organomet.Chem.Rev.(A)*, 1970, **6**, 65.

142. C.H.Popence, *Science*, 1926, **64**, 525.

143. B.W.Travis, *J.Econ.Entomol.*, 1943, **36**, 56.

144. S.M.Egidio, F.Schaposnik, *British Medical Journal*, 1949, **2**, 791.

145. A.Heyndrick, *Progress in Chemical Toxicology*, ed. A.Stolman, **4**, Academic Press, 1969.

146. H.Heydlauf, *European J.Pharm.*, 1969, **6**, 340.

147. P.J.Gehring, P.B.Hammond, *J.Pharmocol.Exp.Ther.*, 1967, **155**, 187.

148. J.S.Britten, M.Blank, *Biochem. And Biophys. Acta*, 1968, **159**, 160.

149. C.E.Inturrisi, *Biochem. And Biophys. Acta*, 1969, **178**, 630.

150. F.J.Kayne, J.Reuben, *J.Amer.Chem.Soc.*, 1970, **92**, 220.

151. *Journal of the Franklin Institute*, 1957, **264**, 48.

152. A.V.Churakov, D.A.Lemenovskii, L.G.Kuz'mina, *J.Orgmet.Chem.*, 1995, **C81** 489.

153. T.E.Butterwolf, T.L.Hubler, A.L.Rheingold, *J.Orgmet.Chem.*, 1992, **431**, 199.

154. M.D.Rausch, B.E.Edwards, R.D.Rogers, J.L.Atwood, *J.Am.Chem.Soc.*, 1983, **105**, 3882.

155. R.G.Holm, P.L.Donnelly, *J.Inorg.Nucl.Chem.*, 1986, **28**, 1887.

156. E.C.Taylor, Y.Maki, A.McKillop, *J.Org.Chem.*, 1969, **34**, 1170.

157. D.L.Reger, J.E.Collins, R.Layland, R.D.Adams, *Inorg.Chem.*, 1996, **35**, 1372.

158. G.Ferguson, M.C.Jennings, F.J.Lalor, C.Shanahan, *Acta.Cryst.*, 1991, **C47**, 2079.

159. A.H.Cowley, R.L.Geerts, C.M.Nunn, S.Trofimenko, *J.Orgmet.Chem.*, 1989, **365**, 19.

160. A.J.Amoroso, J.C.Jeffery, P.L.Jones, J.A.McCleverty, E.Psillakis, M.D.Ward, *J.Chem.Soc., Chem.Comm.*, 1995, 1175.

161. A.L.Rheingold, R.L.Ostrander, B.S.Haggerty, S.Trofimenko, *Inorg.Chem.*, 1994, **33**, 3666.

162. A.L.Rheingold, L.M.Liable-Sands, G.P.A.Yap, S.Trofimenko, *J.Chem.Soc., Chem.Comm.*, 1996, 1233.

163. E.Libertini, K.Yoon, G.Parkin, *Polyhedron*, 1993, **12**, 2539.

164. D.D.LeCloux, C.J.Tokar, M.Osawa, R.P.Houser, M.C.Keyes, W.B.Tolman, *Organometallics*, 1994, **13**, 2855.

165. A.G.Lee, *J.Chem.Soc.(A)*, 1971, 880.

166. Y.P.Mascarenhas, I.Vencato, M.C.Carracal, J.M.Varela, J.S.Casas, J.Sordo, *J.Orgmet.Chem.*, 1988, **344**, 137.

167. H.Kurosawa, *'Comprehensive Organometallic Chemistry'*, eds. G.Wilkinson, F.G.A.Stone, E.W.Abel, Permagon, Oxford, 1982, **1**, 725.

168. R.T.Griffin, K.Henrick, R.W.Matthews, M.McPartlin, *J.Chem.Soc., Dalton Trans.*, 1980, 1550.

169. P.J.Burke, L.A.Gray, P.J.C.Hayward, R.W.Matthews, M.McPartlin, D.G.Gillies, *J.Orgmet.Chem.*, 1977, **136**, C7.

170. G.B.Deacon, S.J.Faulks, B.M.Gatehouse, A.J.Jozsa, *Inorg.Chim.Acta*, 1977, **21**, L1.

171. K.Henrick, R.W.Matthews, P.A.Tasker, *Acta Cryst.*, 1978, **B34**, 935.

172. Y.M.Chow, D.Britton, *Acta Cryst.*, 1975, **B31**, 1922.

173. Y.M.Chow, D.Britton, *Acta Cryst.*, 1975, **B31**, 1929.

174. W.Schwarz, G.Mann, J.Weidlein, *J.Orgmet.Chem.*, 1976, **122**, 303.

175. K.Freudenberg, G.Uthemann, *Chem.Ber.*, 1919, **52**, 1509.

176. J.S.Casas, E.E.Castellano, A.Castiñeiras, A.Sanchez, J.Sordo, E.M.Vázquez-López, J.Zuckerman-Schpector, *J.Chem.Soc., Dalton Trans.*, 1995, 1403.

177. J.F.Hinton, *Mag.Res.in Chem.*, 1987, **25**, 659.

178. A.Blascette, P.G.Jones, A.Michalides, M.Nävake, *J.Orgmet.Chem.*, 1991, **415**, 25.

179. S.E.Jefs, R.W.H.Small, I.J.Worrall, *Acta Cryst.*, 1984, **C40**, 1329.

180. K.Henrick, M.McPartlin, R.W.Matthews, G.B.Deacon, R.J.Phillips, *J.Orgmet.Chem.*, 1980, **193**, 13.

181. T.N.Srivastava, K.K.Bajpai, *J.Inorg.Nucl.Chem.*, 1972, **34**, 1458.

182. A.G.Davies, *'Organotin Chemistry'*, VCH Verlagsgesellschaft mbH, Weinheim, 1997.

183. N.N.Greenwood, A.Earnshaw, *'Chemistry of Elements'*, Permagon Press Ltd., 1984.

184. F.R.Hartley, *'The Chemistry of the Metal-Carbon Bond'*, 1989, **5**, 465.

185. J.Bravo, M.B.Cordero, J.S.Casas, A.Sánchez, J.Sordo, E.E.Castellano, J.Zuckerman-Schpector, *J.Orgmet.Chem.*, 1994, **482**, 147.

186. R.Cea-Olivares, O.Jiménez-Sandoval, G.Espinosa-Pérez, C.Silvestru, *J.Orgmet.Chem.*, 1994, **484**, 33.

187. J.L.Wardell, *'Comprehensive Organometallic Chemistry'*, eds. G.Wilkinson, F.G.A.Stone, E.W.Abel, Permagon, Oxford, 1982, **2**, 863.

188. K.C.Molloy, T.G.Purcell, D.Cunningham, P.McArdle, T.Higgins, *Appl.Organometal.Chem.*, 1987, **1**, 119.

189. A-F Shahida, I.A-A Jassim, F.Weller, *J.Orgmet.Chem.*, 1984, **268**, 125.

190. G.M.Sheldrick, *Acta Cryst.*, 1990, **A46**, 467.

191. G.M.Sheldrick, *J.Appl.Cryst.*, Universität Göttingen, 1995 (In Preparation).

NUMERICAL INDEX OF NEW COMPOUNDS

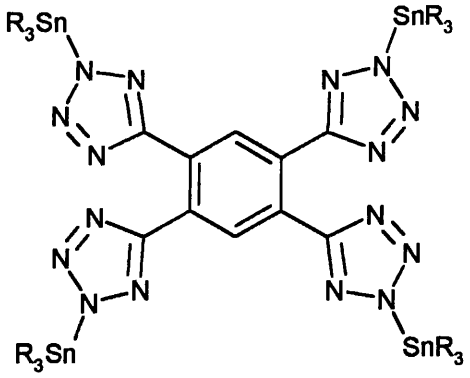

R = Bu (**1**)

R = Et.3½H_2O (**2**)

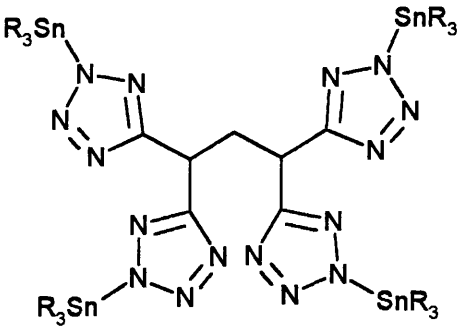

R = Bu (**3**)

R = Et.4H_2O (**4**)

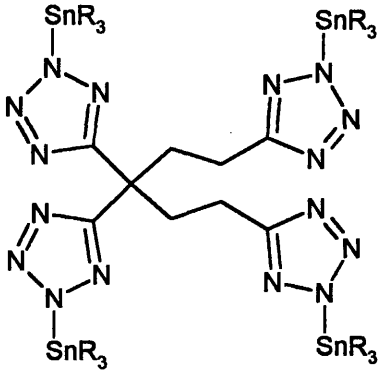

R = Bu (**5**)

R = Et (**6**)

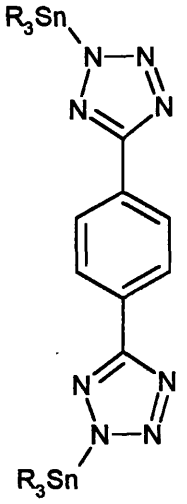

R = Bu.H_2O(**7**)

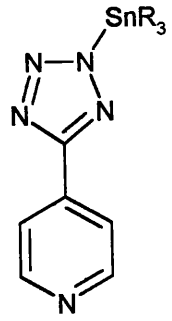

R = Bu (**8**)

R = Et (**9**)

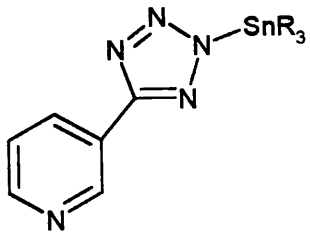

R = Bu (**10**)

R = Et.H_2O (**11**)

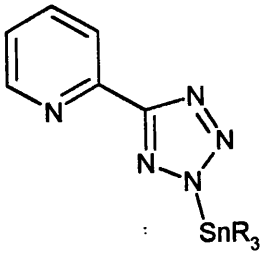

R = Bu (**12**)

R = Et.MeOH (**13**)

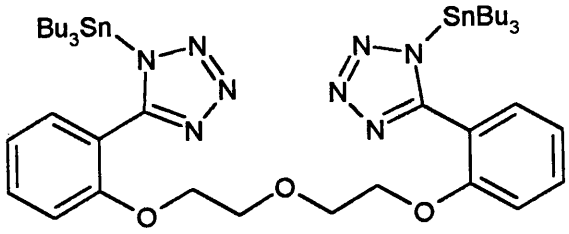

(**14**)

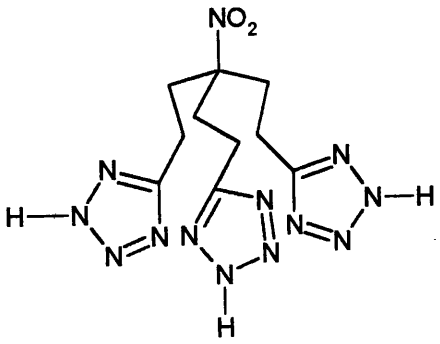

.MeOH (**15**)

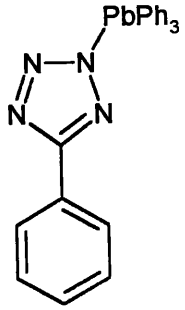

.MeOH (**16**)

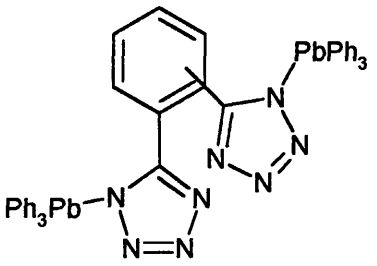

1,2 isomer.2MeOH (**17**)

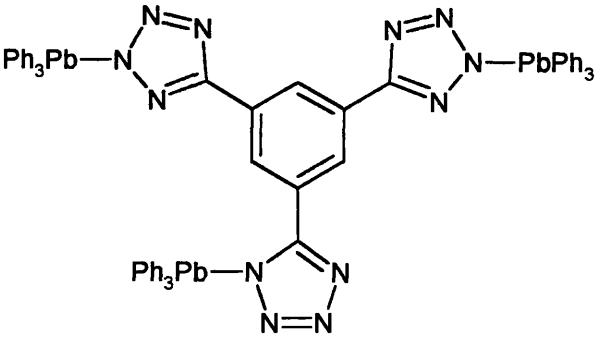

.$3H_2O$(**20**)

1,3 isomer.2MeOH (**18**)

1,4 isomer.$2H_2O$ (**19**)

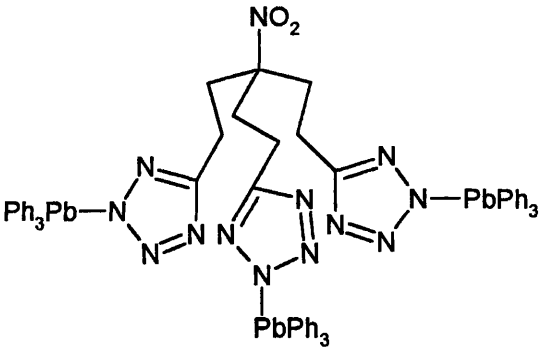

.$6H_2O$ (**21**)

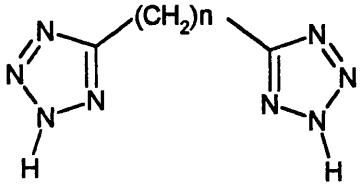

n = 2 (**22**)

n = 4 (**23**)

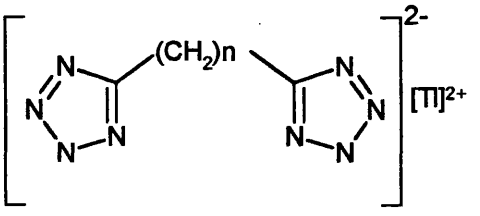

n = 1 (**24**)

n = 4 (**25**)

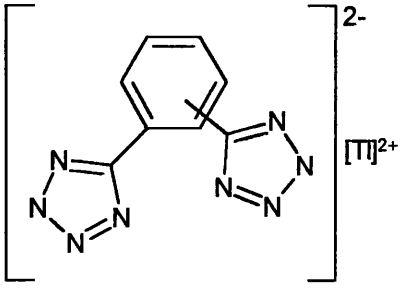

1,3 isomer.$2H_2O$ (**26**)

1,4 isomer (**27**)

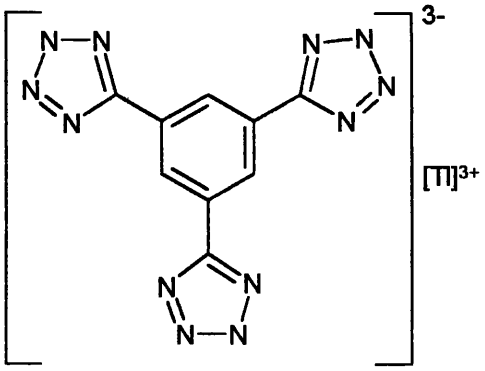

.$3H_2O$ (**28**)

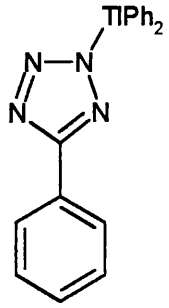

.MeOH (**29**)

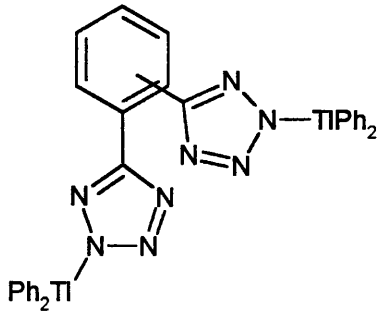

1,2 isomer.$Ph_2TlCl.2H_2O.2MeOH$ (**30**)

1,3 isomer.$2H_2O$ (**31**)

1,4 isomer.$0.5Ph_2TlCl.2H_2O$ (**32**)

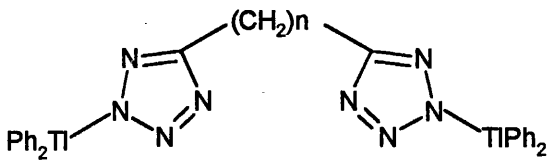

n = $1.2H_2O$ (**33**)

n = 2. $2H_2O$ (**34**)

n = 4.2MeOH (**35**)

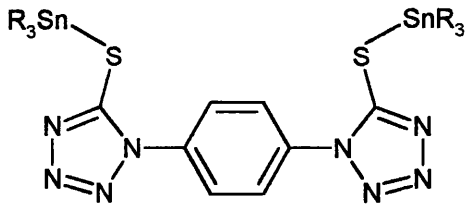

R = Bu (**36**) R = Me.2MeOH (**40**)

R = Et (**37**) R = Ph (**41**)

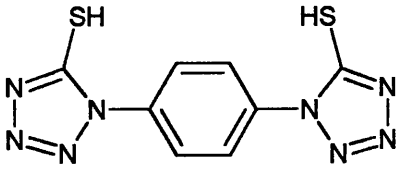

.MeOH (**38**)

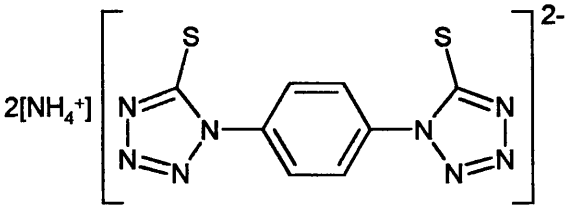

(**39**)

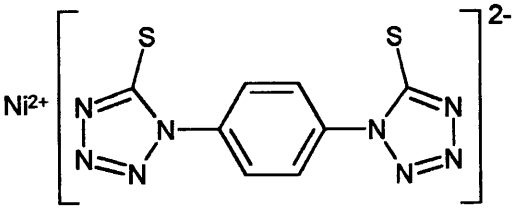

.6H_2O (**42**)

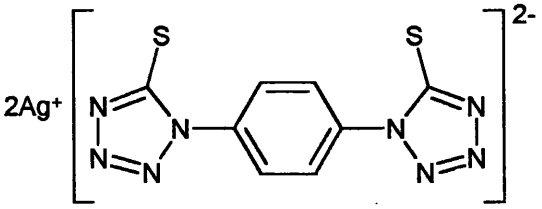

.2H_2O (**43**)

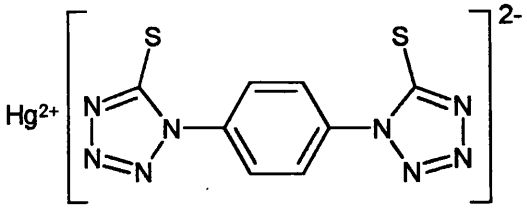

.2H_2O (**44**)

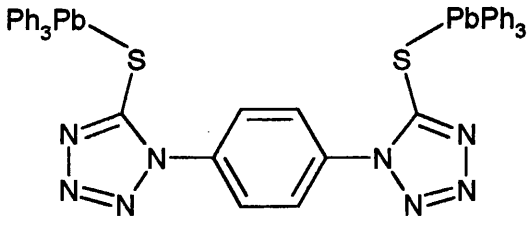

.0.5$CH_3C_6H_5$ (**45**)

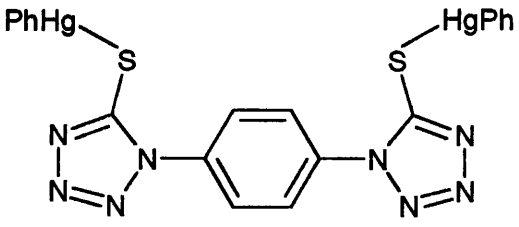

(**46**)

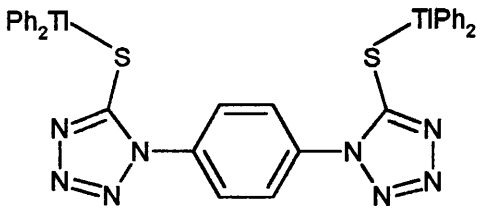

.2H_2O (**47**)